

# **Stony Brook University**



OFFICIAL COPY

**The official electronic file of this thesis or dissertation is maintained by the University Libraries on behalf of The Graduate School at Stony Brook University.**

**© All Rights Reserved by Author.**

**Design, Synthesis and Biological Evaluation of Novel Curcumin Analogues  
as Inhibitors of Matrix Metalloproteinases and Pro-inflammatory Cytokines**

A Dissertation Presented

by

**Yu Zhang**

to

The Graduate School

in Partial Fulfillment of the

Requirements

for the Degree of

**Doctor of Philosophy**

in

**Chemistry**

**(Chemical Biology)**

Stony Brook University

**December 2012**

Copyright by  
Yu Zhang  
2012

**Stony Brook University**

The Graduate School

**Yu Zhang**

We, the dissertation committee for the above candidate for the  
Doctor of Philosophy degree, hereby recommend  
acceptance of this dissertation.

**Francis Johnson – Dissertation Advisor  
Professor, Department of Chemistry**

**Kathlyn A. Parker – Chairperson of Defense  
Professor, Department of Chemistry**

**Robert C. Kerber – Committee Member of Defense  
Professor, Department of Chemistry**

**Carlos de los Santos – External Committee Member of Defense  
Professor, Department of Pharmacological Sciences, Stony Brook University**

This dissertation is accepted by the Graduate School

Charles Taber  
Interim Dean of the Graduate School

Abstract of the Dissertation

**Design, Synthesis and Biological Evaluation of Novel Curcumin Analogues  
as Inhibitors of Matrix Metalloproteinases and Pro-inflammatory Cytokines**

by

**Yu Zhang**

**Doctor of Philosophy**

in

**Chemistry**

**(Chemical Biology)**

Stony Brook University

**2012**

There are two principal reasons why we age: 1) the toxicity of oxygen species; 2) the continuous degradation of collagen by groups of enzymes such as the matrix metalloproteinases (MMPs). The MMPs are a group of more than 25 structurally zinc-containing enzymes that are involved in the degradation of numerous extracellular, pericellular and non-matrix proteins. In many disease conditions their levels and proteinase activity rise, producing pathological and serious structural damage. Tetracyclines (TCs) are known inhibitors of mammalian-derived MMPs, and non-antibiotic formulations of doxycycline are FDA-approved to treat periodontitis and the chronic inflammatory skin disease, rosacea. However, a significant limitation is that the FDA only permits the use of subantimicrobial doses of these antibiotics for these diseases to prevent antibiotic side-effects. Therefore a series of chemically-modified TCs (CMTs), which are no longer anti-bacterial at any dose, were developed, but a significant side-effect was increased

photosensitivity. Accordingly, in order to avoid these limitations, a series of chemically-modified curcumins (CMCs) were prepared and evaluated as new MMP inhibitors because they have the same zinc-binding site as the TCs, namely a polyenolic assembly. The current lead compound, CMC2.24 [a bis-(demethoxy) phenylaminocarbonyl derivative of curcumin], exhibits inhibitory  $IC_{50}$  values *in vitro*, ranging from 2-8 $\mu$ M against two collagenases (MMP-8 and MMP-13), two gelatinases (MMP-2 and MMP-9), MMP-3, MMP-7 and MMP-12. The zinc-binding as well as the acidity constants of these CMCs were evaluated and correlated to their potency as MMP-inhibitors *in vitro*. An *in vitro* lipophilicity study and *in vivo* pharmacokinetics were also carried out for curcumin and CMC2.24. The results show that CMC2.24 is more bioavailable in rat serum, and is retained in organ tissues such as the liver, heart, spleen, lung, kidney and brain in comparison with curcumin, which showed much lower levels of retention in these tissues. It was also found that the production of the pro-inflammatory cytokines and the chemokines including TNF- $\alpha$ , IL-1 $\beta$  and MCP-1 was significantly reduced by CMC2.24 and a related trione (CMC2.5) in cell culture. Collateral studies with CMC2.24 involving its effects on various disease models are discussed.

## Dedication

谨以此论文献给我亲爱的父母和祖父母，感谢他们的抚育，教导，支持，鼓励！

This thesis is dedicated to my parents, Mr. Zhiqiang Zhang and Ms. Wei Liang, for it is their love, support and encouragement that bring a project like this to fruition.

Also to my grandparents, Mr. Shushan Zhang and Ms. Yujie Gong, for it is the good care they have been taking of since the first day I was born.

*“You raise me up,  
So I can stand on mountains;  
You raise me up,  
To walk on stormy seas;  
I am strong,  
When I am on your shoulders;  
You raise me up,  
To more than I can be.”*

*----Brendan Graham, Irish novelist and composer*

## Table of Contents

<b>DEDICATION</b>	<b>V</b>
<b>LIST OF FIGURES</b>	<b>XI</b>
<b>LIST OF TABLES</b>	<b>XX</b>
<b>LIST OF SCHEMES</b>	<b>XXIII</b>
<b>LIST OF ABBREVIATIONS</b>	<b>XXIV</b>
<b>ACKNOWLEDGMENTS</b>	<b>XXVIII</b>
<b>CHAPTER 1. INTRODUCTION</b>	<b>1</b>
<b>References</b>	<b>5</b>
<b>CHAPTER 2. LITERATURE REVIEW</b>	<b>8</b>
<b>PART 1. MATRIX METALLOPROTEINASES (MMPS)</b>	<b>8</b>
<b>A. History</b>	<b>8</b>
<b>B. The Extracellular Matrix (ECM) and Basement Membrane (BM)</b>	<b>9</b>
<b>C. Structure and classification</b>	<b>10</b>
1. Structural features of MMPs	10
2. Classification of MMPs	11
a. Collagenases	13
b. Gelatinases	14
c. Stromelysins	16
d. Matrilysin	16
e. Metalloelastase	17
f. Membrane-type MMPs	17
g. Others	18
<b>D. MMPs involvement in diseases</b>	<b>18</b>
1. MMPs in Cancer	19
2. MMPs in Periodontitis	20
3. MMPs in Arthritis	21



4. MMPs in other diseases	21
<b>E. MMP inhibitors</b>	<b>21</b>
1. Endogenous inhibitors	21
2. Synthetic inhibitors	23
a. Tetracyclines	23
b. Other MMP inhibitors	27
3. Structure comparison of doxycycline, thermorubin, bis-aryol methanes and curcumin	29
<b>PART 2. CURCUMIN</b>	<b>32</b>
<b>F. History</b>	<b>32</b>
<b>G. Therapeutic use of curcumin</b>	<b>33</b>
1. Anti-cancer activity	34
2. Anti-inflammatory activity	35
3. Anti-oxidant activity	35
<b>H. Bioavailability of curcumin</b>	<b>36</b>
<b>References</b>	<b>38</b>
<b>CHAPTER 3. SYNTHESIS OF CHEMICALLY-MODIFIED CURCUMINS BY A MODIFIED PABON REACTION</b>	<b>58</b>
<b>A. Introduction</b>	<b>58</b>
<b>B. Side chain modification</b>	<b>60</b>
<b>C. Introduction of a methoxy/ethoxy carbonyl group on C-4</b>	<b>62</b>
<b>D. Tetrahydro-curcumin analogue</b>	<b>66</b>
<b>E. Unsymmetrical curcumin analogues</b>	<b>67</b>
<b>F. Introduction of an N-phenylaminocarbonyl group on C-4</b>	<b>68</b>
<b>G. Introduction of a solubilizing group on CMC2.24</b>	<b>70</b>
<b>Materials and Methods</b>	<b>74</b>
1. General procedure for the synthesis of 4-substituted-2,4-pentanediones	75
2. General method for the synthesis of the curcumin analogues	78
<b>References</b>	<b>86</b>
<b>CHAPTER 4. <i>IN VITRO</i> POTENCY OF CURCUMIN AND CHEMICALLY-MODIFIED CURCUMINS (CMCS)</b>	<b>90</b>

<b>A. Introduction</b>	<b>90</b>
<b>B. Preliminary study of curcumin and CMCs in MMP-9 inhibition by an HPLC method</b>	<b>90</b>
<b>C. <i>In vitro</i> potency against nine different MMPs by curcumin and the related CMCs</b>	<b>93</b>
<b>D. Inhibition of MMP-9 by newer curcumin analogues</b>	<b>124</b>
<b>Materials and Methods</b>	<b>125</b>
1. HPLC MMP inhibition assay	125
2. Fluorogenic MMP inhibition assay	126
<b>References</b>	<b>127</b>
<b>CHAPTER 5. PK<sub>A</sub>, ZINC- AND BOVINE SERUM ALBUMIN BINDING, AND ANTIMICROBIAL STUDIES ON CURCUMIN, CMC2.5 AND CMC2.24</b>	<b>130</b>
<b>A. Introduction</b>	<b>130</b>
<b>B. pK<sub>a</sub> measurement</b>	<b>131</b>
<b>C. Zinc binding study</b>	<b>141</b>
<b>D. Bovine Serum Albumin (BSA) binding study</b>	<b>145</b>
<b>E. <i>In vitro</i> antimicrobial activity of curcumin, CMC2.5 and CMC2.24</b>	<b>149</b>
1. Minimum Inhibitory Concentration (MIC)	149
2. β-galactosidase inhibition	150
<b>Materials and Methods</b>	<b>152</b>
1. pH equilibria	152
2. Zn <sup>2+</sup> and BSA binding	153
3. Data processing	154
4. MIC test	154
5. <i>In vitro</i> β-galactosidase synthesis	155
<b>References</b>	<b>156</b>
<b>CHAPTER 6. AN <i>IN VITRO</i> LIPOPHILICITY AND AN <i>IN VIVO</i> PHARMACOKINETIC STUDY OF CURCUMIN AND CMC2.24</b>	<b>159</b>
<b>A. Introduction</b>	<b>159</b>
<b>B. <i>In vitro</i> lipophilicity</b>	<b>160</b>
<b>C. <i>In vivo</i> pharmacokinetics by oral route</b>	<b>162</b>
<b>D. <i>In vivo</i> pharmacokinetics by <i>i.v.</i> route</b>	<b>163</b>

<b>Materials and Methods</b>	<b>184</b>
1. Standard curve	184
2. Serum analysis	184
3. Pellets analysis	185
4. Organ analysis	185
<b>References</b>	<b>186</b>
<b>CHAPTER 7. X-RAY CRYSTALLOGRAPHY OF THE MMP-8 CATALYTIC SUBUNIT WITH AND WITHOUT CURCUMIN AND CMC2.24 AS INHIBITORS</b>	<b>188</b>
<b>A. Introduction</b>	<b>188</b>
1. X-ray crystallography	188
2. X-ray crystallography study of MMP-8	189
<b>B. Recombinant protein expression with His-tag</b>	<b>192</b>
<b>C. RECOMBINANT PROTEIN EXPRESSION WITHOUT HIS-TAG</b>	<b>195</b>
<b>D. Crystallization of MMP-8 with or without the inhibitor present</b>	<b>198</b>
<b>Materials and Methods</b>	<b>200</b>
1. Cloning and protein expression of MMP-8 in an MBP fusion system	200
2. Nickel NTA chromatography for purification of the MBP-fusion protein	201
3. Q-Sepharose for purification of the MMP-8 catalytic subunit	202
4. Cloning and protein expression of MMP-8 in pET-22b(+) vector	202
5. Protein purification of MMP-8 catalytic subunit by purification of inclusion bodies	203
6. Gel Filtration Chromatography	203
7. Crystallization	204
<b>References</b>	<b>204</b>
<b>CHAPTER 8. COLLATERAL STUDIES AND CONCLUSION</b>	<b>209</b>
<b>A. Introduction</b>	<b>209</b>
<b>B. Cell Culture Studies</b>	<b>210</b>
<b>C. Tissue Culture Studies</b>	<b>214</b>
<b>D. <i>In Vivo</i> Studies.</b>	<b>216</b>
1. Type-I diabetes	216
2. Wound-healing	219
3. Acute respiratory distress syndrome (ARDS)	222

<b>E. Conclusion</b>	<b>225</b>
<b>References</b>	<b>228</b>
<b>BIBLIOGRAPHY</b>	<b>231</b>
<b>APPENDIX</b>	<b>266</b>
<b>A. Report on the boron analysis of CMC2.24</b>	<b>266</b>

## List of Figures

Figure 1.1 Doxycycline, Thermorubin, Bis-Aroyl Methanes and Curcumin	2
Figure 1.2 Bis-Aroyl Methanes (BAMs)	3
Figure 1.3 Development of novel MMP inhibitors related to curcumin	4
Figure 2.1 General domain structures of MMPs	10
Figure 2.2 MMPs in various diseases	19
Figure 2.3 Structures of tetracyclines and chemically-modified tetracyclines	25
Figure 2.4 Structures of Batimastat and Marimastat	28
Figure 2.5 Structures of BAM1.11 and BAM 1.12	31
Figure 2.6 Structures of curcumin, demethoxycurcumin and bis-demethoxycurumin	33
Figure 2.7 Curcumin used in various diseases	34
Figure 2.8 List of curcumin metabolites via different administrations	37
Figure 3.1 Structures of compounds 1-5	61
Figure 3.2 Structures of compounds 6-18	65
Figure 3.3 Structures of Compounds 20, 21	68
Figure 3.4 Structures of compounds 22-24	70
Figure 3.5 Structures of compounds 25, 26	73
Figure 4.1 MMP-1 inhibition assay	96
Figure 4.1a Test 1 in MMP-1 inhibition assay	96
Figure 4.1b Test 2 in MMP-1 inhibition assay	96
Figure 4.1c Test 3 in MMP-1 inhibition assay	97
Figure 4.1d Test 4 in MMP-1 inhibition assay	97
Figure 4.1e IC <sub>50</sub> of curcumin and selected CMCs against MMP-1	98

Figure 4.2 MMP-2 inhibition assay	99
Figure 4.2a Test 1 in MMP-2 inhibition assay	99
Figure 4.2b Test 2 in MMP-2 inhibition assay	99
Figure 4.2c Test 3 in MMP-2 inhibition assay	100
Figure 4.2d Test 4 in MMP-2 inhibition assay	100
Figure 4.2e IC <sub>50</sub> of curcumin and selected CMCs against MMP-2	101
Figure 4.3 MMP-3 inhibition assay	102
Figure 4.3a Test 1 in MMP-3 inhibition assay	102
Figure 4.3b Test 2 in MMP-3 inhibition assay	102
Figure 4.3c Test 3 in MMP-3 inhibition assay	103
Figure 4.3d Test 4 in MMP-3 inhibition assay	103
Figure 4.3e IC <sub>50</sub> of curcumin and selected CMCs against MMP-3	104
Figure 4.4 MMP-7 inhibition assay	105
Figure 4.4a Test 1 in MMP-7 inhibition assay	105
Figure 4.4b Test 2 in MMP-7 inhibition assay	105
Figure 4.4c Test 3 in MMP-7 inhibition assay	106
Figure 4.4d Test 4 in MMP-7 inhibition assay	106
Figure 4.4e IC <sub>50</sub> of curcumin and selected CMCs against MMP-7	107
Figure 4.5 MMP-8 inhibition assay	108
Figure 4.5a Test 1 in MMP-8 inhibition assay	108
Figure 4.5b Test 2 in MMP-8 inhibition assay	108
Figure 4.5c Test 3 in MMP-8 inhibition assay	109
Figure 4.5d Test 4 in MMP-8 inhibition assay	109

Figure 4.5e IC <sub>50</sub> of curcumin and selected CMCs against MMP-8	110
Figure 4.6 MMP-9 inhibition assay	111
Figure 4.6a Test 1 in MMP-9 inhibition assay	111
Figure 4.6b Test 2 in MMP-9 inhibition assay	111
Figure 4.6c Test 3 in MMP-9 inhibition assay	112
Figure 4.6d IC <sub>50</sub> of curcumin and selected CMCs against MMP-9	113
Figure 4.7 MMP-12 inhibition assay	114
Figure 4.7a Test 1 in MMP-12 inhibition assay	114
Figure 4.7b Test 2 in MMP-12 inhibition assay	114
Figure 4.7c Test 3 in MMP-12 inhibition assay	115
Figure 4.7d Test 4 in MMP-12 inhibition assay	115
Figure 4.7e IC <sub>50</sub> of curcumin and selected CMCs against MMP-12	116
Figure 4.8 MMP-13 inhibition assay	117
Figure 4.8a Test 1 in MMP-13 inhibition assay	117
Figure 4.8b Test 2 in MMP-13 inhibition assay	117
Figure 4.8c Test 3 in MMP-13 inhibition assay	118
Figure 4.8d IC <sub>50</sub> of curcumin and selected CMCs against MMP-13	119
Figure 4.9 MMP-14 inhibition assay	120
Figure 4.9a Test 1 in MMP-14 inhibition assay	120
Figure 4.9b Test 2 in MMP-14 inhibition assay	120
Figure 4.9c Test 3 in MMP-14 inhibition assay	121
Figure 4.9d Test 4 in MMP-14 inhibition assay	121
Figure 4.9e IC <sub>50</sub> of curcumin and selected CMCs against MMP-14	122

Figure 4.10 IC <sub>50</sub> of newer CMCs against MMP-9	125
Figure 5.1 Spectra for pH titration	133
Figure 5.1a Spectra for pH titration of curcumin	133
Figure 5.1b Spectra for pH titration of curcumin intermediate	133
Figure 5.1c Spectra for pH titration of CMC2.5	134
Figure 5.1d Spectra for pH titration of CMC2.24	134
Figure 5.2 Fittings at selected wavelengths for curcumin, CMC2.5 and CMC2.24	135
Figure 5.2a Fitting of curcumin, reading up at pH 7.2: 380, 390, 400, 425nm	135
Figure 5.2b Fitting of curcumin, reading down at pH 11.0: 460, 482, 495, 515, 530, 550, 570nm	135
Figure 5.2c Fitting of curcumin intermediate, reading down at pH 7.2: 448,460, 470, 490, 500, 515, 530, 550nm	136
Figure 5.2d Fitting of CMC2.5: reading up at pH 3.0: 329, 344, 446nm	136
Figure 5.2e Fitting of CMC2.24, open circle, 329nm, filled circle, 356nm; open square, 428nm	137
Figure 5.3 Calculated spectra for curcumin, curcumin intermediate, CMC2.5 and CMC2.24	137
Figure 5.3a Calculated spectra for curcumin, reading down at 470nm: D <sup>3-</sup> , HD <sup>2-</sup> , H <sub>2</sub> D <sup>-</sup> , H <sub>3</sub> D	137
Figure 5.3b Calculated spectra for curcumin intermediate, reading down at 470nm: D <sup>3-</sup> , HD <sup>2-</sup> , H <sub>2</sub> D <sup>-</sup> , H <sub>3</sub> D	138
Figure 5.3c Calculated spectra for CMC2.5, reading down at 440nm: H <sub>3</sub> D, HD <sup>2-</sup> , D <sup>3-</sup>	138
Figure 5.3d Calculated spectra for CMC2.24, reading down at 440 nm: H <sub>3</sub> D, H <sub>2</sub> D <sup>-</sup> , HD <sup>2-</sup> , D <sup>3-</sup>	139
Figure 5.4 Time-dependent spectra for curcumin and CMC2.5	139



Figure 5.4a Spectra of curcumin, pH 8.94, through the isosbestic point at 448.71nm, 2sec intervals to 24sec; darker, displaced lines, 40, 60, 80, 100sec	139
Figure 5.4b Spectra of curcumin in 88 $\mu$ M BSA, 1h intervals	140
Figure 5.4c Spectra of CMC 2.5, pH 7.00, 5sec intervals	140
Figure 5.5 Spectra for zinc binding study for curcumin, CMC2.5 and CMC2.24	142
Figure 5.5a Zinc binding of curcumin	142
Figure 5.5b Zinc binding of CMC2.5	142
Figure 5.5c Zinc binding of CMC2.24	143
Figure 5.6 Fitted spectra for zinc binding for CMC2.5 and CMC2.24 at selected wavelengths	143
Figure 5.6a Fitted zinc binding of CMC2.5 at 413nm	143
Figure 5.6b Fitted zinc binding of CMC2.24 at 329nm, open; 415nm, filled	144
Figure 5.7 Spectra for bovine serum albumin binding study	146
Figure 5.7a Bovine serum albumin binding of curcumin	146
Figure 5.7b Bovine serum albumin binding of CMC2.24 (14.5mM)	146
Figure 5.7c Bovine serum albumin (13.0 $\mu$ M) binding of CMC2.24	147
Figure 5.7d Bovine serum albumin (6.0 $\mu$ M) binding of CMC2.24	147
Figure 5.8 Fitted spectra for BSA binding at selected wavelengths	148
Figure 5.8a Fitted spectra for BSA binding of curcumin at 500nm, 525nm	148
Figure 5.8b Fitted spectra for BSA binding of CMC2.24, 330nm, 421nm	148
Figure 5.9 $\beta$ -galactosidase inhibition of curcumin and CMC2.24	152
Figure 6.1 <i>In vitro</i> lipophilicity of doxycycline, CMT-3, curcumin and CMC2.24	161
Figure 6.1a Lipophilicity study of doxycycline	161
Figure 6.1b Lipophilicity study of CMT-3	161

Figure 6.1c Lipophilicity study of curcumin	161
Figure 6.1d Lipophilicity study of CMC2.24	161
Figure 6.2 HPLC spectra of rat serum samples after oral dosages of curcumin and CMC2.24	162
Figure 6.2a Blood sample from rats with no administration of curcumin or CMC2.24	162
Figure 6.2b Blood sample from rats with oral administration of curcumin, 2h after dosage	162
Figure 6.2c Blood sample from rats with oral administration of curcumin, 6h after dosage	163
Figure 6.2d Blood sample from rats with oral administration of CMC2.24, 2h after dosage	163
Figure 6.2e Blood sample from rats with oral administration of CMC2.24, 6h after dosage	163
Figure 6.3 Standard curves for curcumin, CMC2.24 and doxycycline	166
Figure 6.3a Curcumin standard curve	166
Figure 6.3b CMC2.24 standard curve	166
Figure 6.3c Doxycycline standard curve	166
Figure 6.4 <i>In vivo</i> pharmacokinetics of curcumin, CMC2.24 and doxycycline	169
Figure 6.4a <i>In vivo</i> pharmacokinetics of curcumin in rat serum at 0.5h, 1h, 2h and 4h	169
Figure 6.4b <i>In vivo</i> pharmacokinetics of CMC2.24 in rat serum at 0.5h, 1h, 2h and 4h	169
Figure 6.4c <i>In vivo</i> pharmacokinetics of doxycycline in rat serum at 0.5h, 1h, 2h and 4h	169
Figure 6.5 HPLC analysis of rat serum samples by <i>i.v.</i> route of curcumin and CMC2.24	170
Figure 6.5a Blood sample from rats with no curcumin or CMC2.24	170
Figure 6.5b Blood sample from rats with <i>i.v.</i> administration of curcumin, 5min	170
Figure 6.5c Blood sample from rats with <i>i.v.</i> administration of curcumin, 10min	171
Figure 6.5d Blood sample from rats with <i>i.v.</i> administration of curcumin, 20min	171
Figure 6.5e Blood sample from rats with <i>i.v.</i> administration of CMC2.24, 5min	171
Figure 6.5f Blood sample from rats with <i>i.v.</i> administration of CMC2.24, 10min	171

Figure 6.5g Blood sample from rats with i.v. administration of CMC2.24, 20min	172
Figure 6.6 <i>In vivo</i> pharmacokinetics of curcumin and CMC2.24 within 20min	174
Figure 6.6a <i>In vivo</i> pharmacokinetics of curcumin in rat serum at 5min, 10min and 20min	174
Figure 6.6b <i>In vivo</i> pharmacokinetics of CMC2.24 in rat serum at 5min, 10min and 20min	174
Figure 6.7 <i>In vivo</i> pharmacokinetics of curcumin and CMC2.24 in rat serum within 4h	176
Figure 6.7a <i>In vivo</i> pharmacokinetics of curcumin in rat serum within 4h	176
Figure 6.7b <i>In vivo</i> pharmacokinetics of CMC2.24 in rat serum within 4h	176
Figure 6.8 Comparison of curcumin and CMC2.24 in rat serum	177
Figure 6.9 Comparison of curcumin and CMC2.24 in rat blood pellets within 20min	179
Figure 6.10 <i>In vivo</i> pharmacokinetics of curcumin and CMC2.24 in rat organs	181
Figure 6.10a <i>In vivo</i> pharmacokinetics of curcumin in rat organs including liver, heart, spleen, kidney, lung and brain at 1h after <i>i.v.</i> injection	181
Figure 6.10b <i>In vivo</i> pharmacokinetics of curcumin in rat organs including liver, heart, spleen, kidney, lung and brain at 1h after <i>i.v.</i> injection	181
Figure 6.11 Comparison of the distribution of curcumin and CMC2.24 in rat organs	183
Figure 7.1 General procedures of X-ray crystallography	189
Figure 7.2 Crystal structure of MMP-8 catalytic domain with Batimastat	190
Figure 7.3 Structure of Batimastat (BB-94)	191
Figure 7.4 Primary structure of MMP-8 catalytic domain	193
Figure 7.5 SDS gel of MMP-8 catalytic subunit after nickel column purification	194
Figure 7.6 SDS gel of MMP-8 catalytic subunit after Q-Sepharose purification	194
Figure 7.7 Circular Dichroism determination of MMP-8 refolding after dialysis	196
Figure 7.8 SDS gel of MMP-8 after dialysis	196

Figure 7.9 MALDI determination of MMP-8 after dialysis	197
Figure 7.10 Gel filtration after dialysis	197
Figure 7.11 Density map from the X-ray data collection without any inhibitor	199
Figure 7.12 Density map from the X-ray data collection with an inhibitor CMC2.24	199
Figure 8.1 Illustration of the attenuating effect of curcumin and CMC2.24 on MMP-9 levels in conditioned media from human monocytes stimulated by LPS in cell culture	211
Figure 8.1a The effect of curcumin on MMP-9 levels	211
Figure 8.1b The effect of CMC2.24 on MMP-9 levels	211
Figure 8.2 CMC2.24 (2 and 5 $\mu\text{M}$ ) inhibits the activities of inflammatory mediators (cytokine levels) TNF- $\alpha$ and IL-1 $\beta$ produced by human monocytes stimulated with <i>P.gingivalis</i> LPS (50ng/ml). Each bar represents the mean of 3 cultures $\pm$ S.E.M.	211
Figure 8.2a CMC2.24 (2 and 5 $\mu\text{M}$ ) inhibits the activities of TNF- $\alpha$	212
Figure 8.2b CMC2.24 (2 and 5 $\mu\text{M}$ ) inhibits the activities of IL-1 $\beta$	212
Figure 8.3 Effect of CMC2.23 and CMC2.24 ( $\mu\text{M}$ ) against prostate (PC-3) and pancreatic (MiaPaCa) cancer cells in culture	213
Figure 8.3a Effect of CMC2.23 and CMC2.24 ( $\mu\text{M}$ ) against prostate (PC-3) cancer cells in culture	213
Figure 8.3b Effect of CMC2.23 and CMC2.24 ( $\mu\text{M}$ ) against pancreatic (MiaPaCa) cancer cells in culture	213
Figure 8.4 Analysis of $^{35}\text{SO}_4^{2-}$ release following treatment with curcumin and CMCs (10 $\mu\text{M}$ ) after 72 Hours	215
Figure 8.5 Effect of CMC2.24 on levels of MMP-9 secreted by peritoneal macrophages from diabetic rats	217

Figure 8.5a Effect of CMC2.24 on levels of MMP-9 secreted by peritoneal macrophages from diabetic rats	217
Figure 8.5b Densitometric scanning of CMC2.24 on levels of MMP-9 secreted by peritoneal macrophages from diabetic rats	218
Figure 8.5c Blood glucose levels of normal and diabetic rats	218
Figure 8.6 Chronic wounds	219
Figure 8.7 Proposed mechanism of wound healing	219
Figure 8.8 Clinical appearances of wound healing studies	221
Figure 8.8a Standardized skin wounds in normal and diabetic rats	221
Figure 8.8b Healing (% reduction) of skin wounds in normal, diabetic, and diabetic rats treated with vehicle alone or with topical or systemic administration of CMC2.24	221
Figure 8.9 Normal lung histology	222
Figure 8.10 Histology of lung tissue in the mouse model of ARDS	223
Figure 8.11 ARDS treatment with curcumin, CMC2.5 and CMC2.24	224
Figure 8.12 Pre-clinical developments of novel curcumin analogues as inhibitors of MMPs	227

## List of Tables

Table 2.1 Matrix metalloproteinases (MMPs) and their principle substrates	12
Table 2.2 Classification of tissue inhibitor of metalloproteinases (TIMPs)	22
Table 2.3 <i>In vitro</i> potency of tetracycline and doxycycline	26
Table 2.4 <i>In vitro</i> potency of Batimastat and Marimastat	28
Table 2.5 Antibiotic activity of thermorubin	30
Table 2.6 <i>In vitro</i> potency of BAM1.11 and BAM1.12	31
Table 2.7 Serum concentrations of curcumin by oral administration	36
Table 3.1 Symmetric curcumin analogues 1-5 by side chain modification	61
Table 3.2 Symmetric curcumin analogues 6-18	65
Table 3.3 Symmetric curcumin analogues 22-24	70
Table 4.1 <i>In vitro</i> IC <sub>50</sub> (μM) of curcumin and the CMCs against MMP-9	92
Table 4.2 IC <sub>50</sub> of curcumin and CMCs against MMP-1	98
Table 4.3 IC <sub>50</sub> of curcumin and selected CMCs against MMP-2	101
Table 4.4 IC <sub>50</sub> of curcumin and selected CMCs against MMP-3	104
Table 4.5 IC <sub>50</sub> of curcumin and selected CMCs against MMP-7	107
Table 4.6 IC <sub>50</sub> of curcumin and selected CMCs against MMP-8	110
Table 4.7 IC <sub>50</sub> of curcumin and selected CMCs against MMP-9	113
Table 4.8 IC <sub>50</sub> of curcumin and selected CMCs against MMP-12	116
Table 4.9 IC <sub>50</sub> of curcumin and selected CMCs against MMP-13	119
Table 4.10 IC <sub>50</sub> of curcumin and selected CMCs against MMP-14	122
Table 4.11 <i>In vitro</i> potency of curcumin and selected chemically-modified curcumins (CMCs)	123

Table 4.12 IC <sub>50</sub> of newer CMCs against MMP-9	124
Table 5.1 pK <sub>a</sub> of curcumin, CMC2.5 and CMC2.24	132
Table 5.2 Minimum inhibitory concentrations (MIC) in µg/mL of curcumin and CMCs	150
Table 5.3 β-galactosidase inhibition of curcumin and CMC2.24	151
Table 6.1 Standard curves for curcumin, CMC2.24 and doxycycline	165
Table 6.1a Standard curve for curcumin at concentrations at 1 µM, 5 µM, 10 µM and 50 µM	165
Table 6.1b Standard curve for CMC2.24 at concentrations at 1 µM, 5 µM, 10 µM and 50 µM	165
Table 6.1c Standard curve for doxycycline at concentrations at 1 µM, 5 µM, 10 µM and 50 µM	165
Table 6.2 <i>In vivo</i> pharmacokinetics of curcumin, CMC2.24 and doxycycline	168
Table 6.2a <i>In vivo</i> pharmacokinetics of curcumin in rat serum at 0.5h, 1h, 2h and 4h	168
Table 6.2b <i>In vivo</i> pharmacokinetics of CMC2.24 in rat serum at 0.5h, 1h, 2h and 4h	168
Table 6.2c <i>In vivo</i> pharmacokinetics of doxycycline in rat serum at 0.5h, 1h, 2h and 4h	168
Table 6.3 <i>In vivo</i> pharmacokinetics of curcumin and CMC2.24 in 20min	173
Table 6.3a <i>In vivo</i> pharmacokinetics of curcumin in rat serum at 5min, 10min and 20min	173
Table 6.3b <i>In vivo</i> pharmacokinetics of CMC2.24 in rat serum at 5min, 10min and 20min	173
Table 6.4 Summary of concentrations of curcumin and CMC2.24 in rat serum	175
Table 6.5 <i>In vivo</i> pharmacokinetics of curcumin and CMC2.24 in rat blood pellets	178
Table 6.5a <i>In vivo</i> pharmacokinetics of curcumin and CMC2.24 in rat blood pellets at 5min, 10min and 20min	178
Table 6.5b Comparison of curcumin and CMC2.24 in rat blood pellets at 5min, 10min and 20min	178
Table 6.6 <i>In vivo</i> pharmacokinetics of curcumin in rat organs	180

Table 6.6a <i>In vivo</i> pharmacokinetics of curcumin in rat organs including liver, heart, spleen, kidney, lung and brain at 1h after <i>i.v.</i> injection	180
Table 6.6b <i>In vivo</i> pharmacokinetics of CMC2.24 in rat organs including liver, heart, spleen, kidney, lung and brain at 1h after <i>i.v.</i> injection	180
Table 6.7 Comparison of the distribution of curcumin and CMC2.24 in rat organs	182



## List of Schemes

Scheme 3.1 Synthesis of curcumin by Pabon reaction	58
Scheme 3.2 Boron complex and equilibrium for Pabon reaction	59
Scheme 3.3 Synthesis of 1-5 by modified Pabon reaction	60
Scheme 3.4 Synthesis of Compounds 6-18	63
Scheme 3.5 Synthesis of tetrahydro-curcumin analogue 19	66
Scheme 3.6 Synthesis of asymmetric curcumin analogues 20, 21	67
Scheme 3.7 Synthesis of compounds 22-24	69
Scheme 3.8 Synthesis of compounds 25-27	72
Scheme 3.9 Synthesis of compound 28 from compound 27	73
Scheme 3.10 Synthesis of compound 4c	74
Scheme 5.1 Structures of curcumin, CMC2.5 and CMC2.24	131
Scheme 8.1 Structures of curcumin, CMC2.5 and CMC2.24	210

## List of Abbreviations

ADME: Absorption, distribution, metabolism and excretion

APMA: p-Aminophenylmercuric acetate

ARDS: Acute respiratory distress syndrome

BAM: Bis-aryl methane

CD: Circular dichroism

CMC: Chemically-modified curcumin

CMT: Chemically-modified tetracycline

COOT: Crystallographic object oriented toolkit

CRP: C-reactive protein

DMSO: Dimethyl sulfoxide

Dnp: 2,4-Dinitrophenyl

Dpa: N-3-(2, 4-Dinitrophenyl)-L-2,3-diaminopropionyl

ECM: Extracellular matrix

ESI-MS: Electrospray ionization mass spectrometry

FDA: U.S. Food and Drug Administration

FPLC: Fast protein liquid chromatography

HPLC: High performance liquid chromatography

IC<sub>50</sub>: The half maximal inhibitory concentration

IND: Investigational new drug

i.p.: Intraperitoneal

IPTG: Isopropyl β-D-1-thiogalactopyranoside

i.v.: Intravenous

LDL: Low-density lipoprotein

LPS: Lipopolysaccharide

MALDI: Matrix-assisted laser desorption/ionization

MBP: Maltose binding protein

Mca: (7-Methoxycoumarin-4-yl)acetyl

MIC: Minimum inhibitory concentration

MMP: Matrix metalloproteinase

MW: Molecular weight

NMR: Nuclear magnetic resonance

Nval: Norvaline

OA: Osteoarthritis

PBMC: Peripheral blood mononuclear cells

PDB: Protein data bank

PMN: Polymorphonuclear

SAR: Structure-activity relationship

SDS-PAGE: Sodium dodecyl sulfate polyacrylamide gel electrophoresis

STZ: Streptozotocin

TCs: Tetracyclines

TIMPs: Tissue inhibitors of matrix metalloproteinases

TEV: Tobacco etch virus

TLC: Thin-layer chromatography

Xaa: Acidic amino acid

## Preface

*“I have never let my schooling interfere with my education.”*

---Mark Twain, American author

*“Prediction is very difficult, especially about the future.”*

---Niels Henrik David Bohr, Danish physicist

Inspired by my high school teacher’s remark, “Chemistry is a science of finding, representing and creating nature, and it is the one field of making full use of my logical thinking merit.”, I chose chemistry as my major because it is abstruse, challenging and interesting.

I came to Stony Brook for graduate study in the fall of 2007 after I completed my bachelor degree in Jilin University, China. I still remember what my father told me before I boarded the plane from Beijing to New York, “Be confident, capable and committed!”, which guided me through all my days for the past five years.

In the spring of 2008, I began my research project in Dr. Francis Johnson’s lab. I have been focusing on the project *Design, Synthesis and Biological Evaluation of Novel Curcumin Analogues and Bis-Aroyl Methanes as Inhibitors of Matrix Metalloproteinases and Pro-Inflammatory Cytokines for Diseases of Tissue Loss*. This project was derived from the idea of the therapeutical use of thermorubin, a known antibiotic.

Back to 2004, Dr. Johnson came to Center for Biotechnology at Stony Brook University to further pursue the biological efficacy of thermorubin, and then he was introduced to Dr. Lorne M. Golub, the inventor of two FDA approved drugs, non-antibacterial (sub-antimicrobial dose)

tetracyclines. At that time, thermorubin was initially examined as an inhibitor against the proteinase activity of *P. acnes*. However, the antimicrobial activity and poor solubility potentially limit the long-term therapeutic use for the inhibition of cytokines and chemokines and microbial proteinases. Then a series of bis-aroil methanes (BAMs) were synthesized, because of their similar 1,3-diketone moiety related to the tetracyclines. Preliminary data on the BAMs showed great inhibitory interest against pro-inflammatory cytokines and chemokines.

Because curcumin is structurally the vinyl homologue of BAMs, I carried out the design and synthesis of a series chemically-modified curcumins under the mentorship of Drs. Johnson and Golub, with increasing potency as proteinases inhibitors, based on the studies of structure activity relationship (SAR).

While this thesis delves into the discovery and development of novel MMP inhibitors in depth, I hope more general messages can be extracted, that have relevance well beyond this sector. Fortunately in consulting with our research team, especially Drs. Johnson and Golub, I have been on the lookout for what can be leveraged from their experience. Much has been learned, and much more will be learned.

Everything has to come to an end, meanwhile it is a beginning of another story. I would like to quote Dr. Johnson from the symposium to celebrate his 80<sup>th</sup> year birthday, “Be passionate, patient and persistent!” With this in mind, I sincerely hope the scientific discoveries we have made toward the new type of MMP inhibitor will improve human health and well being.

## Acknowledgments

A thesis like this would simply not have been possible without the help and support of many dedicated people.

I really want to express my deepest appreciation to my advisor, Dr. Francis Johnson, for his guidance, support and encouragement of my research. Dr. Johnson is truly a friend, who introduced me to the drug discovery arena. Dr. Johnson has been inspiring me with his enthusiasm, knowledge and expertise all the time. The most important thing I have learned from Dr. Johnson in the past five years is not just the solution of questions, but the way to solve problems: how to think independently and act independently.

I am particularly indebted to Dr. Lorne M. Golub, who guided me throughout the whole project, helped me formulate ideas of research work and provided me continuous helpful feedback. As my “co-advisor”, Dr. Golub shaped my thinking about many of the core issues I confronted in this thesis and my publications, not only providing insight into the biology behind the whole project, but also offering me the opportunities to make decisions on my own and to build my confidence.

I was blessed with an incredibly talented and dedicated research team. I would like to thank Dr. Hsi-Ming Lee, who gave me invaluable assistance on my research work on biochemistry. I am grateful to Dr. Arnold Wishnia, who was tenacious in processing and analyzing the data on biophysics. I would like to thank Dr. Stephen G. Walker, for his assistance in the antimicrobial study. I am also grateful to Dr. Miguel Garcia-Diaz, for his guidance and suggestions through the X-ray crystallography studies. I would like to thank our collaborators in United States, Canada and Brazil for their endeavor to move this project forward.

I am sincerely grateful to my committee members, Dr. Kathlyn A. Parker, Dr. Robert C. Kerber and Dr. Carlos de los Santos for their suggestions and comments on the project. I was fortunate to benefit from the discussions on my research work. I am also sincerely grateful to Department of Chemistry and Department of Pharmacological Sciences at Stony Brook University for the support of my graduate study and research work. I would like to thank Chem-Master International, Inc. for their generous support of chemicals and reagents.

I am beholden to my family, friends and colleagues, who made my graduate study in Stony Brook a truly wonderful journey.

## Vita, Publications and Fields of Study

### Education

Ph.D. in Chemistry, Stony Brook University 2007-2012

B.S. in Chemistry, Jilin University, China 2003-2007

### Publications

1. **Zhang, Y.**; Gu, Y.; Lee, H.M.; Hambarjjeva, E.; Vrankova, K.; Golub, L.M.; Johnson, F. Design, Synthesis and Biological Activity of New Polyenolic Inhibitors of Matrix Metalloproteinases: A Focus on Chemically-Modified Curcumins. *Curr. Med. Chem.*, **2012**, *19*, 4348-4358
2. **Zhang, Y.**; Golub, L.M.; Johnson, F.; Wishnia, A. pKa, Zinc- and Serum Albumin-Binding of Curcumin and Two Novel Biologically-Active Chemically-Modified Curcumins. *Curr. Med. Chem.*, **2012**, *19*, 4367-4375
3. Gao, W.; Cui, D.; Liu, X.; **Zhang, Y.**; Mu, Y. Rare-earth metal bis(alkyl)s supported by a quinolinyl anilido-Imine ligand: synthesis and catalysis on living polymerization of  $\epsilon$ -caprolactone. *Organometallics*, **2008**, *27*, 5889-5893

### Abstracts

1. Clemens, M.; Napolitano, N.; Lee, H.M.; **Zhang, Y.**; Johnson, F.; Golub, L.M.; Gu, Y. Chemically modified curcumin normalizes chronic inflammation in diabetic rats. *J. Dent. Res.*, **2012**, *91*, Special Issue 1526



2. Napolitano, N.; Clemems, M.; Lee, H.M.; **Zhang, Y.**; Johnson, F.; Golub, L.M.; Gu, Y. Novel curcumin derivatives suppress inflammatory mediators in periodontally-relevant cells. *J. Dent. Res.*, **2012**, *91*, Special Issue 1527
3. Elburki, M.; Lee, H.M.; Gupta, N.; Balacky, P.; Zhang, Y.; Johnson, F.; **Zhang, Y.**; Golub, L.M. Chemically-modified curcumins inhibit alveolar bone loss in diabetic rats with periodontitis. *J. Dent. Res.*, **2012**, *91*, Special Issue 1528
4. Yu, H.W.; Zhang, Y.; **Zhang, Y.**; Lee, H.M.; McClain, S.A.; Johnson, F.; Golub, L.M.. A novel chemically-modified curcumin (CMC2.24) improves diabetic wound-healing. *J. Dent. Res.*, **2012**, *91*, Special Issue 1529
5. **Zhang, Y.**; Lee, H.M.; Golub, L.M.; Hambardjjeva, E.; Tong, S.; Pierre, B.; Vrankova, K.; Johnson, F. Synthesis of poly-enolic zinc-binding compounds, new inhibitors of matrix metalloproteinases and inflammatory mediators for periodontitis and other diseases. *Abstracts of papers, 241<sup>st</sup> ACS National Meeting, MEDI 242, Anaheim, CA, March, 2011*
6. Golub, L. M.; Lee, H. M.; Zhang, Y.; London, L.; Grewal, J. S.; Sorsa, T.; Hambardjjeva, E.; **Zhang, Y.**; Johnson, F. New collagenase inhibitors for periodontitis and other diseases of tissue erosion. *International Association for Dental Research, Barcelona, Spain, July, 2010*

### **Fields of Study**

Organic Chemistry: organic compound synthesis, purification and process development

Analytical Chemistry: chemical structure analysis, characterization and determination

Physical Chemistry: acidity, metal and protein binding study

Enzymology: *in vitro* optimization (IC<sub>50</sub>) and *in vivo* validation

Pharmacokinetics: *in vivo* drug distribution and metabolism

Structure Biology: cloning, protein expression and purification, and X-ray crystallography

## Chapter 1. Introduction

Matrix metalloproteinases (MMPs) are a family of more than 25 zinc-containing endopeptidases responsible for tissue degradation. MMP-1, also called Collagenase-1, discovered by Gross *et al.* in 1962, is an animal-derived neutral proteinase that could degrade triple helical collagen fibrils into  $\frac{1}{4}$  and  $\frac{3}{4}$  fragments under physiological conditions of pH and temperature.<sup>1</sup> Subsequently additional MMPs have been found that they can degrade almost all of the constituents of the extracellular matrix (ECM) including collagens and elastins. When the levels of MMPs are excessively expressed under pathological conditions, the degradation by MMPs in the ECM can cause the destruction of collagen, connective tissue and bone tissue.<sup>2,3</sup> Scientists in both academia and industry have long tried to develop compounds to inhibit pathologically excessive MMP activity for human diseases such as periodontal disease, arthritis, postmenopausal osteoporosis, cardiovascular disease and cancer.<sup>4-6</sup> Basal levels of MMPs are essential for normal connective tissue turnover and remodeling under physiological conditions, whereas the excessive inhibition of MMPs can cause various side effects such as musculoskeletal side-effects, including muscle aches, pain, weakness and cramps.<sup>7,8</sup> To date, the only governmental MMP inhibitor drugs available (USA, Canada, Europe) to clinicians for the treatment of periodontitis and chronic skin disease or any other disease are several formulations of sub-antimicrobial doses of doxycycline. This drug arose because of the discovery in 1983 by Golub *et al.* that an old family of drugs, tetracyclines (TCs), could inhibit mammalian collagenases, and several other matrix metalloproteinases (MMPs), and by non-antimicrobial mechanisms.<sup>9-12</sup> Studies have also shown that tetracyclines not only inhibit MMPs including collagenases and gelatinases from a variety cells including macrophages and polymorphonuclear (PMN) leukocytes, but also inhibit the activation of MMPs from their latent forms, and can decrease Pro-MMP synthesis. With this

in mind, beyond the development of two FDA-approved orally available drugs, Periostat® for the treatment of periodontitis and Oracea® for chronic inflammatory skin disease, several chemically-modified tetracyclines were developed, lacking antimicrobial activity but possessing the MMP inhibitory activity.<sup>10-12</sup> CMT-3, one of the chemically-modified tetracyclines, appeared to be the most potent inhibitor against a variety of cytokines and chemokines in addition to MMPs, and was found to be active in a clinical study of Kaposi's sarcoma with anti-angiogenic activity.<sup>13,14</sup> A significant drawback of the tetracyclines as well as the non-antimicrobial chemically-modified tetracyclines is the side-effect of increased photosensitivity at higher doses, which gave the concern in its systematic long-term use.<sup>15,16</sup>

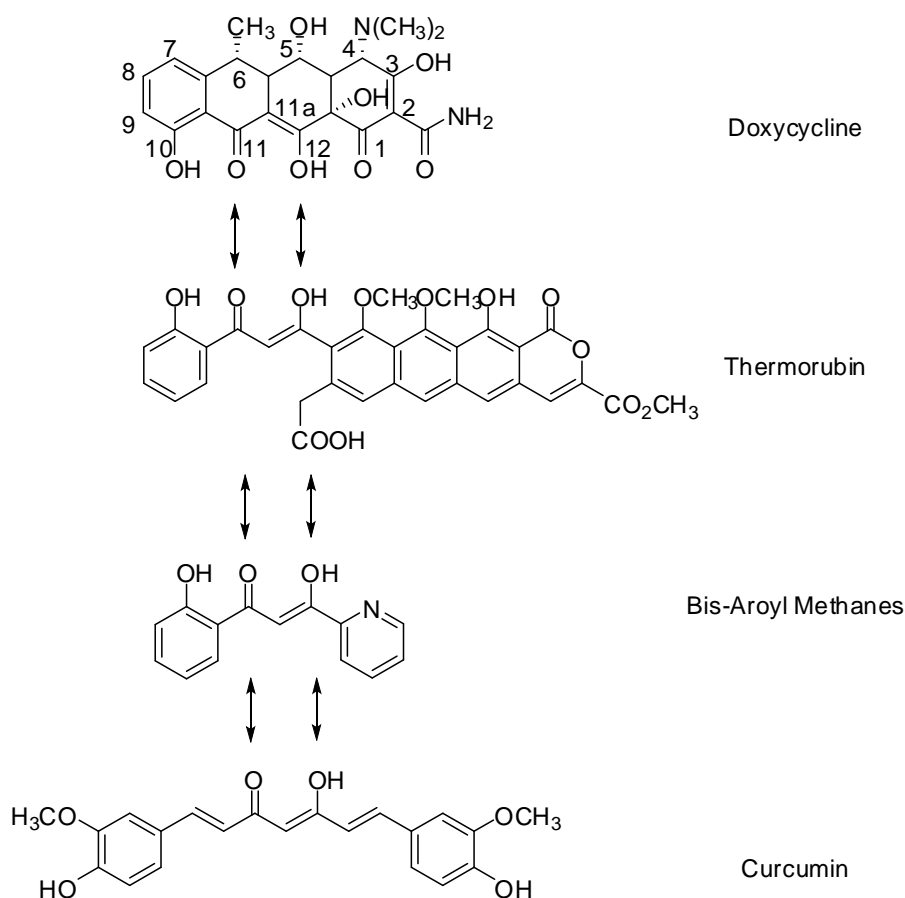


Figure 1.1 Doxycycline, Thermorubin, Bis-Aroyl Methanes and Curcumin

Since the enolic  $\beta$ -diketone moiety of tetracyclines at carbon 11, 11a and 12 is responsible for the inhibition of MMPs through the binding to the zinc atom in the catalytic domain of these enzymes, thermorubin, a natural product isolated from a thermophilic fungus *Thermomyces* in the countryside near Pavia, Italy, was first examined as an MMP inhibitor using the proteinase activity of *P. acnes* as a model because the side chain functionality of thermorubin mimics the linear array of oxygen atoms in tetracycline (Figure 1.1). However, the antimicrobial activity of thermorubin potentially limits the long-term therapeutic use for the inhibition of cytokines and chemokines including MMPs.<sup>17</sup> Bis-aroyl methanes (BAMs) appeared to be a hybrid form of thermorubin and tetracycline since all molecules contain a  $\beta$ -diketone moiety (Figure 1.2). Preliminary studies (unpublished) on the BAMs as inhibitors of MMPs showed reasonable but not improved activity in contrast to the TCs. BAM 1.11 and BAM1.12 each showed *in vitro* IC<sub>50</sub> of 53  $\mu$ M and 60  $\mu$ M against human-derived neutrophil collagenase (MMP-8), and no evidence of toxicity was observed after 5 hour incubation with monocytes. BAM1.11 and BAM1.12 each showed 90% and 100% of inhibition against interleukin-1 $\beta$  (IL-1 $\beta$ ), the pro-inflammatory cytokine up to 50  $\mu$ M in monocytes cells in culture, stimulated by lipopolysaccharide (LPS). However, because of the limitations on the improvement of acidity of these compounds as well as the maintenance of the planarity, we started to focus on a series of bis-vinyl homologues of BAMs, namely chemically-modified curcumins (CMCs).

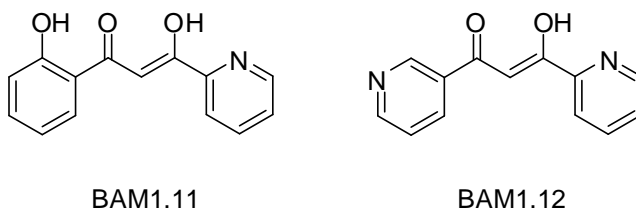


Figure 1.2 Bis-Aroyl Methanes (BAMs)

Curcumin [1,7-bis-(4-hydroxy-3-methoxyphenyl)-1,6-heptadiene-3,5-dione], is the bis-vinyl homologue of BAMs, and also possesses a  $\beta$ -diketone assembly responsible for the metal ion-binding. Curcumin is a natural dietary ingredient of turmeric, derived from the perennial herb *Curcuma longa L.* Curcumin has been used as an herbal treatment for various diseases including pulmonary, gastrointestinal, liver diseases, non-healing wounds and cancer due to its anti-inflammatory, anti-oxidant, anti-angiogenesis, pro-apoptotic and anti-cancer activity.<sup>18-23</sup> Evidence of efficacy has been shown in several *in vitro* and *in vivo* systems. However, the poor oral bioavailability, due to the poor solubility, has limited the therapeutic use of this compound in clinical studies. The current study has focused on a series of enolic bi- and tri-carbonyl compounds, chemically-modified curcumins (CMCs), with the objective of improving the solubility and metal binding characteristics, and additionally improving the biological activity against pro-inflammatory chemokines and cytokines, and principally the MMPs (Figure 1.3).

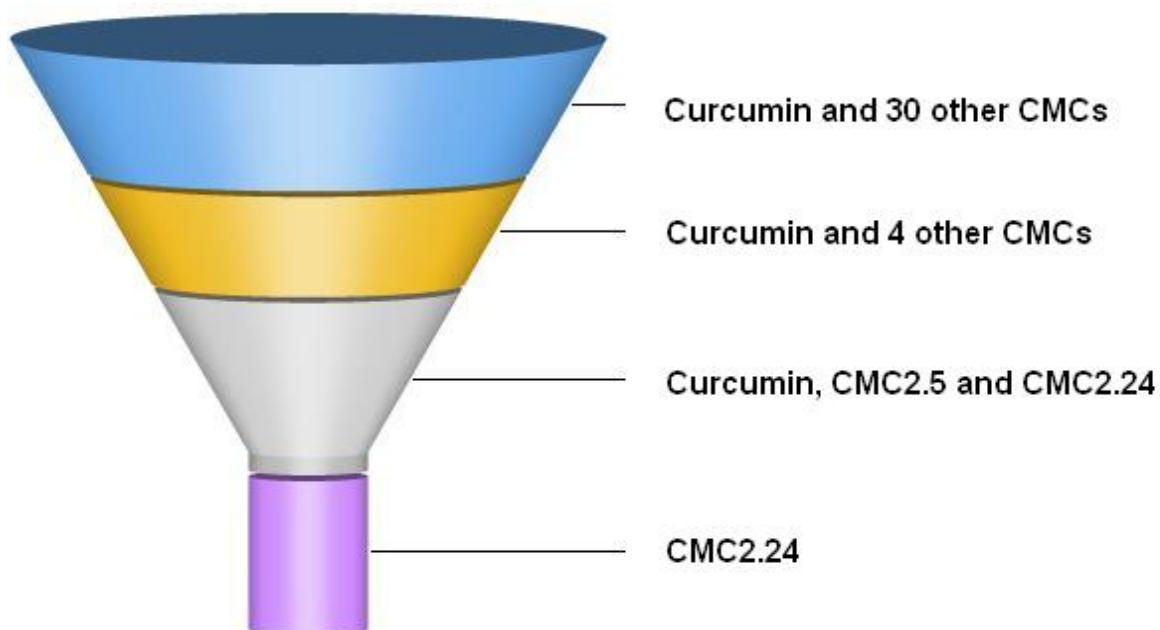


Figure 1.3 Development of novel MMP inhibitors related to curcumin

## References

1. Gross, J.; Lapiere, C.M. Collagenolytic activity in amphibian tissues - a tissue culture assay. *Proc. Natl. Acad. Sci. USA*, **1962**, *48*, 1014-1022
2. Sorsa T.; Tjäderhane L.; Kontinen Y.T.; Lauhrio A.; Salo, T.; Lee, H.M.; Golub, L.M.; Brown, D.L.; Mäntylä P. Matrix metalloproteinases: contribution to pathogenesis, diagnosis and treatment for periodontal inflammation. *Ann. Med.*, **2006**, *38*, 306-321
3. Visse R.; Nagase H. Matrix metalloproteinases and tissue inhibitors of metalloproteinases: structure, function, and biochemistry. *Circ Res.*, **2003**, *92*, 827-839
4. Coussens, L. M.; Fingleton, B.; Matrisian, L. M. Matrix metalloproteinase inhibitors and cancer: trials and tribulations. *Science*, **2002**, *295*, 2387-2392
5. Overall, C. M.; Lopez-Otin, C. Strategies for MMP inhibition in cancer: innovations for the post-trial era. *Nature Rev. Cancer*, **2002**, *2*, 657-672
6. Whittaker, M.; Floyd, C.D.; Brown, P.; Gearing, A.J.H. Design and therapeutic application of matrix metalloproteinase inhibitors. *Chem. Rev.*, **1999**, *99*, 2735-2776.
7. Dove, A. MMP inhibitors: Glimmers of hope amidst clinical failures. *Nature Med.*, **2002**, *8*, 95
8. Peterson, J.T. The importance of estimating the therapeutic index in the development of matrix metalloproteinase inhibitors. *Cardio. Res.*, **2006**, *69*, 677-687
9. Golub, L.M.; Lee, H.M.; Lehrer, G.; Nemiroff, A.; McNamara, T.F.; Kaplan, R.; Ramamurthy, N.S. Minocycline reduces gingival collagenolytic activity during diabetes: Preliminary observations and a proposed new mechanism of action. *J. Periodont. Res.*, **1983**, *18*, 516-526
10. Golub, L.M.; Greenwald, R.A.; Ramamurthy, N.S.; McNamara, T.F.; Rifkin, B.R.

Tetracyclines inhibit connective tissue breakdown: New therapeutic implications for an old family of drugs. *Crit. Revs Oral Biol. Med.*, **1991**, 2, 297-322

11. Golub, L.M.; Wolff, M.; Roberts, S.; Lee, H.M.; Leung, M.; Payonk, G.S. Treating periodontal diseases by blocking tissue-destructive enzymes. *J. Am. Dent. Assoc.*, **1994**, 125,163-169

12. Golub, L.M.; Lee, H.M.; Ryan, M.E.; Giannobile, W.V.; Payne, J.; Sorsa, T. Tetracyclines inhibit connective tissue breakdown by multiple non-antimicrobial mechanisms. *Adv. Dent. Res.*, **1998**, 12, 12-26

13. Dezube, B.J.; Krown, S.E.; Lee, J.Y.; Bauer, K.S.; Aboulafia, D.M. Randomized Phase II trial of matrix metalloproteinase inhibitor COL-3 in AIDS-related Kaposi's sarcoma: an AIDS malignancy consortium study. *Journal of Clinical Oncology*, **2006**, 24, 1389-1394

14. Richards, C.; Pantanowitz, L.; Dezube, B.J. Antimicrobial and non-antimicrobial tetracyclines in human cancer trials. *Pharmacological Research*, **2011**, 63, 151-156

15. Sandberg, S.; Glette, J.; Hopen, G.; Solberg, C.O. Doxycycline induced photodamage to human neutrophils and tryptophan. *Photochem. Photobiol.*, **1984** 39, 43-48

16. Riaz, M.; Pilpel, N. Effects of ultraviolet light on lecithin monolayers in the presence of fluorescein dyes and tetracycline drugs. *J. Pharm. Pharmacol.*, **1983**, 35, 215-218

17. Johnson, F.; Chandra, B.; Iden, C.R.; Naiksatam, P.; Kahen, R.; Okaya, Y.; Lin, S. Y. Thermorubin. 1. Structure studies. *J. Am. Chem. Soc.*, **1980**,102, 5580-5585

18. Bachmeier, B.E.; Mohrenz, I.V.; Mirisola, V.; Schleicher, E.; Romeo, F.; Hohneke, C.; Jochum, M.; Nerlich, A.G.; Pfeffer, U. Curcumin downregulates the inflammatory cytokines CXCL1 and -2 in breast cancer cells via NFkB. *Carcinogenesis*, **2008**, 29, 779-789

19. Kaur, G.; Tirkey, N.; Bharrhan, S.; Chanana, V.; Rishi, P.; Chopra, K. Inhibition of

oxidative stress and cytokine activity by curcumin in amelioration of endotoxin-induced experimental hepatotoxicity. *Clin. Exp. Immunol.*, **2006**, *145*, 313-321

20. Begum, A.N. Jones, M.R.; Lim, G.P.; Morihara, T.; Kim, P.; Heath, D.D.; Rock, C.L.; Pruitt, M.A.; Yang F.; Hudspeth, B.; Hu, S.; Faull, K.F.; Teter, B.; Cole, G.M.; Frautschy, S.A. Curcumin structure-function, bioavailability, and efficacy in models of neuroinflammation and Alzheimer's disease. *J. Pharmacol. Exp. Ther.*, **2008**, *326*, 196-208

21. Banerji, A.; Chakrabarti, J.; Mitra, A.; Chatterjee, A. Effect of curcumin on gelatinase A (MMP-2) activity in B16F10 melanoma cells. *Cancer Lett.*, **2004**, *211*, 235-242

22. Woo, M.S.; Jung, S.H.; Kim, S.Y.; Hyun, J.W.; Ko, K.H.; Kim, W.K.; Kim, H.S. Curcumin suppresses phorbol ester-induced matrix metalloproteinase-9 expression by inhibiting the PKC to MAPK signaling pathways in human astrogloma cells. *Biochem. Biophys. Res. Commun.*, **2005**, *335*, 1017-1025

23. Baum L.; Ng, A. Curcumin interaction with copper and iron suggests one possible mechanism of action in Alzheimer's disease animal models. *J. Alzheimers Dis.*, **2004**, *6*, 367-377



## Chapter 2. Literature review

### Part 1. Matrix metalloproteinases (MMPs)

#### A. History

Matrix metalloproteinases (MMPs) are a group of more than 25 structurally-related zinc-containing enzymes that play an important role in the degradation of the main components of the extracellular matrix (ECM).<sup>1,2</sup> The first collagenolytic enzyme was discovered by Gross *et al.* in 1962.<sup>3</sup> In their study, the enzyme, now known as MMP-1, was recovered from the culture medium of tadpole tail resorbing fragments, and was shown to be able to degrade the triple-helical collagen molecule into two fragments, approximately one quarter distance from the C-terminus under physiological conditions of pH and temperature. Then in 1968, the inactive form of the enzyme, Pro-MMP-1, was first isolated.<sup>4</sup> Both the MMPs and their endogenous inhibitors of the active forms of MMPs, [mainly the tissue inhibitors of the MMPs (designated TIMPs)], play an important role in a variety of physiological and pathological conditions that involve tissue remodeling, ranging from periodontal disease, arthritis, stroke, wound healing to cancer.<sup>5,6</sup> TIMPs were discovered in 1975 by Bauer *et al.* during their tissue culture studies and isolated by Woolley *et al.* from serum.<sup>7,8</sup> Because collagen and the other constituents of the ECM exist throughout the body, and are regulated by MMPs, the development of synthetic inhibitors has been a target for academic groups and the pharmaceutical industry during the past 30 years.<sup>9-13</sup> Principally this thesis concerns the development of a new type of MMP inhibitor that has little toxicity and shows promise in the amelioration of a variety of diseases.

## **B. The Extracellular Matrix (ECM) and Basement Membrane (BM)**

The extracellular matrix (ECM) is defined as the extracellular material around the cells, consisting of fibrous components (e.g., collagens, elastins, fibronectins) and non-fibrous components (e.g., proteoglycans and polysaccharides).<sup>14</sup> The ECM was initially considered as only providing mechanical support to tissue and cells as a static space-filling complex, but studies later showed that the ECM also controls and regulates the behaviors of cells through feedback loops, exhibiting an influence on a variety of cellular events such as adhesion, migration, proliferation, differentiation and survival.<sup>15</sup> Of all of the components in the ECM, collagen plays a very important role in the connective tissue of mammals. There are five common types of collagens, namely type I-V.<sup>16</sup> These can be subject to different types of diseases that cause connective tissue degradation, in systems such as skin, vascular ligature, bone and cartilage. Each fundamental structural unit of collagen molecule (MW about 300 kD) is a long (300 nm), thin (1.5 nm diameter) protein with three coiled subunits woven together in a characteristic right-handed triple helix: two  $\alpha 1$  chains and one  $\alpha 2$  chain (about 1,000 amino acids each).<sup>17</sup> The three  $\alpha$  chains that form the triple helical collagen molecule comprise the structure where Glycine-X-Y is the repeating peptide triplet, in which X and Y can be any amino acid but are frequently proline and 4 (or 3)-hydroxyproline. After the synthesis of collagen molecule in fibroblasts (as pro-collagen), ascorbic acid (vitamin C) plays an important role in regulating the function of propyl hydroxylase during the posttranslational hydroxylation of proline residues.<sup>18</sup> Collagen cross-linking is the ability of collagen fibrils to polymerize with adjacent fibrils, while excessive levels of cross-linking leads to the deterioration of tissue function. Fibronectin is another important protein of the ECM. It is a glycoprotein which plays a prominent role in cell adhesion and migration, because it binds to matrix molecules throughout many of the organ

domains.<sup>19</sup> The basement membrane (BM) acts as a specialized ECM, which connects cells (e.g., epithelial cells, endothelial cells) to adjacent connective tissues.<sup>20</sup> BM functions as a scaffold, where cells can differentiate and migrate, and eventually regulates connective tissue-repair and remodeling processes after injury. MMPs are responsible for the physiological turnover and remodeling of nearly all components of ECM and BM, especially collagen. Unfortunately, pathological levels of these enzymes are associated with a variety of tissue-destructive diseases, including but not limited to aging, osteoarthritis and cancer.<sup>16-20</sup>

### C. Structure and classification

#### 1. Structural features of MMPs

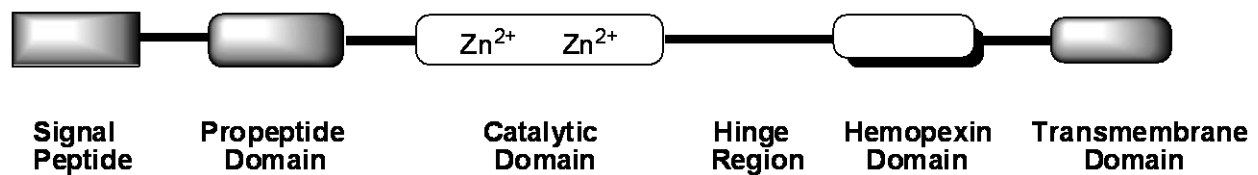


Figure 2.1 General domain structures of MMPs  
(Modified from Whittaker *et al.*<sup>21</sup>)

MMPs exhibit an almost 40% identity in their primary structures, and this includes both the prodomain and the catalytic domain (Figure 2.1).<sup>21</sup> The structural domains of MMPs include a signal peptide, a propeptide domain, a catalytic domain, a hinge region and a hemopexin domain, and a transmembrane domain, the latter being found only in certain types of membrane-type MMPs.<sup>22</sup> The prodomain usually consists of approximately 80 amino acids, and contains a conserved cysteine in the sequence -PRCGXPD- that binds to the zinc atom in the catalytic domain. The N-terminal signal peptide is responsible for the secretion and removal of the proenzyme. The propeptide domain maintains the latency of MMPs before its removal in the MMP activation process. The catalytic domain (approximately 170 residues) contains two  $\alpha$ -

helices and five  $\beta$ -sheets with two zinc atoms, one of which, the catalytic zinc atom, is chelated by three adjacent histidine residues and is responsible for the proteolytic activity of the MMPs.<sup>23,24</sup> All MMPs except MMP-7, MMP-20, MMP-21 contain a hemopexin domain, and a hinge region which connects the latter to the catalytic domain. The function for the hemopexin domain varies with different MMPs. For example, in the collagenases, it is responsible for the TIMP and substrate binding, whereas in gelatinases, it is only responsible for the interaction with TIMPs.<sup>25</sup> The transmembrane domain as well as a furin-activation site is found in only certain MMPs, such as membrane-type MMPs, in which furin is one member of subtilisin-like proprotein convertase family, responsible for the activation of proenzymes.<sup>26</sup> In the ECM, MMPs exist as Pro-MMP forms, which are inactive. There are two steps involved in the MMP extracellular activation related to cysteine switch mechanism: 1) uncovering of the zinc ion from the propeptide in which zinc interacts with cysteine residue through the thiol group in the cysteine complex, and 2) cleavage of the propeptide by other endopeptidases such as membrane-type MMPs. The *in vitro* activation of MMPs also involves the chemical processing whereby the sulfur atom is inactivated by alkylation reagents, disulfides formation, oxidation, or mercury (or silver) salt formation.<sup>27-30</sup>

## **2. Classification of MMPs**

MMP classification is based on the different substrate specificities observed during *in vitro* studies of the individual enzymes. There are five sub-groups of MMPs in total: collagenases, gelatinases, stomelysins, membrane-type, and unclassified. These are listed in Table 2.1.<sup>11-13</sup>

Table 2.1 Matrix metalloproteinases (MMPs) and their principle substrates  
(Modified from references<sup>11-13</sup>)

<b>Group</b>	<b>Enzyme</b>	<b>MMP</b>	<b>Principal Substrates</b>
<b>Collagenases</b>	Fibroblast Collagenase	MMP-1	Fibrillar Collagens, PG Core Protein
	Neutrophil Collagenase	MMP-8	Fibrillar Collagens, $\alpha$ 1 Proteinase Inhibitor (Serpin)
	Collagenase-3	MMP-13	Fibrillar Collagens, PG Core Protein
	Collagenase-4	MMP-18	Collagen I
<b>Gelatinases</b>	Gelatinase A	MMP-2	Gelatin, Elastin, Fibronectin, Collagens IV, V and VI, Cardiac Myocyte Intracellular Contractile Proteins
	Gelatinase B	MMP-9	Gelatin, Elastin, Fibronectin, Collagen I, IV and V
<b>Stromelysins</b>	Stromelysin-1	MMP-3	Fibronectin, Non-Fibrillar Collagens, Laminin
	Stromelysin-2	MMP-10	Fibronectin, Non-Fibrillar Collagens, Laminin
	Stromelysin-3	MMP-11	Gelatin, Fibrillar Collagens, $\alpha$ 1 Proteinase Inhibitor (Serpin)
<b>Membrane-type</b>	MT1-MMP	MMP-14	Pro-MMP-2, Fibrillar Collagens, Gelatin, Elastin, Casein, Fibronectin, Vitronectin, Aggrecan

	MT2-MMP	MMP-15	Pro-MMP-2, Gelatin, Fibronectin, Laminin, Nidogen, Tenascin
	MT3-MMP	MMP-16	Pro-MMP-2, Collagen III, Gelatin
	MT4-MMP	MMP-17	Pro-MMP-2, Gelatin
	MT5-MMP	MMP-24	Pro-MMP-2
	MT6-MMP	MMP-25	Pro-MMP-2
<b>Unclassified</b>	Matrilysin	MMP-7	Fibronectin, Collagen IV and X, Laminin, Aggrecan, Casein, Decorin, Insulin
	Macrophage Metalloelastase	MMP-12	Elastin, Fibronectin, Proteoglycan, $\alpha$ 1-Antitrypsin
	RASI-1	MMP-19	Gelatin
	Enamelysin	MMP-20	Amelogenin, Aggrecan
	CA-MMP	MMP-23	Mca-peptide
	Matrilysin-2	MMP-26	Fibrinogen, Fibronectin, Vitronectin
	Epilysin	MMP-28	Casein

#### ***a. Collagenases***

There are four collagenases (1-4) in the MMP family, namely MMP-1, MMP-8, MMP-13 and MMP-18. These enzymes possess the activity of cleaving native fibrillar triple-helical type I, II and III collagens.<sup>31,32</sup> The Glu-Ile/Leu peptide bond is the cleavage site of the collagen  $\alpha$ -chain, which generates two collagen cleavage fragments, one three times the size of the other on scission.<sup>33</sup>

MMP-1 was the first MMP discovered by Gross *et al.* as mentioned earlier.<sup>3</sup> This exists in two forms, one which is glycosylated having a molecular weight (MW) of 57 kD, and one

unglycosylated having a MW of 52kD.<sup>34</sup> MMP-1 is a constitutive enzyme, and is crucial in diverse physiological processes such as tissue morphogenesis, wound repair and remodeling of collagen extracellular matrix in various physiological and pathological situations. In addition to the role in the turnover of collagen fibrils, MMP-1 is very important in the regulation of cellular behavior for the cleavage of non-matrix substrates and cell surface molecules.<sup>35</sup>

MMP-8, also known as neutrophil collagenase, is an inducible enzyme mainly produced in neutrophils by polymorphonuclear (PMN) leukocytes in bone marrow maturation.<sup>36,37</sup> The glycosylated form of MMP-8 is stored in intracellular granules, where the external stimuli can trigger the degranulation and then release MMP-8. MMP-8 is also found in chondrocytes, odontoblasts, monocyte/macrophage, etc.<sup>38,39</sup> MMP-8 is able to regulate the inflammatory response induced by carcinogens, thus playing a protective role in several pathological conditions including inflammation and cancer, but excessive MMP-8 leads to diseases.<sup>40</sup>

ProMMP-8 can be activated by reactive oxygen species as well as endopeptidases, like other MMPs (e.g., MMP-3, MMP-14), and certain bacterial proteases.<sup>41,42</sup>

MMP-13 was first found in breast cancer cells, and later found to be expressed in other cells including chondrocytes, gingival epithelial cells and osteoblasts.<sup>43,44</sup> MMP-13 is elevated in several pathological conditions of arthritis, periodontitis and various carcinomas.<sup>45</sup> MMP-13 can cleave a variety of components in basement membranes, and shows relatively greater efficiency in cleaving type-II collagen in contrast to types-I and -III.<sup>46</sup> Also MMP-13 appears to be the major collagenase in rats and mice in contrast to other collagenases.<sup>47</sup>

### ***b. Gelatinases***

There are two gelatinases in the MMP family, namely gelatinases A and B, respectively MMP-2 and MMP-9.<sup>48-51</sup> Both of these have head-to-tail repeats located in their catalytic domains, which

are responsible for the binding of gelatin substrate to fibronectin, and which possess the specific activity to further degrade denatured collagens.<sup>52,53</sup> It has been found that TIMPs 1-3 can inhibit both MMP-2 and MMP-9 with different specificities: TIMP-1 is more specific for MMP-9, whereas TIMP-2 is more specific for MMP-2, and TIMP-3 shows almost the same inhibitory activity toward MMP-2 and MMP-9.<sup>54</sup> MMP-2 was first found by Sellers *et al.* in rabbit bone, displaying gelatinase activity, and further confirmed by Liotta *et al.* in their studies on the degradation of type-IV collagen in basement membrane.<sup>55,56</sup> MMP-2 has been found to be expressed in a variety cell lines, and in endothelial cells associated with different types of carcinomas.<sup>34,56</sup> MMP-2 plays a crucial role in the regulation of the ECM, but when the levels of MMP-2 are elevated in cancer cells, increased malignant tumor cell migration has been observed.<sup>11</sup> The activation of MMP-2 is involved in the membrane-type MMPs as well as TIMP-2 on cell surface.<sup>57,58</sup> Pro-MMP-2 has an MW of 72kD, whereas the activated form has an MW of 62kD.

MMP-9 was found in human macrophages by Vartio *et al.* in 1982.<sup>59</sup> It is essential for several remodeling processes such as wound healing, inflammation and cancer metastasis.<sup>60</sup> Compared to MMP-2, MMP-9 does not have extensive degradation activity toward type-I, -II or -III collagen. The secretion of MMP-9 is also observed in PMN neutrophils, from which it is released from tertiary granules under immune response.<sup>61</sup> Human Pro-MMP-9 has a larger MW (92kD) than most of the others because of the extensive N- and O- glycosylation.<sup>51</sup> The active form of MMP-9 ranges from 65 to 82kD due to either N- or C-termini proteolytic degradation.<sup>62,63</sup> Pro-MMP-9 can be activated by human trypsin-2 (serine proteinase) and reactive oxygen species.<sup>38,61</sup> Under the pathological conditions of various inflammatory and malignant diseases (e.g., periodontitis), the production of MMP-9 is elevated. Also several chemokines and cytokines [e.g. tumor



necrosis factor- $\alpha$  (TNF- $\alpha$ ), interleukin-1 (IL-1)] play an important role in the up-stream expression and activation of this enzyme.<sup>61</sup>

### ***c. Stromelysins***

There are three stromelysins in the MMP family, namely Stromelysin-1 (MMP-3), Stromelysin-2 (MMP-10) and Stromelysin-3 (MMP-11). MMP-3 and -10 are responsible for a variety of physiological processes, such as the degradation of specific substrates within the ECM, and activation and inactivation of other proteinases, such as other Pro-MMP members.<sup>64,65</sup> The *in vivo* activation of stromelysins involves serine proteinases, such as neutrophil elastase, chymotrypsin or trypsin.<sup>64</sup> MMP-3 possesses higher efficacy in the proteolysis of specific substrates in contrast to MMP-10.<sup>11</sup> When MMP-3 is activated, it is able to degrade several structural proteins in the ECM, and also able to activate other MMPs like Pro-MMP-1, -8, -13 and -9 in contrast to its weak activity against elastin.<sup>11</sup> MMP-11 is always classified as a stromelysin-like MMP. It is expressed in breast carcinoma cell lines and is responsible for the degradation of the serpins (endogenous serine proteinase inhibitors).<sup>66</sup> There are two different glycosylated forms of Pro-MMP-3 secreted as 60kD and 57kD, the latter being the major constituent.

### ***d. Matrilysin***

MMP-7, also called matrilysin, appears to be the smallest MMP found so far, which only contains the propeptide and catalytic subunits in the domain structure. MMP-7 was first found in rat uterus.<sup>67,68</sup> Because MMP-7 does not have a hemopexin C-terminal domain, the latent form and active form have MWs of only 28kD and 19kD, respectively. MMP-7 is active against a variety of peptide substrates in the ECM, and responsible for the activation of Pro-MMP-1, -2 and -9. MMP-7 has been shown to be involved in early-stage carcinoma development and late-

stage cancer cell invasion (metastasis).<sup>69</sup> MMP-7, as well as MMP-13, is produced by the cancer cells themselves, while other MMPs are mainly expressed by the surrounding cells of the epithelial tumors.

#### *e. Metalloelastase*

MMP-12, macrophage metalloelastase, was found in the macrophages of mice and possesses degradation activity against elastin.<sup>70</sup> The proenzyme of MMP-12 has an MW of 54kD, and the active form has an MW of 22kD after the cleavage of the hemopexin domain from the catalytic domain at the C-terminal end. The activation of Pro-MMP-12 proceeds through one intermediate form of 45kD after the N-terminal processing.<sup>71</sup> The importance of MMP-12 has been shown in alveolar macrophages of lung diseases, such as acute lung injury and chronic inflammatory airway diseases, where it contributes to the exacerbation of these conditions.<sup>72</sup>

#### *f. Membrane-type MMPs*

There are 6 members in the membrane-type MMP (MT-MMP) class, namely, MT1-MMP (MMP-14), MT2-MMP (MMP-15), MT3-MMP (MMP-16), MT4-MMP (MMP-17), MT5-MMP (MMP-24) and MT6-MMP (MMP-25).<sup>73,74</sup> MT-MMPs are covalently linked to the cellular membrane through the transmembrane domain of each enzyme, close to the end of the hemopexin domain at the C-terminal end, whereas MMP-17 and MMP-25 are bound to the cell surface through the domain extension at the C-terminus.<sup>58</sup> Beside the domain structures which are similar to other MMPs, there is a furin-like motif located between the pro-domains and catalytic domains except for the case of MMP-17.<sup>73</sup> In addition to degrading substrates in the ECM, MT-MMPs also play an important role in the activation of other Pro-MMPs. For example, MMP-14 and MMP-16 are responsible for the activation of Pro-MMP-2 in the membrane of cells, while MMP-14 can also activate several other Pro-MMPs including Pro-MMP-8, -9 and -13.<sup>73-75</sup> In

addition, MT-MMPs are able to degrade substrates such as type-I, -II and -III collagens.<sup>73</sup> MMP-14 has a latent form of 63kD in MW and once activated, the MW of this enzyme is reduced to 60kD. The activation of MMP-14 can be achieved by the use of the intracellular neutral proteinase, furin.<sup>76,77</sup>

#### ***g. Others***

Several other MMPs are also known. For example, MMP-19, possessing similar activity to that of stromelysins, is expressed in tissues including the lung, spleen and prostate, and is crucial in the process of angiogenesis.<sup>78,79</sup> MMP-20, enamelysin, was found in tooth enamel, and is responsible for the degradation of ECM substrates such as amelogenin.<sup>80</sup> MMP-28, epilysin, was found in the epidermis, and is also expressed in tissues such as the heart and brain.<sup>81</sup> Others are likely to be found given their extensive involvement in tissue remodeling.

#### **D. MMPs involvement in diseases**

The role of MMPs in tissue remodeling in the ECM comprises mainly the degradation and removal of the extracellular components as mentioned before.<sup>82</sup> When MMPs levels are elevated, they can exacerbate various diseases, and breakdown connective tissue including cartilage and bone.<sup>83</sup> The molecules in the ECM, such as proteoglycans, elastins and fibronectins, are important in cell functions including interactions between various cells and the induction of proteinase activity. As a result, in addition to their regulations of physiological turnover and remodeling, MMPs play an important role in a number of pathological conditions characterized by diseases, including but not limited to arthritis, periodontal disease, postmenopausal osteoporosis, cardiovascular disease and cancer. Because MMPs have a physiological role at low levels, excessive inhibition as a therapeutic goal has been mis-guided; accordingly, “mild”

inhibition, as advocated by Golub *et al.* and Sorsa *et al.* appears to be effective without producing side-effects in human clinical trials.<sup>6,48</sup>

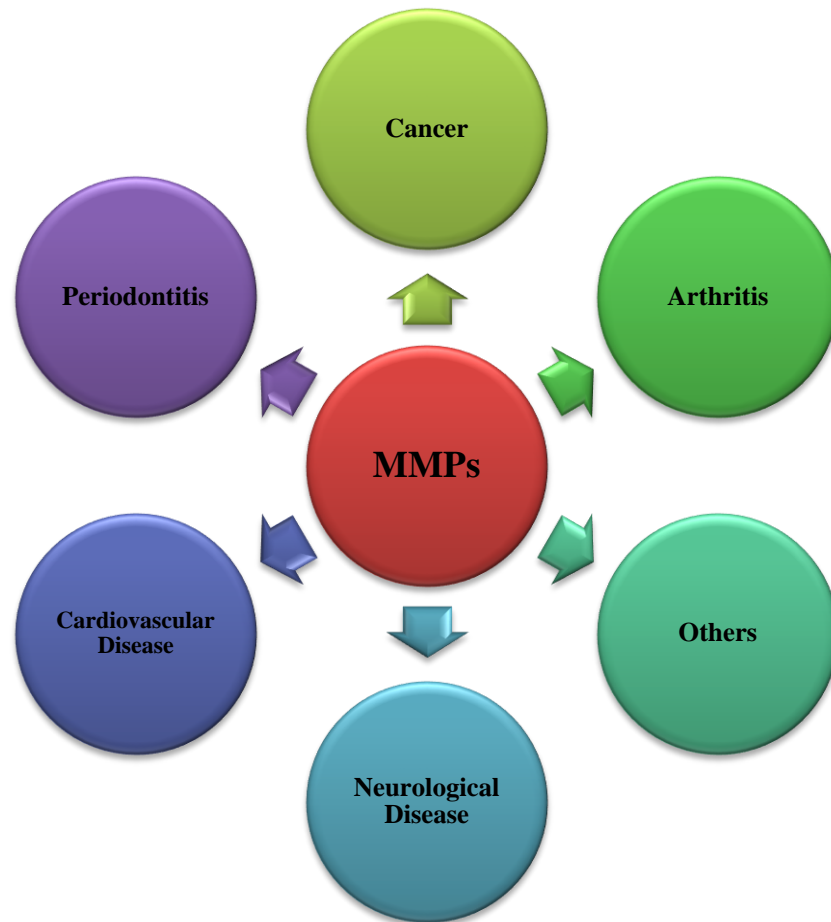


Figure 2.2 MMPs in various diseases

### 1. MMPs in Cancer

The degradation of extracellular substrates and basement membrane by MMPs, together with the regulation of TIMPs, is essential in tumor invasion.<sup>84-86</sup> Elevated levels of MMPs including MMP-1, -2, -3, -7, -9, 10, -11, -13 and -14 have been found in various human tumors including cancers of the breast, colon, lung, skin, pancreas, etc.<sup>87,88</sup> Studies also suggest that tumor cell growth factors, as well as the ECM components of the tumor cells, may also be the target for the MMP degradation. The invasion by tumor cells is believed to be the most critical step in tumor

growth, including mainly tumor cell adhesion (to the ECM), proteolytic degradation of the ECM and migration of tumor cells, followed by the detachment of malignant tumor cells from the ECM.<sup>87,89</sup> For example, MMP-9, in the initial studies, was found to be induced by chemokines and cytokines, and expressed to excessive levels by carcinoma cells.<sup>90</sup> MMP-2 is also responsible for the regulation of laminin-5, an ECM substrate which is essential to tumor cell migration in breast epithelium by the cleavage of residue 578 and initiates the mobility of the tumor cells.<sup>91</sup> MMP-12 was found to be associated with a variety of carcinomas in the degradation of microfibrils related to the elastins.<sup>92,93</sup> MMP-3 and MMP-7 play an important role in cancer cell apoptosis. MMP-3 is responsible for the epithelial cell pro-apoptosis, and MMP-7 is able to induce the apoptosis of epithelial cells by initiating the promoter, Fas ligand, by the cleavage of which, cancer cells are prevented from undergoing apoptosis under the condition of chemotherapeutic agents.<sup>94,95</sup> Angiogenesis, the formation of new blood vessels, plays a crucial role in providing nutrients and oxygen in both physiological and pathological conditions.<sup>96</sup> In pathological condition, the degradation of basement membranes by different types of MMPs provides the prerequisites for angiogenesis, in order to transport the essential nutrients to the cancer cells for tumor growth and metastasis.<sup>97</sup> For example, in addition to its role in the growth of the vascular epithelium, MMP-9 was found to be expressed and induced during the metastasis of the lung and ovarian carcinomas.<sup>98,99</sup>

## **2. MMPs in Periodontitis**

The initiation of an immune response by periodontal bacteria is due to the lipopolysaccharides (LPS), which are the major components of bacterial membranes and lead to periodontal degradation. This induction causes the expression of various chemokines and cytokines, e.g. interleukin-1 (IL-1) and tumour necrosis factor- $\alpha$  (TNF- $\alpha$ ).<sup>100,101</sup> Periodontal degradation was

found in tissues including gingiva, alveolar bone and periodontal ligament. MMP-8, a neutrophil collagenase, and MMP-13, are involved in several physiological and pathological conditions of host response initiation of periodontal disease.<sup>102,103</sup>

### **3. MMPs in Arthritis**

MMPs are the major enzymes that degrade the cartilage matrix (mainly type-II collagen) in osteoarthritis and rheumatoid arthritis.<sup>104</sup> MMP-3 was found to be upregulated in the pathological conditions of arthritis in contrast to other MMPs, because MMP-3 can degrade type-II collagen and aggrecan (the cartilage-specific proteoglycan core protein), and can also activate several other Pro-MMPs including Pro-MMP-1, Pro-MMP-8, Pro-MMP-9, etc.<sup>105</sup>

### **4. MMPs in other diseases**

MMPs are found to be highly expressed at pathological levels in several other diseases including cardiovascular disease, neurological disease (including Alzheimer's disease), and several lung conditions such as acute respiratory distress syndrome (ARDS) and chronic obstructive pulmonary disease (COPD). MMP-9, in particular, is overexpressed by mononuclear phagocytes, and found to be associated with abdominal aortic aneurysm (AAA), the ruptured aneurysm in cardiovascular disease.<sup>106</sup> Both MMP-2 and MMP-9 are induced by amyloid- $\beta$  peptide, the deposit of neuritic plaques, in Alzheimer's disease.<sup>107</sup>

## **E. MMP inhibitors**

### **1. Endogenous inhibitors**

There are generally two types of endogenous inhibitors of MMPs. One is  $\alpha$ 2-macroglobulin, the glycoprotein in plasma, which entraps proteinases including MMPs within the protein complex.

Thus  $\alpha$ 2-macroglobulin has the ability to regulate the MMPs in the plasma and tissue fluids. In

contrast to  $\alpha$ 2-macroglobulin, the other class of MMP inhibitor, namely the tissue inhibitor of metalloproteinases (TIMPs), is more specific and comprises a family of four different proteins, namely TIMP-1, -2, -3 and -4. (Table 2.2)

Table 2.2 Classification of tissue inhibitor of metalloproteinases (TIMPs)  
(Modified from Zitka *et al.*<sup>108</sup>)

	TIMP-1	TIMP-2	TIMP-3	TIMP-4
Inhibited MMPs	All MMPs except MMP-14	All MMPs	MMP-1, -2, -3, -9, -13	MMP-1, -2, -3, -7, -9
MW (kD)	28	21	24	22
Tissues	ovary, bone, uterus	placenta, lung brain	kidney, lung, uterus, brain	brain, heart, muscle
Expression <i>in vitro</i>	inducible	constitutive	inducible	constitutive (restricted)
Localization	diffusible	diffusible	ECM associated	diffusible

The main function of the TIMPs is to control the degradation by the MMPs in the ECM.<sup>82,109</sup>

TIMP-1, -2, -3 and -4 are similar in the structures of their domains. However, they appear to have unique roles due to their substrate specificities.<sup>110</sup> TIMPs bind to MMPs with 1:1

stoichiometry ratio in the MMP-TIMP complex.<sup>11,84</sup> TIMP-1 was first found by Bauer *et al.* as a

protein that inhibits cultured skin fibroblasts in 1975, and later studies showed that TIMP-1

could bind to the hemopexin domains of MMPs including MMP-2 and MMP-9, thus it is

responsible for the regulation of the activity of these enzymes.<sup>111,112</sup> The inhibition mechanism of

TIMPs against MMPs involves the cysteine switch, where MMPs are inactivated by the down-

regulation of disulfide bond formation in cysteines, due to the reductive catalysis of TIMPs.<sup>27</sup> TIMP-3 was found to be expressed in embryo fibroblast cells by Blenis *et al.* in 1983, and appears to be more active in MMP inhibition in comparison to other TIMPs.<sup>113,114</sup> TIMP-4 is expressed abundantly in kidney and colon, and in the inhibition of Pro-MMP-2, it is similar to that of TIMP-2.<sup>115,116</sup>

## **2. Synthetic inhibitors**

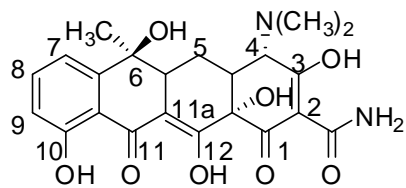
Because MMPs play a key role in the degradation of the ECM and are related to a variety of diseases, the development of MMP inhibitors has been a target of both academic groups and pharmaceutical industry.<sup>117,118</sup> Most of the synthetic inhibitors target the zinc ions in the catalytic domains of MMPs, and some of them showed great potency *in vitro*, but failed in clinical trials due to no evidence of response.<sup>119</sup> The only semi-synthetic MMP inhibitor approved by the FDA is subantimicrobial doses of doxycycline, developed by Golub *et al.*, initially as a treatment for periodontitis, later developed as a treatment for rosacea, a chronic skin disease, under the trade names of Periostat® and Oracea® respectively.<sup>5,6</sup>

### ***a. Tetracyclines***

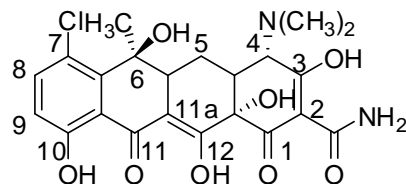
The first tetracycline possessing antibiotic activity was found in the soil organism *Streptomyces aureofaciens* by Duggar in 1948, namely chlortetracycline or Aureomycin. Chlortetracycline showed superior antibiotic activity in contrast to penicillin, the first antibiotic in the history of the world discovered by Fleming in 1928, and chlortetracycline showed antibiotic activity against both Gram-negative and Gram-positive organisms with little toxicity.<sup>120</sup> Since then, natural tetracyclines including chlortetracycline, tetracycline and oxytetracycline have been used in anti-microbial agents for the treatment of various infections.<sup>121</sup> In 1983, Golub *et al.* found that minocycline (later chemically-modified tetracyclines, 1991) could inhibit collagenase



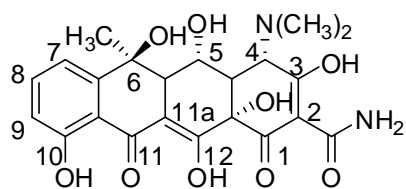
activity in a diabetic rat model, and could also regulate several other MMPs by a non-antimicrobial mechanism of tetracycline in tissue degradation and remodeling.<sup>5,6,48,102,103</sup> These studies confirmed that tetracyclines can inhibit MMPs even after the removal of the dimethylamino group at Carbon-4 which is responsible for the antimicrobial activity. This discovery led to the development of more than 30 chemically-modified tetracyclines (CMTs) and their use in the treatment of various disease including periodontitis, arthritis, osteoporosis, etc., mainly by the regulations of MMPs in tissue remodeling.<sup>122</sup> (Figure 2.3)



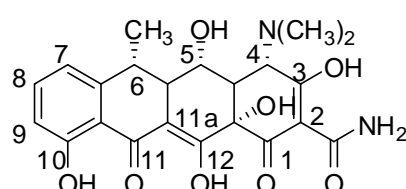
Tetracycline



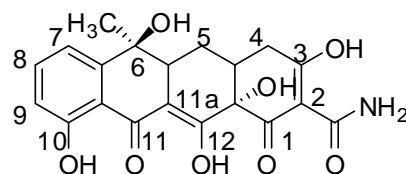
Chlortetracycline



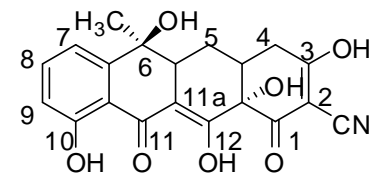
Oxytetracycline



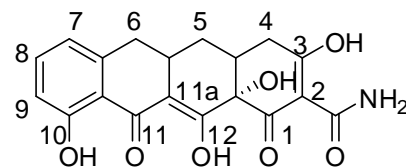
Doxycycline



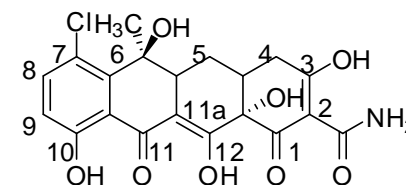
CMT-1



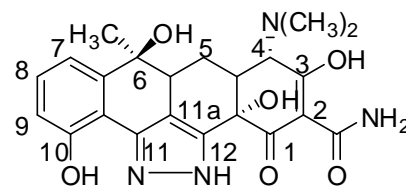
CMT-2



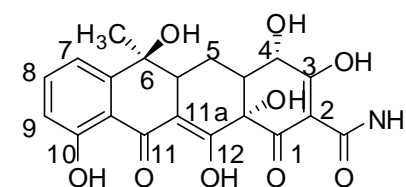
CMT-3



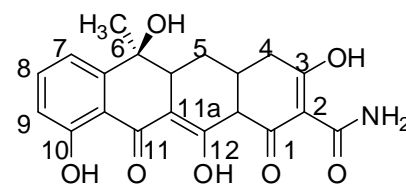
CMT-4



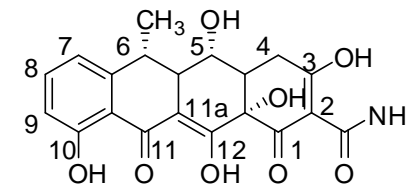
CMT-5



CMT-6



CMT-7



CMT-8

Figure 2.3 Structures of tetracyclines and chemically-modified tetracyclines

Studies were carried out on several tetracyclines (TCs) *in vitro* and *in vivo*. *In vitro* IC<sub>50</sub>s of tetracyclines are summarized below. Of all the TCs and CMTs, doxycycline appeared to be the most potent MMP inhibitor.

Table 2.3 *In vitro* potency of tetracycline and doxycycline  
(Modified from references<sup>122,123</sup>)

	Tetracycline	Doxycycline
MMP-1	>200 μM	15 μM
MMP-8	30 μM	30 μM
MMP-13	<1 μM	10 μM

CMT-1(4-de-dimethylaminotetracycline) was the first chemically-modified non-antibiotic tetracycline to be examined. CMTs-2, -3, -4 can inhibit the polymorphonuclear (PMN) collagenases, whereas CMT-5, the pyrazole derivative of TC (lacking the zinc binding site) was not active. Also, CMTs-1, -3, -6, -7, -8 and doxycycline were found to inhibit bone resorption *in vivo*.<sup>123-125</sup> From the *in vivo* data, it was found that CMT-3 possessed superior inhibitory activity against purified collagenases from tissues including those of the gingiva, osteoblasts and lung cancer cells. CMT-3 was also found to be effective as an anti-angiogenic agent in patients with Kaposi's sarcoma. Tetracyclines were not only the direct inhibitors of MMPs activity, but also the inhibitors of the activation of the MMPs from the proenzyme form.<sup>125,126</sup> Studies also showed TCs could inhibit the expression of MMPs in various cells, including epithelial cells. In this regard, this discovery was translated into the development of two FDA-approved, orally-administered drug substances, namely Periostat® for the treatment of chronic inflammatory oral-bone-destructive periodontitis, and Oracea® for chronic inflammatory skin disease, both

formulated as an “FDA limited sub-antimicrobial” dose of doxycycline. However, a significant side-effect of the tetracyclines and especially their non-antimicrobial congeners such as CMT-3, is increased photosensitivity, particularly at higher doses, and this limits their long-term use.<sup>127,128</sup>

### ***b. Other MMP inhibitors***

Because MMPs are involved in various pathological conditions including cancer, periodontitis, arthritis, etc., the development of MMP inhibitors has been a therapeutic target virtually ever since the first of these was discovered by Gross in 1962. Beside chemically-modified tetracyclines, the earlier generation of MMP inhibitors in 1980s were primarily (but not limited to) hydroxamic acids, possessing the zinc binding group derived from the cleavage site of collagen molecule as the sequence of Ile-Ala-Gly and Leu-Leu-Ala.<sup>129,130</sup> Batimastat (BB-94), developed by British Biotech, showed great potency against MMPs *in vitro* (data shown in Table 2.4), and has been evaluated against tumors including breast carcinoma.<sup>131,132</sup> Marimastat (BB-2516), the second generation hydroxamic acid derivative showed increased activity not only against MMPs but also against certain angiotensin-converting enzymes and enkephalinases including TACE (TNF- $\alpha$  converting enzyme). Marimastat superseded Batimastat in clinical studies for cancer and other diseases. However, the clinical study of Marimastat was negative, and it had no desirable activity against cancer in contrast to the preclinical studies, and caused musculo-skeletal side-effects.<sup>133</sup> The further development of Marimastat therefore was terminated.<sup>134</sup>

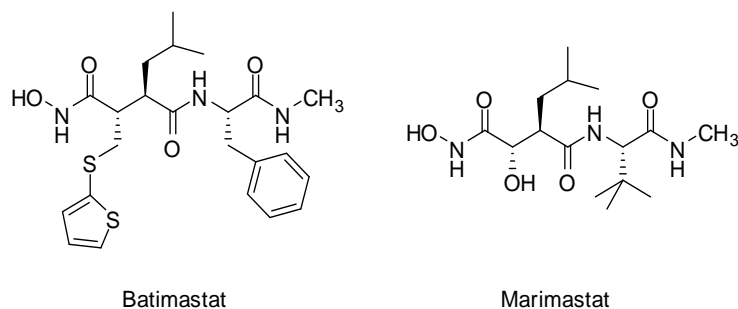


Figure 2.4 Structures of Batimastat and Marimastat

Table 2.4 *In vitro* potency of Batimastat and Marimastat

	Batimastat (BB-94)	Marimastat (BB-2516)
MMP-1	3nM	5nM
MMP-8	10nM	2nM
MMP-2	4nM	6nM
MMP-9	1nM	3nM
MMP-3	Not Determined	200nM
MMP-7	Not Determined	20nM
TACE(TNF- $\alpha$ converting enzyme)	Not Determined	3800nM

Other MMP inhibitors including functional groups such as hydroxamate, thiol, pyrimidine, hydroxypyron and bisphosphonates were developed mainly for cancer treatment, arthritis and cardiovascular disease. However, no other inhibitors, except doxycycline, were approved by the FDA for clinical use.<sup>135-137</sup>

### 3. Structure comparison of doxycycline, thermorubin, bis-aroyl methanes and curcumin

As for tetracyclines, the active site responsible for the inhibition of MMPs is the enolic  $\beta$ -diketone moiety at carbon 11, 11a and 12, by means of the binding to zinc atom in the catalytic domain of these enzymes, based on the studies carried out by Golub *et al.*<sup>5,122</sup> In a search for potential MMP inhibitors, we directed our initial studies to the antibiotic, thermorubin, which has the same  $\beta$ -diketone moiety in its side-chain (present in the nucleus of the tetracyclines).

Thermorubin is an antibiotic substance, first discovered by Craveri *et al.* who isolated it from a thermophilic fungus *Thermomyces antibioticus* (collected in the countryside near Pavia, Italy) which grows best at 50°C rather than the normal temperature of 37°C.<sup>138</sup> Subsequently it was then isolated by a Japanese group who initially gave it the designation BT3-3, until its identity with the Italian product was established. Of the crude fungal extract, thermorubin is the principal product and has a pigment-like character being orange-red in color and rather insoluble in most common solvents. Maximum production occurs at 20-24h in submerged culture (120-200 $\mu$ g/ml) and extraction was accomplished at pH 4.5 with chloroform to give thermorubin as a pure compound containing a molecule of chloroform. The purified material has activity against both Gram-positive and Gram-negative bacteria.<sup>139,140</sup> Against the former, its level of activity approximates that of penicillin or lincomycin, but it has lower activity against Gram-negative bacteria and is not active against yeasts or filamentous fungi. Typical MIC values are given in Table 2.5. Of great interest is the fact that its LD<sub>50</sub> in mice is 300mg/kg body weight when the substance is administered by peritoneal injection. Introduction of 3mg/kg by this route over a three-day period affords 100% protection against an experimental *S. aureus* infection. *In vitro* it is less active in the presence of serum albumin. Oral or subcutaneous administration is ineffective, undoubtedly attributable to the low solubility of the drug in aqueous humour.

Table 2.5 Antibiotic activity of thermorubin

Test Organism	Minimum inhibitory Concentration (MIC) ( $\mu\text{g/mL}$ )
<i>Sarcina lutea</i> ATCC 9341	0.005
<i>Staphylococcus aureus</i> ATCC 6538	0.005
<i>Staphylococcus aureus</i> PV 43 (penicillin resistant)	0.005
<i>Streptococcus pyogenes</i> ATCC 12384	0.05
<i>Streptococcus faecalis</i> ATCC 10541	0.5
<i>Corynebacterium simplex</i> LE B5	0.2
<i>Corynebacterium equi</i> ISM 16111	0.5
<i>Shigella flexneri</i> ATCC 11836	1
<i>Escherichia coli</i> ATCC 10536	2
<i>Klebsiella pneumoniae</i> ATCC 10031	10
<i>Proteus vulgaris</i> ATCC 881	10
<i>Salmonella paratyphi</i> ATCC 9150	20
<i>Pseudomonas aeruginosa</i> ATT 10145	100
<i>Mycobacterium tuberculosis</i> var. <i>hominis</i> H 37 RV	100

Thermorubin was first examined as an inhibitor using the proteinase activity of *P. acnes* as a model because the side chain functionality of thermorubin mimics the linear array of oxygen atoms in tetracycline. The results revealed that thermorubin possesses inhibitory activity against *P. acnes*, a causative factor in acne whereas the MMPs play a pathogenic role. However, the antimicrobial activity and poor solubility of thermorubin potentially limit the long-term

therapeutic use for the inhibition of cytokines and chemokines including MMPs. We then shifted onto a family of bis-aryl methanes (BAMs), which possess the same 1,3-diketone moiety presented in the tetracyclines to which they are distantly related. Preliminary data on the BAMs (unpublished), show that several BAMs are able to inhibit human-derived MMPs *in vitro*. BAM1.11 ( $IC_{50}=53\ \mu\text{M}$ ) and BAM1.12 ( $IC_{50}=60\ \mu\text{M}$ ) showed great inhibitory interest against human-derived neutrophil collagenase (MMP-8). The inhibition of pro-inflammatory cytokines and chemokines such as tumor necrosis factor- $\alpha$  (TNF- $\alpha$ ), interleukin-1 $\beta$  (IL-1 $\beta$ ), monocyte chemotactic protein-1 (MCP-1) and interleukin-6 (IL-6) was also carried out for BAM1.11 and BAM1.12.

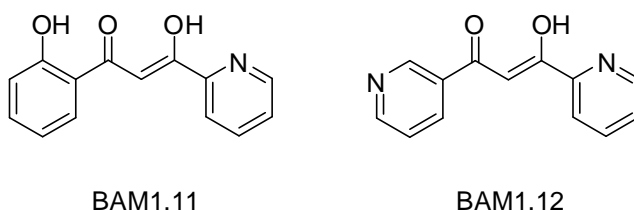


Figure 2.5 Structures of BAM1.11 and BAM 1.12

Table 2.6 *In vitro* potency of BAM1.11 and BAM1.12

Inhibition	BAM1.11	BAM1.12
MMP-8( $IC_{50}$ )	53 $\mu\text{M}$	60 $\mu\text{M}$
Cytotoxicity (Monocytes)	2 $\mu\text{M}$ -0%	2 $\mu\text{M}$ -0%
	25 $\mu\text{M}$ -0%	25 $\mu\text{M}$ -0%
	50 $\mu\text{M}$ -0%	50 $\mu\text{M}$ -0%
TNF- $\alpha$ (%)	2 $\mu\text{M}$ -0%	2 $\mu\text{M}$ -0%
	25 $\mu\text{M}$ -0%	25 $\mu\text{M}$ -26%
	50 $\mu\text{M}$ -0%	50 $\mu\text{M}$ -26%



IL-1 $\beta$ (%)	2 $\mu$ M-0%	2 $\mu$ M-0%
	25 $\mu$ M-13%	25 $\mu$ M-90%
	50 $\mu$ M-100%	50 $\mu$ M-90%
MCP-1 (%)	2 $\mu$ M-68%	2 $\mu$ M-0%
	25 $\mu$ M-70%	25 $\mu$ M-74%
	50 $\mu$ M-73%	50 $\mu$ M-65%
IL-6 (%)	2 $\mu$ M-0%	2 $\mu$ M-10%
	25 $\mu$ M-0%	25 $\mu$ M-10%
	50 $\mu$ M-0%	50 $\mu$ M-38%

However, because of the limitations of the improving of acidity of BAM compounds as well as the maintaining of the planarity (as in the tetracycline), we switched our focus to a series of bis-vinyl homologues of the BAMs, namely the bi-phenolic chemically-modified curcumins (CMCs), which also possess the  $\beta$ -diketone assembly, necessary for zinc binding.

## Part 2. Curcumin

### F. History

Curcumin [1,7-bis-(4-hydroxy-3-methoxyphenyl)-1,6-heptadiene-3,5-dione], is a natural product found in turmeric. The latter substance also known as “curry powder” is used as a flavoring spice, a coloring compound and a therapeutic agent. It is derived from the perennial herb *Curcuma longa L.* that grows in Asian countries particularly India and China. Curcumin was first isolated initially by Vogel *et al.* in 1815, and its structure was elucidated by Lampe *et al.* in

1910.<sup>141</sup> There are two other compounds related to curcumin that also occur in turmeric, namely demethoxycurcumin and bis-demethoxycurcumin. (Figure 2.6)

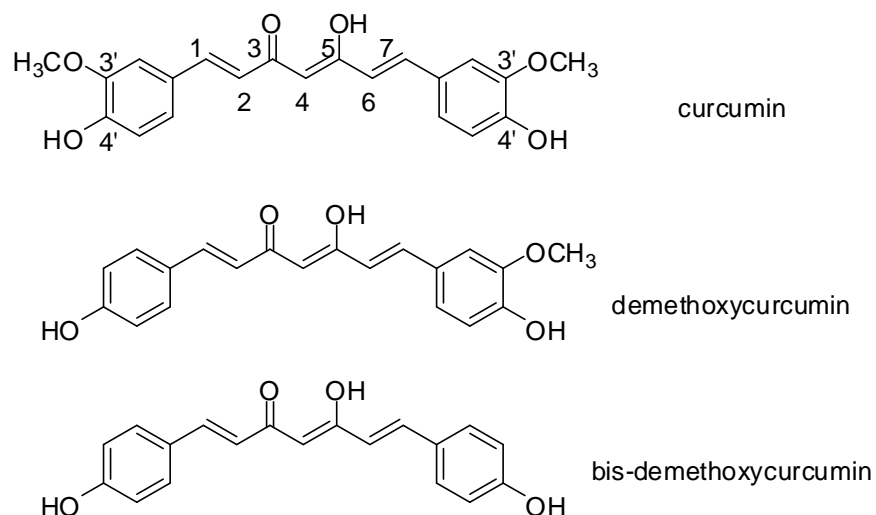


Figure 2.6 Structures of curcumin, demethoxycurcumin and bis-demethoxycurcumin

### G. Therapeutic use of curcumin

Curcumin has been used therapeutically as an herbal medicine for a variety of conditions including pulmonary, gastrointestinal and liver diseases, and also as a remedy for non-healing wounds and in the treatment of cancer.<sup>142-144</sup> Curcumin was found to possess a variety of therapeutic efficacies including the ability to inhibit proliferation and metastasis of various carcinomas, the down-regulation of transcription factors including nuclear factor kappa-light-chain-enhancer of activated B cells (NF- $\kappa$ B), the down-regulation of the expression of chemokines and cytokines including TNF- $\alpha$ , and the suppression of protein kinases and growth factors. (Figure 2.7)

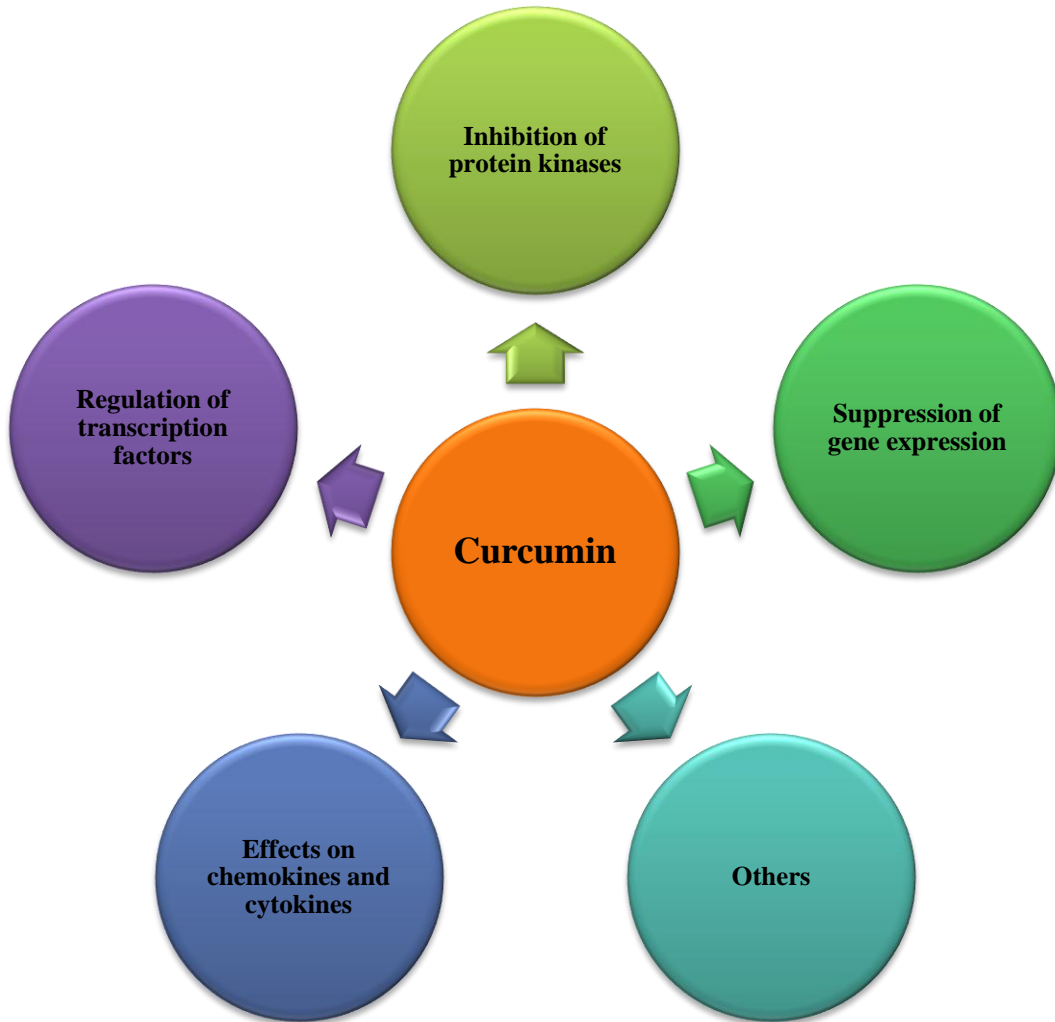


Figure 2.7 Curcumin used in various diseases

### 1. Anti-cancer activity

Curcumin has been evaluated in a variety of human cancer studies, including head and neck cancer, breast cancer, prostate cancer, colon cancer, pancreatic cancer and others.<sup>145-152</sup> The anti-cancer activity of curcumin is mainly due to its role in suppressing the cellular pathways which are responsible for carcinogenesis and the activation of apoptosis in tumor cells. Curcumin is also able to suppress the DNA mutagenesis, caused by UV irradiation.<sup>151</sup> It also inhibits the cyclin D1, the subunit of cyclin-dependent kinases (CDK) 4 (Cdk4) and 6 (Cdk6), that are

regulators of cellular mitosis.<sup>150</sup> Curcumin can also inhibit the P<sub>450</sub> hepatic cytochromes that are involved in both Phase I and Phase II metabolism of xenobiotic substances.<sup>153</sup> Curcumin has also been shown to suppress a variety of transcription factor activation processes, which are responsible for carcinogenesis, including nuclear factor kappa-light-chain-enhancer of activated B cells (NF- $\kappa$ B), cyclooxygenase 2 (COX-2) and tumor necrosis factor (TNF).<sup>149</sup> Both preclinical and clinical studies have already shown the efficacy of curcumin in the treatment of various cancers. In the study carried out by Lal *et al.*, the efficacy of curcumin in the clinical treatment of idiopathic inflammatory orbital pseudotumors is described.<sup>154</sup> The 2-year trial contained eight patients who received an oral dosage of 375mg thrice daily. Four patients out of five who completed the whole study recovered without any recurrence. In addition, no evidence of toxicity was observed.

## **2. Anti-inflammatory activity**

Beside anti-cancer activity, curcumin also possess significant anti-inflammatory effects.<sup>155</sup> It was found to inhibit NF- $\kappa$ B, which regulates the gene expression of a variety of pro-inflammatory cytokines and chemokines including TNF- $\alpha$ , IL-6 and IL-8.<sup>147,149</sup> Curcumin also inhibits the inhibitor kappa B kinase (I $\kappa$ K), which regulates the release and activation (phosphorylation) of NF- $\kappa$ B. Also studies on the inhibition of prostaglandin E2 biosynthesis using curcumin revealed an inhibitory activity toward microsomal prostaglandin E2 synthase-1 enzyme. Above all, curcumin has been used as an anti-inflammatory agent in many pathological conditions including arthritis, Alzheimer's disease and cardiovascular disease.<sup>156-159</sup>

## **3. Anti-oxidant activity**

Curcumin also possesses anti-oxidant activity in both *in vitro* and *in vivo* systems. The phenolic hydroxyl groups in the curcumin molecule are considered to be responsible for its anti-oxidant

activity.<sup>160</sup> The anti-oxidant activity plays an important role in both physiological and pathological conditions including cardiovascular diseases, aging, etc. In cardiovascular diseases, curcumin was found to induce the expression of endogenous anti-oxidants and to suppress the peroxidation of lipids.<sup>161</sup>

## H. Bioavailability of curcumin

Curcumin is reasonably soluble in a variety of organic solvents including alcohols, tetrahydrofuran, dichloromethane, dimethylsulfoxide and dimethylformamide. However, it is very insoluble in aqueous solution including water and physiological buffer.<sup>162</sup> This poor solubility contributes to the poor absorption seen in animal models and human studies, whereas it was found that most of curcumin remained in the stomach and intestine.<sup>163-166</sup> (Table 2.7) When curcumin was administered to humans in doses as high as 12g, a concentration of only 51.2ng/mL was found in serum after 4 hours of dosage.<sup>165</sup>

Table 2.7 Serum concentrations of curcumin by oral administration  
(Modified from references<sup>163-166</sup>)

Species	Oral Dosage	Concentration in Serum
Rat	1g/kg	0.5 µg/mL
Rat	2g/kg	1.4 µg/mL
Human	2g	6.0ng/mL
Human	10g	50.5ng/mL
Human	12g	51.2ng/mL

In addition, the rapid metabolism of curcumin represents a second concern for its bioavailability. Studies have shown that curcumin is metabolized to curcumin glucuronide and curcumin

sulphate by oral administration. Also it undergoes metabolic reduction to dihydrocurcumin, tetrahydrocurcumin and hexahydrocurcuminol. These metabolites were found after intravenous and intraperitoneal administration (Figure 2.8).<sup>167,168</sup> It has still not been determined fully, whether curcumin metabolites are active or not. However, some studies do show that curcumin glucuronides and tetrahydrocurcumin are not as active as curcumin in anti-inflammatory and antiproliferative effects including the suppression of COX-2 activity.<sup>169,170</sup>

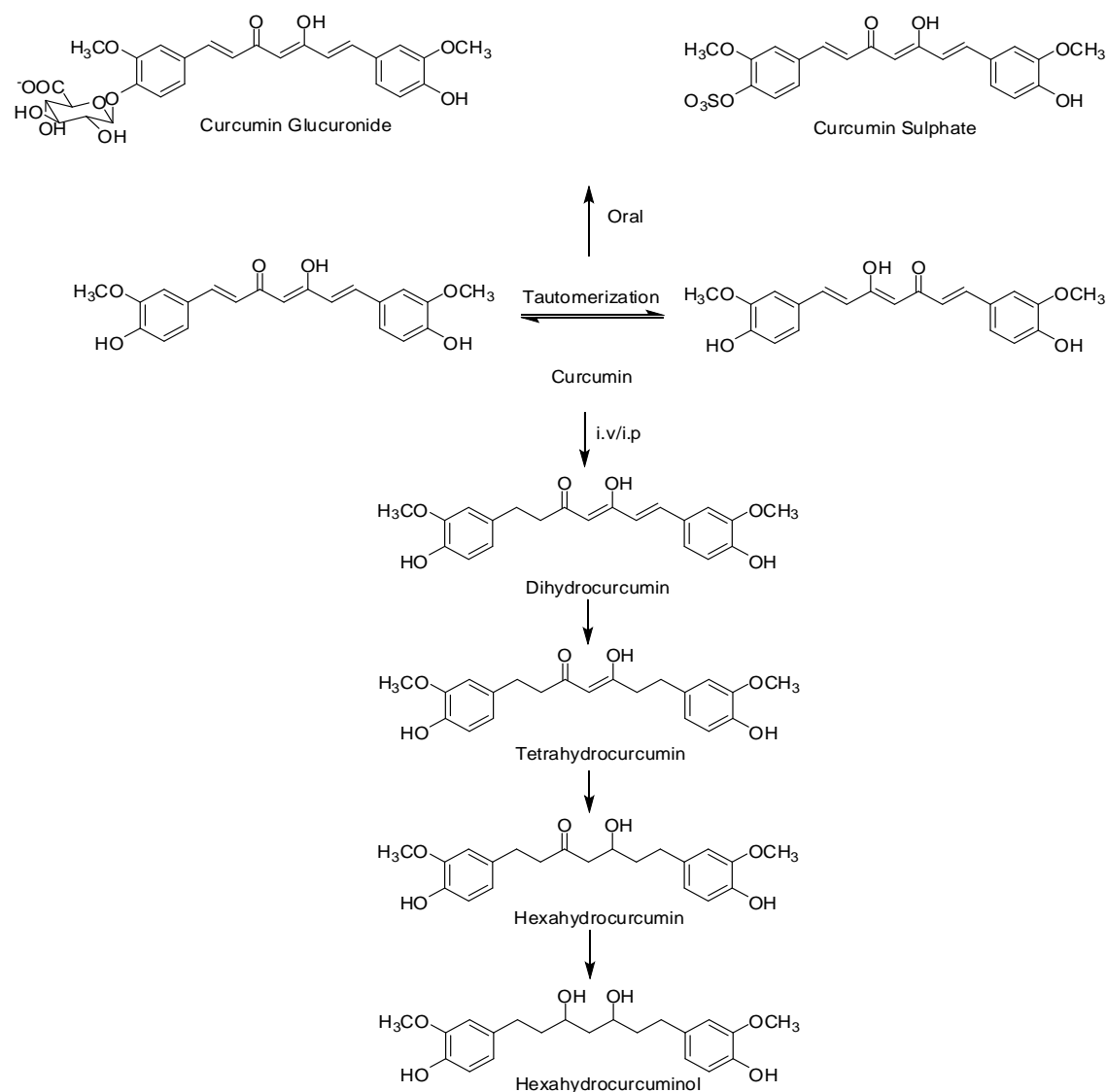


Figure 2.8 List of curcumin metabolites via different administrations

## References

1. Egeblad, M.; Werb, Z. New functions for the matrix metalloproteinases in cancer progression. *Nat. Rev. Cancer*, **2002**, *2*, 161-174
2. Hojilla, C.V.; Mohammed, F.F.; Khokha, R. Matrix metalloproteinases and their tissue inhibitors direct cell fate during cancer development. *Br. J. Cancer*, **2003**, *89*, 1817-1821
3. Gross, J.; Lapiere, C.M. Collagenolytic activity in amphibian tissues: a tissue culture assay. *Proc. Natl. Acad. Sci. USA*, **1962**, *48*, 1014-1022
4. Curry, T.E.; Osteen, K.G. The matrix metalloproteinases system: changes, regulations, and impact throughout the ovarian and uterine reproductive cycle. *Endocr. Rev.*, **2003**, *24*, 429-465
5. Golub, L.M.; Lee, H.M.; Lehrer, G.; Nemiroff, A.; McNamara, T.F.; Kaplan, R.; Ramamurthy, N.S. Minocycline reduces gingival collagenolytic activity during diabetes: Preliminary observations and a proposed new mechanism of action. *J. Periodont. Res.*, **1983**, *18*, 516-526
6. Sorsa T.; Tjäderhane L.; Kontinen Y.T.; Lauhrio A.; Salo, T.; Lee, H.M.; Golub, L.M.; Brown, D.L.; Mäntylä P. Matrix metalloproteinases: contribution to pathogenesis, diagnosis and treatment for periodontal inflammation. *Ann. Med.*, **2006**, *38*, 306-321
7. Bauer, E.A.; Stricklin, G.P.; Jeffrey, J.J.; Eisen, A.Z. Collagenase production by human skin fibroblasts. *Biochem. Biophys. Res. Commun.*, **1975**, *64*, 232-240
8. Wooley, D.E.; Roberts, D.R.; evanson, J.M. Inhibition of human collagenase activity by a small molecular weight serum protein. *Biochem. Biophys. Res. Commun.*, **1975**, *66*, 747-754
9. Coussens, L. M.; Fingleton, B.; Matrisian, L. M. Matrix metalloproteinase inhibitors and cancer: trials and tribulations. *Science*, **2002**, *295*, 2387-2392

10. Overall, C. M.; Lopez-Otin, C. Strategies for MMP inhibition in cancer: innovations for the post-trial era. *Nature Rev. Cancer*, **2002**, *2*, 657-672
11. Visse R.; Nagase H. Matrix metalloproteinases and tissue inhibitors of metalloproteinases: structure, function, and biochemistry. *Circ. Res.*, **2003**, *92*, 827-839
12. Whittaker, M.; Floyd, C. D.; Brown, P.; Gearing, A. J. H. Design and Therapeutic Application of Matrix Metalloproteinase Inhibitors. *Chem. Rev.*, **1999**, *99*, 2735-2776
13. Dove, A. MMP inhibitors: Glimmers of hope amidst clinical failures. *Nature Med.*, **2002**, *8*, 95
14. Alberts, B.; Johnson, A.; Lewis, J.; Raff, M.; Roberts, K.; Walter, P. Molecular biology of the cell. **2002**, fourth edition, Garland Science, 1103-1105
15. Hynes, R.O. The extracellular matrix: not just pretty fibrils. *Science*, **2009**, *326*, 1216-1219
16. Di Lullo, G.A.; Sweeney, S.M.; Korkko, J.; Ala-Kokko, L.; San Antonio, J. D. Mapping the Ligand-binding Sites and Disease-associated Mutations on the Most Abundant Protein in the Human, Type I Collagen. *J. Biol. Chem.*, **2002**, *277*, 4223-4231
17. Hulmes, D. J. Building collagen molecules, fibrils, and suprafibrillar structures. *J. Struct. Biol.*, **2002**, *137*, 2-10
18. Hulmes, D.J. The collagen superfamily-diverse structures and assemblies. *Essays Biochem.*, **1992**, *27*, 49-67
19. Pankov, R.; Yamada, K.M. Fibronectin at a glance. *Journal of Cell Science*, **2002**, *115*, 3861-3863
20. Brown, B.; Lindberg, K.; Reing, J.; Stolz, D.B.; Badylak, S.F. The Basement Membrane Component of Biologic Scaffolds Derived from Extracellular Matrix. *Tissue Engineering*, **2006**,



12, 519-526

21. Whittaker, M.; Floyd, C.D.; Brown, P.; Gearing, A.J. H. Design and Therapeutic Application of Matrix Metalloproteinase Inhibitors. *Chem. Rev.*, **1999**, *99*, 2735-2776
22. Song, F.; Wisithphrom, K.; Zhou, J.; Windsor, L.J. *Frontiers in Bioscience*, **2006**, *11*, 3100 -3120
23. Bode, W.; Gomis-Rüth, F.X.; Stöckler, W. Astacins, serralysins, snake venom and matrix metalloproteinases exhibit identical zinc-binding environments (HEXXHXXGXXH and Met-turn) and topologies and should be grouped into a common family, the 'metzincins'. *FEBS Lett.*, **1993**, *27*, 134-140
24. Stöcker, W.; Grams, F.; Baumann, U.; Reinemer, P.; Gomis-Rüth, F.X.; McKay, D.B.; Bode, W. The metzincins-topological and sequential relations between the astacins, adamalysins, serralysins, and matrixins (collagenases) define a superfamily of zinc-peptidases. *Protein Sci.*, **1995**, *4*, 823-840
25. Allan, J.A.; Docherty, A.J.; Barker, P.J.; Huskisson, N.S.; Reynolds, J.J.; Murphy, G. Binding of gelatinases A and B to type-I collagen and other matrix components. *Biochem. J.*, **1995**, *309*, 299-306
26. Polette, M.; Birembaut, P. Membrane-type metalloproteinases in tumor invasion. *Int. J. Biochem. Cell Biol.*, **1998**, *30*, 1195-1202
27. Springman, E.B.; Angleton, E.L.; Birkedalhansen, H.; Vanwart, H.E. Multiple-modes of activation of latent human fibroblast collagenase-evidence for the role of a Cys-73 active-site zinc complex in latency and a cysteine switch mechanism for activation. *Proc. Natl. Acad. Sci. USA*, **1990**, *87*, 364-368
28. Vanwart, H.E.; Birkedalhansen, H. The cysteine switch-a principle of regulation of

metalloproteinase activity with potential applicability to the entire matrix metalloproteinase gene family. *Proc. Natl. Acad. Sci. USA*, **1990**, *87*, 5578-5582

29. Suzuki, M. Raab, G.; Moses, M.A.; Fernandez, C.A.; Klagsbrun, M. Matrix metalloproteinases-3 releases active heparin-binding EGF-like growth factor by cleavage at a specific juxtamembrane site. *J. Biol. Chem.*, **1997**, *272*, 31730-31737

30. Strongin, A.Y.; Collier, I.; Bannikov, G.; Marmer, B.L.; Grant, G.A. Goldberg, G.I. Mechanism of cell-surface activation of 72-kda type-Iv collagenase-isolation of the activated form of the membrane metalloproteinase. *J. Biol. Chem.*, **1995**, *270*, 5331-5338

31. Kafienah, W.; Bromme, D.; Buttle, D.J.; Croucher, L.J.; Hollander, A.P. Human cathepsin K cleaves native type I and II collagens at the N-terminal end of the triple matrix. *Biochem.*, **1998**, *331*, 727-732

32. Murphy, G.; Allan, J.A.; Willenbrock, F.; Cockett, M.I.; O'Connell, J.P.; Docherty, A.J. The role of the C-terminal domain in collagenase and stromelysin specificity. *J. Biol. Chem.*, **1992**, *267*, 9612-9618

33. Stolow, M.A.; Bauzon, D.D.; Li, J.; Sedgwick, T.; Liang, V.C.; Sang, Q.A.; Shi, Y.B. Identification and characterization of a novel collagenase in *Xenopus laevis*: possible roles during frog development. *Mol. Biol. Cell*, **1996**, *7*, 1471-1483

34. Birkedal-Hansen, H.; Moore, W.G.; Bodden, M.K.; Windsor, L.J.; Birkedal-Hansen, B.; DeCarlo, A.; Engler, J.A. Matrix metalloproteinases: a review. *Crit. Rev. Oral. Biol. Med.*, **1993**, *4*, 197-250

35. Meikle, M.C.; Bord, S.; Hembry, R.M.; Comston, J.; Croucher, P.I.; Reynolds, J.J. Human osteoblasts in culture synthesize collagenase and other matrix metalloproteinases in response to osteotropic hormones and cytokines. *J. Cell Sci.*, **1992**, *103*, 1093-1099

36. Ding, Y.; Uitto, V.J.; Haapasalo, M.; Lounatmaa, K.; Konttinen, Y.T.; Salo, T.; Gienier, D.; Sorsa, T. Membrane components of *Treponema denticola* trigger proteinase release from human polymorphonuclear leukocytes. *J. Dent. Res.*, **1996**, *75*, 1986-1993
37. Sorsa, T.; Tjaderhane, L.; Salo, T. Matrix metalloproteinases (MMPs) in oral diseases. *Oral. Dis.*, **2004**, *10*, 311-318
38. Weiss, S.J.; Peppin, G.; Ortiz, X.; Ragsdale, C.; Test, S.T. Oxidative autoactivation of latent collagenase by human neutrophils. *Science*, **1985**, *227*, 747-749
39. Prikk, K.; Maisi, P.; Pirila, E.; Sepper, R.; Salo, T.; Wahlgren, J.; Sorsa, T. In vivo collagenase-2 (MMP-8) expression by human bronchial epithelial cells and monocytes/macrophages in bronchiectasis. *J. Pathol.*, **2001**, *194*, 232-238
40. Balbin, M.; Fueyo, A.; Tester, A.M.; Pendas, A.M.; Pitiot, A.S.; Astudillo, A.; Overall, C.M.; Shapiro, S.D.; López-Otín, C. Loss of collagenase-2 confers increased skin tumor susceptibility to male mice. *Nat. Genet.*, **2003**, *35*, 252-257
41. Sorsa, T.; Ingman, T.; Suomalainen, K.; Haapasalo, M.; Konttinen, Y.T.; Lindy, O.; Saari, H.; Uitto, V.J. Identification of proteases from periodontopathogenic bacteria as activators of latent human neutrophil and fibroblast-type interstitial collagenases. *Infect. Immun.*, **1992**, *60*, 4491-4495
42. Saari, H.; Suomalainen, K.; Lindy, O.; Konttinen, Y.T.; Sorsa, T. Activation of latent human neutrophil collagenase by reactive oxygen species and serine proteases. *Biochem. Biophys. Res. Commun.*, **1990**, *171*, 979-987
43. Freije, J.M.; Diez-Itza, I.; Balbín, M.; Sánchez, L.M.; Blasco, R.; Tolivia, J.; López-Otín, C. Molecular cloning and expression of collagenase-3, a novel human matrix metalloproteinase produced by breast carcinomas. *J. Biol. Chem.*, **1994**, *269*, 16766-16773.

44. Knauper, V.; Lopez-Otin, C.; Smith, B.; Knight, G.; Murphy, G. Biochemical characterization of human collagenase-3. *J. Biol. Chem.*, **1996**, *271*, 1544-1550
45. Konttinen, Y.T.; Salo, T.; Hanemaaijer, R.; Valleala, H.; Sorsa, T.; Sutinen, M.; Ceponis, A.; Xu, J.W.; Santavirta, S.; Teronen, O.; López-Otín, C. Collagenase-3 (MMP-13) and its activators in rheumatoid arthritis: localization in the pannus-hard tissue junction and inhibition by alendronate. *Matrix Biol.*, **1999**, *18*, 401-412
46. Lindy, O.; Konttinen, Y.T.; Sorsa, T.; Ding, Y.; Santavirta, S.; Ceponis, A.; López-Otín, C. Matrix metalloproteinase 13 (collagenase-3) in human rheumatoid synovium. *Arthritis Rheum.*, **1997**, *40*, 1391-1399
47. Ylipalosaari, M.; Thomas, G.J.; Nystrom, M.; Salhimi, S.; Marshall, J.F.; Huotari, V.; Tervahartiala, T.; Sorsa, T.; Salo, T. Alpha v beta 6 integrin down-regulates the MMP-13 expression in oral squamous cell carcinoma cells. *Exp. Cell Res.*, **2005**, *309*, 273-283
48. Golub, L.M.; Wolff, M.; Roberts, S.; Lee, H.M.; Leung, M.; Payonk, G.S. Treating periodontal diseases by blocking tissue-destructive enzymes. *J. Am. Dent. Assoc.*, **1994**, *125*, 163-171
49. McCawley, L.J.; Matrisian, L.M. Matrix metalloproteinases: they're not just for matrix anymore! *Curr. Opin. Cell Biol.*, **2001**, *13*, 534-540
50. Murphy, G.; Knauper, V. Relating matrix metalloproteinase structure to function: why the 'hemopexin' domain? *Matrix Biol.*, 1997, *15*, 511-518
51. Murphy, G.; Crabbe, T. Gelatinases A and B. *Methods Enzymol.*, **1995**, *248*, 470-484
52. Wilhelm, S.M.; Collier, I.E.; Marmer, B.L.; Eisen, A.Z.; Grant, G.A.; Goldberg, G.I. SV 40-transformed human lung fibroblasts secrete a 92 kDa type IV collagenase which is identical to that secreted by normal human macrophages. *J. Biol. Chem.*, **1989**, *264*, 17213-17221

53. Huhtala, P. Chow, L.T.; Tryggvason, K. Structure of the human type IV collagenase gene. *J. Biol. Chem.*, **1990**, *265*, 11077-11082
54. Coussens, L.M.; Werb, Z. Matrix metalloproteinases and the development of cancer. *Chem. Biol.*, **1996**, *3*, 895-904
55. Sellers, A.; Reynolds, J.J.; Meikle, M.C. Neutral metallo-proteinases of rabbit bone. Separation in latent forms of distinct enzymes that when activated degrade collagen, gelatin and proteoglycans. *Biochem. J.*, **1978**, *171*, 493-496
56. Liotta, L.A.; Abe, S.; Robey, P.G.; Martin, G.R. Preferential digestion of basement membrane collagen by an enzyme derived from a metastatic murine tumor. *Proc. Natl. Acad. Sci. USA*, **1979**, *76*, 2268-2272
57. Itoh, Y.; Kajita, M.; Kinoh, H.; Mori, H.; Okada, A.; Seiki, M. Membrane type 4 matrix metalloproteinase (MT4-MMP, MMP-17) is a glycosyl-phosphatidyl inositol-anchored proteinase. *J. Biol. Chem.*, **1999**, *274*, 34260-34266
58. Kojima, S.; Itoh, Y.; Matsumoto, S.; Masuho, Y.; Seiki, M. Membrane-type 6 matrix metalloproteinase is the second glycosyl-phosphatidyl inositol-anchored MMP. *FEBS Lett.*, **2000**, *480*, 142-146
59. Vartio, T.; Hovi, T.; Vaheri, A. Human macrophages synthesize and secrete a major 95,000-dalton gelatin-binding protein distinct from fibronectin. *J. Biol. Chem.*, **1982**, *257*, 8862-8868
60. Ruhul Amin, A.R.; Senga, T.; Oo, M.L.; Thant, A.A.; Hamaguchi, M. Secretion of matrix metalloproteinase-9 by the proinflammatory cytokine, IL-1 beta: a role for the dual signalling pathways, Akt and Erk. *Genes Cells*, **2003**, *8*, 515-523
61. Bjorklund, M.; Koivunen, E. Gelatinase-mediated migration and invasion of cancer cells.

*Biochim. Biophys. Acta.*, **2005**, 25, 37-69

62. Sang, Q.X.; Birkedal-Hansen, H.; Van Wart, H.E. Proteolytic and non-proteolytic activation of human neutrophil progelatinase B. *Biochim. Biophys. Acta.*, **1995**, 1251, 99-108.
63. Fridman, R.; Toth, M.; Pena, D.; Mobashery, S. Activation of progelatinase B (MMP-9) by gelatinase A (MMP-2). *Cancer Res.*, **1995**, 55, 2548-2555
64. Nagase, H. Human stromelysins 1 and 2. *Methods Enzymol.*, **1995**, 248, 449-470
65. Chin, J.R.; Murphy, G.; Werb, Z. Stromelysin, a connective tissue-degrading metalloendopeptidases secreted by stimulated rabbit synovial fibroblasts in parallel with collagenase. Biosynthesis, isolation, characterization, and substrates. *J. Biol. Chem.*, **1985**, 260, 12367-12376
66. Pei, D.; Majmudar, G.; Weiss, S.J. Hydrolytic inactivation of a breast cancer carcinoma cell-derived serpin by human stromelysin-3. *J. Biol. Chem.*, **1994**, 269, 25849-25855
67. Sellers, A.; Woessner, J.F. The extraction of a neutral metalloproteinase from the involuting rat uterus, and its action on cartilage proteoglycan. *Biochem. J.*, **1980**, 189, 521-531
68. Woessner, J.F.; Taplin, C.J. Purification and properties of a small latent matrix metalloproteinases of the rat uterus. *J. Biol. Chem.*, **1988**, 263, 16918-16925
69. Powell, W.C.; Knox, J.D.; Navre, M.; Grogan, T.M.; Kittelson, J.; Nagle, R.B.; Bowden, G.T. Expression of the metalloproteinase matrilysin in DU-145 cells increases their invasive potential in severe combined immunodeficient mice. *Cancer Res.*, **1993**, 53, 417-422
70. Werb, Z.; Gordon, S. Elastase secretion by stimulated macrophages. Characterization and regulation. *J. Exp. Med.*, **1975**, 142, 361-377
71. Shapiro, S.D.; Griffin, G.L.; Gilbert, D.J.; Jenkins, N.A.; Copeland, N.G.; Welgus, H.G.; Senior, R.M.; Ley, T.J. Molecular cloning, chromosomal localization, and bacterial expression of

a murine macrophage metalloelastase. *J. Biol. Chem.*, **1992**, *267*, 4664-4671

72. Warner, R.L.; Lewis, C.S.; Beltran, L.; Youkin, E.M.; Varani, J.; Johnson, K.J. The role of metalloelastase in immune complex-induced acute lung injury. *Am. J. Pathol.*, **2001**, *158*, 2139-2144

73. Seiki M. Membrane-type matrix metalloproteinases. *APMIS.*, **1999**, *107*, 137-143

74. Knauper, V.; Will, H.; Lopez-Otin, C.; Smith, B.; Atkinson, S.J.; Stanton, H.; Hembry, R.M.; Murphy, G. Cellular mechanisms for human procollagenase-3 (MMP-13) activation. Evidence that MT1-MMP (MMP-14) and gelatinase a (MMP-2) are able to generate active enzyme. *J. Biol. Chem.*, **1996**, *271*, 17124-17131

75. Sato, H.; Takino, T.; Okada, Y.; Cao, J.; Shinagawa, A.; Yamamoto, E.; Seiki, M. A matrix metalloproteinase expressed on the surface of invasive cells. *Nature*, **1994**, *370*, 61-65

76. Sato, H.; Kinoshita, T.; Takino, T.; Nakayama, K.; Seiki, M. Activation of a recombinant membrane type 1-matrix metalloproteinase (MT1-MMP) by furin and its interaction with tissue inhibitor of metalloproteinases (TIMP)-2. *FEBS Lett.*, **1996**, *393*, 101-104

77. Pei, D.; Weiss, S.J. Transmembrane-deletion mutants of the membrane-type matrix metalloproteinase-1 process progelatinase A and express intrinsic matrix-degrading activity. *J. Biol. Chem.*, **1996**, *271*, 9135-9140

78. Pendás, A.M.; Knauper, V.; Puente, X.S.; Llano, E.; Mattei, M.G.; Apte, S.; Murphy, G.; López-Otin, C. Identification and characterization of a novel human matrix metalloproteinase with unique structural characteristics, chromosomal location, and tissue distribution. *J. Biol. Chem.*, **1997**, *272*, 4281-4286

79. Kolb, C.; Mauch, S.; Krawinkel, U.; Sedlacek, R. Matrix metalloproteinase-19 in capillary endothelial cells: expression in acutely, but not in chronically, inflamed synovium. *Exp.*

*Cell Res.*, **1999**, 250, 122-130

80. Bartlett, J.D.; Ryu, O.H.; Xue, J.; Simmer, J.P.; Margolis, H.C. Enamelysin mRNA displays a developmentally defined pattern of expression and encodes a protein which degrades amelogenin. *Connect. Tissue Res.*, **1998**, 39, 101-109

81. Lohi, J.; Wilson, C.L.; Roby, J.D.; Parks, W.C. Epilysin, a novel human matrix metalloproteinase (MMP-28) expressed in testis and keratinocytes and in response to injury. *J. Biol. Chem.*, **2001**, 276, 10134-10144

82. Nagase, H.; Visse, R.; Murphy, G. Structure and function of matrix metalloproteinases and TIMPs. *Cardiovasc. Res.*, **2006**, 69, 562-573

83. Peterson, J.T. The importance of estimating the therapeutic index in the development of matrix metalloproteinase inhibitors. *Cardio. Res.*, **2006**, 69, 677-687

84. Hagglund, A.C.; Ny, A.; Leonardsson, G.; Ny, T. Regulation and localization of matrix metalloproteinases and tissue inhibitors of metalloproteinases in the mouse ovary during gonadotropin-induced ovulation. *Endocrinology*, **1999**, 140, 4351-4358

85. Vu, T.H.; Werb, Z. Matrix metalloproteinases: effectors of development and normal physiology. *Genes. Dev.*, **2000**, 14, 2123-2133

86. Hulboy, D.L.; Rudolph, I.A.; Matrisian, L.M. Matrix metalloproteinases as mediators of reproductive function. *Mol. Hum. Reprod.*, **1997**, 3, 27-45

87. Hotary, K.B.; Allen, E.D.; Brooks, P.C.; Datta, N.S.; Long, M.W.; Weiss, S.J. Membrane type I matrix metalloproteinase usurps tumor growth control imposed by the three-dimensional extracellular matrix. *Cell*, **2003**, 114, 33-45

88. Yu, Q.; Stamenkovic, I. Cell surface-localized matrix metalloproteinase-9 proteolytically activates TGF-beta and promotes tumor invasion and angiogenesis. *Genes. Dev.*, **2000**, 14, 163-



89. Wolf, K.; Mazo, I.; Leung, H.; Engelke, K.; Von Andrian, U.H.; Deryugina, E.I.; Strongin, A.Y.; Bocker, E.B.; Friedl, P. Compensation mechanism in tumor cell migration : mesenchymal-amoeboid transition after blocking of pericellular proteolysis. *J. Cell Biol.*, **2003**, *160*, 267-277
90. Okada, N.; Ishida, H.; Murata, N.; Hashimoto, D.; Seyama, Y.; Kubota, S. Matrix metalloproteinase-2 and -9 in bile as a marker of liver metastasis in colorectal cancer. *Biochem. Biophys Res. Commun.*, **2001**, *288*, 212-216
91. Giannelli, G.; Falk-marzillier, J.; Schiraldi, O.; Stetlerstevenson, W.G.; Quaranta, V. Induction of cell migration by matrix metalloproteinase-2 cleavage of laminin-5. *Science*, **1997**, *277*, 225-228
92. Polette, M.; Nawrocki-Raby, B.; Gilles, C.; Clavel, C.; Birembaut, P. Tumour invasion and matrix metalloproteinases. *Crit. Rev. Oncol. Hematol.*, **2004**, *49*, 179-186
93. Jung, S.; Rutka, J.T.; Hinek, A. Tropoelastin and elastin degradation products promote proliferation of human astrocytoma cell lines. *J. Neuropathol. Exp. Neurol.*, **1998**, *57*, 439-448
94. Mitsiades, N.; Yu, W.H.; Poulaki, V.; Tsokos, M.; Stamenkovic, I. Matrix metalloproteinase-7-mediated cleavage of Fas ligand protects tumor cells from chemotherapeutic drug cytotoxicity. *Cancer Res.*, **2001**, *61*, 577-581
95. Powell, W.C.; Fingleton, B.; Wilson, C.L.; Boothby, M.; Matrisian, L.M. The metalloproteinase matrilysin proteolytically generates active soluble Fas ligand and potentiates epithelial cell apoptosis. *Curr. Biol.*, **1999**, *9*, 1441-1447
96. Holmgren, L. Antiangiogenesis restricted tumor dormancy. *Cancer Metast. Rev.*, **1996**, *15*, 241-245
97. Ingber, D. Extracellular matrix as a solid-state regulator in angiogenesis: identification of

new targets for anti-cancer therapy. *Semin. Cancer Biol.*, **1992**, 3, 57-63.

98. Huang, S.Y.; Van Arsdall, M.; Tedjarati, S.; McCarty, M.; Wu, W.J.; Langley, R.; Fidler, I.J. Contributions of stromal metalloproteinases-9 to angiogenesis and growth of human ovarian carcinoma in mice. *J. Natl. Cancer Inst.*, **2002**, 94, 1134-1142

99. Hiratsuka, S.; Nakamura, K.; Iwai, S.; Murakami, M.; Itoh, T.; Kijima, H.; Shipley, J.M.; Senior, R.M.; Shibuya, M. MMP-9 induction by vascular endothelial growth factor receptor-1 is involved in lung-specific metastasis. *Cancer Cell*, **2002**, 2, 289-300

100. Potempa, J.; Banbula, A.; Travis, J. Role of bacterial proteinases in matrix destruction and modulation of host responses. *Periodontol 2000*, **2000**, 24, 153-192

101. Sorsa, T.; Ding, Y.L.; Ingman, T.; Salo, T.; Westerlund, U.; Haapasalo, M.; Tschesche, H.; Kontinen, Y.T. Cellular source, activation and inhibition of dental plaque collagenase. *J. Clin. Periodontol.*, **1995**, 22, 709-717

102. Ryan, M.E.; Ramamurthy, N.S.; Golub, L.M. Matrix metalloproteinases and their inhibitors in periodontal treatment. *Curr. Opin. Periodontol.*, **1996**, 3, 85-96

103. Sorsa, T.; Mäntylä P.; Rönkä H.; Kallio, P.; Kallis, G.B.; Lundqvist, C.; Kinane, D.F.; Salo, T.; Golub, L.M.; Teronen, O.; Tikanoja, S. Scientific basis of a matrix metalloproteinase-8 specific chair-side test for monitoring periodontal and peri-implant health and disease. *Ann. N. Y. Acad. Sci.*, **1999**, 878, 130-140

104. Manicourt, D.H.; Fujimoto, N.; Obata, K.; Thonar, E.J. Levels of circulating collagenase, stromelysin-1, and tissue inhibitor of matrix metalloproteinases 1 in patients with rheumatoid arthritis. Relationship to serum levels of antigenic keratan sulfate and systemic parameters of inflammation. *Arthritis Rheum.*, **1995**, 38, 1031-1039

105. Leff, R.L. Osteoarthritis. Matrix Metalloproteinase inhibition, cartilage loss. Surrogate

markers, and clinical implications. *Ann. N.Y. Acad. Sci.*, **1999**, 878, 201-207

106. Takagi, H.; Manabe, H.; Kawai, N.; Goto, S.N.; Umemoto, T. Circulating matrix metalloproteinase-9 concentrations and abdominal aortic aneurysm presence: a meta-analysis.

*Interact. Cardiovasc. Thorac. Surg.*, **2009**, 9, 437-440

107. Mizoguchi H, Yamada K, Nabeshima T. Matrix metalloproteinases contribute to neuronal dysfunction in animal models of drug dependence, Alzheimer's disease, and epilepsy. *Biochem.*

*Res. Int.*, **2011**, 681385

108. Zitka, O.; Kukacka, J.; Krizkova, S.; Huska, D.; Adam, V.; Masarik, M.; Prusa, R.; Kizek, R. Matrix metalloproteinases. *Current Medicinal Chemistry*, **2010**, 17, 3751-3768

109. Nagase, H.; Woessner, J.F. Jr. Matrix metalloproteinases. *J. Biol. Chem.*, **1999**, 274, 21491-21494

110. Jung, K.; Nowak, L.; Lein, M.; Priem, F.; Schnorr, D.; Loening, S.A. Matrix metalloproteinases 1 and 3, tissue inhibitor of metalloproteinase-1 and the complex of metalloproteinase-1 tissue inhibitor in plasma of patients with prostate cancer. *Int. J. Cancer*, **1997**, 74, 220-223

111. Bauer, E.A.; Stricklin, G.P.; Jeffraey, J.J.; Eisen, A.Z. Collagenase production by human skin fibroblasts. *Biochem. Biophys. Res. Commun.*, **1975**, 64, 232-240

112. Gomez, D.E.; Alonso, D.F.; Yoshiji, H.; Thorgeirsson, U.P. Tissue inhibitors of metalloproteinases- structure, regulation and biological functions. *Eur. J. cell. Biol.*, **1997**, 74, 111-122.

113. Blenis, J.; Hawkes, S.P. Transformation-sensitive protein associated with the cell substratum of chicken embryo fibroblasts. *Proc. Natl. Acad. Sci. USA*, **1983**, 80, 770-774

114. Anana-Apte, B.; Bao, L.; Smith, R.; Iwata, K.; Olsen, b.R.; Zetter, B. Apte, S.S. A review

of tissue inhibitor of metalloproteinases-3 (TIMP-3) and experimental analysis of its effect on primary tumor growth. *Biochem. Cell Biol.*, **1996**, *74*, 853-862

115. Tummalapali, C.M.; Heath, B.J.; Tyagi, S.C. Tissue inhibitor of metalloproteinase-4 instigates apoptosis in transformed cardiac fibroblasts. *J. cell Biochem.*, **2001**, *80*, 512-521

116. Wu, I.M.; Moses, M.A. Molecular cloning and expression analysis of the cDNA encoding rat tissue inhibitor of metalloproteinase-4. *Matrix Biol.*, **1998**, *16*, 339-342

117. Coussens, L. M.; Fingleton, B.; Matrisian, L. M. Matrix metalloproteinase inhibitors and cancer: trials and tribulations. *Science*, **2002**, *295*, 2387-2392

118. Wojtowicz-Praga, S.; torri, J. Johnson, M.; Steen, V.; Marshal, J.; Ness, E.; Dickson, R.; Sale, M.; Rasmussen, H.S.; Chiodo, T.A.; Hawkins, M.J. Phase I trial of Marimastat, a novel matrix metalloproteinase inhibitor, administered orally to patients with advanced lung cancer. *J. Clin. Oncol.*, **1998**, *16*, 2150-2156.

119. Overall, C. M.; Lopez-Otin, C. Strategies for MMP inhibition in cancer: innovations for the post-trial era. *Nature Rev. Cancer*, **2002**, *2*, 657-672

120. Duggar, B.M. Aureomycin: a product of the continuing search for new antibiotics. *Ann. NY Acad. Sci.*, **1948**, *51*, 177-181

121. Minieri, P.P.; Firman, M.C.; Mistretta, A. G.; Abbey, A.; Bricker, C.E.; Rigler, N.E.; Sokol, H. A new broad spectrum antibiotic product of the tetracycline group. *Antibiotics Ann. 1953-54.*, **1954**, 81-87

122. Golub, L.M.; Ramamurthy, N.S.; McNamara, T.F.; Greenwald, R.A.; Rifkin, B.R. Tetracyclines inhibit connective tissue breakdown: new therapeutic implications for an old family of drugs. *Crit. Rev. Oral Biol. Med.*, **1991**, *2*, 297-321

123. Golub, L.M.; Lee, H.M.; Ryan, M.E.; Giannobile, W.V.; Payne, J.; Sorsa, T. Tetracyclines

- inhibit connective tissue breakdown by multiple non-antimicrobial mechanisms. *Adv. Dent. Res.*, **1998**, *12*, 12-26
124. Gabler, W.L.; Creamer, H.R. Suppression of human neutrophil functions by tetracyclines. *J. Periodontal Res.*, **1991**, *26*, 52-58
125. Dezube, B.J.; Krown, S.E.; Lee, J.Y.; Bauer, K.S.; Aboulafia, D.M. Randomized phase II trial of matrix metalloproteinase inhibitor COL-3 in AIDS-related Kaposi's sarcoma: an AIDS Malignancy Consortium Study. *J. Clin. Oncol.*, *2006*, **24**, 1389-1394
126. Richards, C.; Pantanowitz, L.; Dezube, B.J. Antimicrobial and non-antimicrobial tetracyclines in human cancer trials. *Pharmacological Research*. **2011**, *63*, 151-156
127. Sandberg, S.; Glette, J.; Hopen, G.; Solberg, C.O. Doxycycline induced photodamage to human neutrophils and tryptophan. *Photochem. Photobiol.*, **1984**, *39*, 43-48
128. Riaz, M.; Pilpel, N. Effects of ultraviolet light on lecithin monolayers in the presence of fluorescein dyes and tetracycline drugs. *J. Pharm. Pharmacol.*, **1983**, *35*, 215-218
129. Brown, P.D.; Giavazzi, R. Matrix metalloproteinase inhibition: a review of anti-tumour activity. *Ann. Oncol.*, **1995**, *6*, 967-974
130. Brown, P.D. Matrix metalloproteinase inhibitors. *Angiogenesis*, **1998**, *1*, 142-154
131. Sledge, G.W.; Qulali, M.; Goulet, R.; Bone, E.A.; Fife, R. Effect of matrix metalloproteinase inhibitor batimastat on breast cancer regrowth and metastasis in athymic mice. *J. Natl. Cancer Inst.*, **1995**, *87*, 1546-1550
132. Brown, P.D.; Davidson, A.H.; Drummond, A.H.; Gearing, A.; Whittaker, M. Hydroxamic acid matrix metalloproteinase inhibitors. Matrix metalloproteinases in cancer therapy. HUMANA PRESS. **2001**, 113-142
133. Overall, C.M.; Lopez-Otin, C. Strategies for MMP inhibition in cancer: innovations for

the post-trial era. *Nat. Rev. Cancer*, **2002**, 2, 657-672

134. Zucker, S.; Cao, J.; Chen, W.T. Critical appraisal of the use of matrix metalloproteinase inhibitors in cancer treatment. *Oncogene*, **2000**, 19, 6642-6650

135. Overall, C.M.; Kleifeld, O. Towards third generation matrix metalloproteinase inhibitors for cancer therapy. *British Journal of Cancer*, **2006**, 94, 941-946

136. Fisher, J.F.; Mobashery, S. Recent advances in MMP inhibitor design. *Cancer Metastasis Rev.*, **2006**, 25, 115-136

137. Amălinei, C.; Căruntu, I.D.; Giușcă, S.E.; Bălan, R.A. Matrix metalloproteinases involvement in pathologic conditions. *Romanian Journal of Morphology and Embryology*, **2010**, 51, 215-228

138. Caraveri, R.; Coronelli, C.; Pagani, H.; Sensi, P. Thermorubin, a new antibiotic from a thermoactinomycete. *Clin. Med.*, **1964**, 71, 511-521

139. Cavalleri, B.; Turconi, M.; Pallanza, R. Synthesis and antibacterial activity of some derivatives of the antibiotic thermorubin. *J. Antibiot. (Tokyo)*, **1985**, 38, 1752-1760

140. Hayashi, K.; Dombou, M.; Sekiya, M.; Nakajima, H.; Fujita, T. Nakayama, M. Thermorubin and 2-hydroxyphenyl acetic acid, aldose reductase inhibitors. *J. Antibiot. (Tokyo)*, **1995**, 48, 1345-1346

141. Lampe, V.; Milobedzka, J.; Kostanecki, St. V. Zur Kenntnis des Curcumins. *Berichte.*, **1910**, 43, 2163

142. Sharma, O.P. Antioxidant activity of curcumin and related compounds. *Biochem. Pharmacol.*, **1976**, 25, 1811-1812

143. Ruby, A.J.; Kuttan, G; Babu, K.D.; Rajasekharan, K.N.; Kuttan, R. Anti-tumour and antioxidant activity of natural curcuminoids. *Cancer Lett.*, **1995**, 94, 79-83

144. Aggarwal, B.B.; Kumar, A; Bharti, A.C. Anticancer potential of curcumin: preclinical and clinical studies. *Anticancer Res.*, **2003**, *23*, 363-398
145. Caputi, M.; Groeger, A.M.; Esposito, V.; Dean, C.; De Luca, A.; Pacilio, C.; Muller, M.R.; Giordano, G.G.; Baldi, F.; Wolner, E.; Giordano, A. Prognostic role of cyclin D1 in lung cancer: relationship to proliferating cell nuclear antigen. *Am. J. Respir. Cell Mol. Biol.*, **1999**, *20*, 746-750
146. Drobnjak, M.; Osman, I.; Scher, H.I.; Fazzari, M.; Cordon-Cardo, C. Overexpression of cyclin D1 is associated with metastatic prostate cancer to bone. *Clin. Cancer Res.*, **2000**, *6*, 1891-1895
147. Baldwin, A.S. Control of oncogenesis and cancer therapy resistance by the transcription factor NFkappaB. *J. Clin. Invest.*, **2001**, *107*, 241-246
148. Lee, H.; Arsura, M.; Wu, M.; Duyao, M.; Buckler, A.J.; Sonenshein, G.E., Role of Rel-related factors in control of c-myc gene transcription in receptor-mediated apoptosis of the murine B cell WEHI 231 line. *J. Exp. Med.*, **1995**, *181*, 1169-1177
149. Sovak, M.A.; Bellas, R.E.; Kim, D.W.; Zanieski, G.J.; Rogers, A.E.; Traish, A.M.; Sonenshein, G.E. Aberrant nuclear factor-kappaB/Rel expression and the pathogenesis of breast cancer. *J. Clin. Invest.*, **1997**, *100*, 2952-2960
150. Mukhopadhyay, A.; Banerjee, S.; Stafford, L.J.; Xia, C.X.; Liu, M.; Aggarwal, B.B., Curcumininduced suppression of cell proliferation correlates with downregulation of cyclin D1 expression and CDK4-mediated retinoblastoma protein phosphorylation. *Oncogene*, **2002**, *21*, 8852-8862
151. Huang, M.T.; Ma, W.; Yen, P.; Xie, J.G.; Han, J.; Frenkel, K.; Grunberger, D.; Conney, A.H. Inhibitory effects of topical application of low doses of curcumin on 12-O-

tetradecanoylphorbol-13-acetate-induced tumor promotion and oxidized DNA bases in mouse epidermis. *Carcinogenesis*, **1997**, *18*, 83-88

152. Gumbiner, L.M.; Gumerlock, P.H.; Mack, P.C.; Chi, S.G.; deVere White, R.W.; Mohler, J.L.; Pretlow, T.G.; Tricoli, J.V. Overexpression of cyclin D1 is rare in human prostate carcinoma. *Prostate*, **1999**, *38*, 40-45

153. Thapliyal, R.; Maru, G.B. Inhibition of cytochrome p450 isoenzymes by curcumins in vitro and in vivo. *Food Chem. Toxicol.*, **2001**, *39*, 541-547

154. Lal, B.; Kapoor, A.K.; Agrawal, P.K.; Asthana, O.P.; Srimal, R.C. Role of curcumin in idiopathic inflammatory orbital pseudotumours. *Phytother Res.*, **2000**, *14*, 443-447

155. Ravindran, J.; Subbaraju, G.V.; Ramani, M.V.; Sung, B.; Aggarwal, B.B. Bisdemethylcurcumin and structurally related hispolon analogues of curcumin exhibit enhanced prooxidant, anti-proliferative and anti-inflammatory activities in vitro. *Biochem Pharmacol.*, **2010**, *79*, 1658-1666

156. Banji, D.; Pinnapureddy, J.; Banji, O.J.; Kumar, A.R.; Reddy, K.N. Evaluation of the concomitant use of methotrexate and curcumin on Freund's complete adjuvant-induced arthritis and hematological indices in rats. *Indian J. Pharmacol.*, **2011**, *43*, 546-550

157. Mathy-Hartert, M.; Jacquemond-Collet, I.; Priem, F.; Sanchez, C.; Lambert, C.; Henrotin, Y. Curcumin inhibits pro-inflammatory mediators and metalloproteinase-3 production by chondrocytes. *Inflamm. Res.*, **2009**, *58*, 899-908

158. Caesar, I.; Jonson, M.; Nilsson, K.P.; Thor, S.; Hammarström, P. Curcumin promotes A-beta fibrillation and reduces neurotoxicity in transgenic *Drosophila*. *PLoS One*, **2012**, *7*, e31424

159. Wang, L.; Li, C.; Guo, H.; Kern, T.S.; Huang, K.; Zheng, L. Curcumin inhibits neuronal and vascular degeneration in retina after ischemia and reperfusion injury. *PLoS One*, **2011**, *6*,



e23194

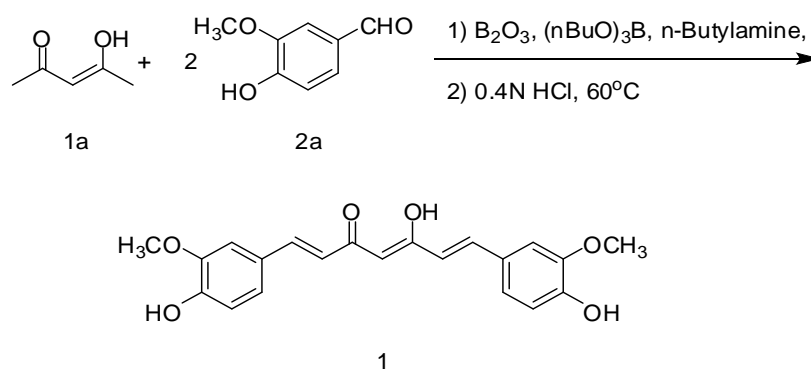
160. Sharma, O.P. Antioxidant activity of curcumin and related compounds. *Biochem Pharmacol.*, **1976**, *25*, 1811-1812
161. Venkatesan, N. Curcumin attenuation of acute adriamycin myocardial toxicity in rats. *Br. J. Pharmacol.*, **1998**, *124*, 425-427
162. Aggarwal, B.B.; Kumar, A; Bharti, A.C. Anticancer potential of curcumin: preclinical and clinical studies. *Anticancer Res.*, **2003**, *23*, 363-398
163. Shoba, G.; Joy, D.; Joseph, T.; Majeed, M.; Rajendran, R.; Srinivas, P. S. Influence of piperine on the pharmacokinetics of curcumin in animals and human volunteers. *Planta. Med.*, **1998**, *64* , 353-356
164. Cheng, A.L.; Hsu, C.H.; Lin, J.K.; Hsu, M.M.; Ho, Y.F.; Shen, T.S.; Ko, J.Y.; Lin, J.T.; Lin, B.R.; Ming-Shiang, W.; Yu, H.S.; Jee, S.H.; Chen, G.S.; Chen, T.M.; Chen, C.A.; Lai, M.K.; Pu, Y.S.; Pan, M.H.; Wang, Y.J.; Tsai, C.C.; Hsieh, C.Y. Phase I clinical trial of curcumin, a chemopreventive agent, in patients with high-risk or pre-malignant lesions. *Anticancer Res.*, **2001**, *21*, 2895-2900
165. Lao, C.D.; Ruffin, M.T.; Normolle, D.; Heath, D.D.; Murray, S.I.; Bailey, J.M.; Boggs, M.E.; Crowell, J; Rock, C.L.; Brenner, D.E. Dose escalation of a curcuminoid formulation. *BMC Complement Altern. Med.*, **2006**, *6*, 10
166. Maiti, K.; Mukherjee, K.; Gantait, A; Saha, B.P.; Mukherjee, P.K. Curcumin–phospholipid complex: Preparation, therapeutic evaluation and pharmacokinetic study in rats. *Int. J. Pharm.*, **2007**, *330*, 155-163
167. Anand, P.; Kunnumakkara, A.B.; Newman, R.A.; Aggarwal, B.B. Bioavailability of curcumin: problems and promises. *Mol. Pharm.*, **2007**, *4*, 807-818

168. Ireson, C.R.; Jones, D.J.; Orr, S.; Coughtrie, M.W.; Boocock, D.J.; Williams, M.L.; Farmer, P.B.; Steward, W.P.; Gescher, A.J. Metabolism of the cancer chemopreventive agent curcumin in human and rat intestine. *Cancer Epidemiol. Biomarkers Prev.*, **2002**, *11*, 105-111
169. Ireson, C.; Orr, S.; Jones, D.J.; Verschoyle, R.; Lim, C.K.; Luo, J.L.; Howells, L.; Plummer, S.; Jukes, R.; Williams, M.; Steward, W.P.; Gescher, A. Characterization of metabolites of the chemopreventive agent curcumin in human and rat hepatocytes and in the rat in vivo, and evaluation of their ability to inhibit phorbol ester-induced prostaglandin E2 production. *Cancer Res.*, **2001**, *61*, 1058-1064
170. Sandur, S.K.; Pandey, M.K.; Sung, B.; Ahn, K.S.; Murakami, A.; Sethi, G.; Limtrakul, P.; Badmaev, V.; Aggarwal, B.B. Curcumin, demethoxycurcumin, bisdemethoxycurcumin, tetrahydrocurcumin, and turmerones differentially regulate antiinflammatory and antiproliferative responses through a ROS independent mechanism. *Carcinogenesis*, **2007**, *28*, 1765-1773

## Chapter 3. Synthesis of chemically-modified curcumins by a modified Pabon reaction

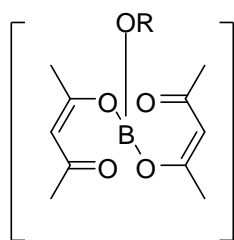
### A. Introduction

Curcumin [1,7-bis-(4-hydroxy-3-methoxyphenyl)-1,6-heptadiene-3,5-dione; **1**], a yellow pigment, comes from the perennial herb *Curcuma longa L.* that grows in Asian countries as mentioned in Chapter 2, and its chemical structure was not elucidated till 1910 by Lampe *et al.*<sup>1</sup> The first synthesis for curcumin carried out by Lampe *et al.* in 1918 contained eight steps beginning with vanillin, but as a method it appeared to lack any practical use.<sup>2</sup> In 1937, Pavolini *et al.* carried out a one-step synthesis of curcumin using 2,4-pentanedione (**1a**), vanillin (**2a**) and boric anhydride, but the yield was only 10%.<sup>3</sup> Since then, curcumin and curcumin analogues have been synthesized by several other methods with much improved yield. Of importance are the procedures of Pabon *et al.*<sup>4</sup> and Pedersen *et al.*<sup>5</sup> In Pabon's paper, curcumin was prepared in two steps: 1) generation of a boron complex from 2,4-pentadione, vanillin and boric anhydride in the presence of n-butylamine and tri-n-butyl borate, where boric anhydride was used to avoid Knoevenagel condensation<sup>5</sup> at C-3 position of 2,4-pentadione, because the boron complex makes the C-3 position of 2,4-pentadione not active in Knoevenagel reaction; 2) hydrolysis of boron complex into curcumin by 0.4N HCl at 60°C. (Scheme3.1)



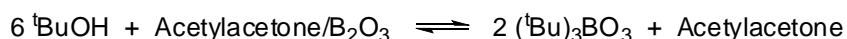
Scheme 3.1 Synthesis of curcumin by Pabon reaction

In the first step of the synthesis of curcumin reported by Pabon *et al.*, two ways were used to generate the boron complex, one was by heating the mixture of vanillin, 2,4-pentadione and boric anhydride at 100°C for 30min, followed by the addition of n-butylamine, while in the second method, reactants were dissolved in ethyl acetate at 60°C. The latter method gave a higher yield (73%) in contrast to the first one (45%). The proposed structure for boron complex from the view of Pabon is shown in Scheme 3.2, however, it's still not elucidated because no analysis was done on the structure of boron complex with 2,4-pentadione. The tri-alkyl borate was used to catalyze the formation of boron complex in the following equilibrium (Scheme 3.2). The first step of Pabon reaction was to generate the boron complex of 2,4-pentadione, then the decomposition of boron complex in dilute acid could give curcumin as the final product.



R=Alkyl Group

Equilibrium:



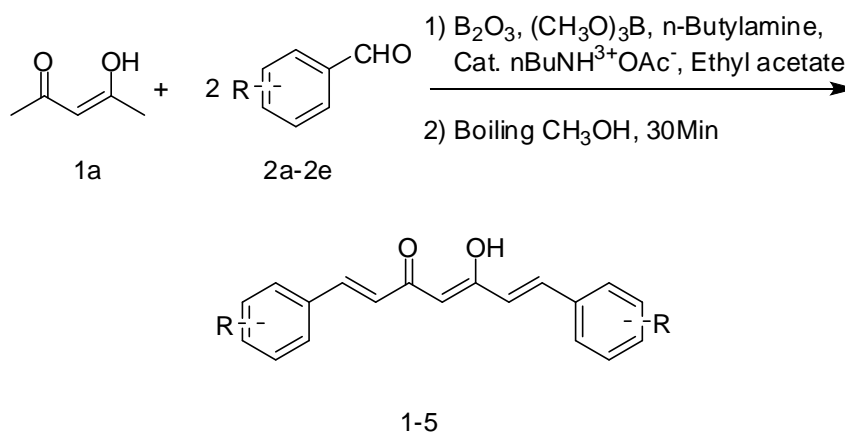
#### Scheme 3.2 Boron complex and equilibrium for Pabon reaction

The equilibrium indicates that alcohol could also decompose the boron complex of curcumin to tri-alkyl borate and free curcumin. Thus, in the variation of the Pabon method, boiling methanol was used instead of diluted acid in order to deprotect the boron complex because in many cases the substances are sensitive or even not stable under the acidic condition. Also trimethyl borate was used instead of tri-n-butyl borate, because the boiling point of trimethyl borate is 68-69°C, lower than that of tri-n-butyl borate, 230°C accordingly, which suggests that excessive trimethyl

borate could be simply removed by co-evaporation with methanol.<sup>6,7</sup> A catalytic amount of n-butylammonium acetate was utilized in addition to n-butylamine, in order to catalyze the formation of the double bonds by helping the dehydration.

### B. Side chain modification

Following the modified Pabon reaction procedure, several compounds were prepared according to Scheme 3.3. 2,4-Pentandione and very finely powdered boron oxide were heated to 120°C for 5min until a pale-yellow viscous liquid formed, then the reaction was cooled to room temperature, followed by the addition of the corresponding aldehyde and trimethyl borate in ethyl acetate. Catalytic amounts of n-butylamine and n-butylammonium acetate were then added. The mixture was stirred, and a red metallic precipitate began to appear after 1 hour. Then the reaction was held at room temperature for 48 hours to complete the process. The precipitate was filtered and collected, and then boiled with methanol to give products **1-5**.



Scheme 3.3 Synthesis of **1-5** by modified Pabon reaction

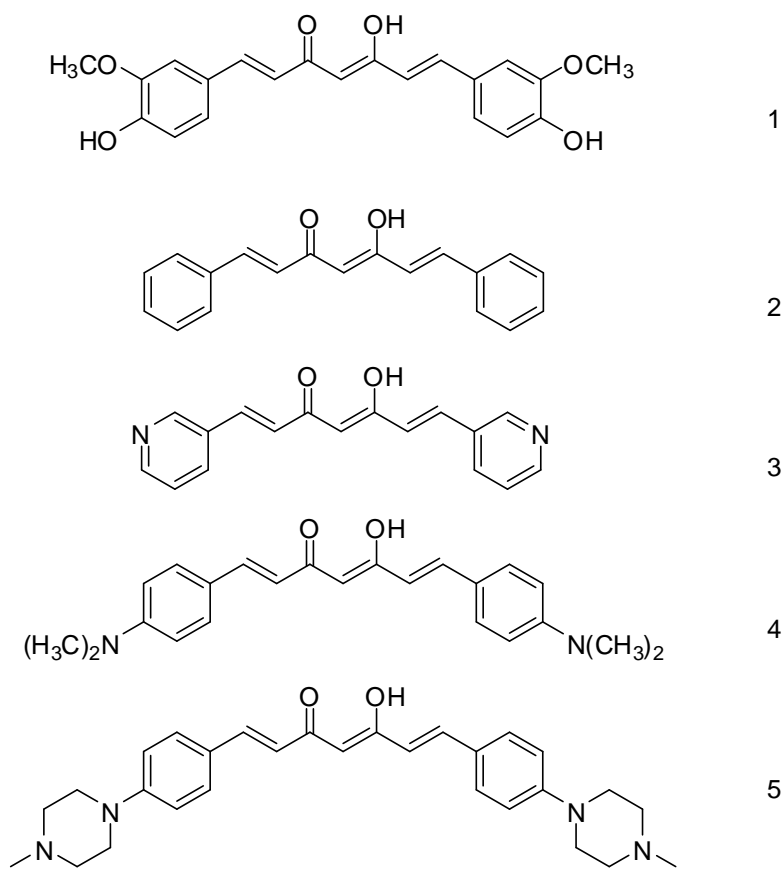


Figure 3.1 Structures of compounds **1-5**

Table 3.1 Symmetric curcumin analogues 1-5 by side chain modification

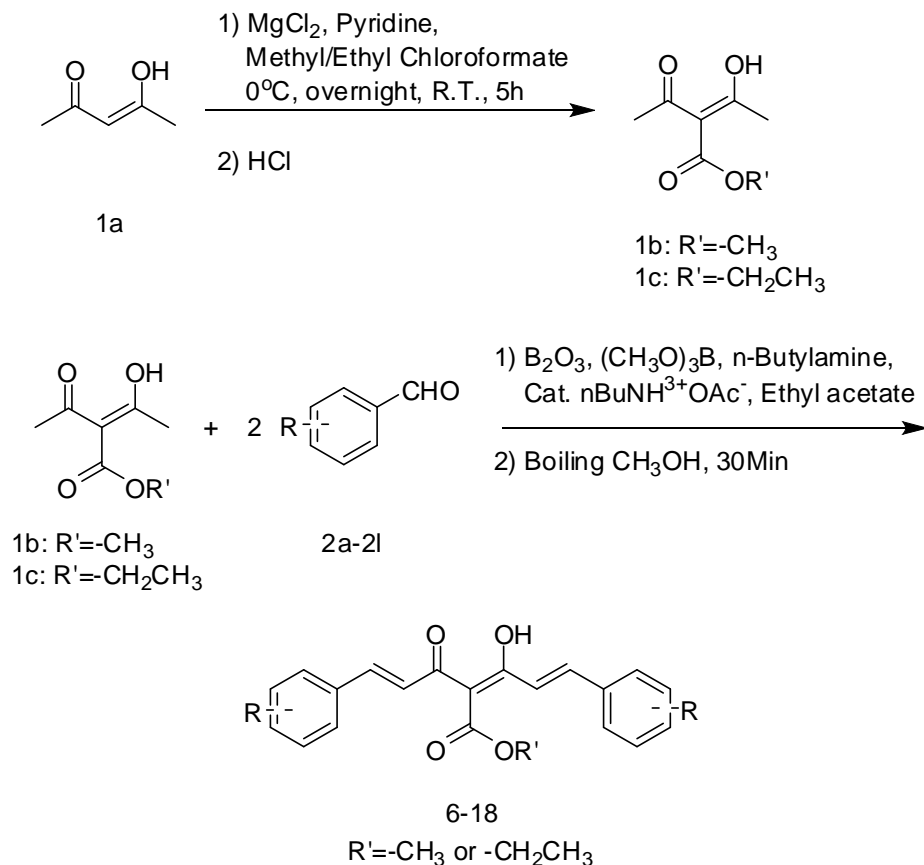
Compound	Name	Yield (%)	Melting Point (°C)
<b>1</b>	Curcumin	77.0	175-176
<b>2</b>	CMC2.2	65.1	141-142
<b>3</b>	CMC2.3	63.2	171-172
<b>4</b>	CMC2.7	61.1	212-214
<b>5</b>	CMC2.19	46.4	239-240

As seen in the table above, compounds **1-5** were synthesized by a modified Pabon reaction, and were obtained in higher yield compared to Pabon's original preparation in the cases of **1** (73%

reported by Pabon), **2** (23% reported by Pabon) and **4** (36% reported by Pabon). The melting points have been repeated for these analogues.<sup>4, 8</sup> These compounds except curcumin did not show any desirable activity against human-derived MMPs. Biological data will be discussed in detail in Chapter 4.

### C. Introduction of a methoxy/ethoxy carbonyl group on C-4

The poor solubility of curcumin limits its bioavailability for therapeutic applications, so an improvement is needed to increase the solubility.<sup>9</sup> Accordingly, the methoxy/ethoxy carbonyl group was introduced at the 4-position to obtain curcumin analogues. Side chain aryl group modification was also developed. The biological data in Chapter 4 reveal that some of these compounds are more potent against human-derived MMPs relative to curcumin. The pK<sub>a</sub> studies shown in Chapter 5 also indicate that CMC2.5 (**7**), the first lead compound among these curcumin analogues, is more acidic and more ionized at physiological pH (pH=7.4-7.6), and correlates with the biological data obtained. The syntheses of these curcumin analogues **6-18** with methyl/ethyl group on C-4 starts from 3-substituted-2,4-pentadione, the precursor for the Pabon reaction.<sup>10</sup> 2,4-Pentandione was first added to a suspension of magnesium chloride in methylene chloride in the presence of pyridine to generate the anion at carbon-7. Then an alkyl chloroformate was added dropwisely at 0°C, followed by the work up of dilute HCl after warming to room temperature over 5 hours. Both **1b** and **1c** were then used in the modified Pabon reaction to give compounds **6-18**. Several functional groups were placed on the phenyl rings including nitro, dimethylamino, pyridinyl and additional methoxy groups.

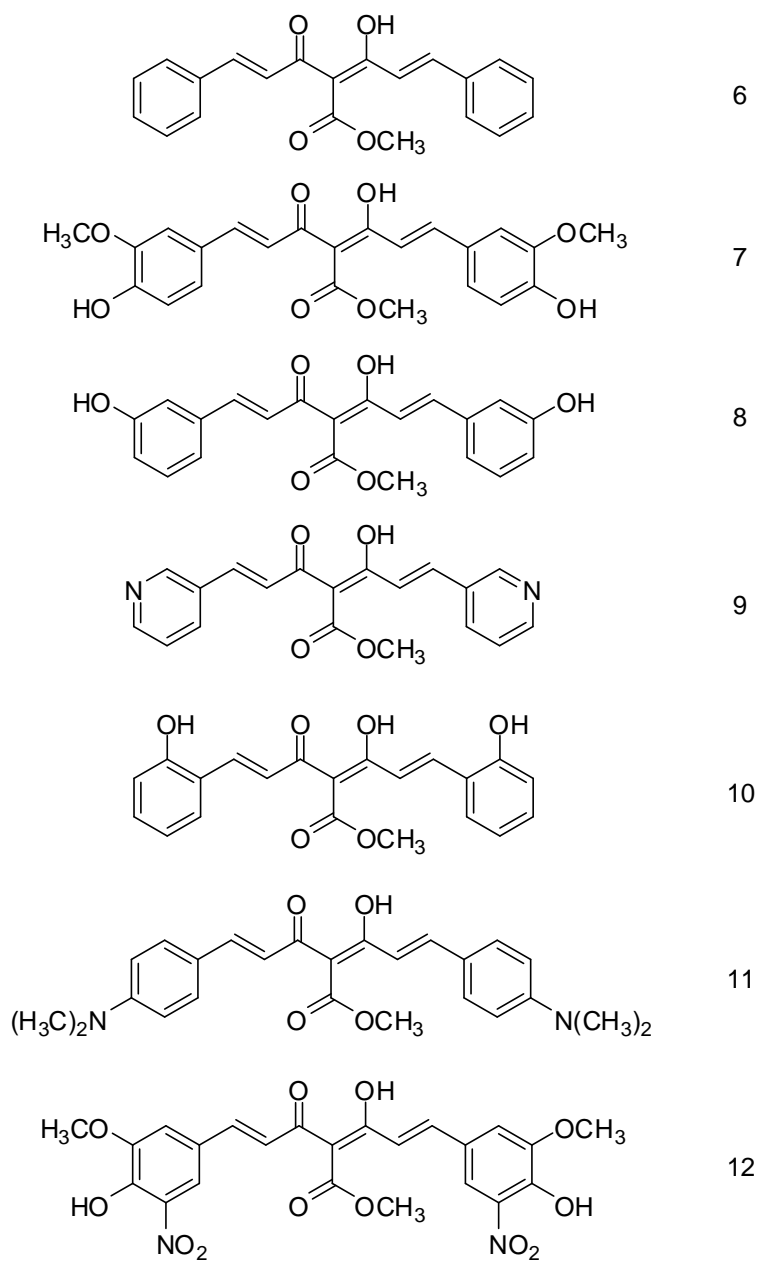


### Scheme 3.4 Synthesis of Compounds **6-18**

Among the curcumin analogues **6-18**, the yields vary dramatically for different substitutions on the phenyl ring. It appears that the introduction of an electron-donating group on the phenyl group, like methoxy group, increases the yield in the Pabon reaction, as can be seen for CMC2.13 (**13**), whereas the introduction of electron-withdrawing groups such as nitro group decreases the yield, as can be seen for CMC2.12 (**12**). However, the yields for the remaining curcumin analogues are around 40-50% except a lower yield was observed for CMC2.18 (**18**), probably because of the steric hindrance in the phenyl ring during the initial condensation. CMC2.16 (**16**) with an ethoxy carbonyl group on C-4 position, was also synthesized. All the biological data for these compounds will be discussed in Chapter 4. Both CMC2.5 (**7**) and



CMC2.14 (**14**) displayed excellent inhibitory activity against human-derived MMPs *in vitro*, so further studies were focused on the modifications of these two compounds.



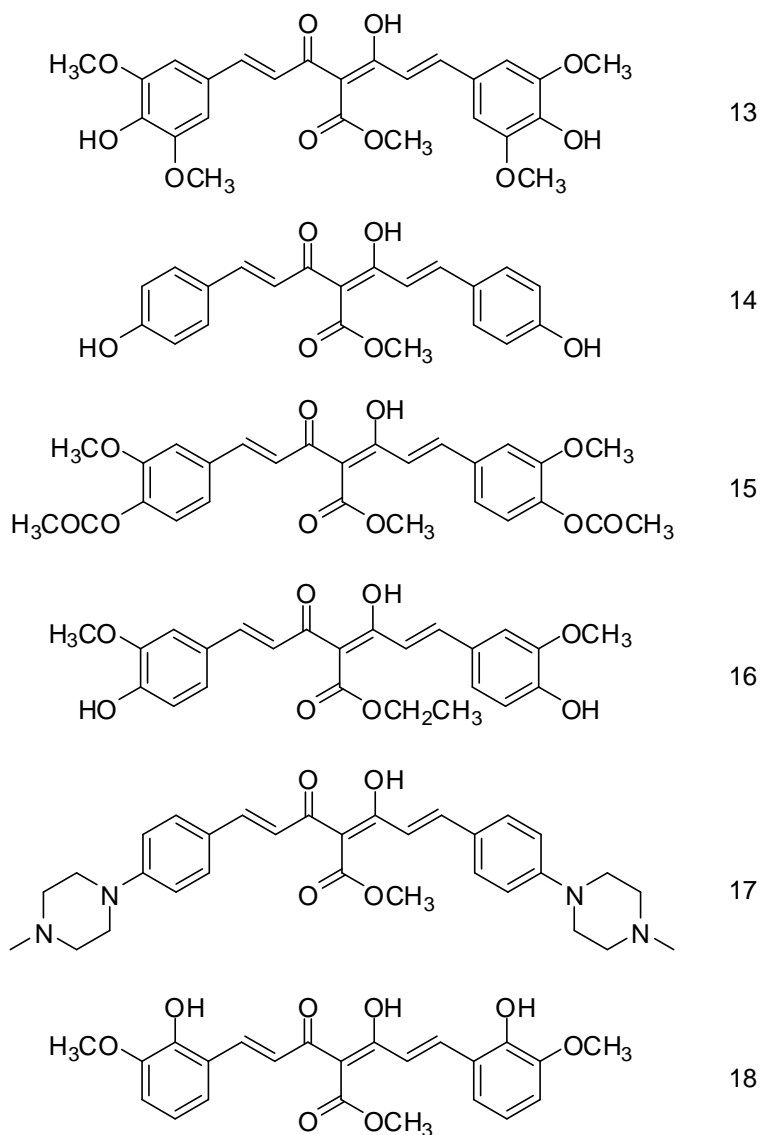


Figure 3.2 Structures of compounds **6-18**

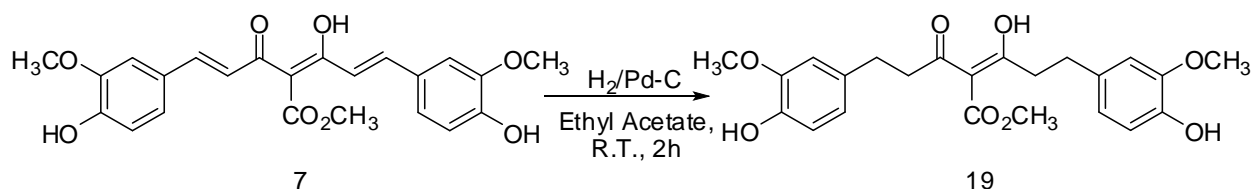
Table 3.2 Symmetric curcumin analogues **6-18**

Compound	Name	Yield (%)	Melting Point (°C)
<b>6</b>	CMC2.4	52.1	126-127
<b>7</b>	CMC2.5	72.0	175-176
<b>8</b>	CMC2.6	40.2	199-189
<b>9</b>	CMC2.8	38.7	195-196

<b>10</b>	CMC2.10	46.3	165-166
<b>11</b>	CMC2.11	45.1	224-225
<b>12</b>	CMC2.12	26.0	207-208
<b>13</b>	CMC2.13	77.0	179-180
<b>14</b>	CMC2.14	49.2	214-216
<b>15</b>	CMC2.15	46.0	169-170
<b>16</b>	CMC2.16	44.6	158-159
<b>17</b>	CMC2.17	49.1	191-192
<b>18</b>	CMC2.18	25.8	201-202

#### D. Tetrahydro-curcumin analogue

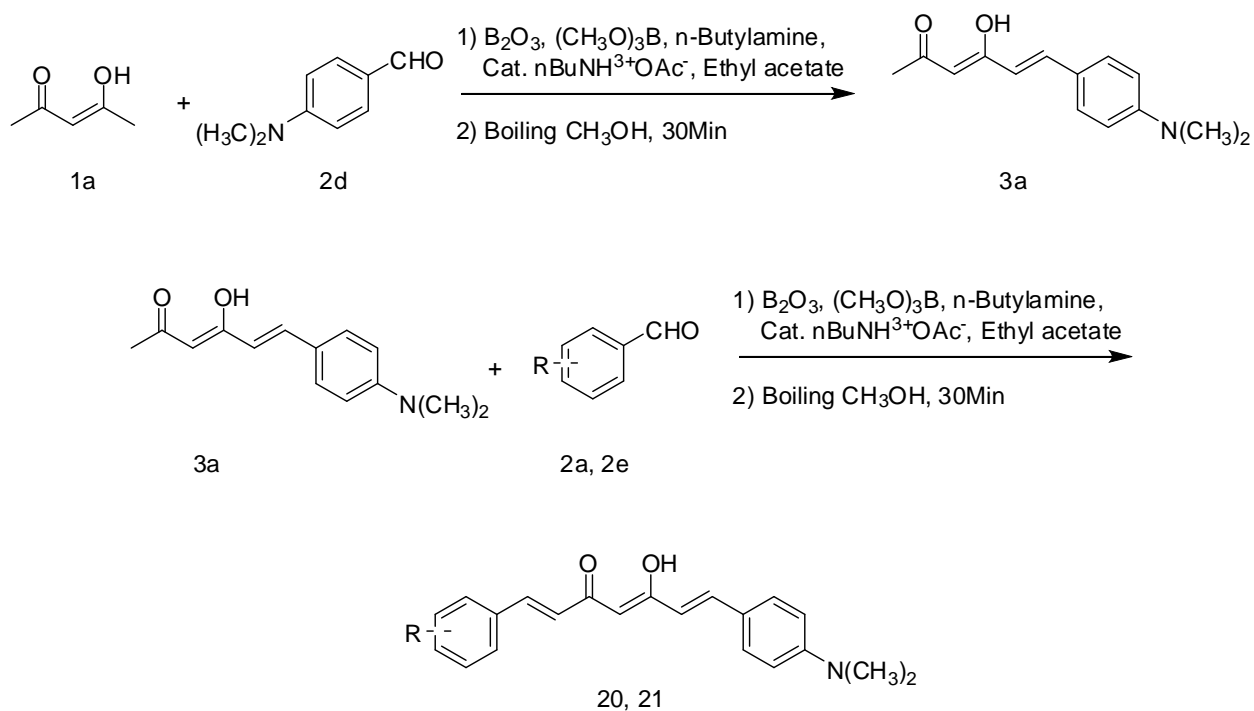
Tetrahydro-curcumin is one of the metabolites of curcumin in rats and human by intravenous route, however, it is still not clear if the metabolites are active or not.<sup>11, 12</sup> One tetrahydro-curcumin analogue CMC2.9 (**19**) was prepared by hydrogenation of CMC2.5 (**7**), the first lead compound from *in vitro* test against human-derived MMPs, in the presence of palladium-on-charcoal in ethyl acetate for 2 hours. However, **19** didn't show any inhibitory activity against MMPs.



Scheme 3.5 Synthesis of tetrahydro-curcumin analogue **19**

## E. Unsymmetrical curcumin analogues

Curcumin is highly symmetric and very insoluble. Modifications were made to the synthetic method to prepare the unsymmetrical curcumin analogue **20** and **21**, which were synthesized by Dr. Kveta Vrankova. Both of these contain a dimethylamino group on one phenyl ring, and 4-hydroxy-3-methoxy for **20**, 4-methyl-piperazinyl group for **21** on the other phenyl ring. The dimethylamino group was expected to increase the solubility in aqueous media, whereas the other functional group would be responsible for the MMP inhibitory activity. However, these two compounds lack potency against human-derived MMPs when tested (see Chapter 4).



Scheme 3.6 Synthesis of asymmetric curcumin analogues **20**, **21**

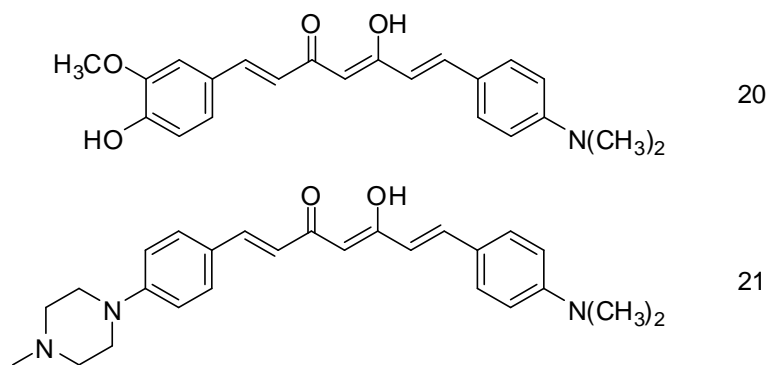
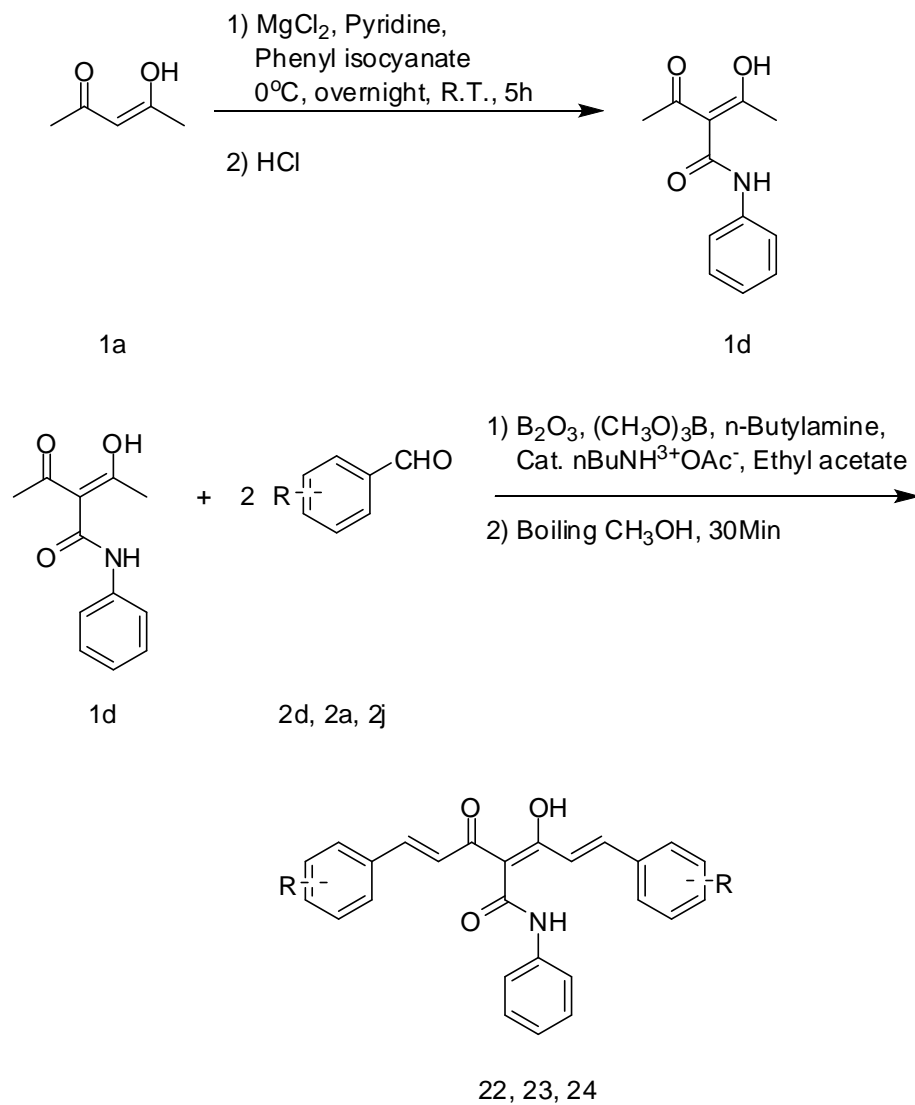


Figure 3.3 Structures of Compounds **20**, **21**

#### F. Introduction of an N-phenylaminocarbonyl group on C-4

Given that CMC2.5 (**7**) and CMC2.14 (**14**) showed desirable inhibitory activities against human-derived MMPs *in vitro* (data shown in Chapter 4), these two compounds were selected as the initial lead compounds as MMP inhibitors. Thereafter an N-phenylaminocarbonyl group was introduced in place of the methoxy carbonyl groups on **7** and **14**. This synthesis starts with a reaction of 2,4-pentanedione and phenyl isocyanate in the presence of magnesium chloride and pyridine to give the 3-arylaminocarbonyl-2,4-pentadione. Three N-phenylaminocarbonyl substituted chemically modified curcumins, namely CMC2.22 (**22**), CMC2.23 (**23**) and CMC2.24 (**24**) were prepared using a modified Pabon reaction as described in this chapter. Compound **23** and **24** both showed great potency against human-derived MMPs *in vitro*, and collateral studies in Chapter 8 also revealed that these two compounds are more potent compared to curcumin in cell culture (chemokine and cytokine inhibition), and *in vivo* studies (periodontitis, arthritis and wound healing).<sup>13-19</sup>



Scheme 3.7 Synthesis of compounds **22-24**

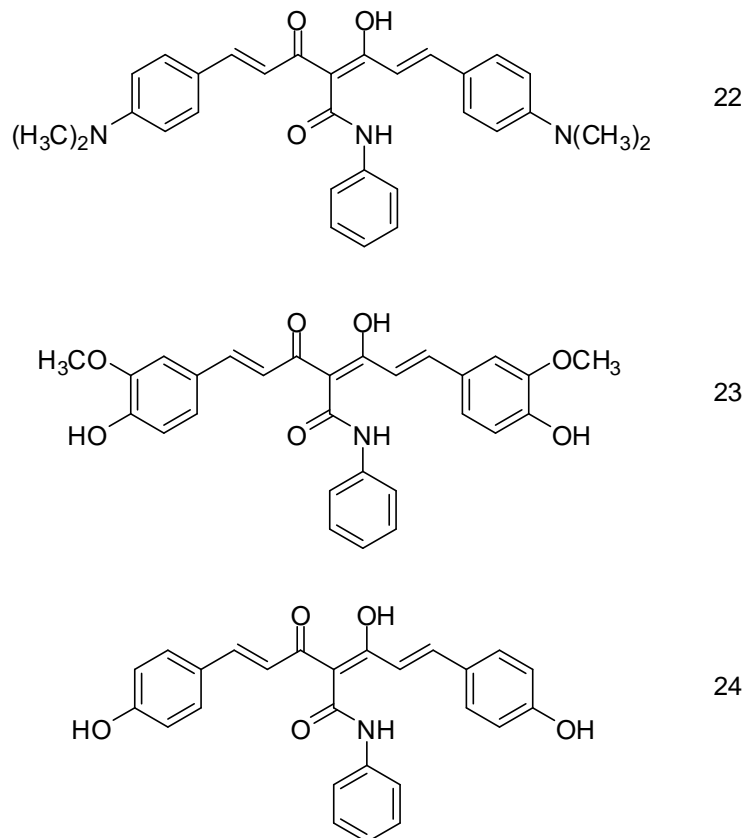


Figure 3.4 Structures of compounds **22-24**

Table 3.3 Symmetric curcumin analogues **22-24**

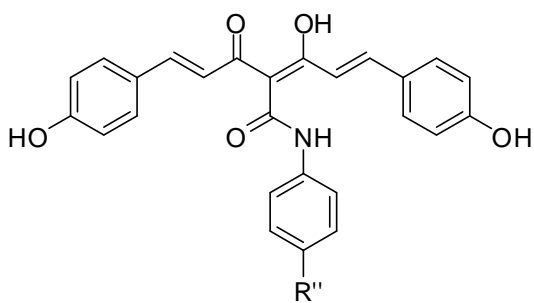
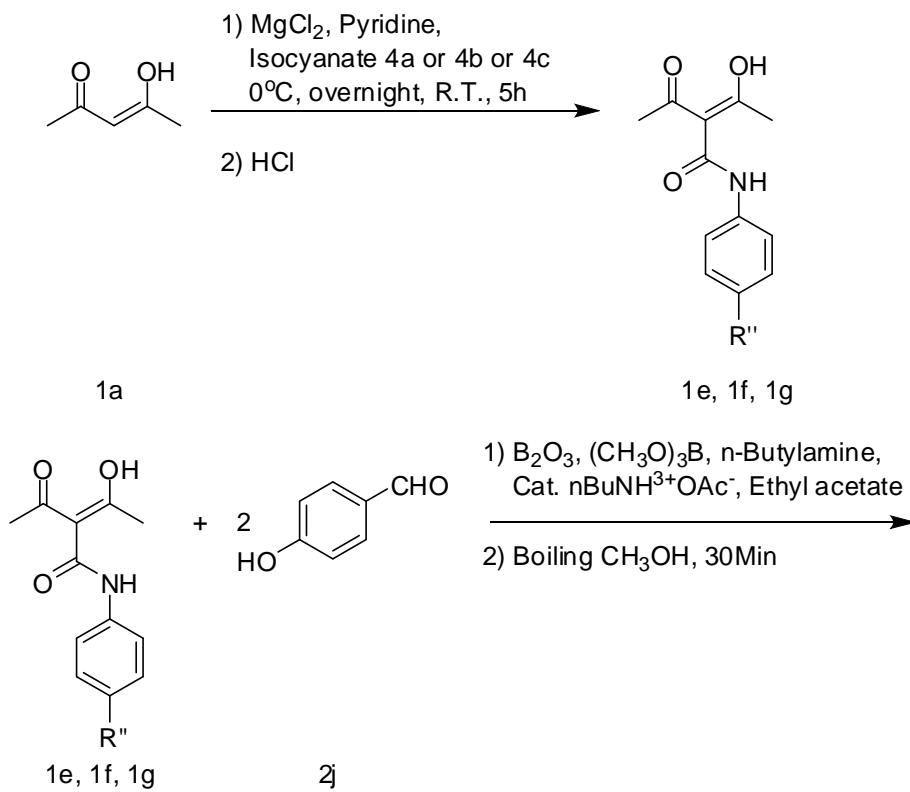
Compound	Name	Yield (%)	Melting Point (°C)
<b>22</b>	CMC2.22	51.7	208-209
<b>23</b>	CMC2.23	46.6	193-194
<b>24</b>	CMC2.24	46.2	220-221

### G. Introduction of a solubilizing group on CMC2.24

Because CMC2.24 (**24**) is tremendously potent in both *in vitro* and *in vivo* studies (data will be shown in the following chapters), modifications were made in an attempt to increase the solubility as well as to maintain the biological efficacy. Firstly, either a chloride or a methoxy group was introduced to the C-4' position in the central phenyl ring of 3-arylamino-carbonyl-2,4-

pentanedione. *In vitro* tests (shown in Chapter 4) revealed that both of these products, namely CMC2.25 (**25**) and CMC2.26 (**26**) are as potent as **24**. In order to obtain compound CMC2.28 (**28**) with potentially increased solubility because of the diol, the corresponding ketal CMC2.27 (**27**) was prepared from 2,4-pentanedione and isocyanate **4c** in the modified Pabon reaction. Isocyanate **4c** was made from the acid **5f** by using diphenylphosphoryl azide which causes a Curtius rearrangement. The product **4c** was used in a condensation with 2,4-pentadione without further purification.<sup>20</sup> Compound **27** was treated with 10% acetic acid in a mixture of methanol and H<sub>2</sub>O to give the desired product **28**. However, according to the *in vitro* data in Chapter 4, these two compounds, **27** and **28**, did not show any desirable inhibitory activity against human-derived MMP-9.

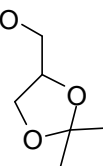




25  $\text{R}'' = -\text{Cl}$

26  $\text{R}'' = -\text{OCH}_3$

27  $\text{R}'' =$



Scheme 3.8 Synthesis of compounds **25-27**

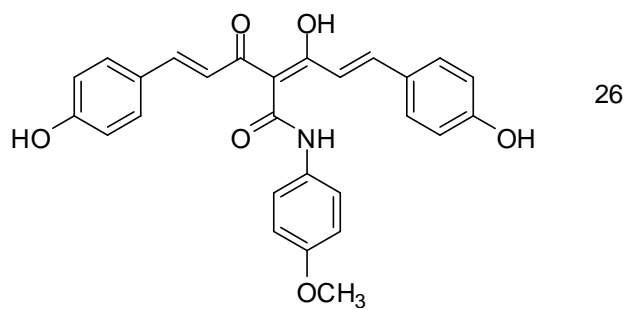
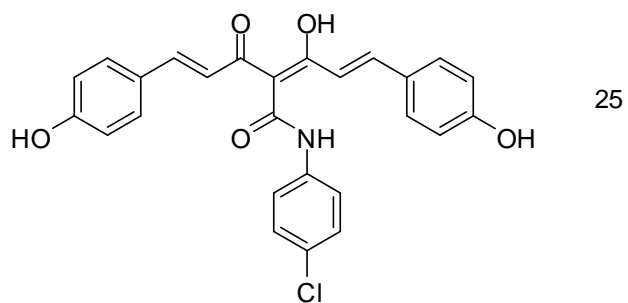
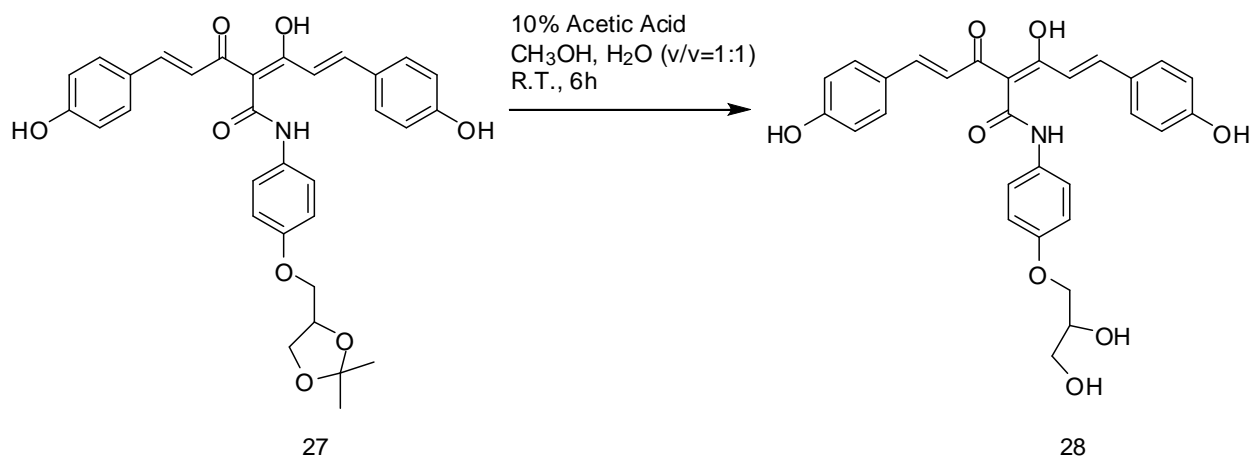
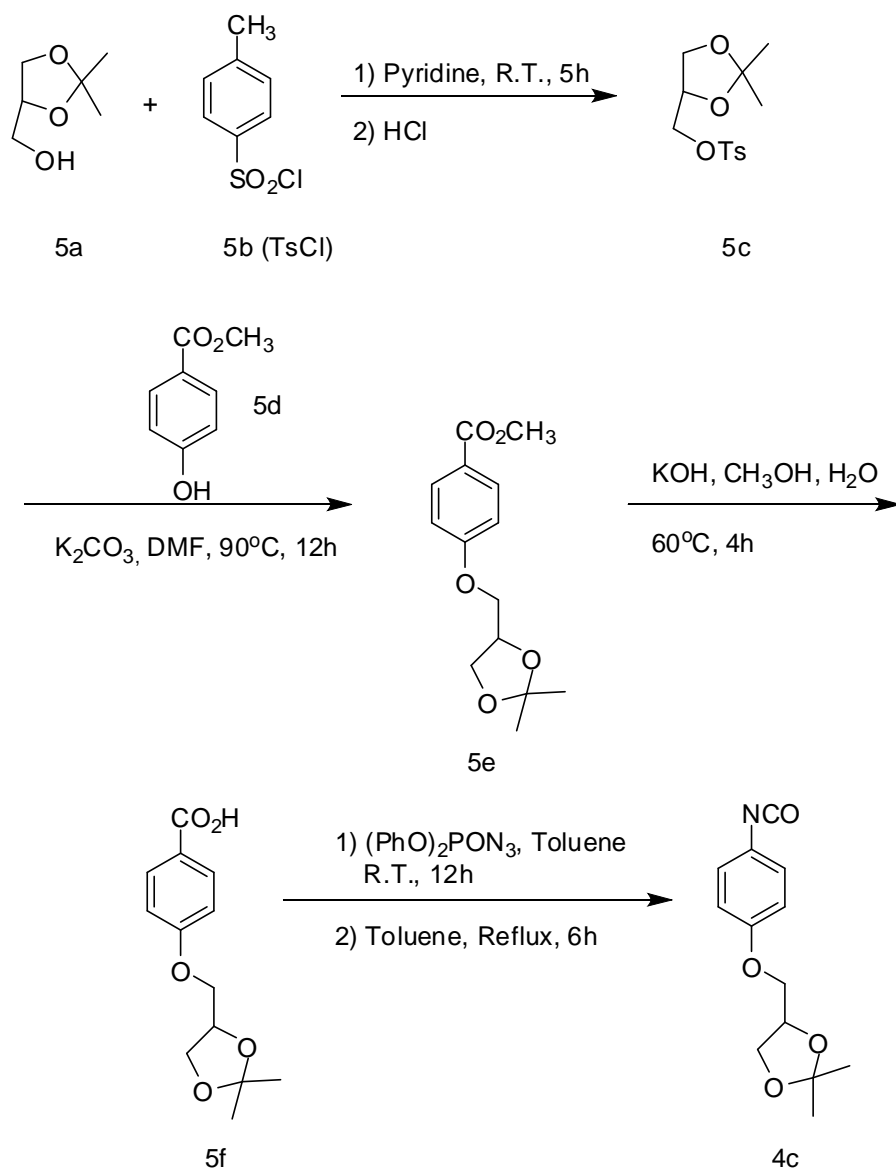


Figure 3.5 Structures of compounds **25**, **26**



Scheme 3.9 Synthesis of compound **28** from compound **27**



Scheme 3.10 Synthesis of compound **4c**

## Materials and Methods

All reagents and solvents employed in this experimental work were reagent grade and were used as such unless otherwise specified. Melting points were taken on a Thomas-Hoover open capillary melting point apparatus and are uncorrected.  $^1\text{H}$  NMR spectra were recorded on a Varian Gemini 300 spectrometer either in  $\text{CDCl}_3$  or  $\text{DMSO-d}_6$ . Chemical shifts are reported in parts per million (ppm) relative to TMS. Mass spectra were recorded on either a Thermo

Electron DSQ GC/MS equipped with a solid probe inlet and EI ionization or an Agilent 1100LC (API-ES)/MSD-VL( $m/z=50-1500$ ) using electrospray ionization. Thin-layer chromatography (TLC) was performed on silica gel sheets (Tiedel-deHa *ën*, Sleeze, Germany). After appropriate purification all new products showed a single spot on TLC analysis in the following solvent systems: 25% ethyl acetate in hexanes and 10% methanol in dichloromethane. Components were visualized by UV light ( $\lambda=254$  nm). Flash column chromatographic separations were carried out on 60A ° (230–400 mesh) silica gel (TSI Chemical Co., Cambridge, MA). All reactants that were moisture or air-sensitive were conducted under dry nitrogen. The starting materials and reagents, unless otherwise specified, were the best grade commercially available (Sigma-Aldrich, Milwaukee, WI or Fluka Chemie GmbH, Sigma-Aldrich, Germany) and were used without further purification.

### **1. General procedure for the synthesis of 4-substituted-2,4-pentanediones**

2,4-Pentanedione (**1a**) (1.00g, 10mmol) was added to a suspension of magnesium chloride (1.35g, 1.2eq) in 20mL methylene chloride, followed by pyridine(2.13mL, 2.5eq), and the mixture was stirred at 0°C for 1h, then either an alkyl chloroformate or a phenyl isocyanate(1.0eq) was added dropwise at 0°C. The mixture was allowed to warm up to room temperature during 8 hours, and then was poured into 3N aqueous HCl solution (10mL) and extracted with methylene chloride (20mL). The organic layer was washed with 20mL brine solution, dried over sodium sulfate and the solvent was removed under vacuo. The product was then either distilled or recrystallized from an appropriate solvent as required. The essential data for each individual compound are given below.

**3-Methoxycarbonyl-2,4-pentanedione (1b):** Colorless liquid, 68.1% yield. Distilled at 45°C, 0.5mmHg.( lit.<sup>10</sup>, bp 75-76°C, 0.3mmHg) <sup>1</sup>H NMR (DMSO-d<sub>6</sub>, 300MHz): δ 3.00(s, 6H), 3.73(s, 3H), 17.76(s, 1H). ESI (-ve) MS m/z 157.1[M-H]<sup>-</sup>.

**3-Ethoxycarbonyl-2,4-pentanedione (1c):** Colorless liquid, 60.5% yield. Distilled at 60°C, 1.4mmHg.(lit.<sup>21</sup>, bp 88-91°C, 8mmHg) <sup>1</sup>H NMR (DMSO-d<sub>6</sub>, 300MHz): δ 1.25(t, 3H) , 2.30(s, 6H), 4.20(q, 2H), 17.75(s, 1H). ESI (-ve) MS m/z 171.2[M-H]<sup>-</sup>.

**3-Phenylaminocarbonyl-2,4-pentanedione (1d):** White solid, 72.0% yield, mp 118-119°C.(lit.<sup>22</sup>, mp 117-119°C) <sup>1</sup>H NMR (DMSO-d<sub>6</sub>, 300MHz): δ 2.15(s, 6H), 7.08(t, 1H), 7.32(t, 2H), 7.64(d, *J*=8.1Hz, 2H), 10.36(s, 1H), 16.46(s, 1H). ESI (-ve) MS m/z 218.1[M-H]<sup>-</sup>.

**3-(4-Chloro)-phenylaminocarbonyl-2,4-pentanedione(1e):** White solid, 30.5% yield, mp 124-125°C <sup>1</sup>H NMR (CDCl<sub>3</sub>, 300 MHz): δ 2.59(s, 3H) , 2.57(s, 3H) , 7.37(d, *J*=8.7Hz, 2H), 7. 55(d, *J*=8.7Hz, 2H), 12.17(s, 1H), 18.45(s, 1H). ESI (-ve) MS m/z 252.7 [M-H]<sup>-</sup>.

**3-(4-Methoxy)-phenylaminocarbonyl-2,4-pentanedione(1f):** White solid, 34.3% yield, mp 130-131°C. <sup>1</sup>H NMR (CDCl<sub>3</sub>, 300 MHz): δ 2.49(s, 3H) , 2.51(s, 3H), 7.08(t, 1H), 6.88(d, *J*=9.0Hz, 2H), 7. 41(d, *J*=8.7Hz, 2H), 11.91(s, 1H), 18.65(s, 1H). ESI(-ve) MS m/z 248.2[M-H]<sup>-</sup>.

**3-(4-((2,2-Dimethyl-1,3-dioxolan-4-yl)methoxy))-phenylaminocarbonyl-2,4-pentanedione(1g):** White solid, 22.3% yield, mp 105-106°C. <sup>1</sup>H NMR (DMSO-d<sub>6</sub>, 300 MHz): δ 1.29(s, 3H), 1.34(s, 3H), 2.14(s, 6H) , 4.43-4.55(m, 1H), 4.05-4.10(m, 2H), 3.95-3.96(m, 1H), 3.69-3.74(m, 1H), 6.92(d, *J*=9.0Hz, 2H), 7. 54(d, *J*=9.0Hz, 2H), 10.21(s, 1H), 16.42(s, 1H). ESI (-ve) MS m/z 348.1[M-H]<sup>-</sup>.

**4-(4-Methylpiperazinyl-1-yl)benzaldehyde (2e):** Potassium carbonate (3.50g, 25.3mmol) was added to a solution of 4-fluorobenzaldehyde (2.71mL, 3.14g, 25.3mmol) and *N*-methylpiperazine (2.55mL, 2.30g, 23mmol) in DMSO (23mL) and the mixture was heated under reflux (120°C)

for 5h. The reaction mixture was then poured into water (450mL) and extracted with ether (4×20mL). The combined organic layers were washed with water, dried over Na<sub>2</sub>SO<sub>4</sub> and evaporated. The crude material was crystallized from a hexane:ethyl acetate (3:1) to afford **2e** as a pale-yellow crystalline solid, yield 46.0 %, mp 56-57°C.(lit.<sup>23</sup>) <sup>1</sup>H NMR (CDCl<sub>3</sub>, 300MHz) δ 2.35(s, 3H), 2.55(t, *J* = 5.1Hz, 4H), 3.42(t, *J* = 5.1Hz, 4H), 6.90-6.94(m, 2H), 7.74-7.77(m, 2H), 9.78(s, 1H). MS (EI) *m/z* (%) 204 (M<sup>+</sup>, 100), 133(30), 132(35).

**(3Z,5E)-6-(4-Dimethylaminophenyl)-4-hydroxyhexa-3,5-dien-2-one (3a)**: 2,4-Pentanedione (10mmol) and boron oxide (0.49 g, 7mmol, 0.7eq) in a 50 mL flask were heated to 120°C for 5min to form pale-yellow suspension. Aldehyde (10mmol, 1.0eq) and trimethyl borate (4.16g, 40mmol, 4.0eq) were dissolved in ethyl acetate (10mL) and gradually added to reaction mixture. While stirring, 0.05mL of butylamine and 0.2mL of butylammonium acetate in dimethylformamide solution (0.136g/mL) were added. After 1hour, a red precipitate started to form. The whole reaction was stirred at room temperature for 48hours. The precipitate was filtered and dried, then dissolved in methanol (50mL) and boiled for 30 min at 60°C. Methanol was removed by rotary evaporation and the crude product (3a) was purified by crystallization from dichloromethane (20mL) and methanol (20mL); orange-red crystals; mp 136-137°C; <sup>1</sup>H NMR (CDCl<sub>3</sub>, 300 MHz) δ 2.13(s, 3H), 3.03(s, 6H), 5.60(s, 1H), 6.27(d, *J* = 15.6 Hz, 1H), 6.65-6.69(m, 2H), 7.41-7.44(m, 2H), 7.56(d, *J*=15.9 Hz, 1H), 18.46(br s, 1H).

**(±)(2,2-Dimethyl-1,3-dioxolan-4-yl)methyl-4-methylbenzenesulfonate(5c)**: 10mmol racemic 2,2-dimethyl-1,3-dioxolane-4-methanol (Soketal, Sigma-Aldrich, Inc., St. Louis, MO) dissolved in Pyridine (20 mL) at room temperature, followed by the addition of 2.1g p-toluenesulfonyl chloride (p-TsCl, 11.0 mmol, 1.1eq). The reaction mixture was left at room temperature for 5 h, and then worked up by 30mL 1.0 N HCl. 30mL dichloromethane was used to extract the

compound, and removed by rotary evaporation to afford compound 5c.<sup>24</sup> Pale yellow viscous liquid, yield 92%. <sup>1</sup>H NMR (CDCl<sub>3</sub>, 300 MHz) δ 1.31(s, 3H), 1.34(s, 3H), 2.45(s, 3H), 3.82-3.85(m, 1H), 3.87-3.94(m, 1H), 3.95-4.00 (m, 2H), 4.28-4.41(m, 1H), 7.36(d, 2H, *J*=8.7Hz), 7.77(d, 2H, *J*=8.7Hz).

**(±)4-((2,2-Dimethyl-1,3-dioxolan-4-yl)methoxy)-methyl-benzoate (5e):** 2.86g 5c(10mmol) was dissolved in 80mL DMF, followed by the addition of 4-Hydroxybenzoate(5d)(1.52g, 10mmol) and potassium carbonate(2.12g, 15mmol) at room temperature. While stirring, the reaction mixture was heated to 90°C for 12h. The reaction mixture was poured into 500mL of H<sub>2</sub>O after cooling down to room temperature. 200mL dichloromethane was used for extraction, and removed by rotary evaporation. White solid, 86.5%. <sup>1</sup>H NMR (CDCl<sub>3</sub>, 300 MHz) δ 1.47(s, 3H), 1.53(s, 3H), 3.97-4.00(m, 1H), 4.04-4.09(m, 1H), 4.14-4.19(m, 1H), 4.22-4.27(m, 1H), 4.52-4.59(m, 1H), 7.00(d, *J*=9.0, 2H), 8.05(d, *J*=9.0, 2H)

**(±)4-((2,2-Dimethyl-1,3-dioxolan-4-yl)methoxy)-benzoic acid (5f):** 2.66g 5e (10mmol) was added to 50mL methanol, followed by the addition of 15mL 1N KOH in H<sub>2</sub>O. The reaction mixture was left to 60°C for 4h. 20mL 0.5N citric acid was used to neutralize the reaction mixture after cooling down to room temperature. 50mL ethyl acetate was used for extraction, and removed by rotary evaporation.<sup>25</sup> White solid, 95.6% Yield. <sup>1</sup>H NMR (CDCl<sub>3</sub>, 300 MHz) δ 1.41(s, 3H), 1.47(s, 3H), 3.88-3.94(m, 1H), 3.99-4.05(m, 1H), 4.09-4.21(m, 2H), 4.47-4.55(m, 1H), 6.96(d, *J*=9.0, 2H), 8.06(d, *J*=9.0, 2H)

## 2. General method for the synthesis of the curcumin analogues

2,4-Pentanedione or a 3-substituted 2,4-pentanedione (10mmol) and very finely powdered boron oxide (0.49 g, 7mmol, 0.7 eq) were placed in a 50mL flask and heated to 120°C for 5min to form a pale-yellow viscous liquid which was cooled to room temperature. The appropriate aldehyde

(20mmol, 2.0 eq) and trimethyl borate (4.16g, 40mmol, 4.0eq) were dissolved in ethyl acetate (10 mL) and gradually added to reaction mixture over 10 minutes. Thereafter, with stirring, 0.05mL butylamine and 0.2mL butylammonium acetate in dimethylformamide solution (0.136g/mL) was then added. After 1 hour, a red-colored precipitate began to form and stirring was continued at room temperature for 48 hours. The precipitate was removed by filtration, washed with dry ether and air-dried, then dissolved in methanol (50 mL) and boiled for 30 min at 60°C. The methanol was removed by rotary evaporation and the solid crude product was purified by recrystallization from dichloromethane (20 mL) and methanol (20 mL).

**1,7-Bis(4-hydroxy-3-methoxyphenyl)hepta-1E,6E-dien-3,5-dione (1):** From 2,4-pentanedione (**1a**) and 4-hydroxy-3-methoxybenzaldehyde (**2a**); orange crystals, yield 77.0%, mp 175-176°C. (lit.<sup>4</sup>, mp 177-178°C) <sup>1</sup>H NMR (DMSO-d<sub>6</sub>, 300MHz): δ 3.83(s, 6H), 6.05(s, 1H), 6.75(d, *J*=15.6Hz, 2H), 6.81(d, *J*=7.8Hz, 2H), 7.14(d, *J*=8.4Hz, 1H), 7.15(d, *J*=8.1Hz, 1H), 7.31(d, *J*=2.1Hz, 2H), 7.54(d, *J*=15.9 Hz, 2H), 9.66(s, 2H), 16.40 (s, 1H); ESI (-ve) MS *m/z* 367.2[M-H]<sup>-</sup>.

**1,7-Diphenyl-hepta-1E,6E-dien-3,5-dione (2):** From 2,4-pentanedione (**1a**) and benzaldehyde (**2b**); orange crystals, yield 65.1%, mp 141-142°C. (lit.<sup>4</sup> mp 140.5°C) <sup>1</sup>H NMR (DMSO-d<sub>6</sub>, 300MHz): δ 6.21(s, 1H, =CH), 6.96(d, *J*=15.9Hz, 2H, =CH), 7.41-7.48(m, 6H, Ar-H), 6.65(d, *J*=15.9Hz, 2H, =CH), 7.71-7.75(m, 4H, Ar-H), 16.08(s, 1H, -OH enol). ESI (-ve) MS *m/z* 275.2 [M-H]<sup>-</sup>.

**1,7-Bis(3-pyridyl)-hepta-1E,6E-dien-3,5-dione (3):** From 2,4-pentanedione (**1a**) and 3-pyridinecarboxaldehyde (**2c**); yellow solid, yield 62.3%, mp 171-172°C. <sup>1</sup>H NMR (DMSO-d<sub>6</sub>, 300MHz): δ 6.20(s, 1H), 7.12(d, *J*=16.2Hz, 2H), 7.45-7.49(m, 2H), 7.68(d, *J*=15.9Hz, 2H),



8.18(d,  $J=8.4\text{Hz}$ , 2H), 8.57-8.59(m, 2H), 8.90(d,  $J=1.8\text{Hz}$ , 2H), 15.97(s, 1H). ESI (-ve) MS  $m/z$  277.2[M-H]<sup>-</sup>.

**1,7-Bis(4-N,N-dimethylaminophenyl)-hepta-1E,6E-dien-3,5-dione (4)**: From 2,4-pentanedione (**1a**) and 4-(dimethylamino)benzaldehyde (**2d**); purple crystals, yield 61.1%, mp 212-214°C.(lit. [24] mp 214-215°C) <sup>1</sup>H NMR (DMSO- $d_6$ , 300MHz):  $\delta$  2.98(s, 12H), 5.95(s, 1H), 6.59(d,  $J=15.9\text{Hz}$ , 2H), 6.72(d,  $J=9.0\text{Hz}$ , 4H), 7.50(d,  $J=15.6\text{Hz}$ , 2H), 7.53(d,  $J=8.7\text{Hz}$ , 4H), 16.62(s, 1H). ESI (-ve) MS  $m/z$  365.1[M-H]<sup>-</sup>.

**1,7-Bis(4-(4-methylpiperazinyl-1-yl))hepta-1E,6E-dien-3,5-dione (5)**: From 3-methoxycarbonyl-2,4-pentanedione (**1b**) and 4-(4-methylpiperazinyl-1-yl)benzaldehyde (**2e**); orange-red crystals, yield 46.4%, mp 239-240°C. <sup>1</sup>H NMR (CDCl<sub>3</sub>, 300MHz)  $\delta$  2.36(s, 6H), 2.56(t,  $J = 5.1\text{Hz}$ , 8H), 3.32(t,  $J = 5.0\text{Hz}$ , 8H), 5.74(s, 1H), 6.46(d,  $J = 15.6\text{Hz}$ , 2H), 6.87-6.91(m, 4H), 7.45-7.48(m, 4H), 7.58(d,  $J = 15.6\text{Hz}$ , 2H), 16.20(br s, 1H); ESI (-ve) MS  $m/z$  471.2[M-H]<sup>-</sup>.

**1,7-Bis-phenyl-4-methoxycarbonylhepta-1E,6E-dien-3,5-dione (6)** : From 3-methoxycarbonyl-2,4-pentanedione (**1b**) and benzaldehyde (**2b**); white solid, yield 52.1%, mp 126-127°C. <sup>1</sup>H NMR (DMSO- $d_6$ , 300MHz):  $\delta$  3.92(s, 3H), 7.26(d,  $J=15.6\text{Hz}$ , 2H), 7.45-7.47(m, 6H), 7.72-7.75(m, 4H), 7.82(d,  $J=15.6\text{Hz}$ , 2H), 18.07(s, 1H). ESI (-ve) MS  $m/z$  333.2[M-H]<sup>-</sup>.

**1,7-Bis(4-hydroxy-3-methoxyphenyl)-4-methoxycarbonylhepta-1E,6E-dien-3,5-dione (7)**: From 3-methoxycarbonyl-2,4-pentanedione (**1b**) and 4-hydroxy-3-methoxybenzaldehyde (**2a**); yellow crystals, yield 72.0%, mp 175-176°C. <sup>1</sup>H NMR (DMSO- $d_6$ , 300MHz):  $\delta$  3.82(s, 3H), 3.91(s, 6H), 6.84(d,  $J=7.2\text{Hz}$ , 2H), 7.03(d,  $J= 15.6\text{Hz}$ , 2H), 7.19(d,  $J=8.1\text{Hz}$ , 1H), 7.20(d,  $J=8.4\text{Hz}$ , 1H), 7.28(d,  $J=1.5\text{Hz}$ , 2H), 7.73(d,  $J=15.6\text{Hz}$ , 2H), 9.81(s, 2H), 18.31(s, 1H); ESI (-ve) MS  $m/z$  425.2[M-H]<sup>-</sup>.

**1,7-Bis(3-hydroxyphenyl)-4-methoxycarbonylhepta-1E,6E-dien-3,5-dione (8):** From 3-methoxycarbonyl-2,4-pentanedione (**1b**) and 3-hydroxybenzaldehyde (**2f**); yellow crystals, yield 40.2%, mp 188-189°C. <sup>1</sup>H NMR (DMSO-d<sub>6</sub>, 300MHz): δ 3.91(s, 3H), 6.86(d, *J*=7.8Hz, 2H), 7.08-7.28(m, 8H), 7.73(d, *J*=15.3Hz, 2H), 9.70(s, 2H), 18.11(s, 1H). ESI (-ve) MS m/z 365.2[M-H]<sup>-</sup>.

**1,7-Bis(3-pyridyl)-4-methoxycarbonylhepta-1E,6E-dien-3,5-dione (9):** From 3-methoxycarbonyl-2,4-pentanedione (**1b**) and 3-pyridinecarboxaldehyde (**2c**); yellow solid, yield 38.7%, mp 195-196°C. <sup>1</sup>H NMR (DMSO-d<sub>6</sub>, 300MHz): δ 3.92(s, 3H), 7.38(d, *J*= 15.9Hz, 2H), 7.49(t, 2H), 7.86(d, *J*=15.3Hz, 2H), 8.19(d, *J*=7.5Hz, 2H), 8.61(d, *J*=4.2Hz, 2H), 8.90(s, 2H), 17.89(s, 1H). ESI (-ve) MS m/z 335.2[M-H]<sup>-</sup>.

**1,7-Bis(2-hydroxyphenyl)-4-methoxycarbonylhepta-1E,6E-dien-3,5-dione (10):** From 3-methoxycarbonyl-2,4-pentanedione (**1b**) and 2-hydroxybenzaldehyde (**2g**); yellow crystals, yield 46.3%, mp 165-166°C. <sup>1</sup>H NMR (DMSO-d<sub>6</sub>, 300MHz): δ 3.88(s, 3H), 6.84-6.94(m, 4H), 7.26(d, *J*=15.3Hz, 1H), 7.27(d, *J*=15.3Hz, 1H), 7.29(d, *J*=15.6Hz, 2H), 7.58(d, *J*=7.5Hz, 1H), 7.58(d, *J*=8.1Hz, 1H), 8.01(d, *J*=15.6Hz, 2H), 10.42 (s, 2H), 18.11(s, 1H); ESI (-ve) MS m/z 365.2[M-H]<sup>-</sup>.

**1,7-Bis(4-N,N-dimethylaminophenyl)-4-methoxycarbonylhepta-1E,6E-dien-3,5-dione (11)** From 3-methoxycarbonyl-2,4-pentanedione (**1b**) and 4-(dimethylamino)benzaldehyde (**2d**); purple crystals, yield 45.1%, mp 224-225°C. <sup>1</sup>H NMR (DMSO-d<sub>6</sub>, 300MHz): δ 3.01(s, 12H), 3.89(s, 3H), 6.74(d, *J*=8.7Hz, 4H), 6.88(d, *J*=15.3 Hz, 2H), 7.53(d, *J*=9.0 Hz, 4H), 7.70(d, *J*=15.3 Hz, 2H), 18.47(s, 1H); ESI (-ve) MS m/z 419.2[M-H]<sup>-</sup>.

**1,7-Bis(3-nitro-4-hydroxy-5-methoxyphenyl)-4-methoxycarbonylhepta-1E,6E-dien-3,5-dione (12):** From 3-methoxycarbonyl-2,4-pentanedione (**1b**) and 4-hydroxy-3-methoxy-5-

nitrobenzaldehyde (**2h**); orange solid, yield 26.0%, mp 207-208°C. <sup>1</sup>H NMR (DMSO-d<sub>6</sub>, 300MHz): δ 3.92(s, 3H), 3.94(d, *J*=1.5Hz, 6H), 6.98(d, *J*=15.9Hz, 1H), 7.21(d, *J*=13.5Hz, 1H), 7.61(d, *J*=15.9Hz, 1H), 7.63(d, *J*=13.5Hz, 2H), 7.77(d, *J*=15.6Hz, 1H), 7.84(d, *J*=9.3Hz, 2H), 11.03(s, 2H), 18.06(s, 1H). ESI (-ve) MS m/z 515.0 [M-H]<sup>-</sup>.

**1,7-Bis(4-hydroxy-3,5-dimethoxyphenyl)-4-methoxycarbonylhepta-1E,6E-dien-3,5-dione**

(**13**): From 3-methoxycarbonyl-2,4-pentanedione (**1b**) and 4-hydroxy-3,5-dimethoxybenzaldehyde (**2i**); yellow crystals, yield 77.0%, mp 179-180°C. <sup>1</sup>H NMR (DMSO-d<sub>6</sub>, 300MHz): δ 3.82(s, 12H), 3.92(s, 3H), 7.03(s, 5H), 7.09(s, 1H), 7.73(d, *J*=15.6Hz, 2H), 9.18(s, 2H), 18.30(s, 1H); ESI (-ve) MS m/z 485.2[M-H]<sup>-</sup>.

**1,7-Bis(4-hydroxyphenyl)-4-methoxycarbonylhepta-1E,6E-dien-3,5-dione** (**14**):

From 3-methoxycarbonyl-2,4-pentanedione (**1b**) and 4-hydroxybenzaldehyde (**2j**); yellow crystals, yield 49.2%, mp 214-216°C. <sup>1</sup>H NMR (DMSO-d<sub>6</sub>, 300MHz): δ 3.90(s, 3H), 6.83(d, *J*=8.4Hz, 4H), 6.99(d, *J*=15.6Hz, 2H), 7.58(d, *J*=8.7Hz, 4H), 7.73(d, *J*=15.6Hz, 2H), 10.17(s, 2H), 18.27(s, 1H); ESI (-ve) MS m/z 365.2[M-H]<sup>-</sup>.

**1,7-Bis(4-acetoxy-3-methoxyphenyl)-4-methoxycarbonylhepta-1E,6E-dien-3,5-**

**dione** (**15**): From 3-methoxycarbonyl-2,4-pentanedione (**1b**) and 4-acetoxy-3-methoxybenzaldehyde (**2k**); pale-yellow crystals, yield 46.0%, mp 169-170°C. <sup>1</sup>H NMR (DMSO-d<sub>6</sub>, 300MHz): δ 2.27(s, 6H), 3.84(s, 6H), 3.92(s, 3H), 7.17(d, *J*=8.4Hz, 2H), 7.26(d, *J*=15.9Hz, 2H), 7.36(d, *J*=8.1Hz, 2H), 7.49(s, 2H), 7.81(d, *J*=15.3 Hz, 2H), 18.04(s, 1H, -OH); ESI (-ve) MS m/z 509.2[M-H]<sup>-</sup>.

**1,7-Bis(4-hydroxy-3-methoxyphenyl)-4-ethoxycarbonylhepta-1E,6E-dien-3,5-dione** (**16**):

From 3-ethoxycarbonyl-2,4-pentanedione (**1c**) and 4-hydroxy-3-methoxybenzaldehyde (**2a**); yellow crystals, yield 44.6%. mp 158-159°C. <sup>1</sup>H NMR (DMSO-d<sub>6</sub>, 300MHz): δ 1.32-1.37(t, 3H),

3.82(s, 6H), 4.39(q, 2H), 6.84(d,  $J=8.1\text{Hz}$ , 2H), 7.08(d,  $J=15.3\text{Hz}$ , 2H), 7.17(d,  $J=8.1\text{Hz}$ , 1H), 7.17(d,  $J=8.1\text{Hz}$ , 1H), 7.26(d,  $J=1.5\text{Hz}$ , 2H), 7.72(d,  $J=15.9\text{Hz}$ , 2H), 9.80(s, 2H), 18.30(s, 1H); ESI (-ve) MS  $m/z$  439.2[M-H]<sup>-</sup>.

**1,7-Bis(4-(4-methylpiperazinyl-1-yl)phenyl)-4-methoxycarbonylhepta-1E,6E-dien-3,5-dione**

**(17)**: From 3-methoxycarbonyl-2,4-pentanedione (**1b**) and 4-(4-methylpiperazinyl-1-yl)benzaldehyde (**2e**); dark-red crystals, 49.2% yield, mp 191-192°C. <sup>1</sup>H NMR (CDCl<sub>3</sub>, 300MHz)  $\delta$  3.04(s, 6H), 3.94(s, 3H), 6.65-6.69(m, 4H), 7.00(d,  $J = 14.4\text{Hz}$ , 2H), 7.46-7.49 (m, 4H), 7.78 (d,  $J = 15.3\text{Hz}$ , 2H), 15.69 (br s, 1H). ESI (-ve) MS  $m/z$  529.2[M-H]<sup>-</sup>.

**1,7-Bis(2-hydroxy-3-methoxyphenyl)-4-methoxycarbonylhepta-1E,6E-dien-3,5-dione (18)**:

From 3-methoxycarbonyl-2,4-pentanedione (**1b**) and 2-hydroxy-3-methoxybenzaldehyde (**2l**); yellow crystals, yield 25.8%, mp 201-202°C. <sup>1</sup>H NMR (DMSO-d<sub>6</sub>, 300MHz):  $\delta$  3.82(s, 6H), 3.88(s, 3H), 6.83(t, 2H), 7.04(d,  $J=7.5\text{Hz}$ , 2H), 7.18(d,  $J=7.5\text{Hz}$ , 2H), 7.26(d,  $J=15.9\text{Hz}$ , 2H), 8.04(d,  $J=15.6\text{Hz}$ , 2H), 9.62(s, 2H), 18.13(s, 1H); ESI (-ve) MS  $m/z$  425.2[M-H]<sup>-</sup>.

**1,7-bis(4-hydroxy-3-methoxyphenyl)-4-methoxycarbonylheptane-3,5-dione (19)**:

7 (0.426g, 1mmol) was added to 10mL ethyl acetate, followed by catalytic amount of 10% Pd/C. The reaction mixture was stirred under the atmosphere of H<sub>2</sub> for 2 hours, and then filtered through Celite. The solvent was removed by rotary evaporation, and the solid crude product was purified by recrystallization from dichloromethane (4mL) and methanol (6mL). Pale-yellow solid, yield 52.1%, mp 92-94°C. <sup>1</sup>H NMR (DMSO-d<sub>6</sub>, 300MHz):  $\delta$  2.62-2.84(m, 8H), 3.71(s, 3H), 3.72(s, 6H), 6.54(d,  $J=1.8\text{Hz}$ , 1H), 6.57(d,  $J=2.1\text{Hz}$ , 1H), 6.63(d,  $J=2.7\text{Hz}$ , 1H), 6.65(d,  $J=2.7\text{Hz}$ , 1H), 6.74(d,  $J=1.5\text{Hz}$ , 2H), 8.73(s, 2H), 17.57(s, 1H); ESI (-ve) MS  $m/z$  429.2[M-H]<sup>-</sup>.

**1-(4-Dimethylaminophenyl)-7-(4-hydroxy-3-methoxyphenyl)-hepta-1E,6E-dien-3,5-dione**

**(20)**: From 4-hydroxy-3-methoxybenzaldehyde (**2a**) and (3Z,5E)-6-(4-dimethylaminophenyl)-4-

hydroxyhexa-3,5-dien-2-one (**3a**); orange-red crystals; mp 171-172°C; <sup>1</sup>H NMR (CDCl<sub>3</sub>, 300 MHz) δ 3.07(s, 6H), 3.95(s, 3H), 5.77(s, 1H), 5.83(br s, 1H), 6.43(d, J=15.9Hz, 1H), 6.47(d, J=15.9Hz, 1H), 6.66-6.70(m, 2H), 6.93(d, J=9.0Hz, 1H), 7.05(d, J=2.1Hz, 1H), 7.11 (dd, J=8.2, 1.7Hz, 1H), 7.44-7.48(m, 4H), 7.55(d, J=15.9Hz, 1H), 7.63(d, J = 15.9Hz, 1H), 16.20(br s, 1H); MS (EI) m/z (%) 364 (M<sup>+</sup>, 60), 267 (100), 188 (35), 174 (100), 147 (50), 146 (50), 134 (100).

**1-(4-Dimethylaminophenyl)-7-((4-N-methylpiperazin-1-yl)phenyl)-hepta-1E,6E-dien-3,5-dione (21)**: From 4-(4-N-methylpiperazin-1-yl)benzaldehyde (**2e**) and (3Z,5E)-6-(4-dimethylaminophenyl)-4-hydroxyhexa-3,5-dien-2-one (**3a**); orange-red crystals; mp 242-243°C; <sup>1</sup>H NMR (CDCl<sub>3</sub>, 300 MHz) δ 2.36(s, 3H), 2.56(t, J = 5.2Hz, 4H), 3.03(s, 6H), 3.31(t, J = 5.0Hz, 4H), 5.74(s, 1H), 6.43(d, J = 15.6Hz, 1H), 6.46(d, J = 15.6Hz, 1H), 6.66-6.70(m, 2H), 6.87-6.91(m, 2H), 7.44-7.47(m, 4H), 7.57 (d, J = 15.9Hz, 1H), 7.61 (d, J = 15.9Hz, 1H), 16.27 (br s, 1H); MS (EI) m/z (%) 417 (M<sup>+</sup>, 40), 321 (75), 266 (30), 189 (40), 188 (40), 174 (95), 147 (45), 146 (50), 134 (100).

**1,7-Bis(4-dimethylaminophenyl)-4-N-phenylaminocarbonylhepta-1E,6E-dien-3,5-dione (22)**: From 3-phenylaminocarbonyl-2,4-pentanedione (**1c**) and 4-(dimethylamino)benzaldehyde (**2d**); purple crystals, yield 51.7%, mp 208-209°C. <sup>1</sup>H NMR (DMSO-d<sub>6</sub>, 300MHz): δ 2.96(s, 12H), 6.59(d, J=15.6Hz, 2H), 6.69(d, J=8.1Hz, 4H), 7.13(t, 1H), 7.39-7.42(m, 6H), 7.66(d, J=15.3Hz, 2H), 7.73(d, J=8.1Hz, 2H), 10.56(s, 1H), 17.78(s, 1H). ESI (-ve) MS m/z 480.2[M-H].

**1,7-Bis(4-hydroxy-3-methoxyphenyl)-4-N-phenylaminocarbonylhepta-1E,6E-dien-3,5-dione (23)**: From 3-phenylaminocarbonyl-2,4-pentanedione (**1c**) and 4-hydroxy-3-methoxybenzaldehyde (**2a**); orange crystals, yield 46.6%, mp 193-194°C. <sup>1</sup>H NMR (DMSO-d<sub>6</sub>, 300 MHz): δ 3.70(s, 6H), 6.73(d, J=15.6 Hz, 2H), 6.79(d, J=8.1Hz, 2H), 7.08-7.15(m, 5H),

7.37(t, 2H), 7.69(d, J=3.9Hz, 2H), 7.72(d, J=3.9Hz, 2H), 9.79(s, 2H), 10.59(s, 1H), 17.56(s, 1H); ESI (-ve) MS m/z 486.2[M-H]<sup>-</sup>.

**1,7-Bis(4-hydroxyphenyl)-4-N-phenylaminocarbonylhepta-1E,6E-dien-3,5-dione (24):**

From 3-phenylaminocarbonyl-2,4-pentanedione (**1c**) and 4-hydroxybenzaldehyde (**2j**); yellow crystals, yield 46.2%, mp 220-221°C. <sup>1</sup>H NMR (DMSO-d<sub>6</sub>, 300MHz): δ 6.68(d, J=15.6Hz, 4H), 6.79(d, J=8.7Hz, 4H), 7.13(t, 1H), 7.38(t, 2H), 7.45(d, J=9.0 Hz, 2H), 7.70(d, J=6.3Hz, 2H), 7.72(d, J=9.0Hz, 2H), 10.14(s, 2H), 10.61(s, 1H), 17.56(s, 1H); ESI (-ve) MS m/z 426.2[M-H]<sup>-</sup>.

**1,7-Bis(4-hydroxyphenyl)-4-N-(4-chloro)-phenylaminocarbonylhepta-1E,6E-dien-3,5-dione**

**(25):** From 3-(4-chloro)-phenylaminocarbonyl-2,4-pentanedione (**1e**) and 4-hydroxybenzaldehyde (**2j**); orange crystals, yield 41.6%, mp 202-203°C. <sup>1</sup>H NMR (DMSO-d<sub>6</sub>, 300 MHz): δ 6.66(d, J=15.6Hz, 2H), 6.78(d, 4H, J=8.7Hz), 7.41-7.47(t, 6H), 7.71(d, J=15.6Hz, 2H), 7.76(d, J=8.7 Hz, 2H), 10.16(s, 2H), 10.73(s, 1H), 17.59(s, 1H); ESI (-ve) MS m/z 460.6 [M-H]<sup>-</sup>.

**1,7-Bis(4-hydroxyphenyl)-4-N-(4-methoxy)-phenylaminocarbonylhepta-1E,6E-dien-3,5-**

**dione (26):** From 3-(4-methoxy)-phenylaminocarbonyl-2,4-pentanedione(**1f**) and 4-hydroxybenzaldehyde (**2j**); yellow crystals, yield 52.3%, mp 220-221°C. <sup>1</sup>H NMR (DMSO-d<sub>6</sub>, 300 MHz): δ 3.75(s, 3H), 6.67(d, J=15.6Hz, 2H), 6.79(d, J=9.0Hz, 2H), 6.94(d, J=9.0Hz, 2H), 7.45(d, J=9.0 Hz, 4H), 7.63(d, J=9.0Hz, 2H), 7.69(d, J=15.3 Hz, 2H), 10.15(s, 2H), 10.46(s, 1H), 17.51(s, 1H); ESI (-ve) MS m/z 456.2 [M-H]<sup>-</sup>.

**(±)-1,7-Bis(4-hydroxyphenyl)-4-N-(4-((2,2-dimethyl-1,3-dioxolan-4-yl)methoxy))**

**-phenylaminocarbonylhepta-1E,6E-dien-3,5-dione(27)**

From 3-(4-((2,2-dimethyl-1,3-dioxolan-4-yl)methoxy))-phenylaminocarbonyl-2,4-pentanedione(**1g**) and 4-hydroxybenzaldehyde (**2j**); red crystals, yield 17.6%, mp 210-212°C. <sup>1</sup>H

NMR (DMSO-d<sub>6</sub>, 300 MHz):  $\delta$  1.30(s, 3H), 1.36(s, 3H), 3.72-3.77(m, 1H), 3.92-4.12(m, 3H), 4.36-4.46(m, 1H), 6.67(d,  $J=15.3\text{Hz}$ , 2H), 6.79(d,  $J=8.7\text{Hz}$ , 4H), 6.97(d,  $J=9.0\text{Hz}$ , 2H), 7.45(d,  $J=8.7\text{Hz}$ , 4H), 7.63(d,  $J=9.0\text{Hz}$ , 2H), 7.70(d,  $J=15.3\text{Hz}$ , 2H), 10.14(s, 2H), 10.47(s, 1H), 17.52(s, 1H); ESI (-ve) MS m/z 557.2 [M-H]<sup>-</sup>.

**(±)-1,7-Bis(4-hydroxyphenyl)-4-N-(4-(2,3-dihydroxypropoxy)phenyl)-**

**phenylaminocarbonylhepta-1E,6E-dien-3,5-dione(28):** 200mg of **27** was added to 8mL of methanol and H<sub>2</sub>O mixture(v/v=1:1), followed by the addition of 2mL of 10% acetic acid. The reaction was left at room temperature for 6 h until TLC showed no starting material **27**. Then 20mL was used for extraction, and removed by rotary evaporation. Crude product **28** was purified by column chromatography (silica, CH<sub>2</sub>Cl<sub>2</sub>/MeOH = 90:10).<sup>26</sup> Brown solid, yield 24.3%, mp 234-236°C. <sup>1</sup>H NMR (DMSO-d<sub>6</sub>, 300 MHz):  $\delta$  3.42-3.45(m, 2H), 3.72-3.86(m, 3H), 4.62(br, s, 1H), 4.85(br, s, 1H), 6.67(d,  $J=15.9\text{Hz}$ , 2H), 6.75-6.80(m, 4H), 6.94(d,  $J=9.0\text{Hz}$ , 2H), 7.43-7.49(m, 4H), 7.62(d,  $J=9.0\text{Hz}$ , 2H), 7.69(d,  $J=15.3\text{Hz}$ , 2H), 10.15(s, 2H), 10.46(s, 1H), 17.52(s, 1H); ESI (-ve) MS m/z 517.2 [M-H]<sup>-</sup>.

## References

1. Lampe, V.; Milobedzka, J.; Kostanecki, St. V. Zur Kenntnis des Curcumins. *Berichte.*, **1910**, *43*, 2163
2. Lampe, V. Synthese von Curcumin. *Ber. Dtsch. Chem. Ges.*, **1918**, *51*, 1347-1355;
3. Pavolini, T. Nuova sintesi della Curcumina. *Riv. Ital. Essenze, Profumi, Piante Officinali*, **1937**, *19*, 167-168
4. Pabon, H.J.J. A synthesis of curcumin and related compounds. *RECUEIL.*, **1964**, *83*, 379-386

5. Pedersen, U.; Rasmussen, P.B.; Lawesson, S.O. Synthesis of naturally occurring curcuminoids and related compounds. *Liebigs Ann. Chem.*, **1985**, 1557-1569
6. [http://www.chemicalbook.com/ProductMSDSDetailCB1126251\\_EN.htm](http://www.chemicalbook.com/ProductMSDSDetailCB1126251_EN.htm) for physical properties of trimethyl borate
7. [http://www.chemicalbook.com/ChemicalProductProperty\\_EN\\_CB4145842.htm](http://www.chemicalbook.com/ChemicalProductProperty_EN_CB4145842.htm) for physical properties of tributyl borate
8. Chen, S.Y.; Chen, Y.; Li, Y.P.; Chen, S.H.; Tan, J.H.; Ou, T.M.; Gu, L.Q.; Huang, Z.S. Design, synthesis, and biological evaluation of curcumin analogues as multifunctional agents for the treatment of Alzheimer's disease. *Bioorg. Med. Chem.*, **2011**, *19*, 5596-5604
9. Anand, P.; Kunnumakkara, A.B.; Newman, R.A.; Aggarwal, B.B. Bioavailability of curcumin: problems and promises. *Mol. Pharm.*, **2007**, *4*, 807-818
10. Bingham, S.J.; Tyman, J.H.P. Improved synthesis of alkyl diacetylacetates. *Organic Preparations and Procedures INT.*, **2001**, *33*, 357-409
11. Ireson, C.R.; Jones, D.J.; Orr, S.; Coughtrie, M.W.; Boocock, D.J.; Williams, M.L.; Farmer, P.B.; Steward, W.P.; Gescher, A.J. Metabolism of the cancer chemopreventive agent curcumin in human and rat intestine. *Cancer Epidemiol Biomarkers Prev.*, **2002**, *11*, 105-111
12. Ireson, C.; Orr, S.; Jones, D.J.; Verschoyle, R.; Lim, C.K.; Luo, J.L.; Howells, L.; Plummer, S.; Jukes, R.; Williams, M.; Steward, W.P.; Gescher, A. Characterization of metabolites of the chemopreventive agent curcumin in human and rat hepatocytes and in the rat in vivo, and evaluation of their ability to inhibit phorbol ester-induced prostaglandin E2 production. *Cancer Res.*, **2001**, *61*, 1058-1064



13. Clemens, M.; Kang, D.; Napolitano, N.; Lee, H.M.; Golub, L.M.; Gu, Y. LPS or CRP/oxLDL Cholesterol-Complex: Temporal Study of Cytokine/MMP Production. *J. Dent. Res.*, **2011**, *90*, Special Issue 2284
14. Napolitano, N.; Kang, D.; Clemens, M.; Lee, H.M.; Johnson, F.; Golub, L.M.; Gu, Y. Chemically Modified Curcumins Suppress Human Mononuclear Cell Cytokines. *J. Dent. Res.*, **2011**, *90*, Special Issue 2292
15. Clemens, M.; Napolitano, N.; Lee, H.M.; Zhang, Y.; Johnson, F.; Golub, L.M.; Gu, Y. Chemically modified Curcumin Normalizes Chronic Inflammation in Diabetic Rats. *J. Dent. Res.*, **2012**, *91*, Special Issue 1526
16. Napolitano, N.; Clemens, M.; Lee, H.M.; Zhang, Y.; Johnson, F.; Golub, L.M.; Gu, Y. Novel Curcumin Derivatives Suppress Inflammatory Mediators in Periodontally-relevant Cells. *J. Dent. Res.*, **2012**, *91*, Special Issue 1527
17. Elburki, M.; Lee, H.M.; Gupta, N.; Balacky, P.; Zhang, Y.; Johnson, F.; Zhang, Y.; Golub, L.M. Chemically-Modified Curcumins Inhibit Alveolar Bone Loss in Diabetic Rats with Periodontitis. *J. Dent. Res.*, **2012**, *91*, Special Issue 1528
18. Yu, H.W.; Zhang, Y.; Zhang, Y.; Lee, H.M.; McClain, S.A.; Johnson, F.; Golub, L.M.. A Novel Chemically-modified Curcumin (CMC2.24) Improves Diabetic Wound-Healing. *J. Dent. Res.*, **2012**, *91*, Special Issue 1529
19. Katzap, E.; Goldstein, M.J.; Shah, N.V.; Schwartz, J.; Razzano, P.; Golub, L.M.; Johnson, F.; Greenwald, R.; Grande, D. The chondroprotective capability of curcumin (*curcuma longa*) and its derivatives against IL-1 $\beta$  and OsM-mediated chondrolysis. *Trans. Orthoped. Res. Soc.*, **2011**, *36*

20. Banfi, L.; Basso, A.; Bevilacqua, E.; Gandolfo, V.; Giannini, G.; Guanti, G.; Musso, L.; Paravidino, M.; Riva, R. Synthesis and DNA-cleaving activity of lactenediynes conjugated with DNA-complexing moieties. *Bioorg. Med. Chem.*, **2008**, *16*, 3501-3518
21. Buechi, G.; Wuest, H. Synthetic Studies on Damascenones. *Helvetica Chimica Acta*, **1971**, *54*, 1767-1775
22. Eckberg, R.P.; Nelson, J.H.; Kenney, J.W.; Howells, P.N.; Henry, R.A. Reactions of bis(2,4-pentanedionato)nickel(II) with isocyanates and other electrophiles. Electrophilic addition to 2,4-pentanedione catalyzed by bis(2,4-pentanedionato)nickel(II) *Inorganic Chemistry*, **1977**, *16*, 3128-3129
23. O'Brien, P.M.; Sliskovic, D.R.; Blankley, C. J.; Roth, B.D.; Wilson, M.W.; Hamelehle, K.L.; Krause, B.R.; Stanfield, R.L. Inhibitors of Acyl-CoA:Cholesterol O-Acyl Transferase (ACAT) as Hypocholesterolemic Agents. 8. Incorporation of Amide or Amine Functionalities into a Series of Disubstituted Ureas and Carbamates. Effects on ACAT Inhibition in vitro and Efficacy in vivo. *J. Med. Chem.*, **1994**, *37*, 1810-1822
24. Zhou, D.; Lagoja, I.M.; Rozenski, J.; Busson, R.; Van Aerschot, A.; Herdewijn, P. Synthesis and properties of aminopropyl nucleic acids. *Chembiochem*, **2005**, *6*, 2298-2304
25. Khurana, J.M.; Sehgal, A. An efficient and convenient procedure for ester hydrolysis. *OPPI BRIEFS*, **1994**, *26*, 580-583
26. Lawbart, M.L.; Schneider, J.J. Preparation and properties of steroidal 17,20- and 20,21-acetonides epimeric at C-20. I. Derivatives of 5.beta.-pregnan-3.alpha.-ol. *J. Org. Chem.*, **1969**, *34*, 3505-3512

## Chapter 4. *In vitro* potency of curcumin and chemically-modified curcumins (CMCs)

### A. Introduction

The inhibitory concentration at 50% ( $IC_{50}$ ) is a crucial measure of efficacy of a compound in any functions related to biological or biochemical processes. In this chapter, an *in vitro* enzymology study is described for both curcumin and the CMCs using a variety of MMPs. A preliminary *in vitro* MMP-9 inhibitory assay was first conducted for the first 21 synthesized compounds, by using an HPLC method that was used in previous evaluations of tetracycline.<sup>1</sup> Curcumin, CMC2.5, CMC2.14 showed great potency against human-derived MMP-9 *in vitro*, and were then selected for further study. Two other compounds, CMC2.23 and CMC2.24, where an N-phenylamino carbonyl group had been introduced, were evaluated together with the active compounds from the preliminary study. These five compounds, as well as 1,10-phenanthroline, a known zinc chelator and inhibitor of MMPs, were evaluated in the fluorogenic inhibitory assays against MMP-1, -2, -3, -7, -8, -9, -12, -13 and -14 *in vitro*.<sup>2</sup> Each enzyme individually was incubated with the MMP-susceptible fluorogenic peptide substrate, Mca-K-P-L-G-Dpa-A-R-NH<sub>2</sub>. For each compound, the micromolar ( $\mu$ M) concentration of  $IC_{50}$  that was responsible for the proteolytic activity of the MMP was determined from a plot of the percentage of the inhibition versus the concentrations of the inhibitor. CMC2.24 showed great potency against most of the MMPs tested in the assay. In addition, four newer CMCs, namely CMC2.25, CMC2.26, CMC2.27 and CMC2.28, were then studied against human-derived MMP-9 *in vitro* by the fluorogenic assay, where CMC2.25 and CMC2.26 showed similar potency to CMC2.24.

### B. Preliminary study of curcumin and CMCs in MMP-9 inhibition by an HPLC method

In order to evaluate the *in vitro* potency of curcumin and CMCs as inhibitors of MMP-9, the inhibition assay was carried out by an HPLC method.<sup>1</sup> DNP-octapeptide containing a gly-ileu

susceptible linkage was used as substrate, and 1,10-phenanthroline, a zinc cation binding agent traditionally used to quench *in vitro* MMP activity reactions, was used as the positive control for the experiment. All of the data are the average (Ave.) of three analyses with standard error of deviation (S.D.) and mean (S.E.M.). From the data shown in Table 4.1, the first two chemically-modified curcumins that were prepared had unsubstituted phenyl or pyrid-3-yl rings at the termini of the 7-carbon chain (CMC2.2 and CMC2.3), but these two compounds were found to be inactive against human derived MMP-9. At this point a methoxycarbonyl group was introduced at the carbon-4 position of thirteen related CMCs in an attempt to increase both solubility and zinc-binding efficacy. From the preliminary data, some of these methoxycarbonyl analogues including CMC2.5 and CMC2.14 showed significant potency compared to the analogues with no carbon-4 substitution such as CMC2.2 and CMC2.3, and also the analogues with unsubstituted phenyl side chains such CMC2.4. Some other side chain modifications including the introduction of dimethylamino-, nitro-, methoxy-, 4-methylpiperazinyl were also made, namely CMC2.11, CMC2.12, CMC2.13, CMC2.17. Also a tetrahydrocurcumin analogue of CMC2.5 was prepared, namely CMC2.9. However, this compound didn't show any inhibitory efficacy against MMP-9 *in vitro*. One ethoxycarbonyl curcumin analogue was also prepared, namely CMC2.16, which was no more soluble or potent than the analogue, CMC2.5 having a methoxycarbonyl group at carbon-4. When a 4-*N*-methylpiperazinyl substituent was introduced as in CMC2.17 or CMC2.19, in an attempt to increase the solubility, these two compounds were inactive against MMP-9 *in vitro*. Also two unsymmetrical curcumin analogues, namely CMC2.20 and CMC2.21, showed no improved inhibitory activity. Studies were focused on the two significantly active compounds having a 4-methoxycarbonyl, namely CMC2.5, and 4-methoxycarbonyl bis(demethoxy)curcumin (CMC2.14). However, at the time when the N-

phenylamino carbonyl group was introduced at C-4, the substrate, DNP-octapeptide containing gly-ileu susceptible peptide used or the HPLC assay was not available from the supplier. Thus the biological evaluation of the newer compounds was completed by a fluorogenic assay as noted in Section 4.3 of this chapter.

Table 4.1 *In vitro* IC<sub>50</sub> (μM) of curcumin and the CMCs against MMP-9

Note: An HPLC inhibition assay was used. 1,10-Phenanthroline, the standard zinc chelating agent was used as a positive control. DNP-octapeptide containing gly-ileu susceptible peptide was used as the substrate. Each value represents the mean of at 3 analyses (±S.E.M.).

Compound		IC <sub>50</sub> (μM)	% Inhibition at 100 μM
	1,10-Phenanthroline	15.3 ±5.5	100
1	Curcumin	18.5 ±6.5	58.1 ±5.7
2	CMC2.2	>100	<50
3	CMC2.3	>100	<50
4	CMC2.7	>100	<50
5	CMC2.19	43.7 ±4.7	63.9 ±4.2
6	CMC2.4	>100	<50
7	CMC2.5	56.3 ±6.9	67.5 ±8.0
8	CMC2.6	72.6 ±5.2	52.3 ±13.1
9	CMC2.8	>100	<50
10	CMC2.10	23.0 ±4.2	73.3 ±11.9
11	CMC2.11	>100	<50
12	CMC2.12	>100	<50
13	CMC2.13	>100	<50

14	CMC2.14	22.6±1.8	89.2±6.5
15	CMC2.15	61.1±2.6	67.5±12.4
16	CMC2.16	26.3±3.5	76.7±9.6
17	CMC2.17	>100	<50
18	CMC2.18	65.3±4.9	62.8±8.5
19	CMC2.9	>100	<50
20	CMC2.20	>100	<50
21	CMC2.21	>100	<50

### **C. *In vitro* potency against nine different MMPs by curcumin and the related CMCs**

As mentioned in Chapter 2, different MMPs have diverse functions in tissue remodeling and regulation. Herein, curcumin and four CMCs were screened against nine MMPs including MMP-1, -2, -3, -7, -8, -9, -12, -13 and -14 in the *in vitro* fluorogenic MMP inhibition assay.<sup>3,4</sup> MMP-1, collagenase-1, plays an important role in the turnover of various physiological processes such as tissue morphogenesis, wound repair and remodeling of collagen extracellular matrix in various physiological and pathological situations.<sup>5</sup> Curcumin and CMCs are not as potent as 1,10-phenanthroline with respect to the inhibition of this MMP. 1,10-Phenanthroline possesses an IC<sub>50</sub> of 42.0 μM, in contrast to the 65.0-85.0 μM range of inhibition by curcumin and CMCs. This suggests that both curcumin and CMCs are not strong inhibitors for MMP-1, the constitutive MMP responsible for the regulation of many physiological functions (Figure 4.1, Table 4.2). Gelatinase A (MMP-2), plays an important role in a variety of pathological conditions related to different cancers.<sup>6</sup> Curcumin, CMC2.23 and CMC2.24 are highly active against MMP-2 having IC<sub>50</sub>s less than 10.0 μM, especially CMC2.24 having an IC<sub>50</sub> of 4.8 μM in contrast to the positive control 1,10-phenanthroline (IC<sub>50</sub>=73.8 μM) (Figure 4.2, Table 4.3). Stromelysin-1 (MMP-3), is

capable of degrading a number of structural proteins in the ECM, and is also responsible for the activation of several other MMPs such as Pro-MMP-1, -8, -13 and -9.<sup>7</sup> Also, curcumin, CMC2.23 and CMC2.24 were potent inhibitors of this type of enzyme. CMC2.24 possesses an  $IC_{50}$  of 2.9  $\mu$ M, the most potent one in this assay (Figure 4.3, Table 4.4). Matrilysin (MMP-7), appears to be very active in early-stage tumor development and late-stage invasion of cancer cells.<sup>8</sup> The positive control, 1,10-phenanthroline does not display strong potency against MMP-7. However, CMC2.24 is quite potent as the inhibitor of this enzyme with an  $IC_{50}$  of 5.0  $\mu$ M, about 10 fold more potent than curcumin (Figure 4.4, Table 4.5). Neutrophil collagenase (MMP-8), is very important in the regulation of the inflammatory response induced by carcinogens, and it is involved in different types of pathological conditions related to inflammation and cancer.<sup>9</sup> CMC2.23 was the most potent compound in the *in vitro* inhibition of MMP-8, having an  $IC_{50}$  of 2.5  $\mu$ M. Curcumin and the other CMCs are also more potent than the control 1,10-phenanthroline (Figure 4.5, Table 4.6). Gelatinase B (MMP-9), is crucial for numerous tissue remodeling situations that include wound healing, inflammation and cancer metastasis.<sup>10</sup> Both CMC2.23 and CMC2.24 appear to be very potent against MMP-9 in this assay, having  $IC_{50}$ s around 8.0  $\mu$ M, and they are also better inhibitors than curcumin (Figure 4.6, Table 4.7). Macrophage metalloelastase (MMP-12), has been found to play an essential role in alveolar macrophages of lung diseases, such as acute lung injury and chronic inflammatory airway diseases.<sup>11</sup> Curcumin and CMC2.24 are the most potent inhibitors in the assay with  $IC_{50}$ s around 2.0  $\mu$ M (Figure 4.7, Table 4.8). Collagenase-3 (MMP-13), can cleave a variety of components in basement membranes, and was found to be the most abundant collagenase in rats and mice.<sup>12</sup> Again curcumin, CMC2.23 and CMC2.24 displayed great potency against MMP-13 with an  $IC_{50}$  around 3.0  $\mu$ M (Figure 4.8, Table 4.9). MMP-14 (MT1-MMP), possesses the activities to degrade a variety of substrates in

the ECM, and can activate the Pro-MMPs, -8, -9 and -13.<sup>13</sup> CMC2.24 was found to be the most potent inhibitor of MMP-14, having an IC<sub>50</sub> around 15.0 μM (Figure 4.9, Table 4.10). In general, when an N-phenylaminocarbonyl group is introduced at the Carbon-4 position, the MMP inhibitory activity was increased very substantially as is evident from the data for CMC2.23 and CMC2.24, but not in the case of CMC2.22. CMC2.24 proved to be significantly more potent than curcumin, specifically against the MMP-7, -9, -12, and -14, all of which are inducible MMPs and which are active in a variety of inflammatory diseases as well as cancer. However, the constitutive collagenase enzyme MMP-1, was much less affected by either curcumin or the CMCs. The N-phenylamino carbonyl group at Carbon-4 also increased the solubility of these compounds, probably associated with the increased acidity (a tricarbonyl methane versus a dicarbonyl methane; pK<sub>a</sub> data shown in Chapter 5) versus curcumin and because of its amide character. The data shown below indicate that both curcumin and the 4-oxo-substituted curcumins are better MMP inhibitors, in contrast to the standard zinc chelating agent, 1,10-phenanthroline. Two N-phenylamino carbonyl curcumins, CMC2.23 and CMC2.24 were also tested against several chemokines and cytokines in cell culture, and CMC2.24 was selected as the current lead compound for further wound healing, bone remodeling and cancer studies.



Figure 4.1 MMP-1 inhibition assay

Note: A fluorimetric inhibition assay was used, and 1, 10-phenanthroline was used as the positive control for the experiment. IC<sub>50</sub>s were measured from the following plots.

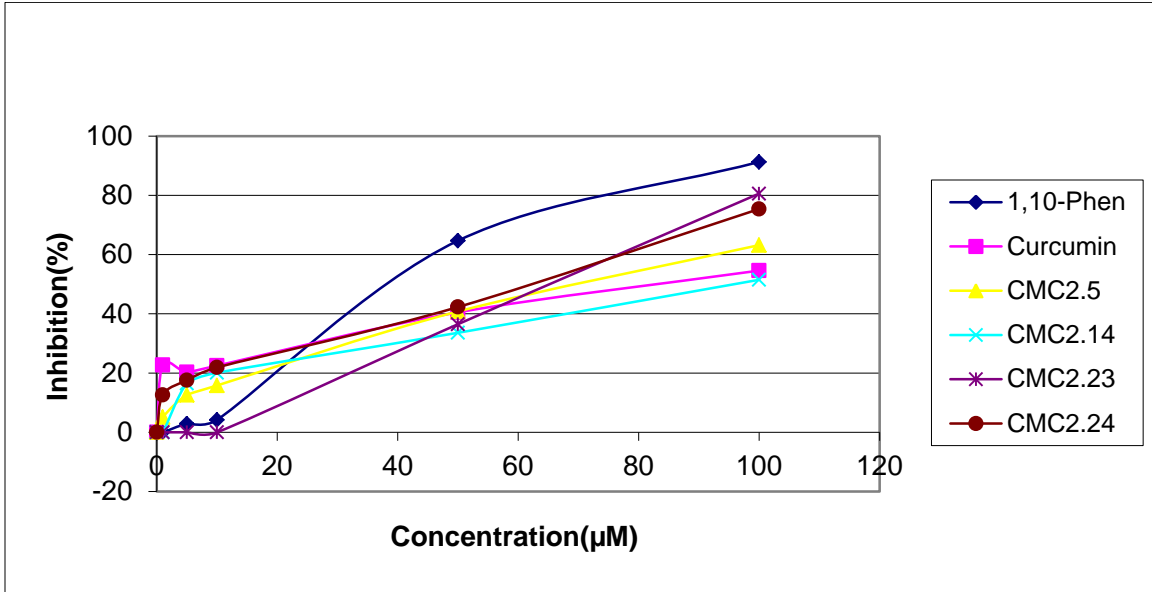


Figure 4.1a Test 1 in MMP-1 inhibition assay

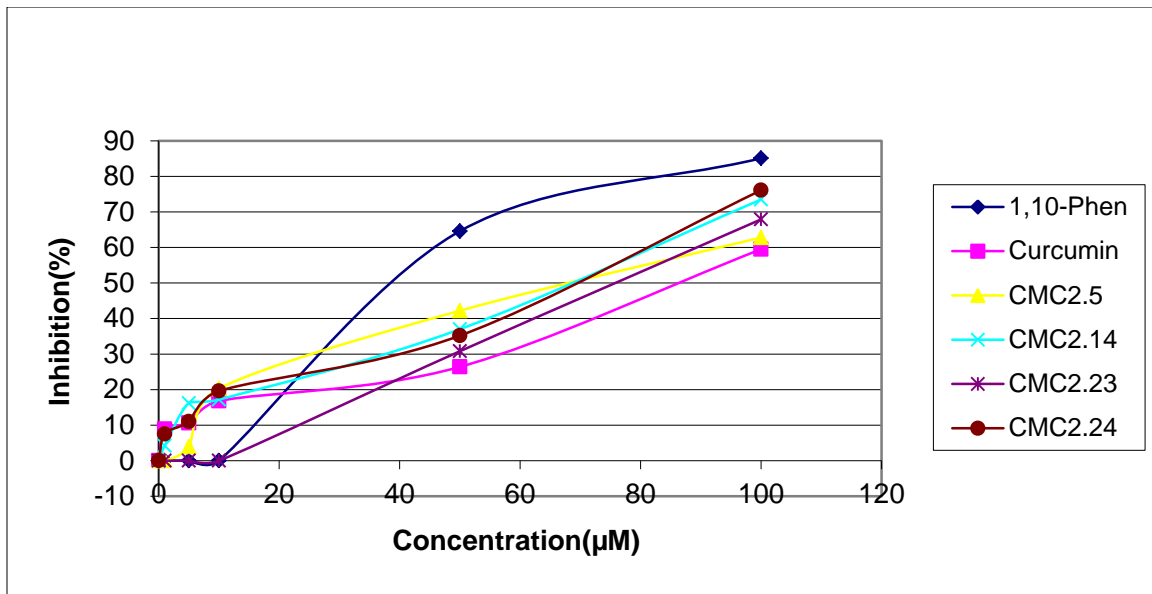


Figure 4.1b Test 2 in MMP-1 inhibition assay

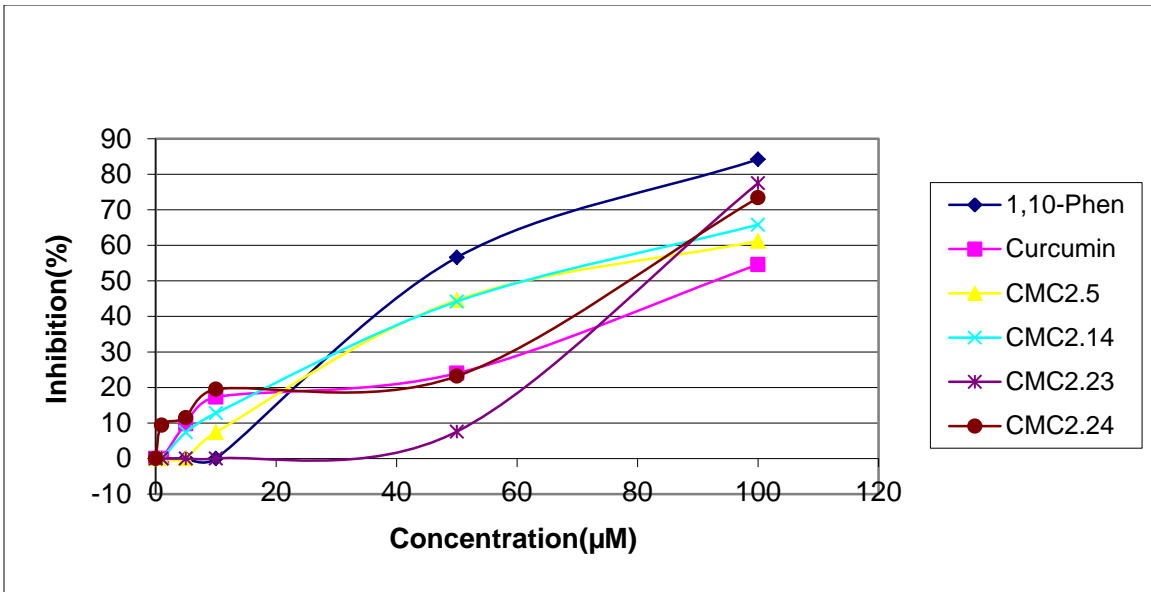


Figure 4.1c Test 3 in MMP-1 inhibition assay

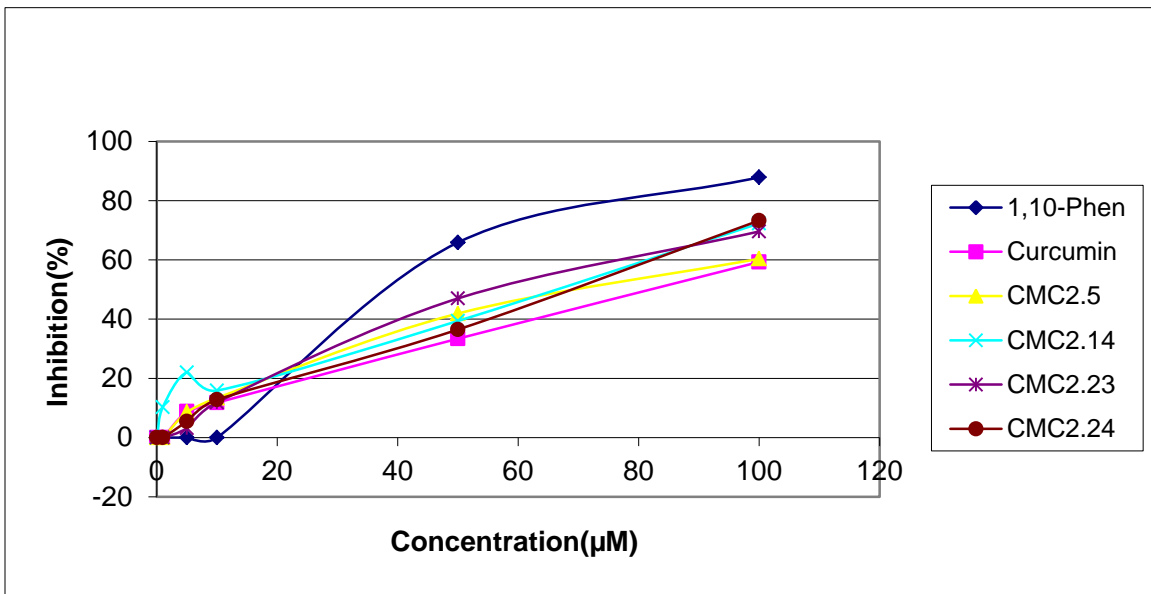


Figure 4.1d Test 4 in MMP-1 inhibition assay

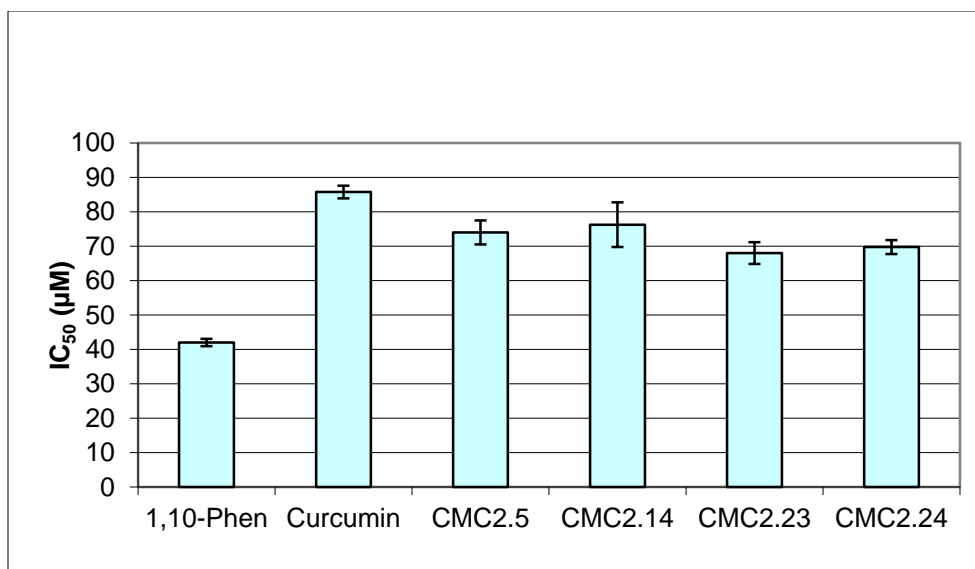


Figure 4.1e IC<sub>50</sub> of curcumin and selected CMCs against MMP-1

Table 4.2 IC<sub>50</sub> of curcumin and CMCs against MMP-1

		1,10- Phen	Curcumin	CMC2.5	CMC2.14	CMC2.23	CMC2.24
Test 1	IC <sub>50</sub> (µM)	42.0	86.0	80.0	93.0	66.0	70.0
Test 2	IC <sub>50</sub> (µM)	40.0	81.0	79.0	80.0	72.0	64.0
Test 3	IC <sub>50</sub> (µM)	45.0	90.0	65.0	67.0	74.0	72.0
Test 4	IC <sub>50</sub> (µM)	41.0	86.0	72.0	65.0	60.0	73.0
	Ave.	42.0	85.8	74.0	76.3	68.0	69.8
	S.D.	2.16	3.68	6.97	12.99	6.32	4.03
	S.E.M.	1.08	1.84	3.49	6.49	3.16	2.01

Figure 4.2 MMP-2 inhibition assay

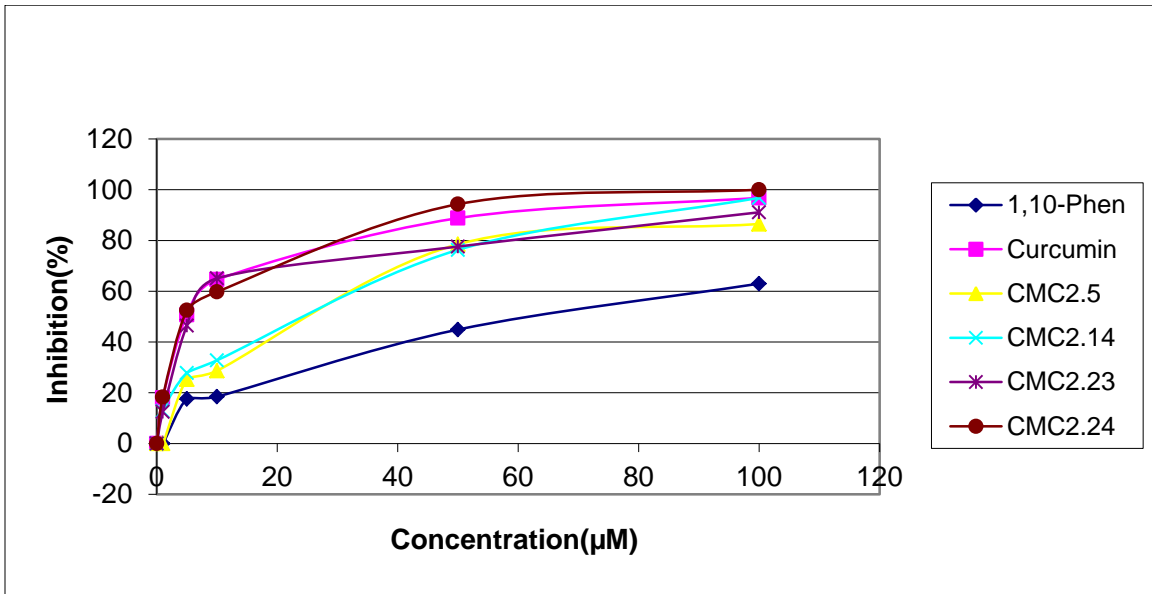


Figure 4.2a Test 1 in MMP-2 inhibition assay

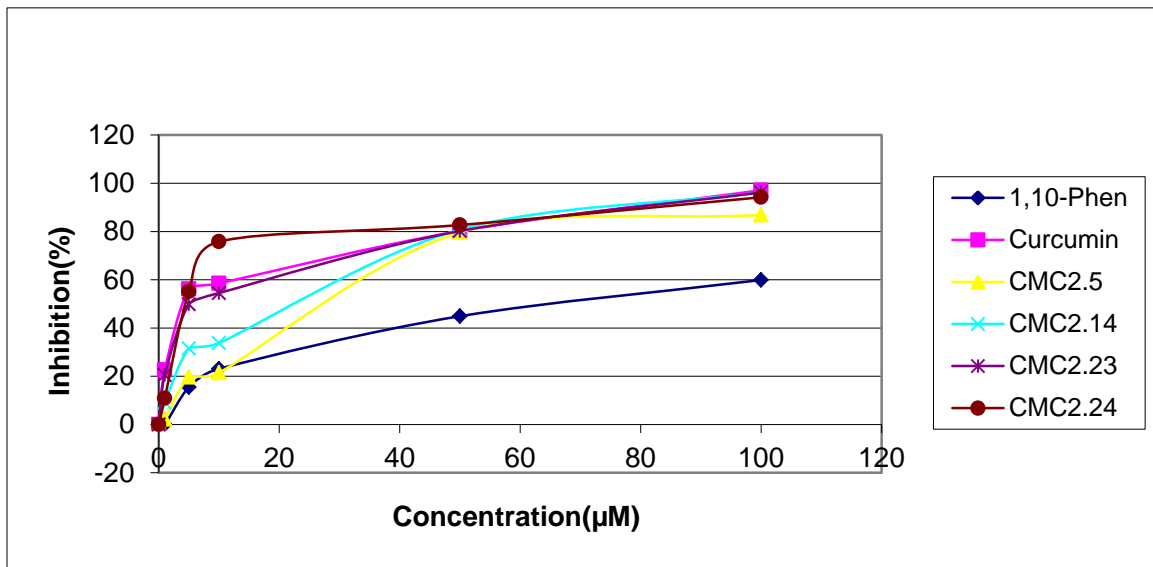


Figure 4.2b Test 2 in MMP-2 inhibition assay

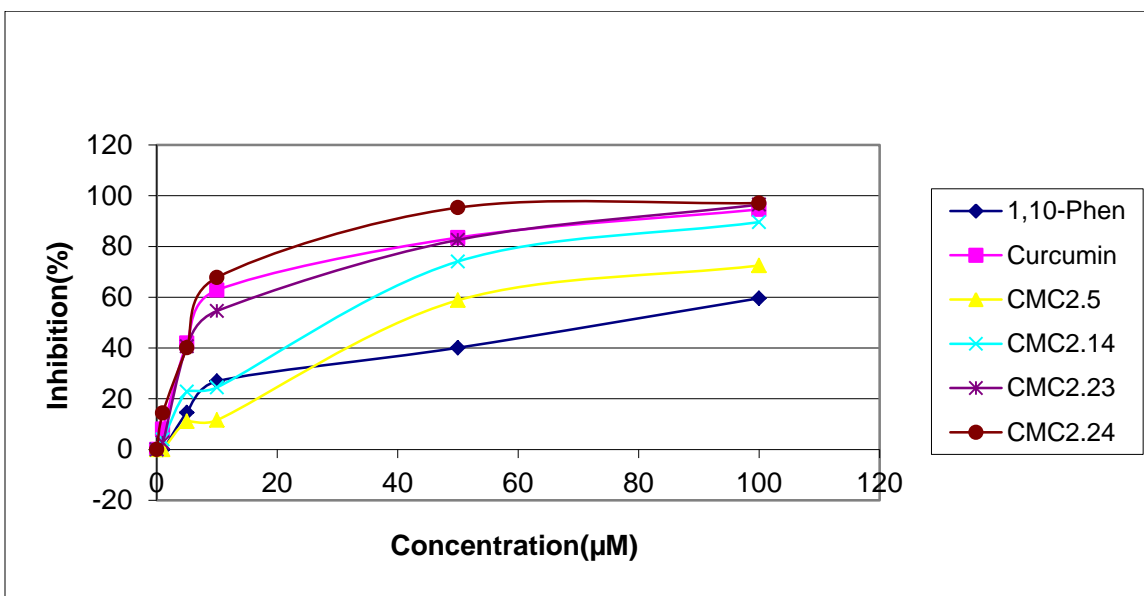


Figure 4.2c Test 3 in MMP-2 inhibition assay

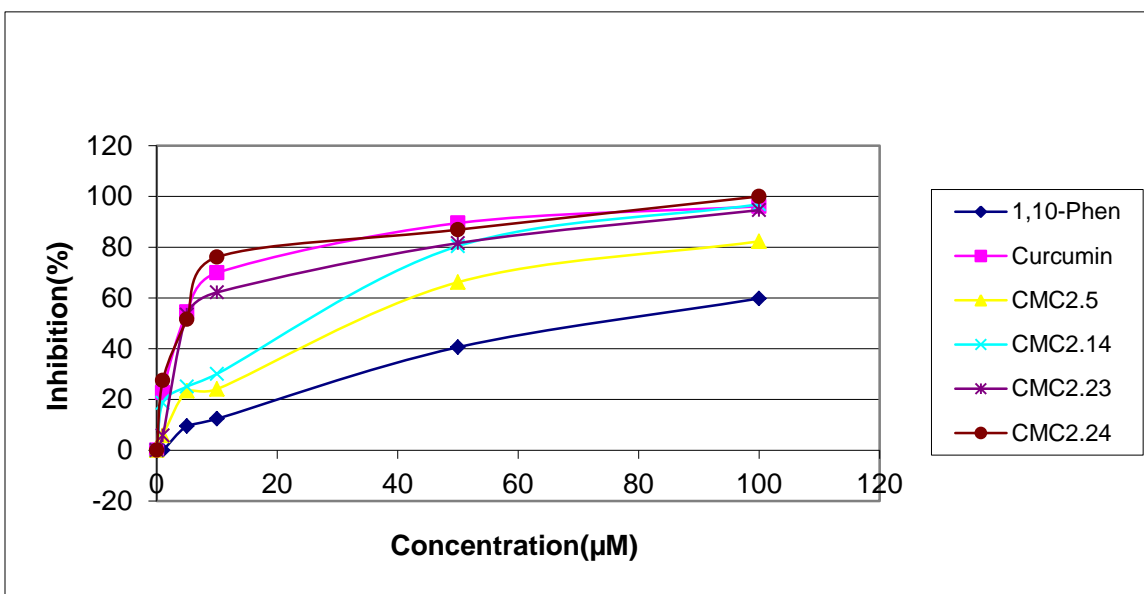


Figure 4.2d Test 4 in MMP-2 inhibition assay

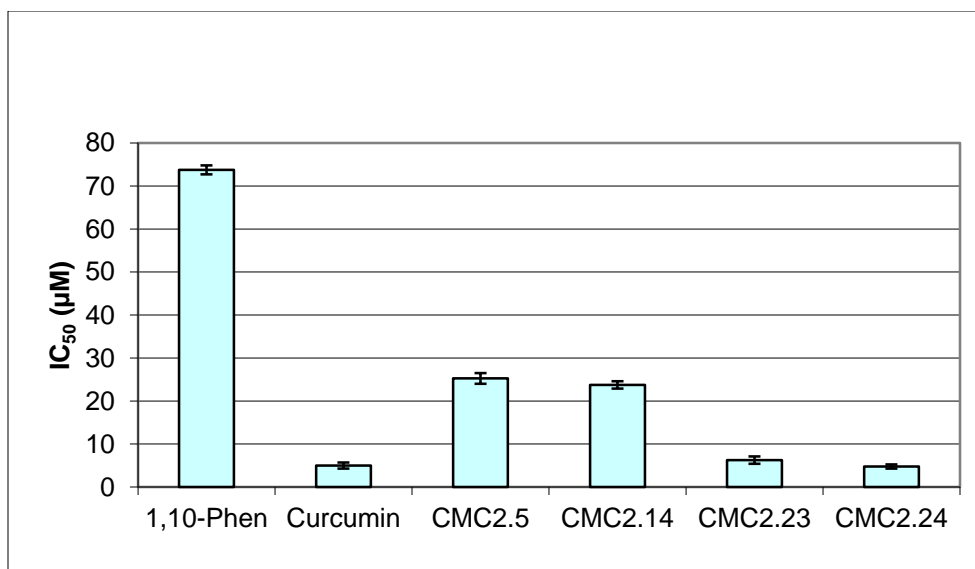


Figure 4.2e IC<sub>50</sub> of curcumin and selected CMCs against MMP-2

Table 4.3 IC<sub>50</sub> of curcumin and selected CMCs against MMP-2

		1,10- Phen	Curcumin	CMC2.5	CMC2.14	CMC2.23	CMC2.24
Test 1	IC <sub>50</sub> (µM)	75.0	5.0	28.0	26.0	6.0	4.0
Test 2	IC <sub>50</sub> (µM)	72.0	4.0	22.0	24.0	7.0	4.0
Test 3	IC <sub>50</sub> (µM)	72.0	7.0	25.0	22.0	8.0	6.0
Test 4	IC <sub>50</sub> (µM)	76.0	4.0	26.0	23.0	4.0	5.0
	Ave.	73.8	5.0	25.3	23.8	6.3	4.8
	S.D.	2.06	1.41	2.50	1.70	1.70	0.96
	S.E.M.	1.03	0.71	1.25	0.85	0.85	0.48

Figure 4.3 MMP-3 inhibition assay

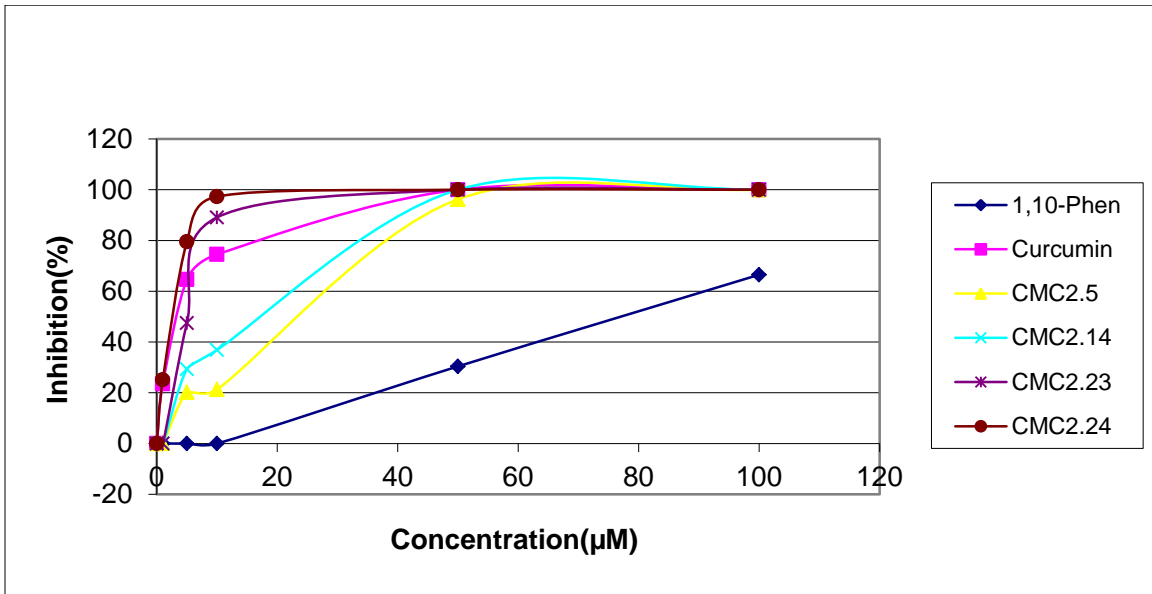


Figure 4.3a Test 1 in MMP-3 inhibition assay

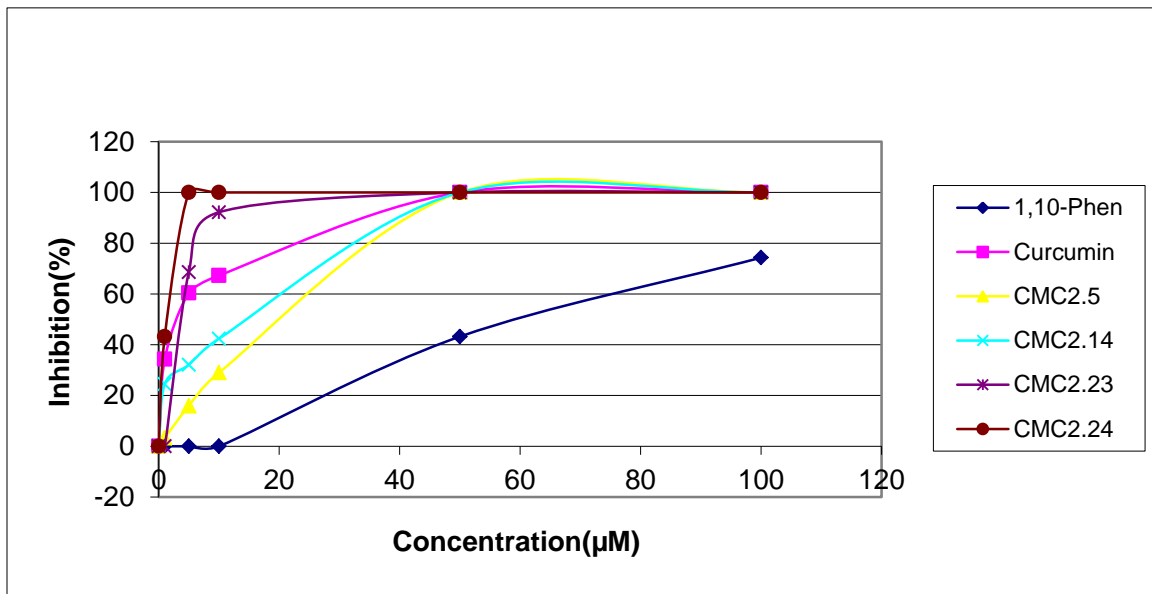


Figure 4.3b Test 2 in MMP-3 inhibition assay

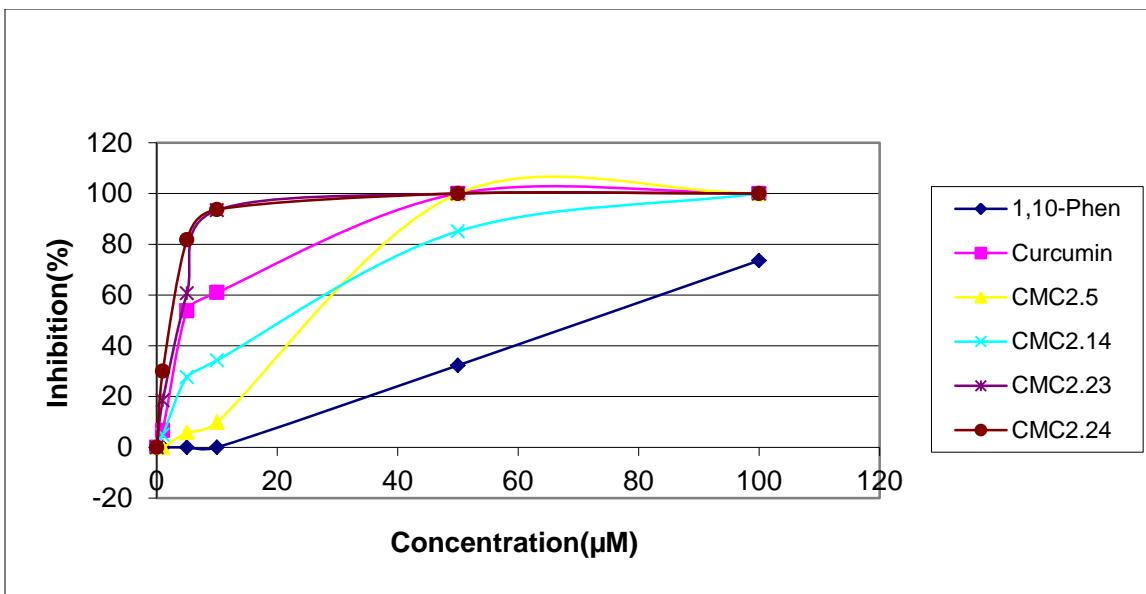


Figure 4.3c Test 3 in MMP-3 inhibition assay

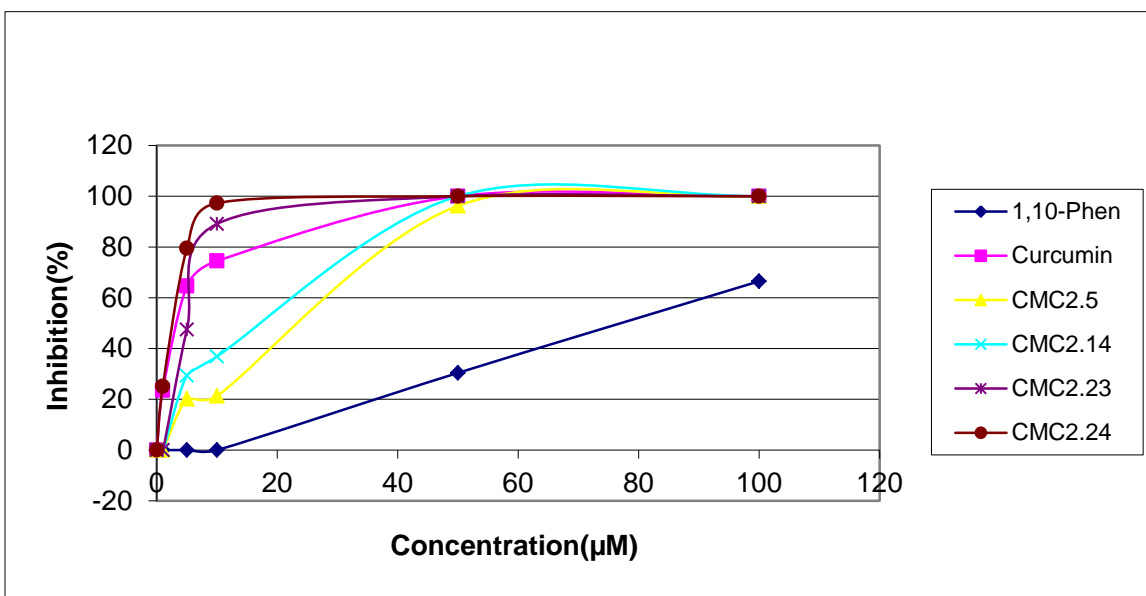


Figure 4.3d Test 4 in MMP-3 inhibition assay



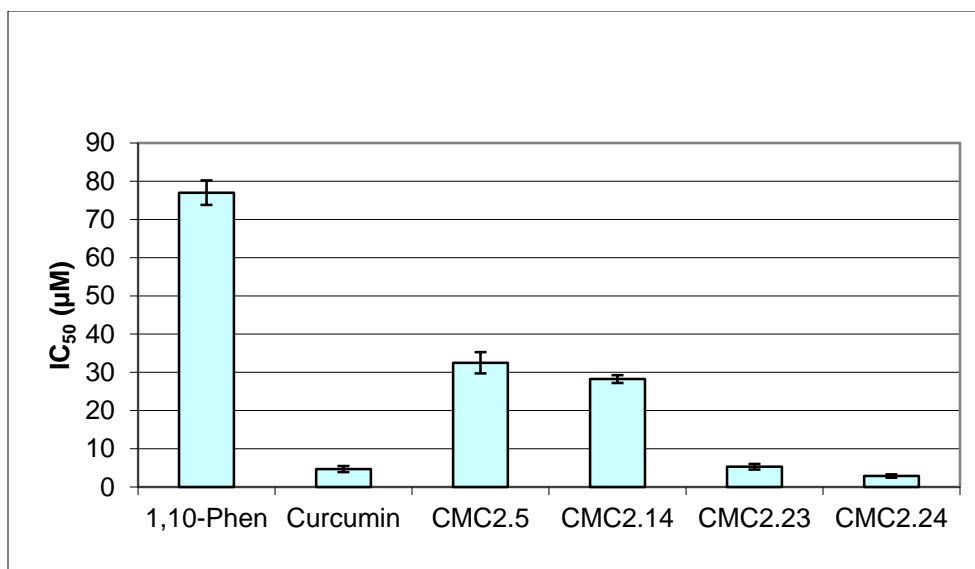


Figure 4.3e IC<sub>50</sub> of curcumin and selected CMCs against MMP-3

Table 4.4 IC<sub>50</sub> of curcumin and selected CMCs against MMP-3

		1,10-Phen	Curcumin	CMC2.5	CMC2.14	CMC2.23	CMC2.24
Test 1	IC <sub>50</sub> (µM)	71.0	3.5	35.0	26.0	4.0	2.0
Test 2	IC <sub>50</sub> (µM)	75.0	4.0	32.0	30.0	6.0	3.0
Test 3	IC <sub>50</sub> (µM)	76.0	4.2	38.0	27.0	4.2	2.5
Test 4	IC <sub>50</sub> (µM)	86.0	7.0	25.0	30.0	7.0	4.0
	Ave.	77.0	4.7	32.5	28.3	5.3	2.9
	S.D.	6.38	1.58	5.57	2.06	1.45	0.85
	S.E.M.	3.19	0.79	2.78	1.03	0.72	0.43

Figure 4.4 MMP-7 inhibition assay

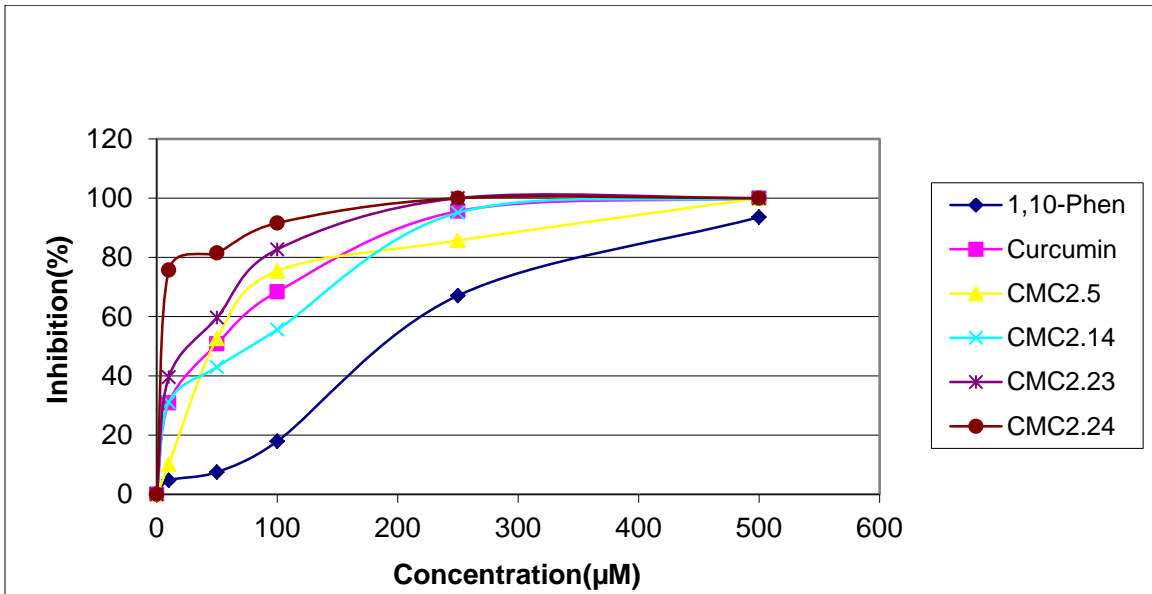


Figure 4.4a Test 1 in MMP-7 inhibition assay

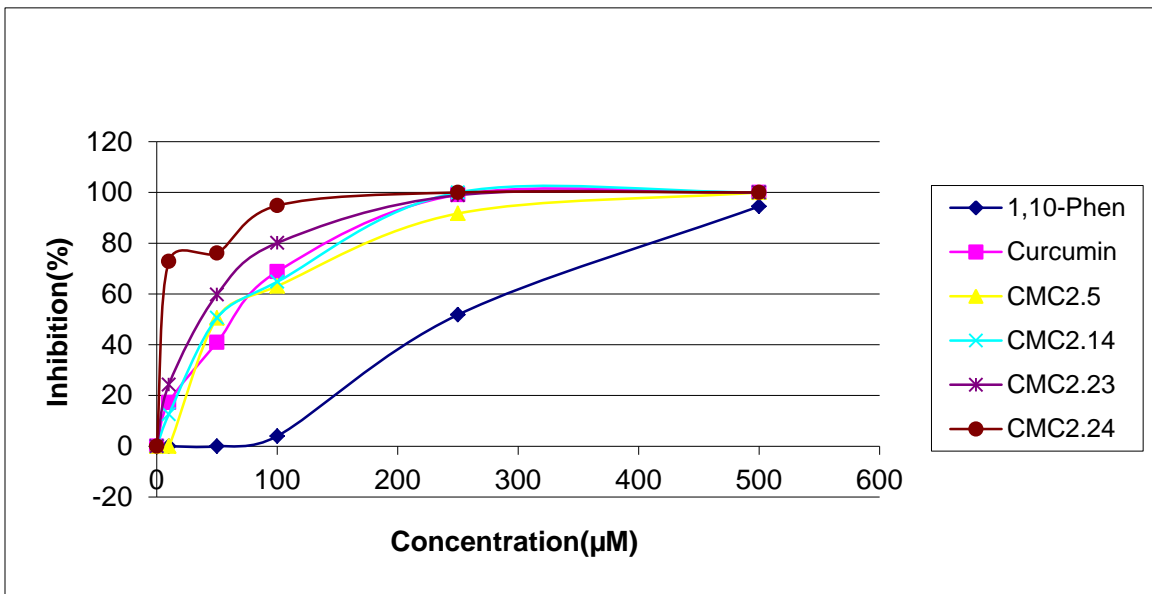


Figure 4.4b Test 2 in MMP-7 inhibition assay

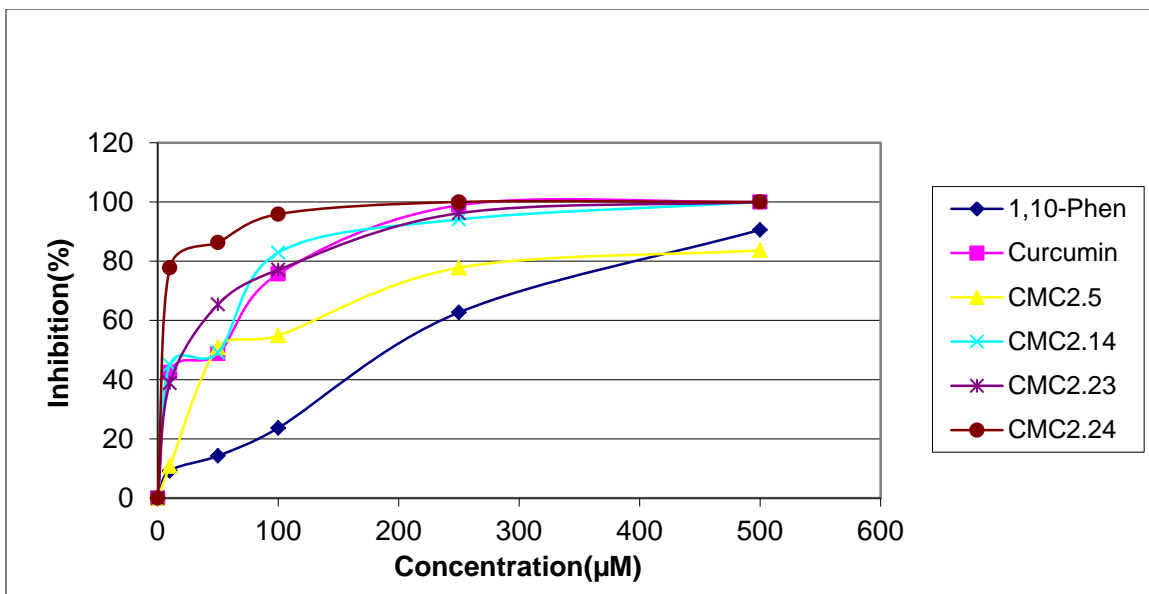


Figure 4.4c Test 3 in MMP-7 inhibition assay

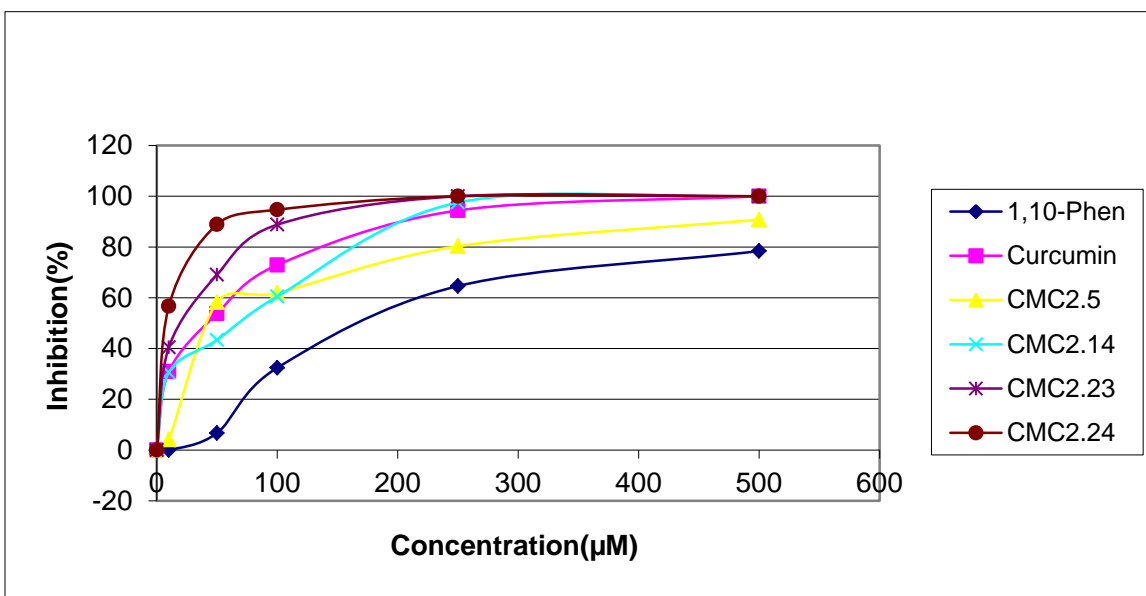


Figure 4.4d Test 4 in MMP-7 inhibition assay

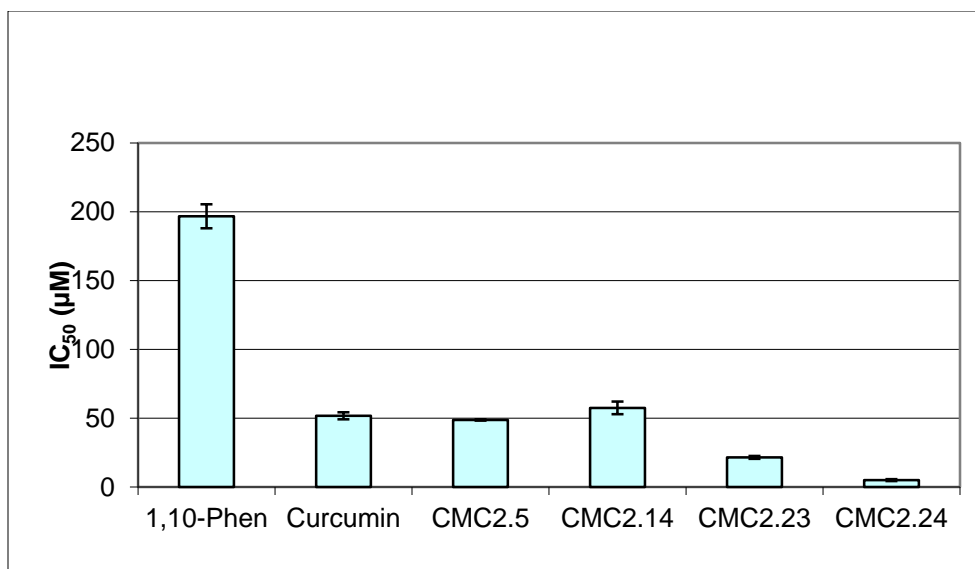


Figure 4.4e IC<sub>50</sub> of curcumin and selected CMCs against MMP-7

Table 4.5 IC<sub>50</sub> of curcumin and selected CMCs against MMP-7

		1,10-Phen	Curcumin	CMC2.5	CMC2.14	CMC2.23	CMC2.24
Test 1	IC <sub>50</sub> (µM)	185.0	49.0	48.0	68.0	19.0	5.0
Test 2	IC <sub>50</sub> (µM)	218.0	56.0	50.0	48.0	21.0	4.0
Test 3	IC <sub>50</sub> (µM)	204.0	56.0	49.0	52.0	24.0	4.0
Test 4	IC <sub>50</sub> (µM)	180.0	46.0	48.0	62.0	22.0	7.0
	Ave.	196.75	51.75	48.75	57.5	21.5	5.0
	S.D.	17.54	5.06	0.96	9.15	2.08	1.41
	S.E.M.	8.77	2.53	0.48	4.57	1.04	0.71

Figure 4.5 MMP-8 inhibition assay

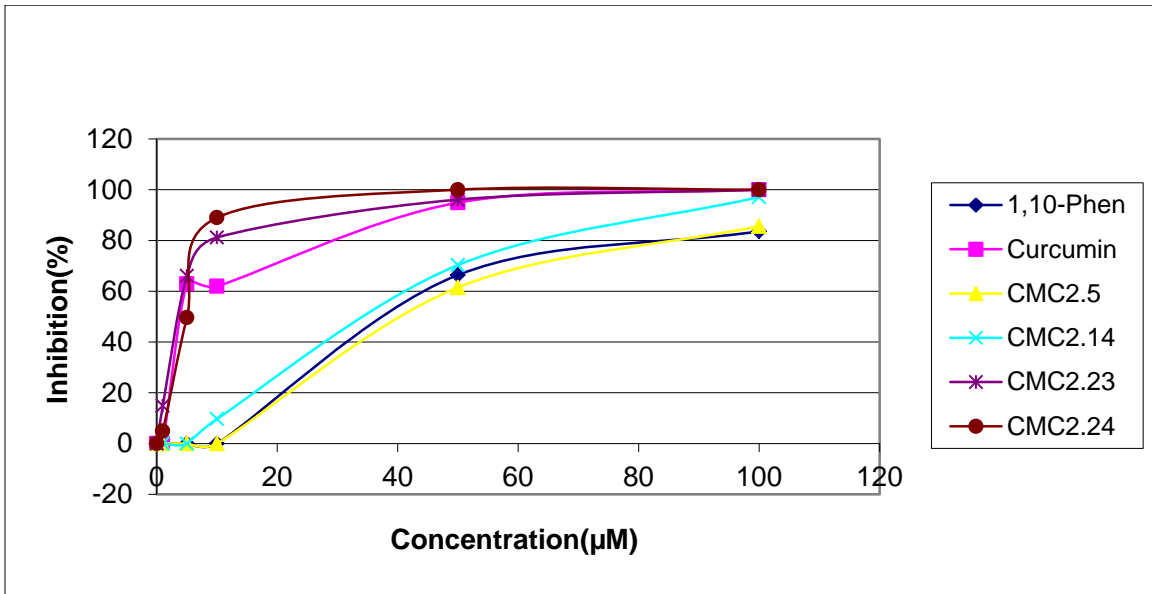


Figure 4.5a Test 1 in MMP-8 inhibition assay

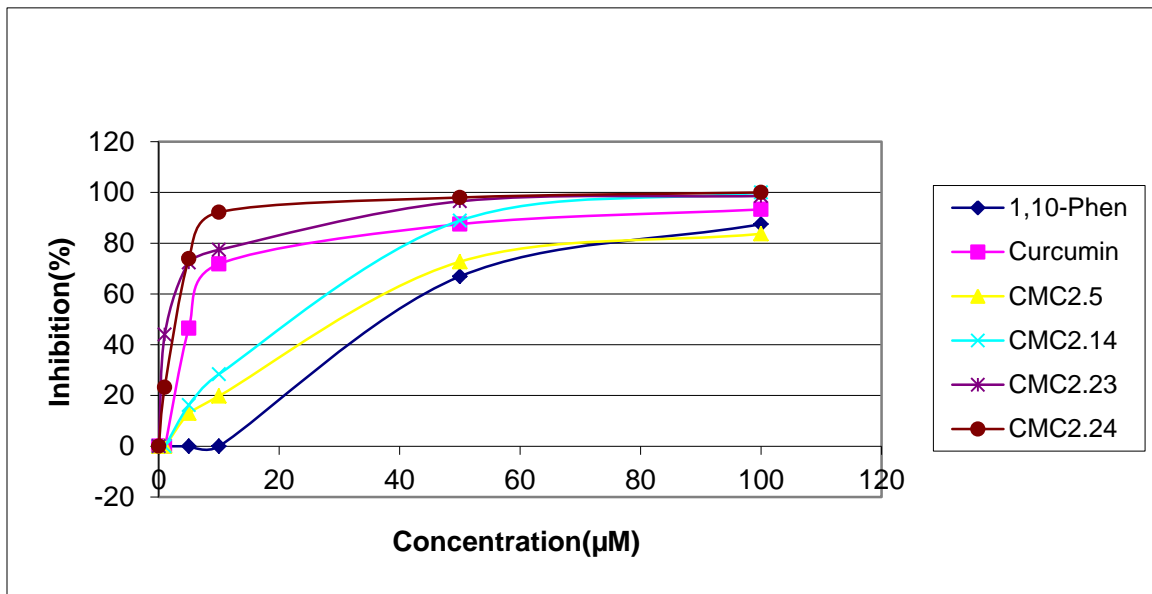


Figure 4.5b Test 2 in MMP-8 inhibition assay

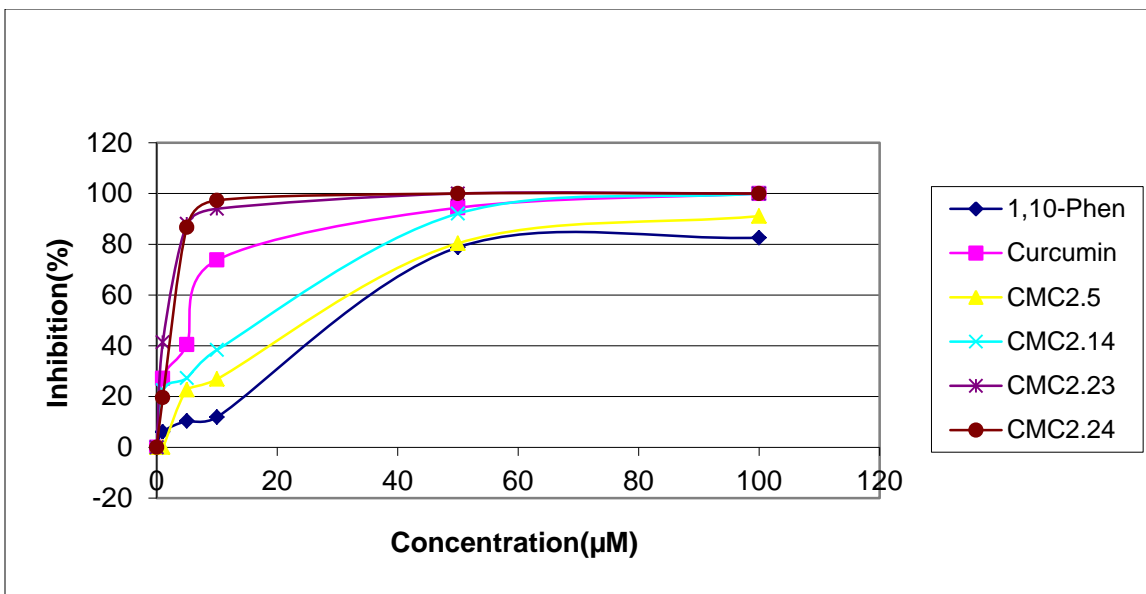


Figure 4.5c Test 3 in MMP-8 inhibition assay

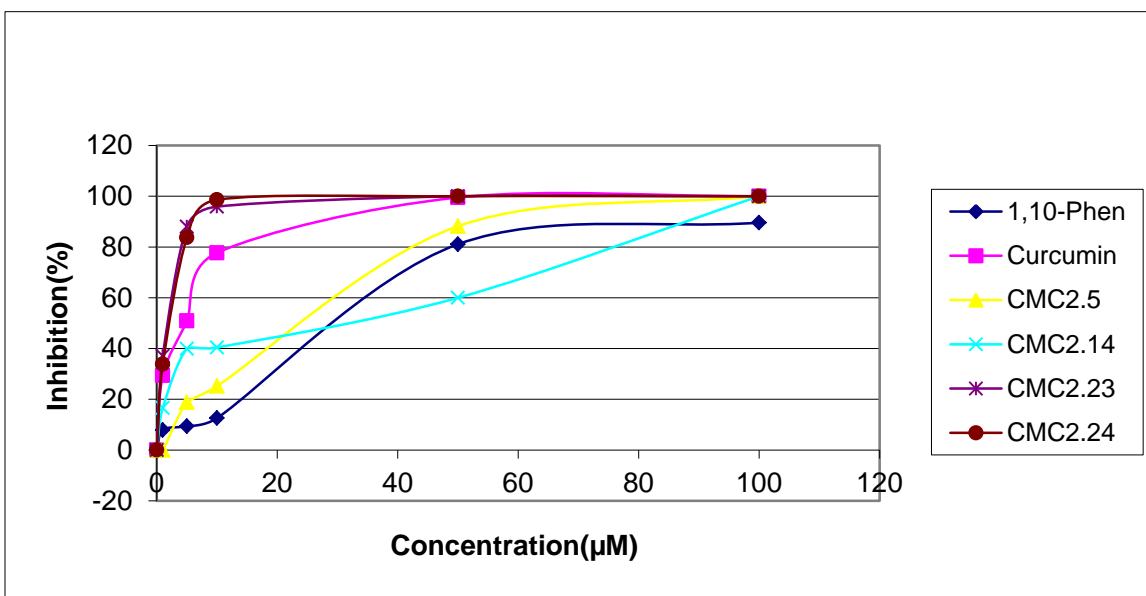


Figure 4.5d Test 4 in MMP-8 inhibition assay

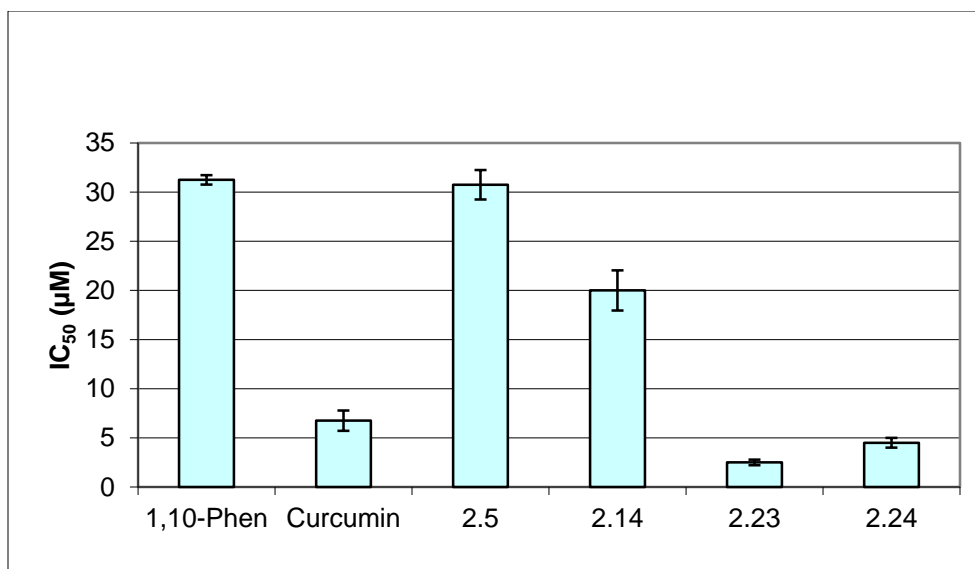


Figure 4.5e IC<sub>50</sub> of curcumin and selected CMCs against MMP-8

Table 4.6 IC<sub>50</sub> of curcumin and selected CMCs against MMP-8

		1,10-Phen	Curcumin	CMC2.5	CMC2.14	CMC2.23	CMC2.24
Test 1	IC <sub>50</sub> (µM)	30.0	5.0	35.0	20.0	3.0	6.0
Test 2	IC <sub>50</sub> (µM)	32.0	8.0	30.0	25.0	2.0	4.0
Test 3	IC <sub>50</sub> (µM)	32.0	9.0	28.0	20.0	2.0	4.0
Test 4	IC <sub>50</sub> (µM)	31.0	5.0	30.0	15.0	3.0	4.0
	Ave.	31.3	6.8	30.8	20.0	2.5	4.5
	S.D.	0.96	2.06	2.99	4.08	0.58	1.00
	S.E.M.	0.48	1.03	1.49	2.04	0.29	0.50

Figure 4.6 MMP-9 inhibition assay

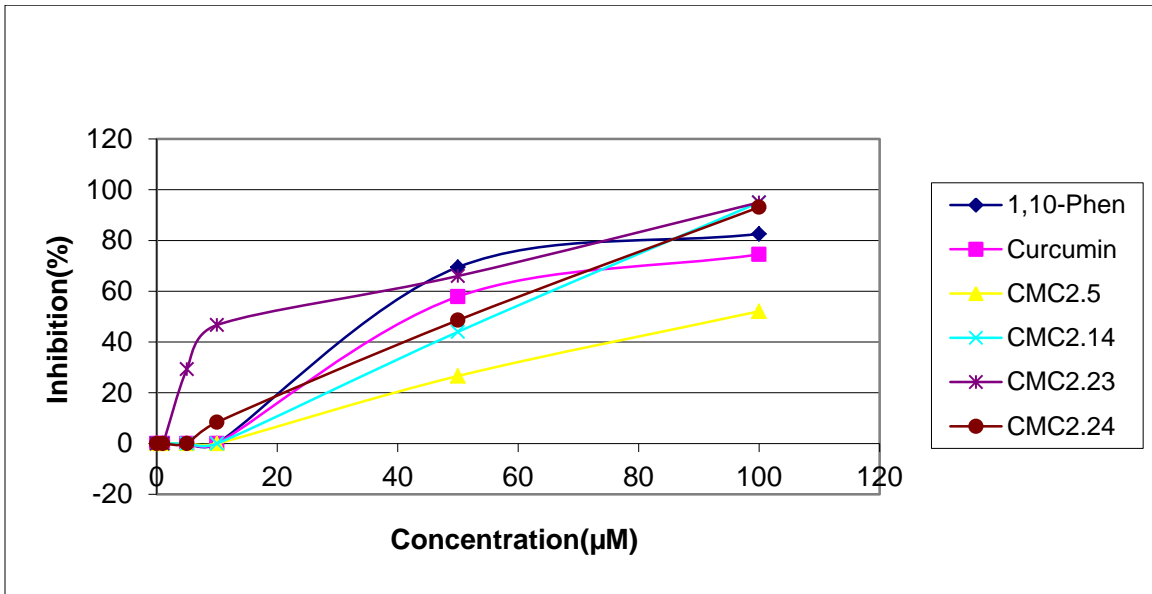


Figure 4.6a Test 1 in MMP-9 inhibition assay

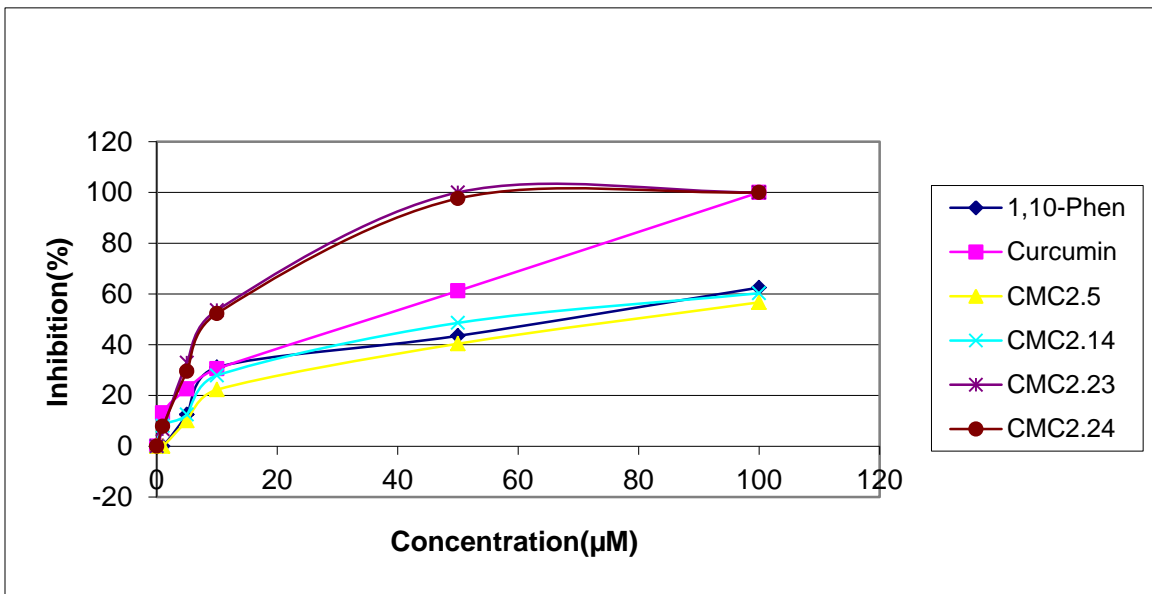


Figure 4.6b Test 2 in MMP-9 inhibition assay



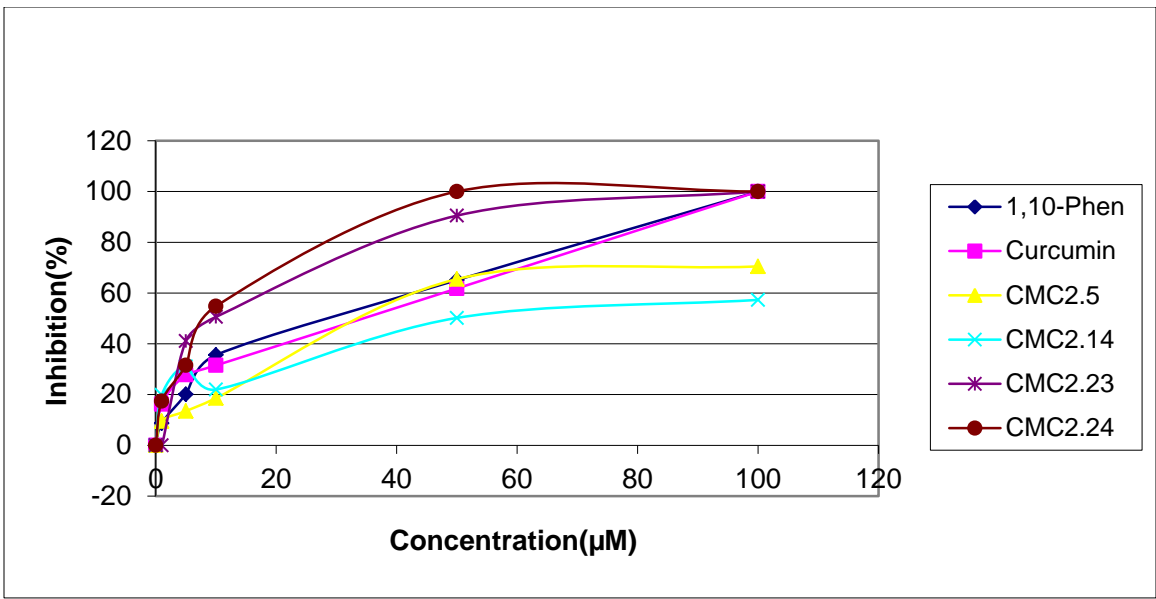


Figure 4.6c Test 3 in MMP-9 inhibition assay

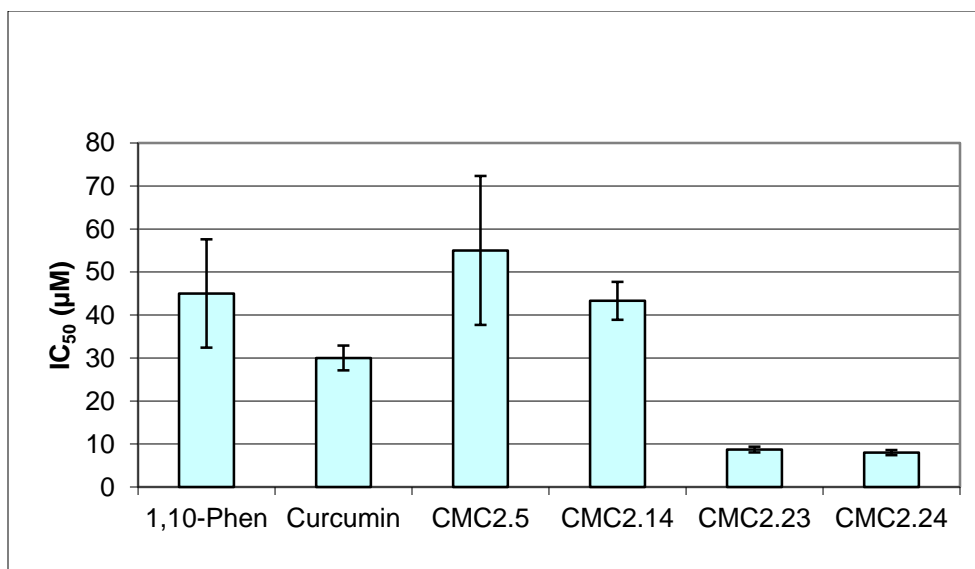


Figure 4.6d IC<sub>50</sub> of curcumin and selected CMCs against MMP-9

Table 4.7 IC<sub>50</sub> of curcumin and selected CMCs against MMP-9

		1,10- Phen	Curcumin	CMC2.5	CMC2.14	CMC2.23	CMC2.24
Test 1	IC <sub>50</sub> (µM)	30.0	35.0	25.0	50.0	10.0	8.0
Test 2	IC <sub>50</sub> (µM)	70.0	30.0	85.0	45.0	8.0	9.0
Test 3	IC <sub>50</sub> (µM)	35.0	25.0	55.0	35.0	8.0	7.0
	Ave.	45.0	30.0	55.0	43.3	8.7	8.0
	S.D.	21.79	5.00	30.00	7.64	1.15	1.00
	S.E.M.	12.58	2.89	17.32	4.41	0.67	0.58

Figure 4.7 MMP-12 inhibition assay

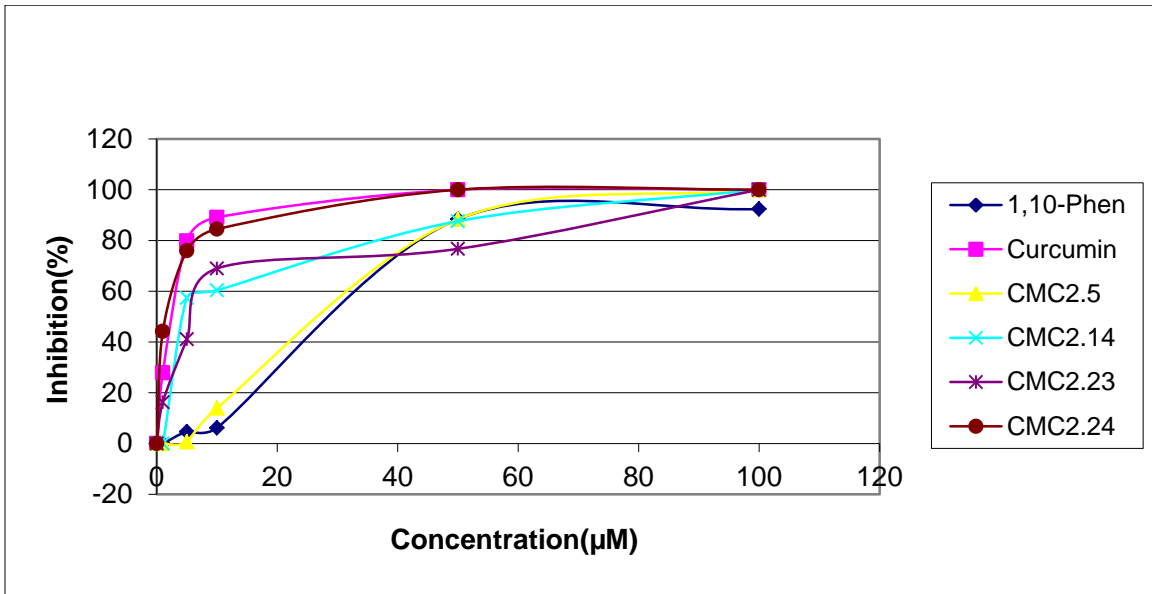


Figure 4.7a Test 1 in MMP-12 inhibition assay

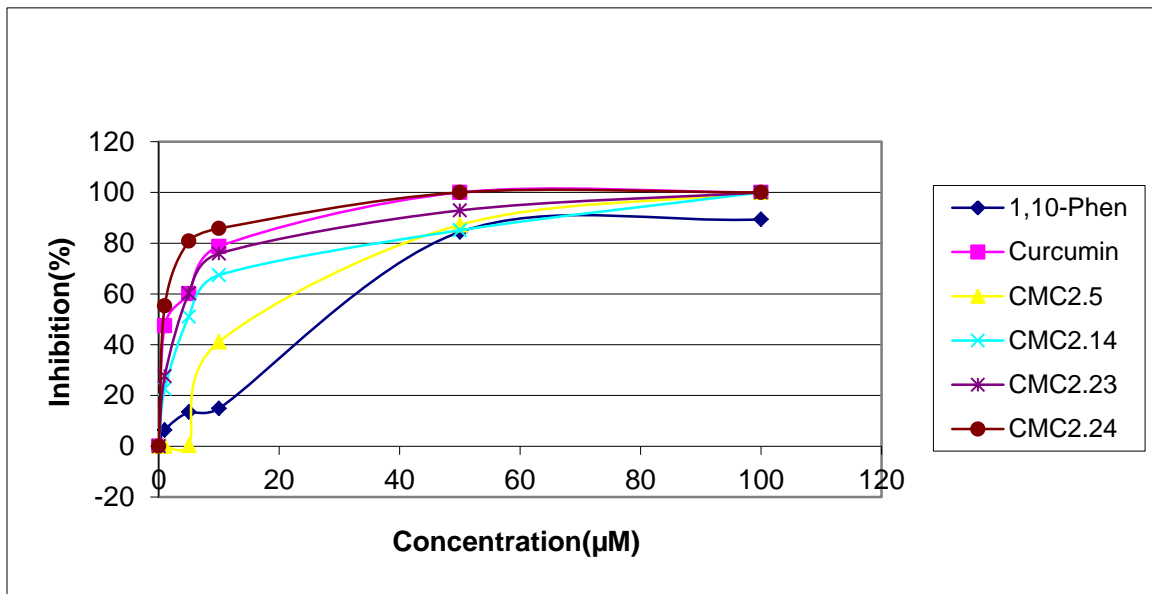


Figure 4.7b Test 2 in MMP-12 inhibition assay

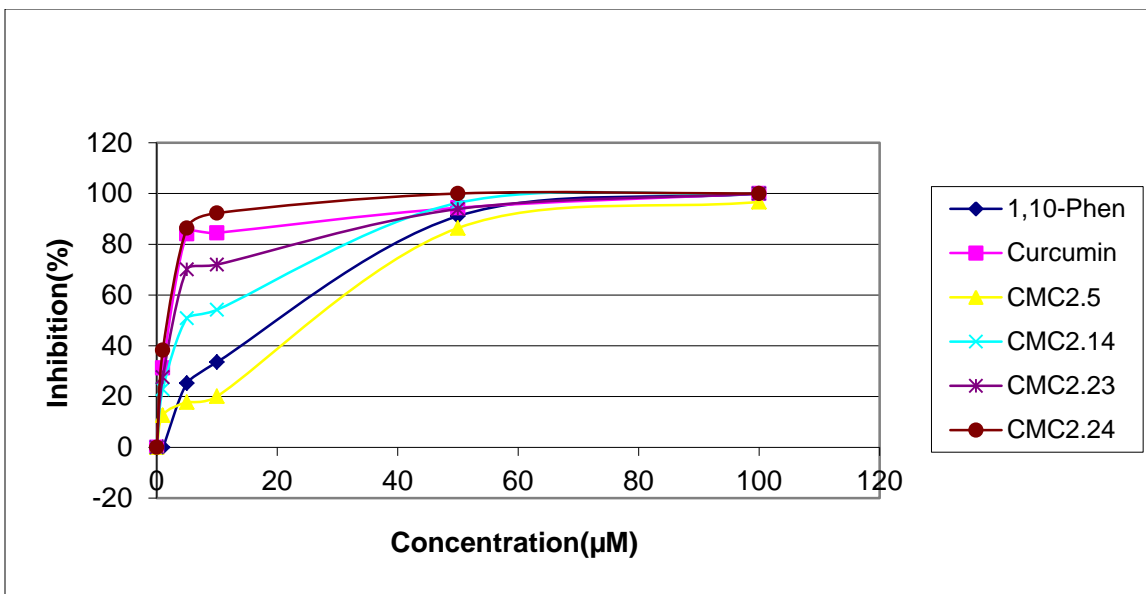


Figure 4.7c Test 3 in MMP-12 inhibition assay

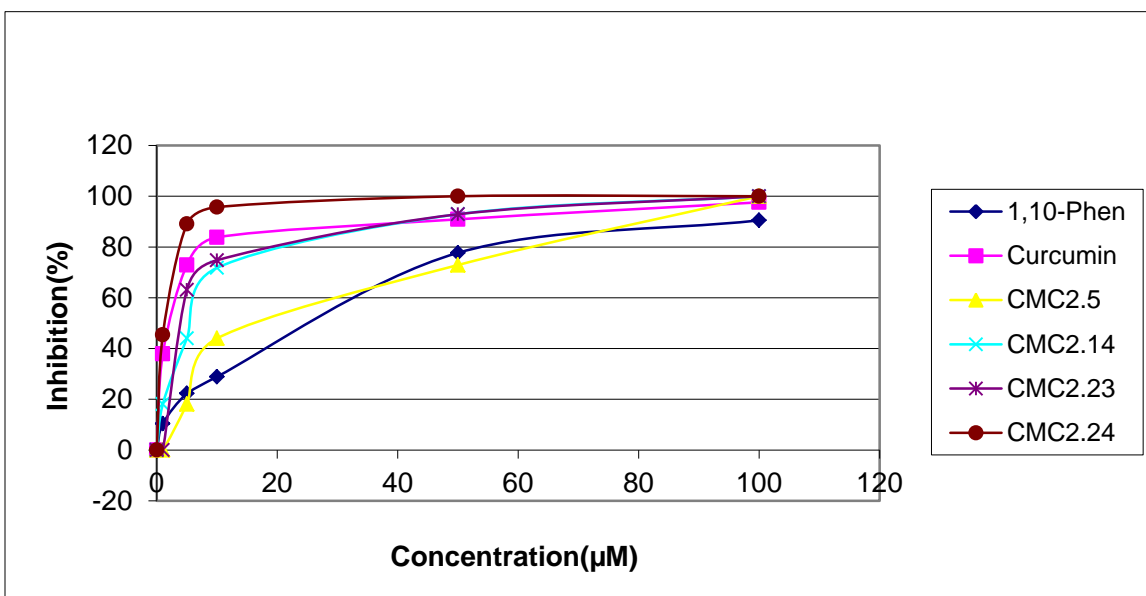


Figure 4.7d Test 4 in MMP-12 inhibition assay

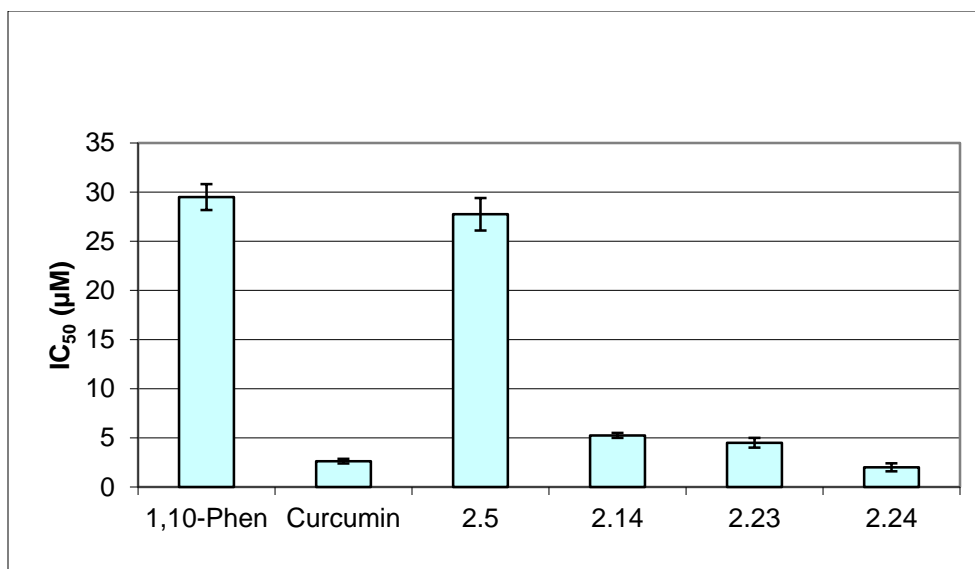


Figure 4.7e IC<sub>50</sub> of curcumin and selected CMCs against MMP-12

Table 4.8 IC<sub>50</sub> of curcumin and selected CMCs against MMP-12

		1,10-Phen	Curcumin	CMC2.5	CMC2.14	CMC2.23	CMC2.24
Test 1	IC <sub>50</sub> (µM)	33.0	3.0	31.0	5.0	6.0	2.0
Test 2	IC <sub>50</sub> (µM)	30.0	3.0	26.0	5.0	4.0	1.0
Test 3	IC <sub>50</sub> (µM)	27.0	2.5	30.0	5.0	4.0	2.0
Test 4	IC <sub>50</sub> (µM)	28.0	2.0	24.0	6.0	4.0	3.0
	Ave.	29.5	2.6	27.8	5.3	4.5	2.0
	S.D.	2.65	0.48	3.30	0.50	1.00	0.82
	S.E.M.	1.32	0.24	1.65	0.25	0.50	0.41

Figure 4.8 MMP-13 inhibition assay

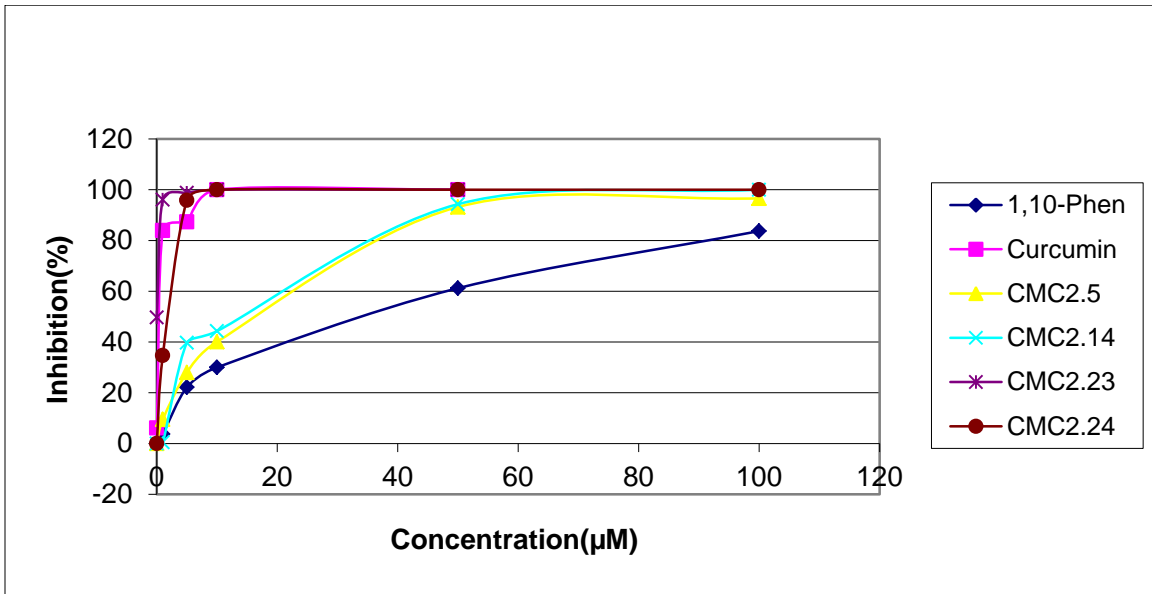


Figure 4.8a Test 1 in MMP-13 inhibition assay

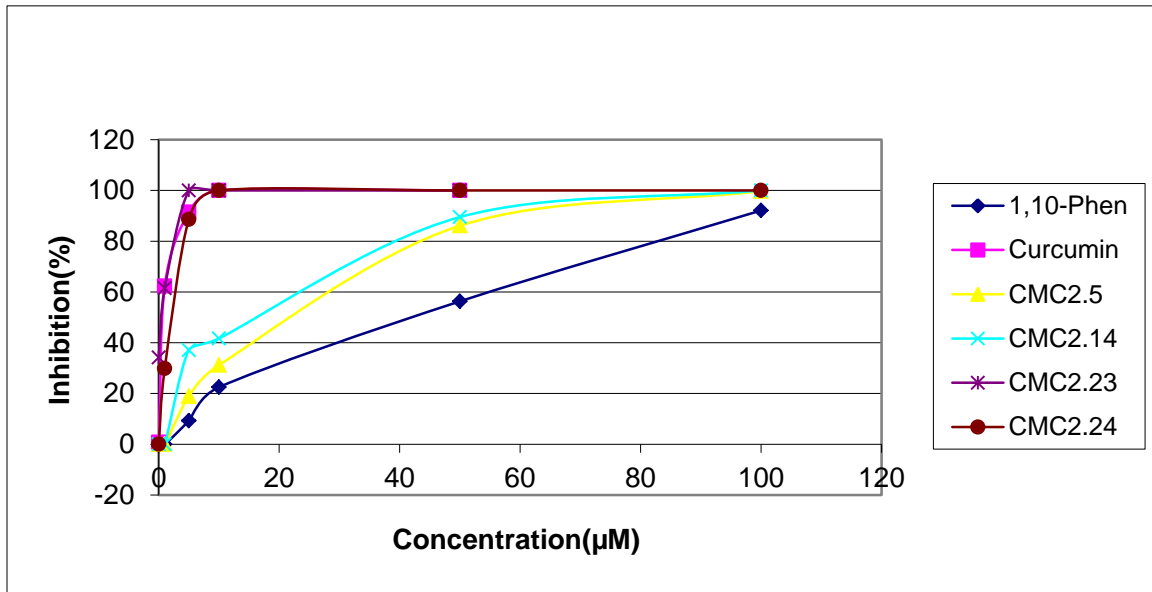


Figure 4.8b Test 2 in MMP-13 inhibition assay

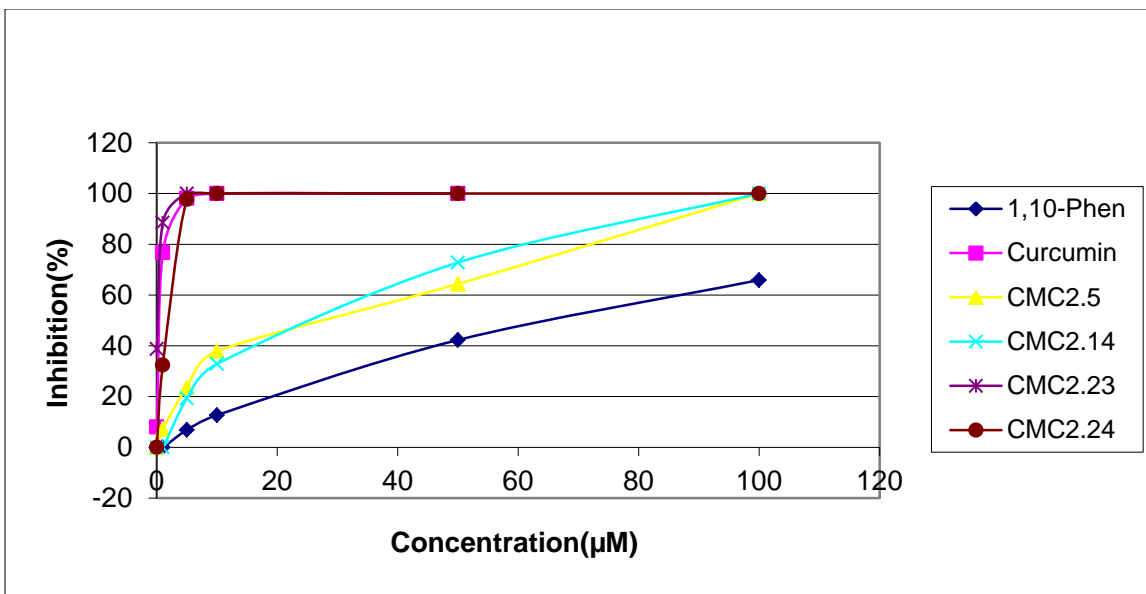


Figure 4.8c Test 3 in MMP-13 inhibition assay

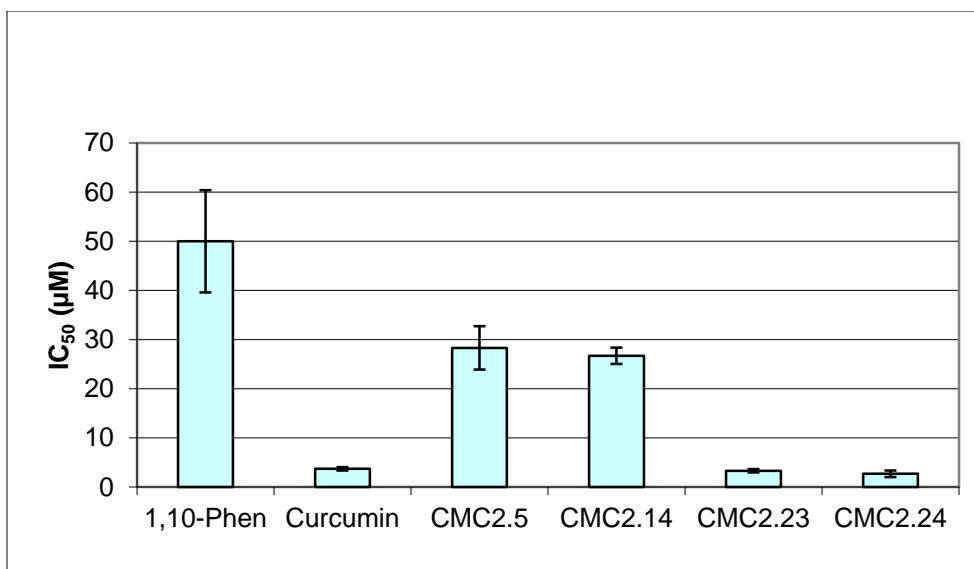


Figure 4.8d IC<sub>50</sub> of curcumin and selected CMCs against MMP-13

Table 4.9 IC<sub>50</sub> of curcumin and selected CMCs against MMP-13

		1,10-Phen	Curcumin	CMC2.5	CMC2.14	CMC2.23	CMC2.24
Test 1	IC <sub>50</sub> (uM)	35.0	4.0	20.0	25.0	3.0	4.0
Test 2	IC <sub>50</sub> (uM)	45.0	4.0	30.0	25.0	4.0	2.0
Test 3	IC <sub>50</sub> (uM)	70.0	3.0	35.0	30.0	3.0	2.0
	Ave.	50.0	3.7	28.3	26.7	3.3	2.7
	S.D.	18.03	0.58	7.64	2.89	0.58	1.15
	S.E.M.	10.41	0.33	4.41	1.67	0.33	0.67



Figure 4.9 MMP-14 inhibition assay

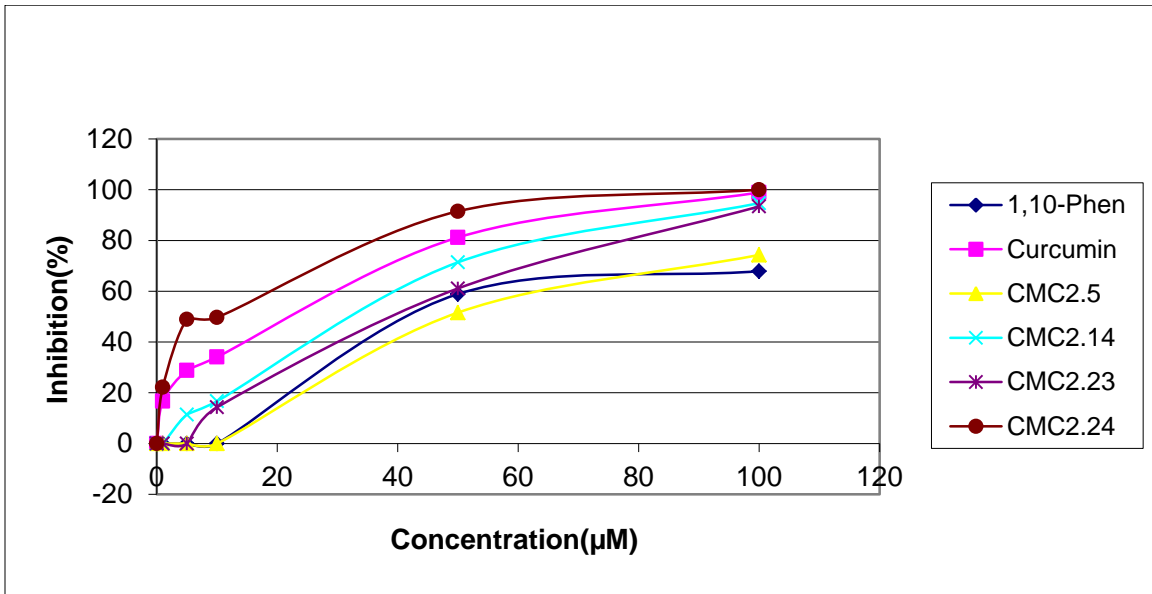


Figure 4.9a Test 1 in MMP-14 inhibition assay

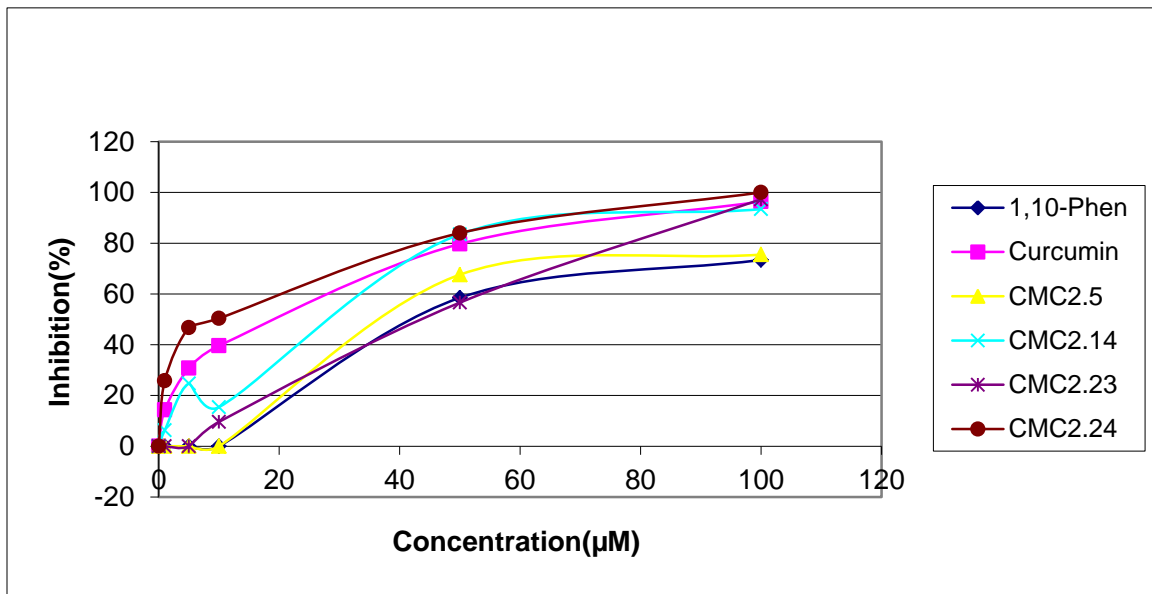


Figure 4.9b Test 2 in MMP-14 inhibition assay

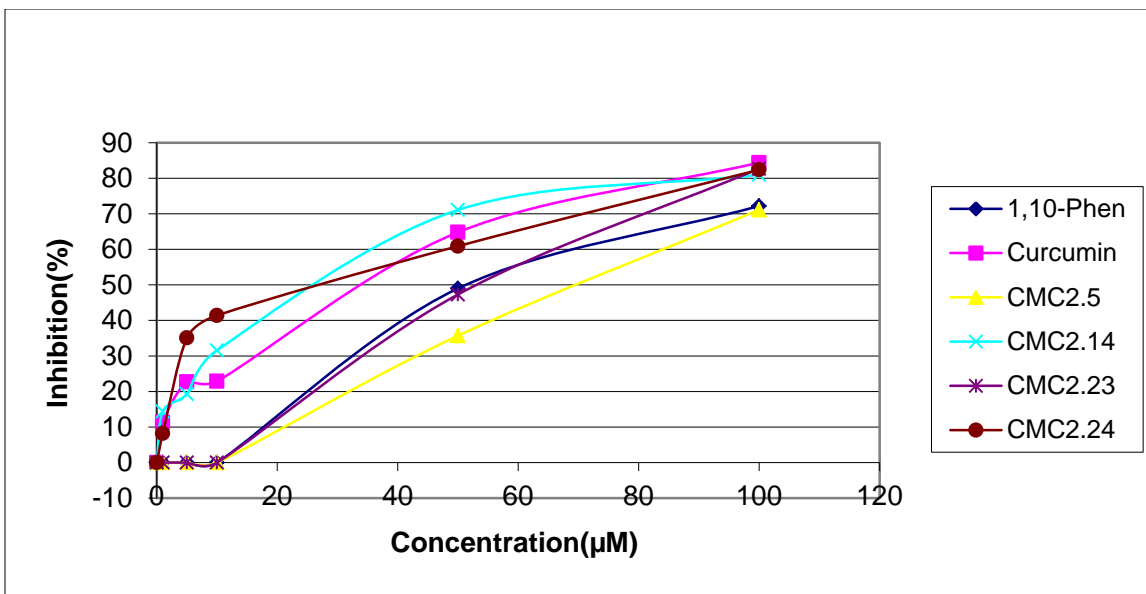


Figure 4.9c Test 3 in MMP-14 inhibition assay

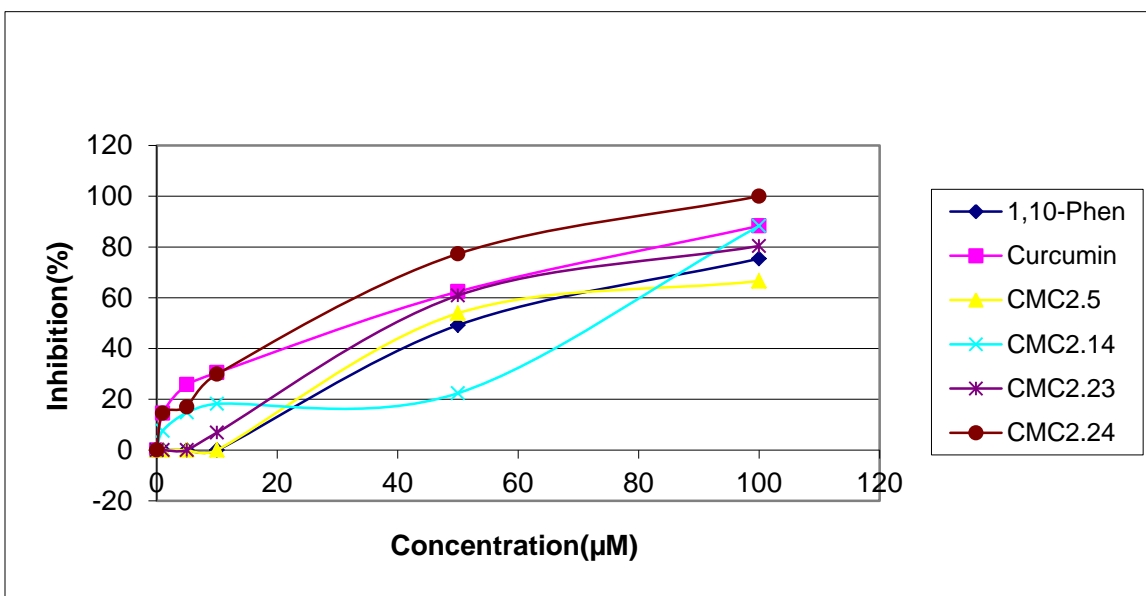


Figure 4.9d Test 4 in MMP-14 inhibition assay

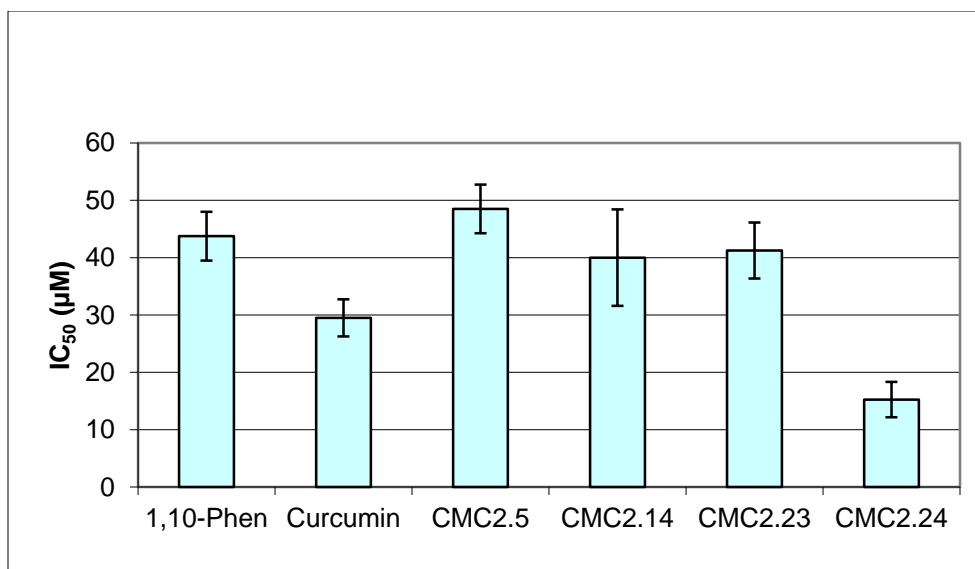


Figure 4.9e IC<sub>50</sub> of curcumin and selected CMCs against MMP-14

Table 4.10 IC<sub>50</sub> of curcumin and selected CMCs against MMP-14

		1,10- Phen	Curcumin	CMC2.5	CMC2.14	CMC2.23	CMC2.24
Test 1	IC <sub>50</sub> (µM)	35.0	25.0	46.0	30.0	32.0	12.0
Test 2	IC <sub>50</sub> (µM)	38.0	24.0	42.0	30.0	38.0	10.0
Test 3	IC <sub>50</sub> (µM)	52.0	31.0	61.0	35.0	55.0	15.0
Test 4	IC <sub>50</sub> (µM)	50.0	38.0	45.0	65.0	40.0	24.0
	Ave.	43.8	29.5	48.5	40.0	41.3	15.3
	S.D.	8.50	6.45	8.50	16.83	9.78	6.18
	S.E.M.	4.25	3.23	4.25	8.42	4.89	3.09

Table 4.11 *In vitro* potency of curcumin and selected chemically-modified curcumins (CMCs)

Note: 1,10-Phenanthroline, was used as the positive control for the fluorogenic MMP inhibitory assay. Curcumin and CMCs were evaluated as inhibitors of nine different mammalian (human-derived) MMPs. IC<sub>50</sub>s (in  $\mu$ M concentration) were measured using a synthetic fluorescent peptide substrate (Mca-Lys-Pro-Leu-Gly-Leu-Dpa-Ala-Arg-NH<sub>2</sub>) for MMPs and which has a cleavage site between Gly and Leu. Each value represents the mean of at 3 or 4 analyses ( $\pm$ S.E.M.).

Compounds		1,10-Phenanthroline	Curcumin	CMC2.5	CMC2.14	CMC2.23	CMC2.24
Collagenases	MMP-1	42.0 $\pm$ 1.1	85.8 $\pm$ 1.8	74.0 $\pm$ 3.5	76.3 $\pm$ 6.5	68.0 $\pm$ 3.2	69.8 $\pm$ 2.0
	MMP-8	31.3 $\pm$ 0.5	6.8 $\pm$ 1.0	30.8 $\pm$ 1.5	20.0 $\pm$ 2.0	2.5 $\pm$ 0.3	4.5 $\pm$ 0.5
	MMP-13	50.0 $\pm$ 10.4	3.7 $\pm$ 0.3	28.3 $\pm$ 4.4	26.7 $\pm$ 1.7	3.3 $\pm$ 0.3	2.7 $\pm$ 0.7
Gelatinases	MMP-2	73.8 $\pm$ 1.0	5.0 $\pm$ 0.7	25.3 $\pm$ 1.3	23.8 $\pm$ 0.9	6.3 $\pm$ 0.9	4.8 $\pm$ 0.5
	MMP-9	45.0 $\pm$ 12.6	30.0 $\pm$ 2.9	55.0 $\pm$ 17.3	43.3 $\pm$ 4.4	8.7 $\pm$ 0.7	8.0 $\pm$ 0.6
Others	MMP-3	77.0 $\pm$ 3.2	4.7 $\pm$ 0.8	32.5 $\pm$ 2.8	28.3 $\pm$ 1.0	5.3 $\pm$ 0.7	2.9 $\pm$ 0.4
	MMP-7	196.8 $\pm$ 8.8	51.8 $\pm$ 2.5	48.8 $\pm$ 0.5	57.5 $\pm$ 4.6	21.5 $\pm$ 1.0	5.0 $\pm$ 0.7
	MMP-12	29.5 $\pm$ 1.3	2.6 $\pm$ 0.2	27.8 $\pm$ 1.7	5.3 $\pm$ 0.3	4.5 $\pm$ 0.5	2.0 $\pm$ 0.4
	MMP-14	43.8 $\pm$ 4.2	29.5 $\pm$ 3.2	48.5 $\pm$ 4.3	40.0 $\pm$ 8.4	41.3 $\pm$ 4.9	15.3 $\pm$ 3.1

#### D. Inhibition of MMP-9 by newer curcumin analogues

Four newer chemically-modified curcumins, namely CMC2.25, CMC2.26, CMC2.27 and CMC2.28 were synthesized based on the lead compound CMC2.24 in order to increase the solubility. These four compounds were evaluated in the MMP-9 *in vitro* assay first, and the data reveal that CMC2.25 (the introduction of chloride on the middle phenyl ring) and CMC2.26 (the introduction of methoxy group on the middle phenyl ring) were as potent as CMC2.24. However, CMC2.27 (the introduction of ketal group on the middle phenyl ring) and CMC2.28 (the introduction of adjacent diol on the middle phenyl ring) didn't show great activity in the inhibition assay against MMP-9 (Table 4.12, Figure 4.10).

Table 4.12 IC<sub>50</sub> of newer CMCs against MMP-9

		1,10-Phen	CMC2.24	CMC2.25	CMC2.26	CMC2.27	CMC2.28
Test 1	IC <sub>50</sub> (μM)	37.0	7.0	5.0	4.0	46.0	63.0
Test 2	IC <sub>50</sub> (μM)	42.0	4.0	6.0	5.0	52.0	61.0
Test 3	IC <sub>50</sub> (μM)	41.0	7.0	8.0	5.0	56.0	68.0
	Ave.	40.0	6.0	6.3	4.7	51.3	64.0
	S.D.	2.64	1.73	1.52	0.57	5.03	3.6
	S.E.M.	1.32	0.86	0.76	0.28	2.51	1.8

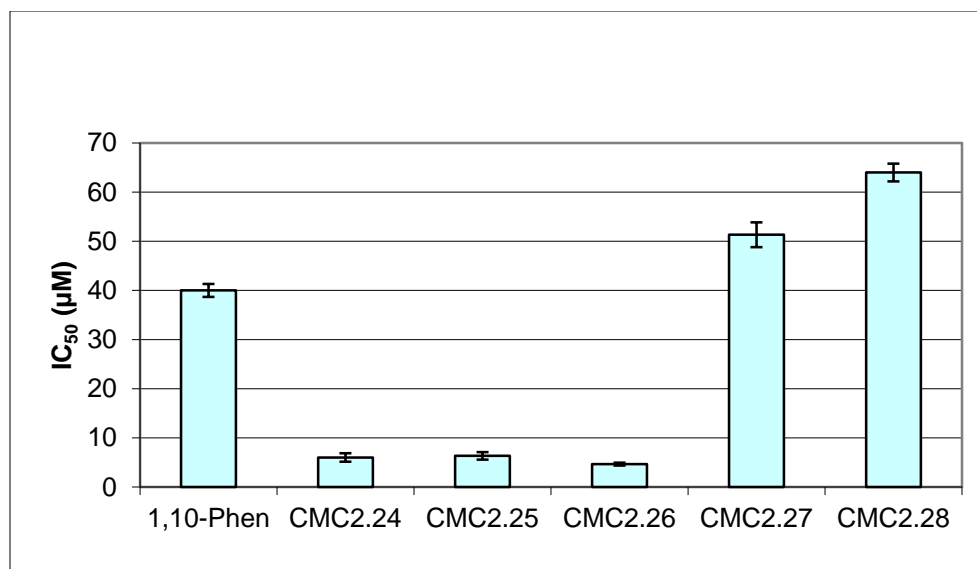


Figure 4.10 IC<sub>50</sub> of newer CMCs against MMP-9

## Materials and Methods

### 1. HPLC MMP inhibition assay

MMP-9 human neutrophil monomer was purchased from Calbiochem, EMD Biosciences, Inc. (La Jolla, CA) and activated by adding *p*-aminophenylmercuric acetate (APMA) purchased from Sigma-Aldrich (St. Louis, MO) to achieve a final concentration of 1mM in DMSO purchased from Sigma-Aldrich (St. Louis, MO). Dnp-Pro-Gln-Gly-Ile-Ala-Gly-Gln-D-Arg-OH, purchased from BACHEM (Torrance, CA) was used as substrate. Stock solutions of 1,10-phenanthroline, curcumin and curcumin analogues were prepared in DMSO at a final concentrations of 1, 5, 10, 25, 50, 100, 250 and 500 µM in the reaction mixture. Both the substrate and the tripeptide breakdown product absorb at 380nm with the same extinction coefficient. 90 µL of 5mM CaCl<sub>2</sub>, 0.2M NaCl and 50mM Tris/HCl pH=7.6 buffer, 1 µL of MMP-9 producing 10-15% lysis of the synthetic peptide substrate, 1 µL of stock solutions of 1,10-phenanthroline, curcumin or curcumin analogues prepared in DMSO and 10 µL of substrate were added and then incubated at 37°C for

4h. The reaction mixture was stopped by adding 100  $\mu$ L of the stop solution (30% acetonitrile in 2M acetic acid, containing 4mM 1,10-phenanthroline); samples were vortexed and centrifuged for 10min at 10,000rpm. An aliquot of 120  $\mu$ L was injected into HPLC (Waters Alliance 2695 System) for analysis (HPLC developing system: 20% Acetonitrile, 80% H<sub>2</sub>O), and the percentage of lysis was calculated and converted to the inhibition percentage.

## 2. Fluorogenic MMP inhibition assay

MMP-1, -2, -3, -7, -8, -12, -13 and -14 were all recombinant human enzymes and were purchased from R&D Systems, Inc. (Minneapolis, MN), whereas MMP-9 human neutrophil monomer was purchased from Calbiochem, EMD Biosciences, Inc. (La Jolla, CA). MMP-1, -2, -3, -7, -8, -9, -12 and -13 were activated by adding *p*-aminophenylmercuric acetate (APMA) purchased from Sigma-Aldrich (St. Louis, MO) to achieve a final concentration of 1mM in DMSO purchased from Sigma-Aldrich (St. Louis, MO). MMP-14 was activated by recombinant human furin, purchased from R&D Systems, Inc. (Minneapolis, MN). The substrate for MMP-1, -2, -7, -8, -9, -12, -13 and -14 was Mca-Pro-Leu-Gly-Leu-Dpa-Ala-Arg-NH<sub>2</sub> fluorogenic peptide substrate IX, purchased from R&D Systems, Inc. (Minneapolis, MN). [Mca: (7-Methoxycoumarin-4-yl) acetyl, Dpa: N-3-(2, 4-Dinitrophenyl)-L-2,3-diaminopropionyl]. The substrate for MMP-3 was Mca-Arg-Pro-Lys-Pro-Val-Glu-Nval-Trp-Arg-Lys(Dnp)-NH<sub>2</sub> fluorogenic peptide substrate II, purchased from R&D Systems, Inc. (Minneapolis, MN). [Mca: (7-Methoxycoumarin-4-yl)acetyl, Nval: Norvaline, Dnp: 2, 4-Dinitrophenyl]. Cleavage of the fluorogenic substrate was measured by the differences in intensities of the excitation and emission wavelengths at 320nm and 405nm, respectively. Stock solutions of 1,10-phenanthroline, curcumin and curcumin analogues were prepared in DMSO at concentrations of 1, 5, 10, 25, 50, 100, 250 and 500  $\mu$ M. 100  $\mu$ L solution containing 80  $\mu$ L of 1mM CaCl<sub>2</sub>, 0.2M

NaCl and 50mM Tris/HCl (pH=7.6) buffer and 10 $\mu$ L of enzyme, were added first to the 96 well plate, followed by the addition of different concentrations of inhibitor (1  $\mu$ L) and substrate (10 $\mu$ L) to a final reaction volume now containing 1% DMSO. The whole mixture was incubated at 37°C for 4h, and Fluoro Count (Packard Instrument Co., CT) was used to measure the increase in fluorescence when the substrate was cleaved. By comparison with the uninhibited degradation from enzyme and substrate, the percentage of inhibition was determined by subtracting the degradation of the enzyme, substrate and inhibitor mixture. The IC<sub>50</sub> for each compound was obtained from a plot of the percentage of inhibition versus the inhibitor concentration.

## References

1. Golub, L.M.; Ciancio, S.; Ramamurthy, N.S.; Leung, M.; McNamara, T.F. Low-dose doxycycline therapy: effect on gingival and crevicular fluid collagenase activity in humans. *J. Periodontal Res.*, **1990**, *25*, 321-330
2. Knight, C.G.; Willenbrock, F; Murphy, G. A novel coumarin-labelled peptide for sensitive continuous assays of the matrix metalloproteinases. *FEBS Lett.*, **1992**, *296*, 263-266
3. Nagase, H.; Enghild, J.J.; Suzuki, K.; Salvesen, G. Stepwise activation mechanisms of the precursor of matrix metalloproteinase 3 (stromelysin) by proteinases and (4-aminophenyl) mercuric acetate. *Biochemistry*, **1990**, *29*, 5783-5789
4. Nagase, H.; Fields, C.G.; Fields, G.B. Design and Characterization of a Fluorogenic Substrate Selectively Hydrolyzed by Stromelysin 1 (Matrix Metalloproteinase-3). *J. Biol. Chem.*, **1994**, *269*, 20952-20957
5. Meikle, M.C.; Bord, S.; Hembry, R.M.; Comston, J.; Croucher, P.I.; Reynolds, J.J. Human osteoblasts in culture synthesize collagenase and other matrix metalloproteinases in response to osteotropic hormones and cytokines. *J. Cell Sci.*, **1992**, *103*, 1093-1099



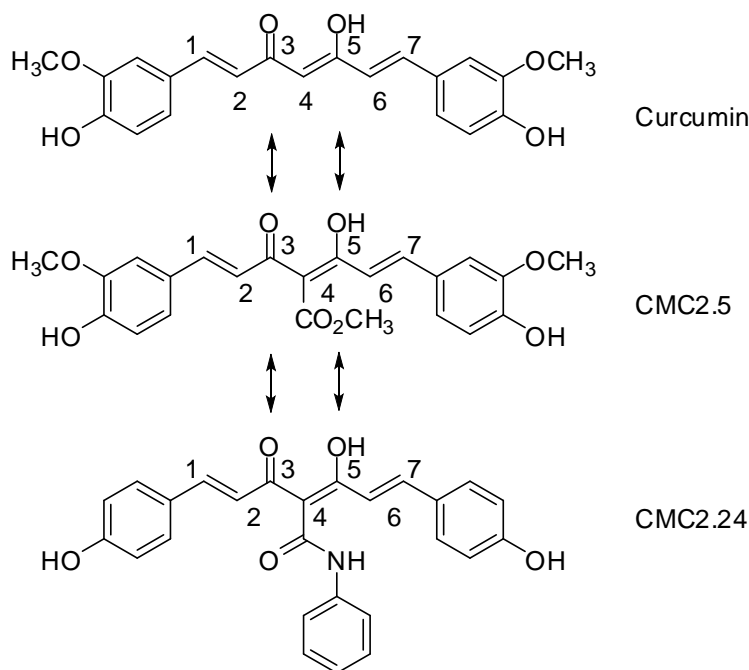
6. Liotta, L.A.; Abe, S.; Robey, P.G.; Martin, G.R. Preferential digestion of basement membrane collagen by an enzyme derived from a metastatic murine tumor. *Proc. Natl. Acad. Sci. USA*, **1979**, *76*, 2268-2272
7. Chin, J.R.; Murphy, G.; Werb, Z. Stromelysin, a connective tissue-degrading metalloendopeptidases secreted by stimulated rabbit synovial fibroblasts in parallel with collagenase. Biosynthesis, isolation, characterization, and substrates. *J. Biol. Chem.*, **1985**, *260*, 12367-12376
8. Powell, W.C.; Knox, J.D.; Navre, M.; Grogan, T.M.; Kittelson, J.; Nagle, R.B.; Bowden, G.T. Expression of the metalloproteinase matrilysin in DU-145 cells increases their invasive potential in severe combined immunodeficient mice. *Cancer Res.*, **1993**, *53*, 417-422
9. Prikk, K.; Maisi, P.; Pirila, E.; Sepper, R.; Salo, T.; Wahlgren, J.; Sorsa, T. In vivo collagenase-2 (MMP-8) expression by human bronchial epithelial cells and monocytes/macrophages in bronchiectasis. *J. Pathol.*, **2001**, *194*, 232-238
10. Wilhelm, S.M.; Collier, I.E.; Marmer, B.L.; Eisen, A.Z.; Grant, G.A.; Goldberg, G.I. SV 40-transformed human lung fibroblasts secrete a 92 kDa type IV collagenase which is identical to that secreted by normal human macrophages. *J. Biol. Chem.*, **1989**, *264*, 17213-17221
11. Warner, R.L.; Lewis, C.S.; Beltran, L.; Youkin, E.M.; Varani, J.; Johnson, K.J. The role of metalloelastase in immune complex-induced acute lung injury. *Am. J. Pathol.*, **2001**, *158*, 2139-2144
12. Konttinen, Y.T.; Salo, T.; Hanemaaijer, R.; Valleala, H.; Sorsa, T.; Sutinen, M.; Ceponis, A.; Xu, J.W.; Santavirta, S.; Teronen, O.; López-Otín, C. Collagenase-3 (MMP-13) and its activators in rheumatoid arthritis: localization in the pannus-hard tissue junction and inhibition by alendronate. *Matrix Biol.*, **1999**, *18*, 401-412

13. Sato, H.; Kinoshita, T.; Takino, T.; Nakayama, K.; Seiki, M. Activation of a recombinant membrane type 1-matrix metalloproteinase (MT1-MMP) by furin and its interaction with tissue inhibitor of metalloproteinases (TIMP)-2. *FEBS Lett.*, **1996**, *393*, 101-104
14. Morimoto, T.; Yamasaki, M.; Nakata, K.; Tsuji, M.; Nakamura, H. The expression of macrophage and neutrophil elastases in rat periradicular lesions. *J. Endod.*, **2008**, *34*, 1072-1076

## Chapter 5. pK<sub>a</sub>, zinc- and bovine serum albumin binding, and antimicrobial studies on curcumin, CMC2.5 and CMC2.24

### A. Introduction

The acid dissociation constant, K<sub>a</sub> is used to quantitatively describe the acidity of a compound in a particular solution. Normally, the logarithmic form pK<sub>a</sub> ( $-\log_{10}K_a$ ) is used to compare the acidities of different compounds. Values of the pK<sub>a</sub>s of the three acidic groups of curcumin have been reported by Bernabé-Pineda *et al.*<sup>1</sup> As mentioned in Chapters 1 and 2, the poor aqueous solubility of curcumin limits its therapeutic use. Two factors might affect the bioavailability: charge type (charging aqueous solubility at physiological pH) and enhanced solubility in the blood. We therefore determined the pK<sub>a</sub>s of the three acidic groups in the compounds: curcumin, CMC2.5 and CMC2.24. It has also been established that some MMP inhibitors appear to act by binding to the enzymic Zn<sup>2+</sup> through a β-diketone assembly.<sup>2-4</sup> We hope that the modified compounds might bind to Zn<sup>2+</sup> more strongly than curcumin does, because of the electron-withdrawing power of the 4-substitutions. We therefore studied Zn<sup>2+</sup> binding to these compounds. A bovine serum albumin assay was also carried out for curcumin and CMC2.24 to determine their binding to the major plasma transport protein, serum albumin.<sup>5-6</sup> Because FDA only permits the use of subantimicrobial doses of antibiotics for other diseases than infections, therefore an antimicrobial assay was carried out for curcumin, CMC2.5 and CMC2.24 accordingly, for both minimum inhibitory concentration (MIC) test and β-galactosidase inhibition, whereas the known antibiotic, doxycycline was used as a positive control.



Scheme 5.1 Structures of curcumin, CMC2.5 and CMC2.24

### B. $pK_a$ measurement

The  $pK_a$ s of curcumin have been reported by Bernabé-Pineda *et al.*, and were found to be  $pK_{a1}=8.38$  for  $H_3D = H_2D^- + H^+$ ,  $pK_{a2}=9.88$  for  $H_2D^- = HD^{2-} + H^+$ , and  $pK_{a3}=10.51$  for  $HD^{2-} = D^{3-} + H^+$  (D is designated here as any deprotonated form of curcumin).<sup>1</sup> In our studies on CMC2.5 and CMC2.24, we obtained the spectra seen in Figure 5.1, which shows the raw spectra as a function of pH. In Figure 5.1 at certain wavelengths, 3 or 4 species were found and correlated with the progressive forms of deprotonation products of curcumin, CMC2.5 and CMC2.24. Figure 5.2 shows the fitted curves extracted from these data, displayed at wavelengths chosen to maximize the contrasts. Figure 5.3 shows the derived spectra of the various species for these three compounds. It was noted that CMC2.5 and CMC2.24 are more acidic with regard to the enolic proton, which correlates with an introduction of the electron-withdrawing group, either methoxycarbonyl or phenylaminocarbonyl group at carbon-4, whereas the two phenolic protons

on either CMC2.5 or CMC2.24 are likewise more acidic than those of curcumin. (Table 5.1) However, for CMC2.5, a third deprotonation was not observed. The standard error for all the  $pK_a$  measurements for curcumin, CMC2.5 and CMC2.24 was less than 0.1 in all cases.

Table 5.1  $pK_a$  of curcumin, CMC2.5 and CMC2.24

Compound	$pK_a$
Curcumin	$pK_{a1}= 8.41, pK_{a2}=9.94, pK_{a3}=11.12$
CMC2.5	$pK_{a1}= 6.50, pK_{a2}= pK_{a3}=8.82$
CMC2.24	$pK_{a1}= 6.98, pK_{a2}=8.40, pK_{a3}=9.80$

For curcumin, the data correlated surprisingly well with the reported  $pK_a$  values.<sup>1</sup> One intermediate species was found after graph fitting, which suggests a tautomeric form of curcumin. An isosbestic point (448.5nm) was found for curcumin at pH 8.9, and then the curve shifted to the lower wavelength. The rate of transformation was remarkably slow when the pH was raised to 11.0. As for CMC2.5, the third  $pK_a$  was not observed because of 1) the striking isobestic point above pH 9.0; 2) the dramatic change in the range of pH 6.5. Two distinct processes were found after the fitting for CMC2.24, in which the rate of transformation became slow around pH 11.0. A time dependence was observed for all three compounds, and the deprotonation process was slow for the protic acids. (Figure 5.4) As had BernabéPineda *et al.*<sup>1</sup> earlier, we observed that the spectra of all three species varied with time, and so we determined the  $pK_a$  values extrapolated to zero. For curcumin, the time-dependence was such that we could determine the spectra for an intermediate compound.

Figure 5.1 Spectra for pH titration

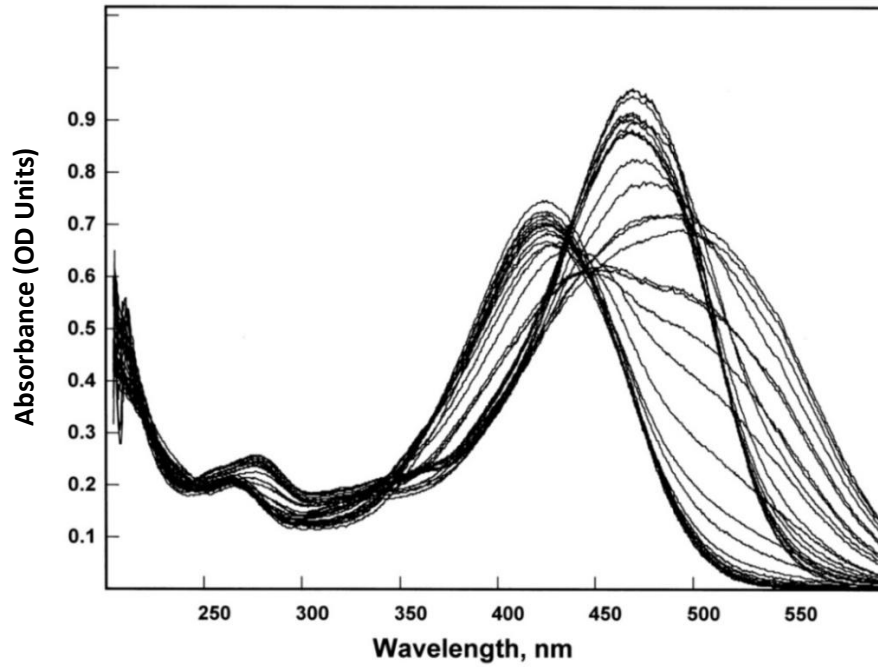


Figure 5.1a Spectra for pH titration of curcumin

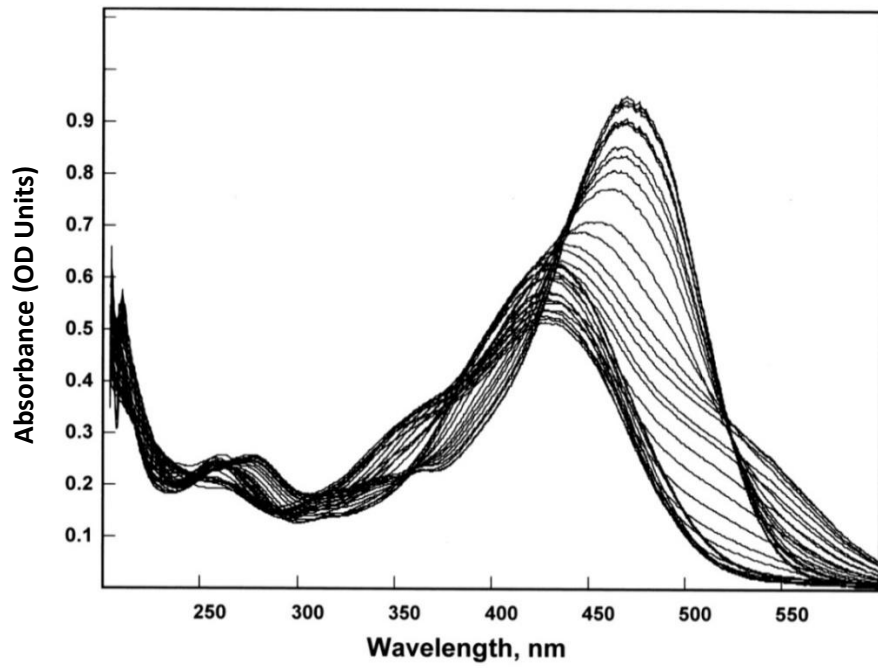


Figure 5.1b Spectra for pH titration of curcumin intermediate

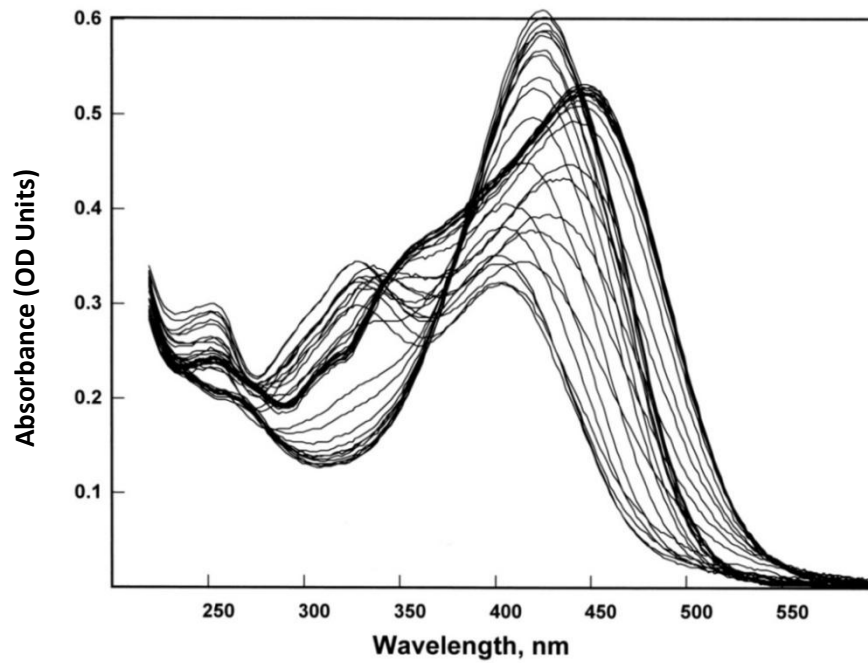


Figure 5.1c Spectra for pH titration of CMC2.5

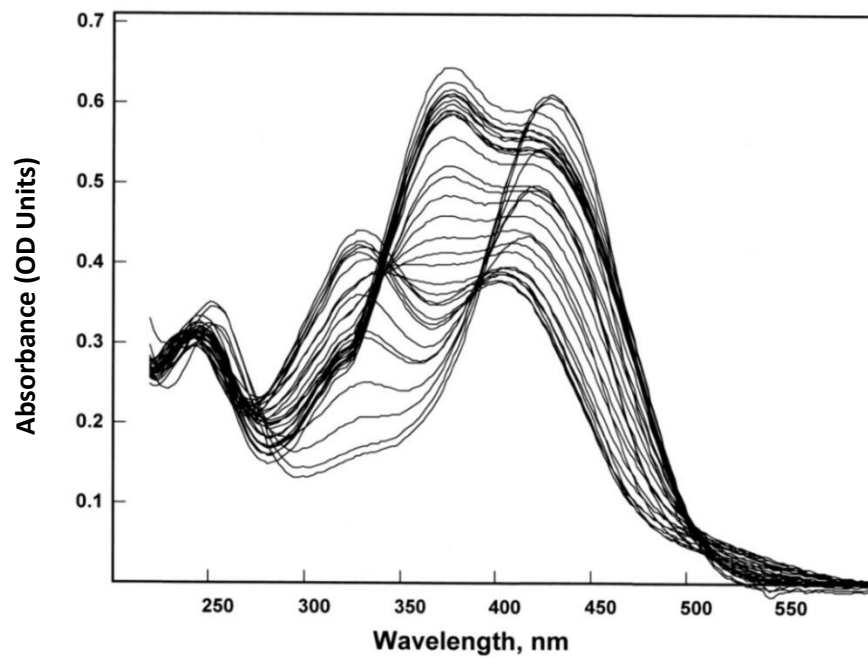


Figure 5.1d Spectra for pH titration of CMC2.24

Figure 5.2 Fittings at selected wavelengths for curcumin, CMC2.5 and CMC2.24

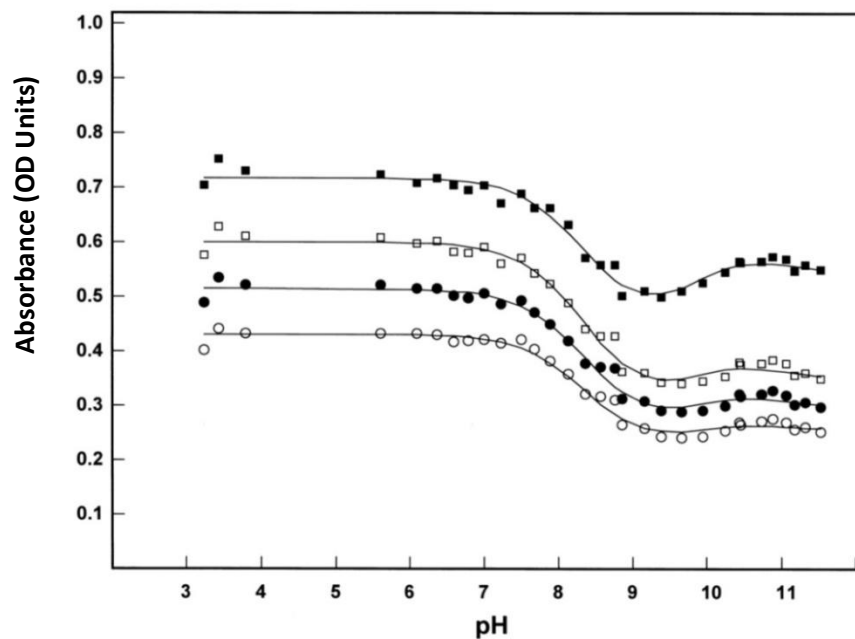


Figure 5.2a Fitting of curcumin, reading up at pH 7.2: 380, 390, 400, 425nm

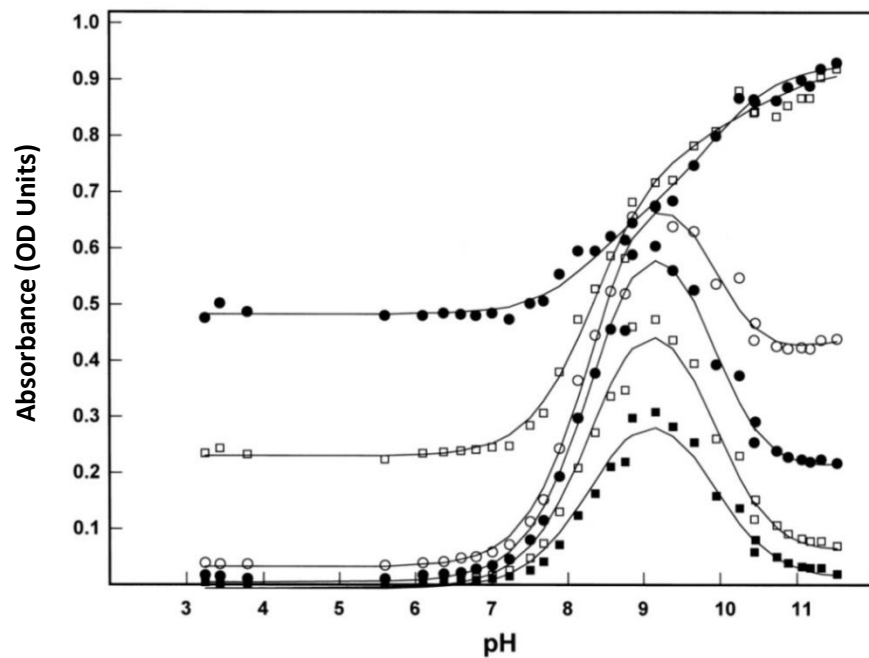


Figure 5.2b Fitting of curcumin, reading down at pH 11.0: 460, 482, 495, 515, 530, 550, 570nm



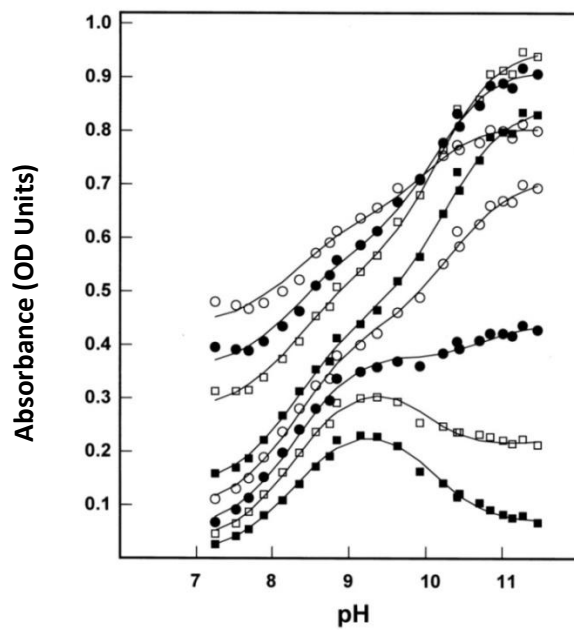


Figure 5.2c Fitting of curcumin intermediate, reading down at pH 7.2: 448,460, 470, 490, 500, 515, 530, 550nm

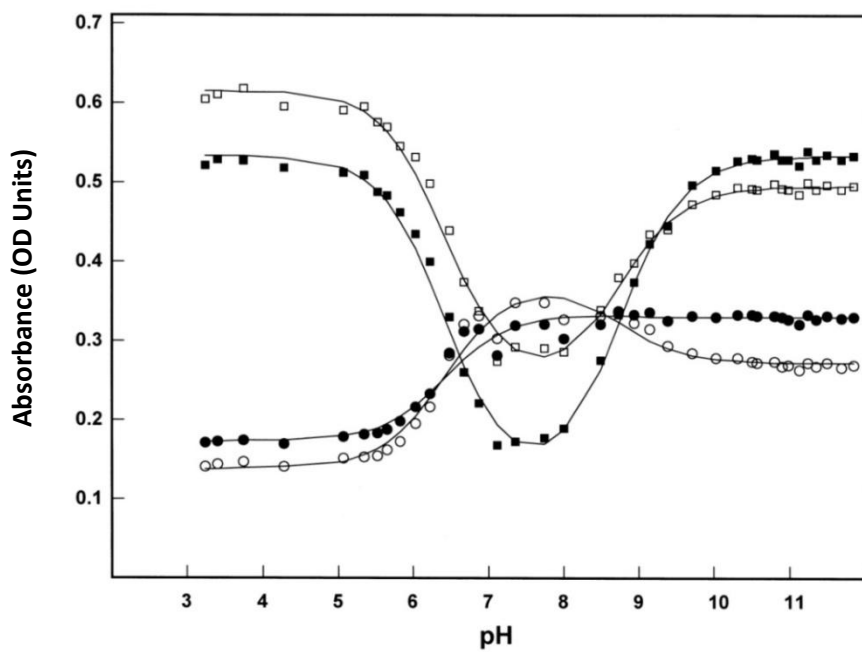


Figure 5.2d Fitting of CMC2.5: reading up at pH 3.0: 329, 344, 446nm

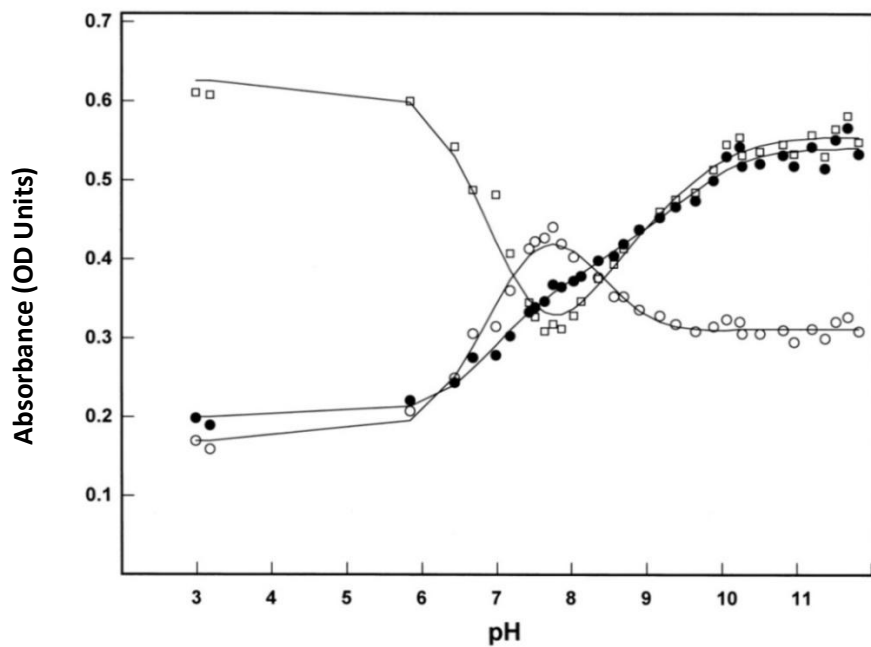


Figure 5.2e Fitting of CMC2.24, open circle, 329nm, filled circle, 356nm; open square, 428nm

Figure 5.3 Calculated spectra for curcumin, curcumin intermediate, CMC2.5 and CMC2.24

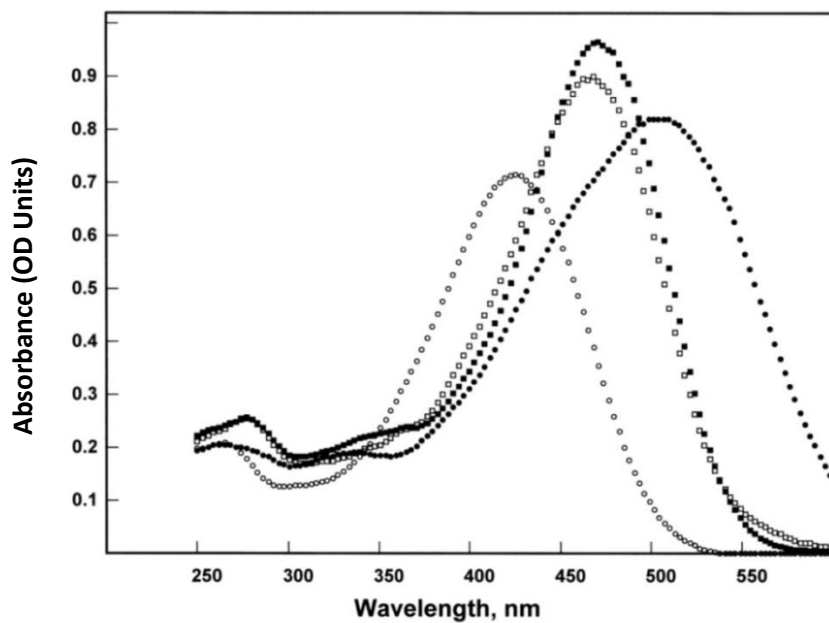


Figure 5.3a Calculated spectra for curcumin, reading down at 470nm:  $D^{3-}$ ,  $HD^{2-}$ ,  $H_2D^-$ ,  $H_3D$

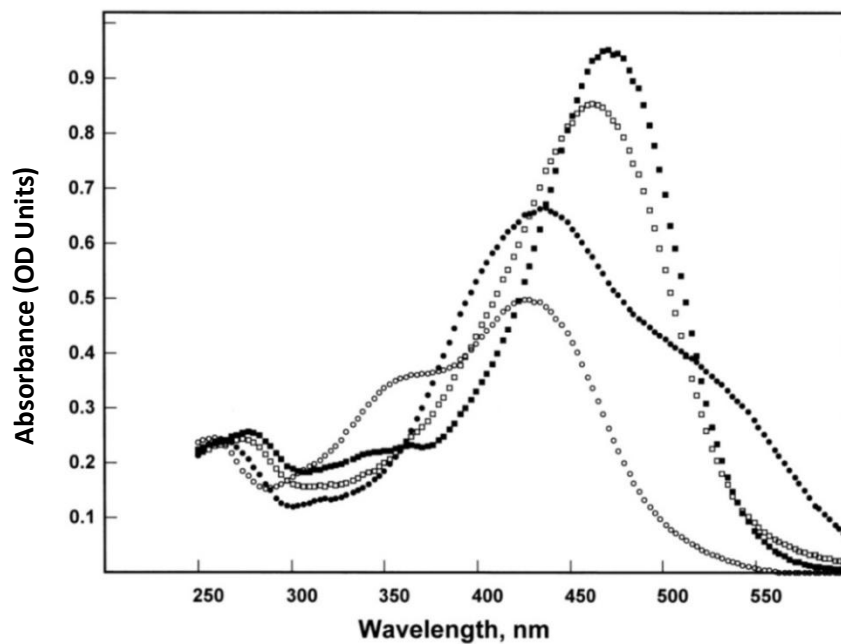


Figure 5.3b Calculated spectra for curcumin intermediate, reading down at 470nm:  $D^{3-}$ ,  $HD^{2-}$ ,  $H_2D^-$ ,  $H_3D$

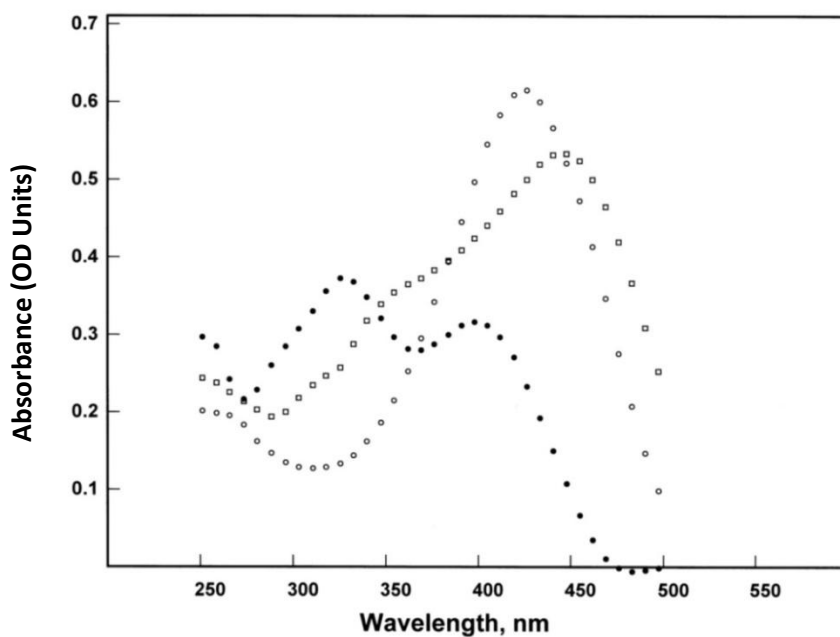


Figure 5.3c Calculated spectra for CMC2.5, reading down at 440nm:  $H_3D$ ,  $HD^{2-}$ ,  $D^{3-}$

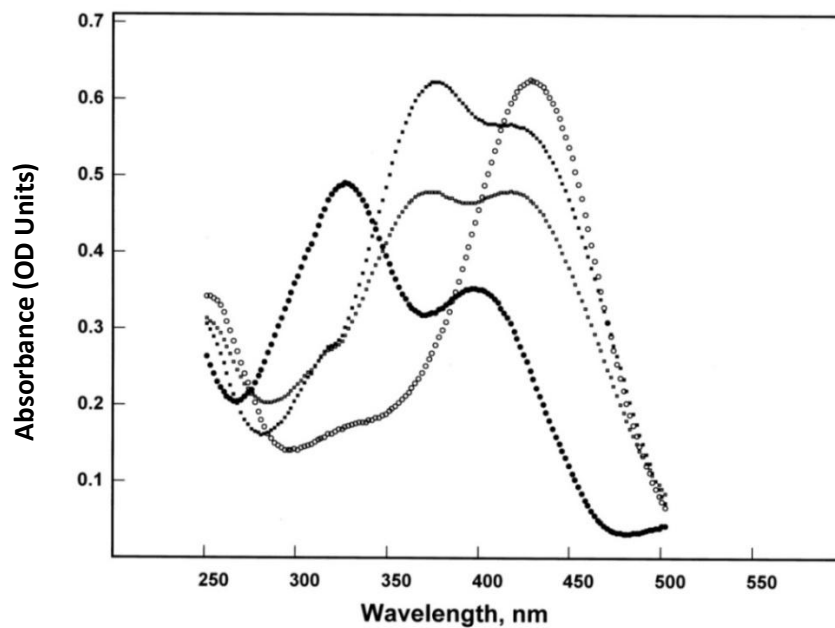


Figure 5.3d Calculated spectra for CMC2.24, reading down at 440 nm:  $H_3D$ ,  $H_2D^-$ ,  $HD^{2-}$ ,  $D^{3-}$

Figure 5.4 Time-dependent spectra for curcumin and CMC2.5

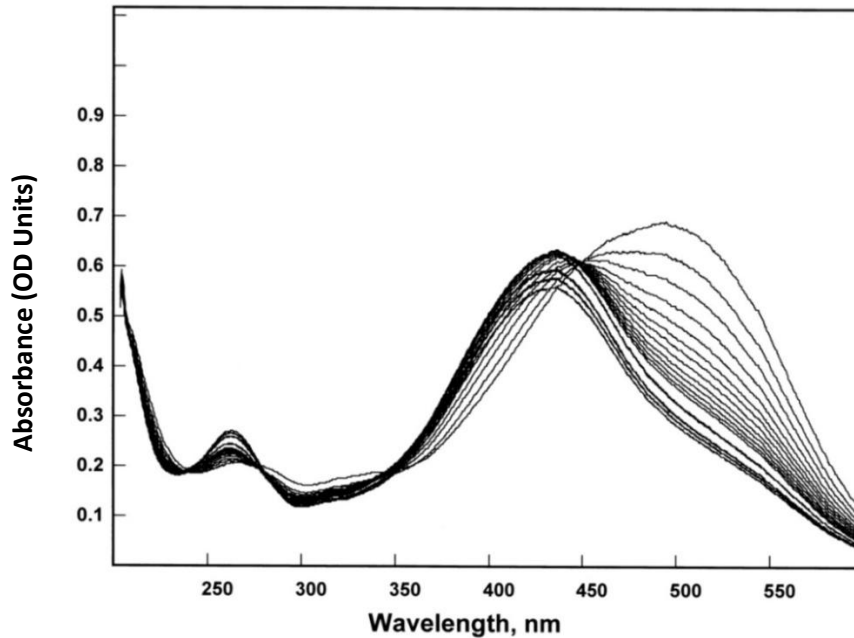


Figure 5.4a Spectra of curcumin, pH 8.94, through the isosbestic point at 448.71nm, 2sec intervals to 24sec; darker, displaced lines, 40, 60, 80, 100sec

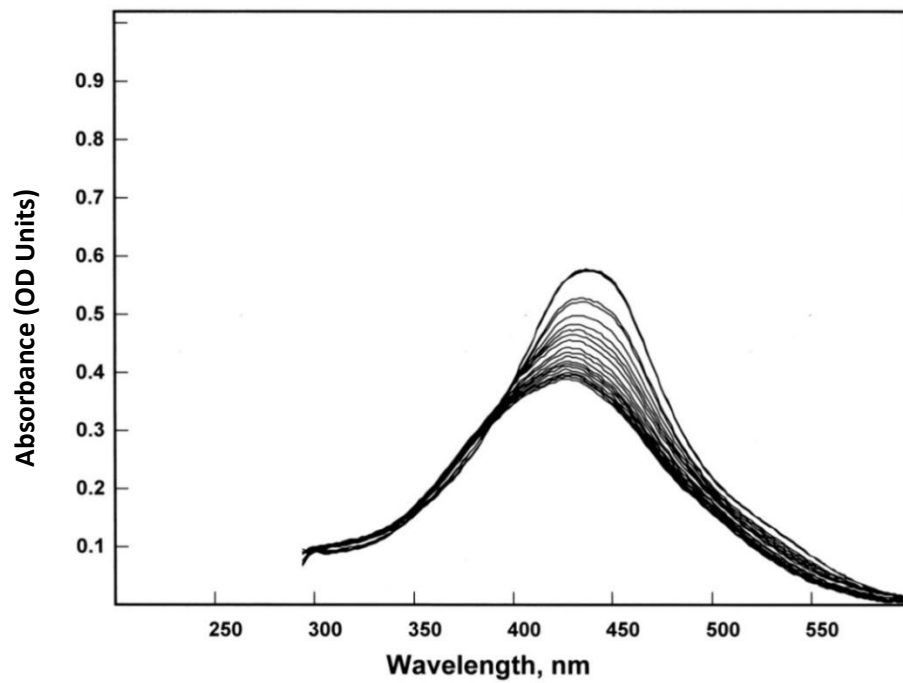


Figure 5.4b Spectra of curcumin in 88  $\mu$ M BSA, 1h intervals

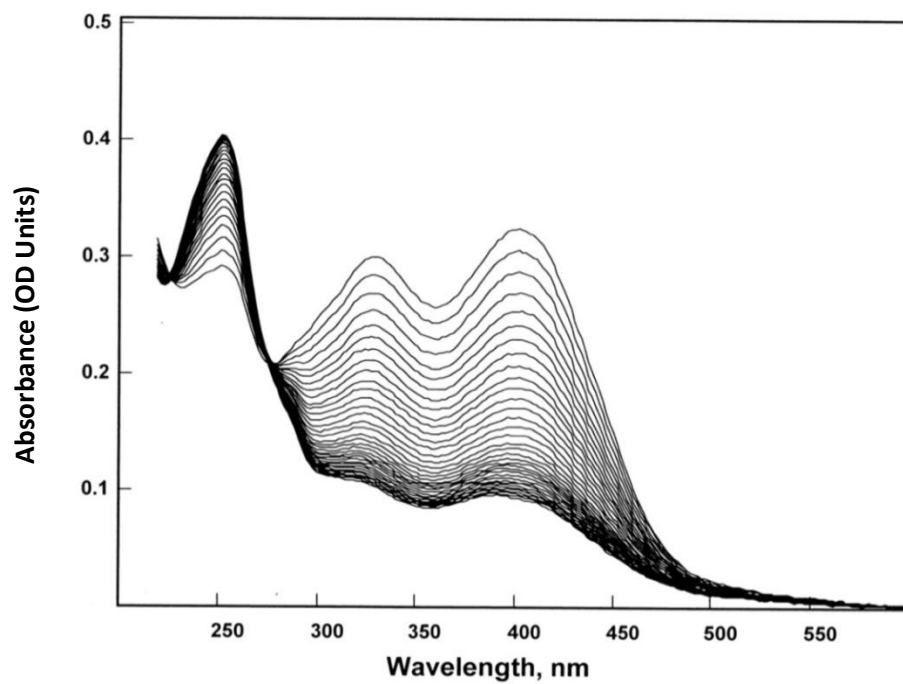


Figure 5.4c Spectra of CMC 2.5, pH 7.00, 5sec intervals

### C. Zinc binding study

Because the MMPs are zinc-dependent enzymes, the binding to zinc ions is a probable contributor to the inhibition, as first shown for doxycycline.<sup>2-4</sup> Therefore zinc binding studies were carried out for curcumin, CMC2.5 and CMC2.24. Figure 5.5 shows the spectra of curcumin, CMC2.5 and CMC2.24 at different concentrations of zinc ions. These data were fitted at multiple wavelengths to extract the derived spectra. Figure 5.6 shows the fitted spectra for these compounds. Several wavelengths were plotted and calculated for the dissociation constant:  $K = (cb - cx)(ca - cx)/cx$ , where  $cb$  is the total concentration of zinc ion,  $ca$  is the concentration of curcumin or a CMC and  $cx$  is the concentration of the complex formed by the zinc with curcumin or a CMC. When  $cb \gg cx$ ,  $K_D$  reduced to  $cb(ca - cx)/cx$ . The dissociation constants found were  $1385 \pm 89 \mu\text{M}$  for curcumin,  $1880 \pm 68 \mu\text{M}$  for CMC2.5 and  $765 \pm 20 \mu\text{M}$  for CMC2.24. CMC2.24 shows slightly stronger binding to zinc ion compared to both curcumin and CMC2.5. It should be noted that the interaction of CMC2.24 with zinc ion would be strong enough to form a complex with the zinc ion in the catalytic domain of MMPs, thus it is responsible for its inhibitory activity. The free energy of binding for CMC2.24, is deduced from  $\Delta G = -RT \ln K$ , and is approximately -28kJ, which would enable the enolate form to bind to the zinc ion strongly.

Figure 5.5 Spectra for zinc binding study for curcumin, CMC2.5 and CMC2.24

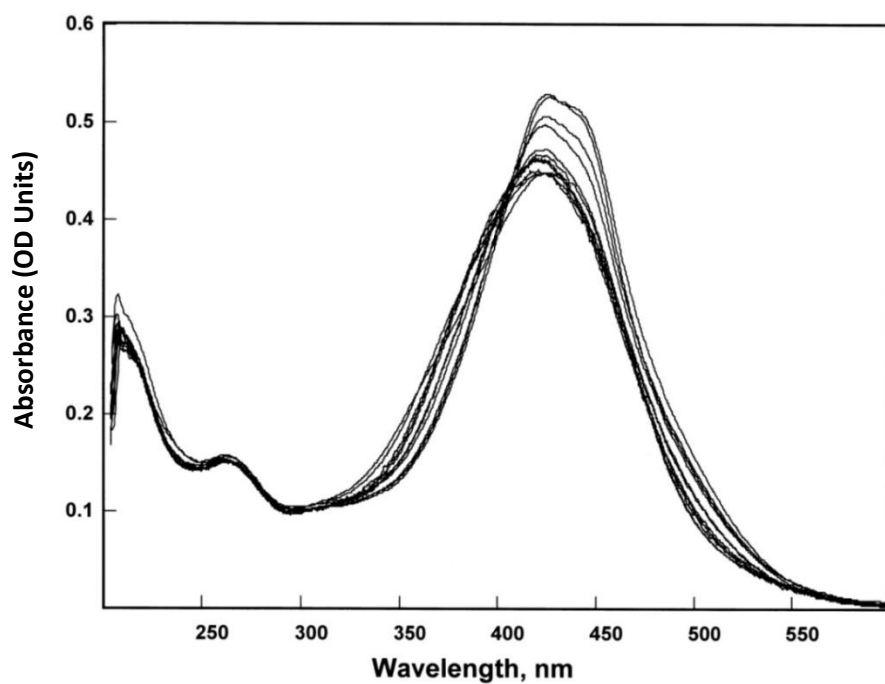


Figure 5.5a Zinc binding of curcumin

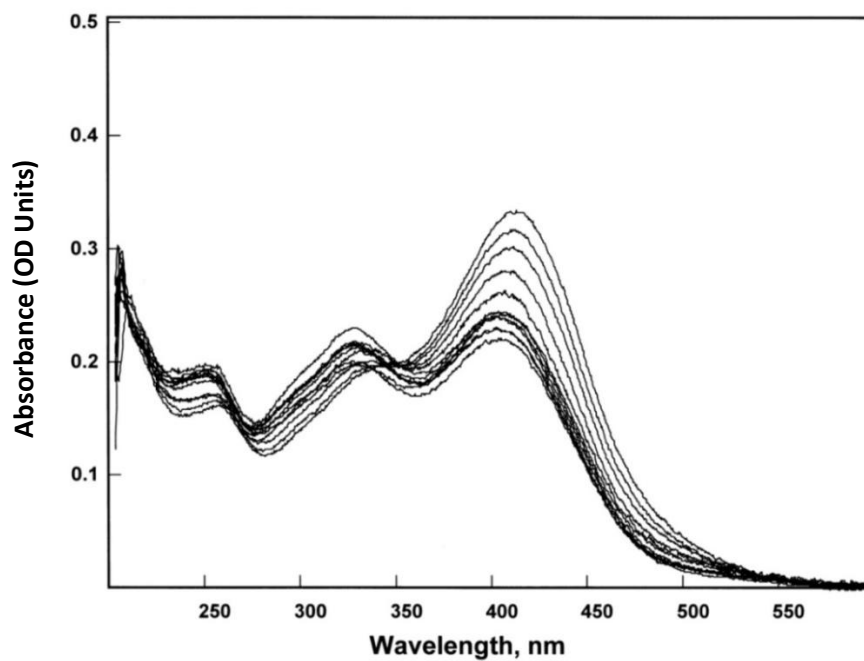


Figure 5.5b Zinc binding of CMC2.5

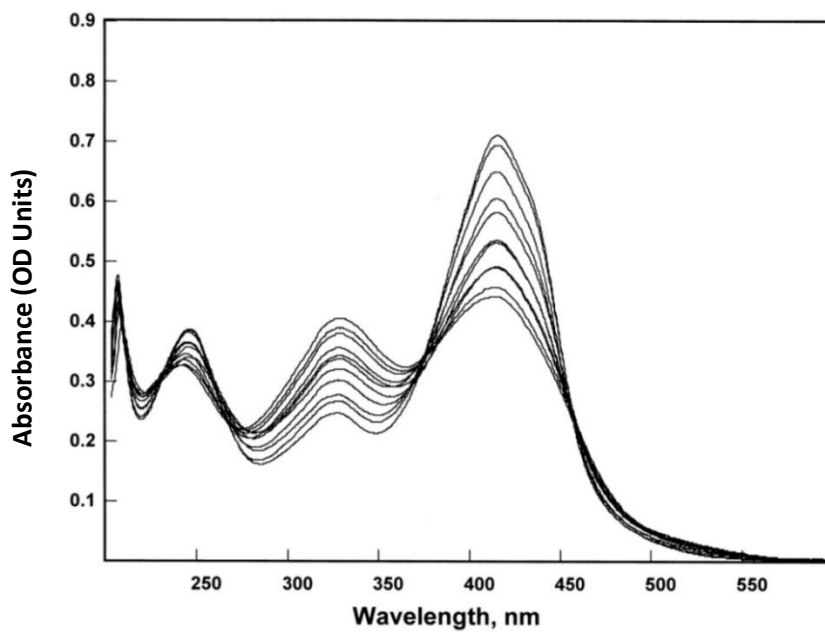


Figure 5.5c Zinc binding of CMC2.24

Figure 5.6 Fitted spectra for zinc binding for CMC2.5 and CMC2.24 at selected wavelengths

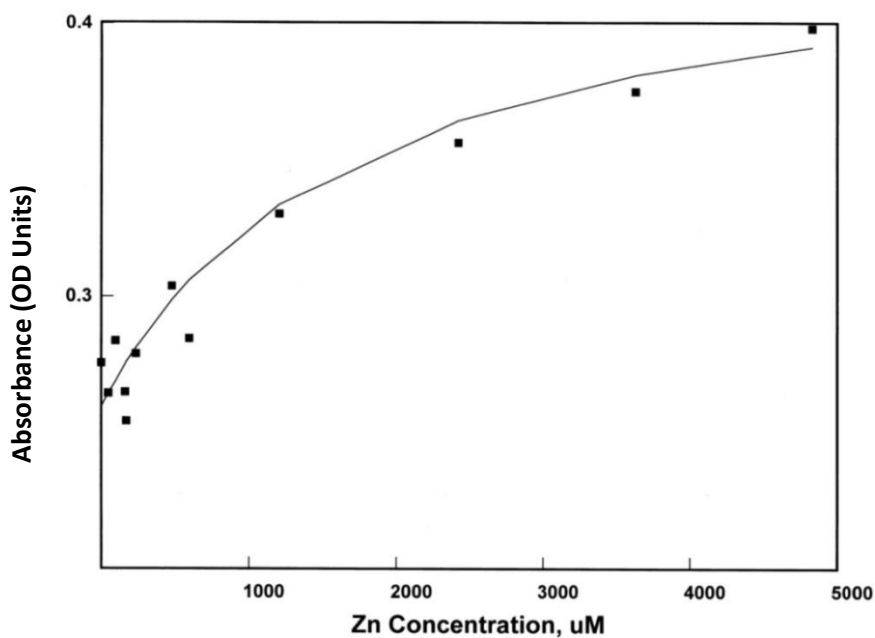


Figure 5.6a Fitted zinc binding of CMC2.5 at 413nm



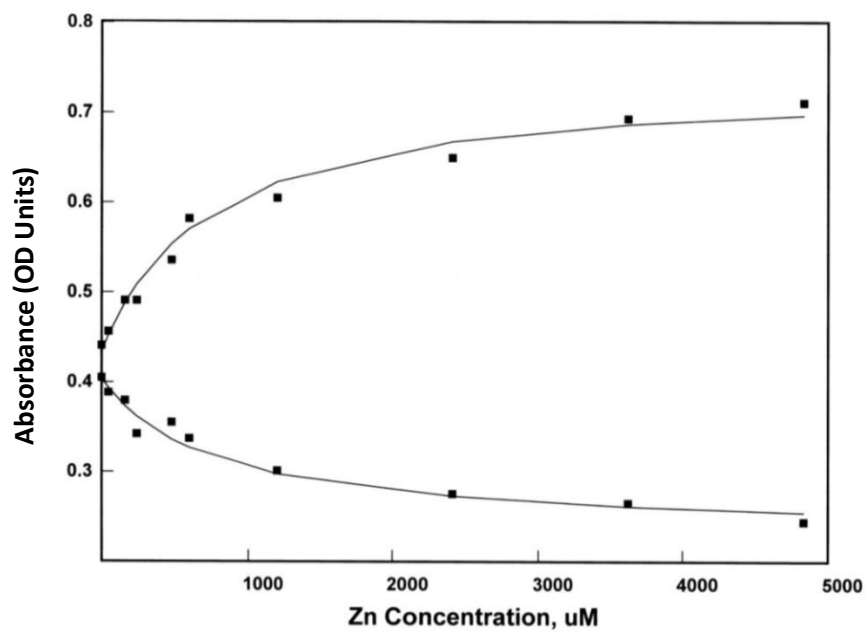


Figure 5.6b Fitted zinc binding of CMC2.24 at 329nm, open; 415nm, filled

#### **D. Bovine Serum Albumin (BSA) binding study**

Given that curcumin and CMCs show relative time-dependence of spectral transformation in various pH buffers, and they are neither soluble enough nor stable enough in salt solutions, it would be crucial to study the binding of these compounds to serum albumin, which resembles the conditions in plasma or extracellular fluid to maintain useful therapeutic concentrations.<sup>5,6</sup>

Accordingly, a serum albumin binding assay was carried out. Serum albumin is the major plasma proteins in mammals. Bovine serum albumin (BSA) was used in the assays of serum binding studies because of structural similarity with human serum albumin (HSA). BSA contains 581 residues and has multiple binding sites with specificities. The binding of BSA to curcumin was studied by Bourassa *et al.*, who reported a dissociation constant  $K_D$  of 30  $\mu\text{M}$  using an indirect fluorescence spectroscopic method at a BSA concentration of 20mg/mL.<sup>7</sup> In the current study, the UV-Visible technique which was used for the  $pK_a$  determination and the zinc binding study was utilized to evaluate the binding to serum by two compounds, namely curcumin and CMC2.24. The observed spectra are shown in Figure 5.7, and the calculated figures are shown in Figure 5.8. The dissociation constants are:  $K_d=1.32 \pm 0.17 \mu\text{M}$  for curcumin and  $K_d=0.56 \pm 0.08 \mu\text{M}$  for CMC2.24. The dissociation constant for curcumin was lower than the one determined by Bourassa *et al.* by an order of magnitude. In human plasma, the concentration of serum albumin is about 700  $\mu\text{M}$ , which strongly suggests that approximately 99.8% of CMC2.24 is bound to the albumin.

Figure 5.7 Spectra for bovine serum albumin binding study

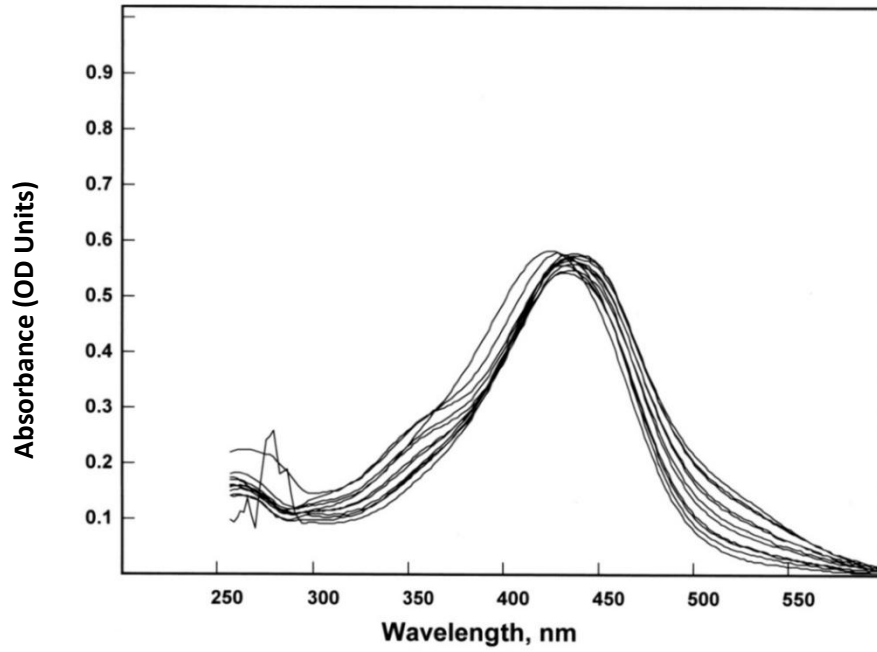


Figure 5.7a Bovine serum albumin binding of curcumin

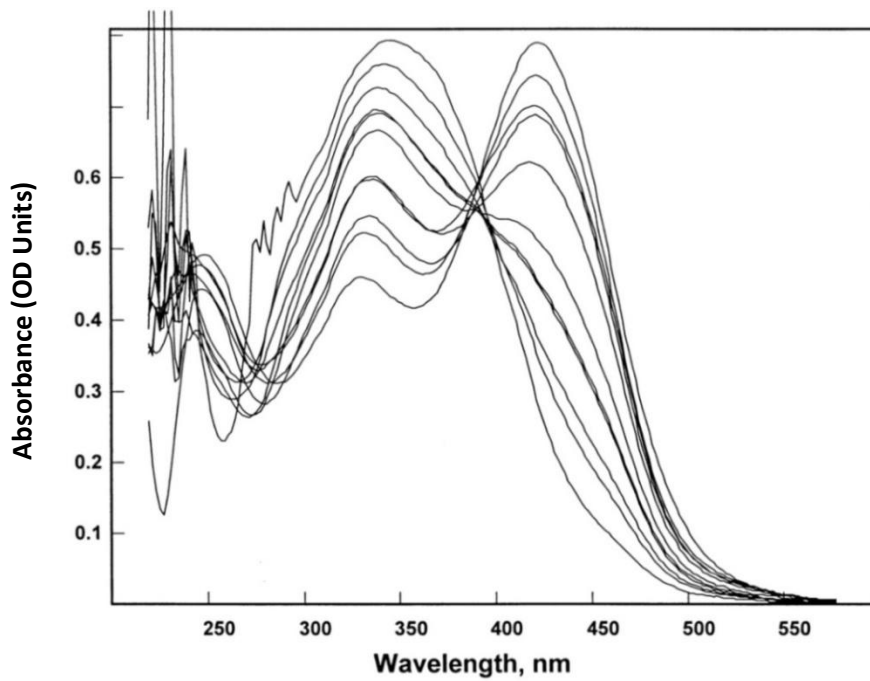


Figure 5.7b Bovine serum albumin binding of CMC2.24 (14.5mM)

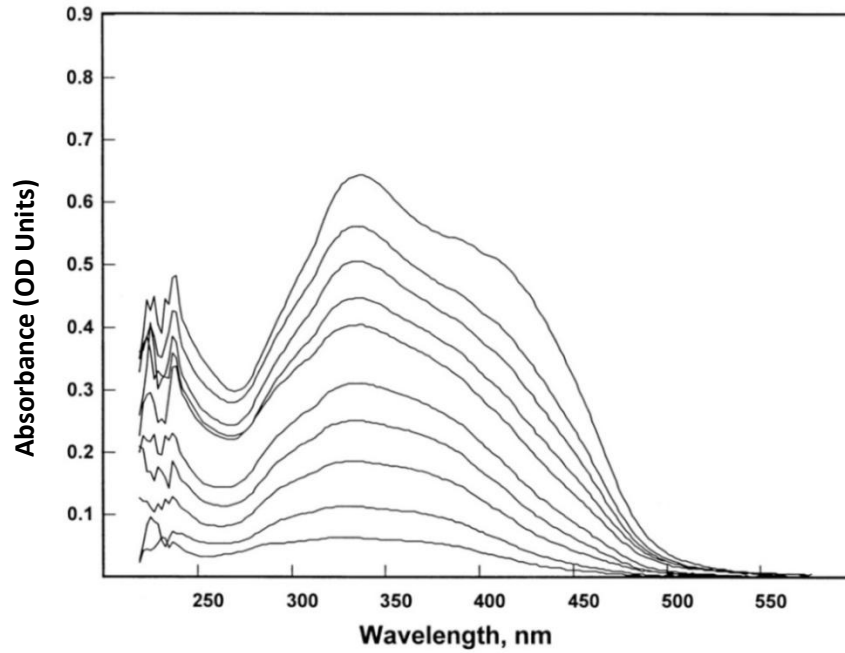


Figure 5.7c Bovine serum albumin (13.0 μM) binding of CMC2.24

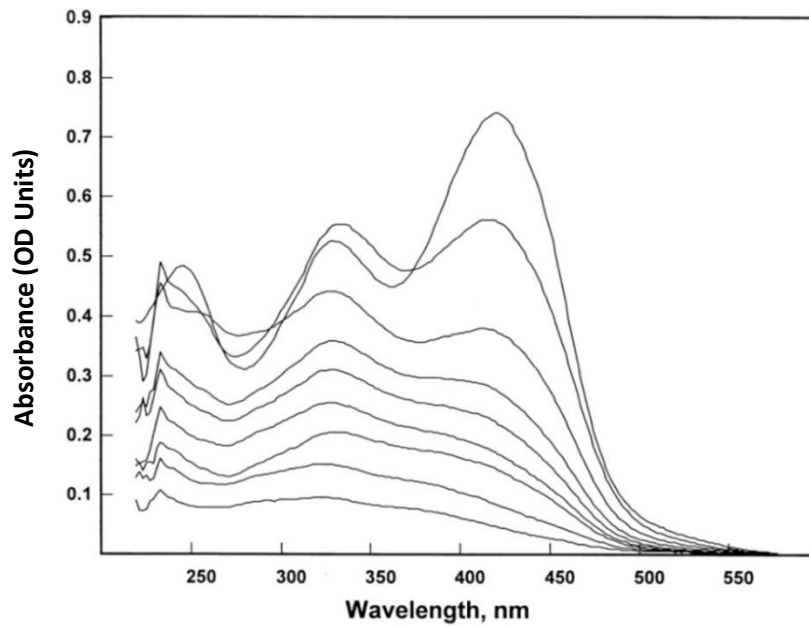


Figure 5.7d Bovine serum albumin (6.0 μM) binding of CMC2.24

Figure 5.8 Fitted spectra for BSA binding at selected wavelengths

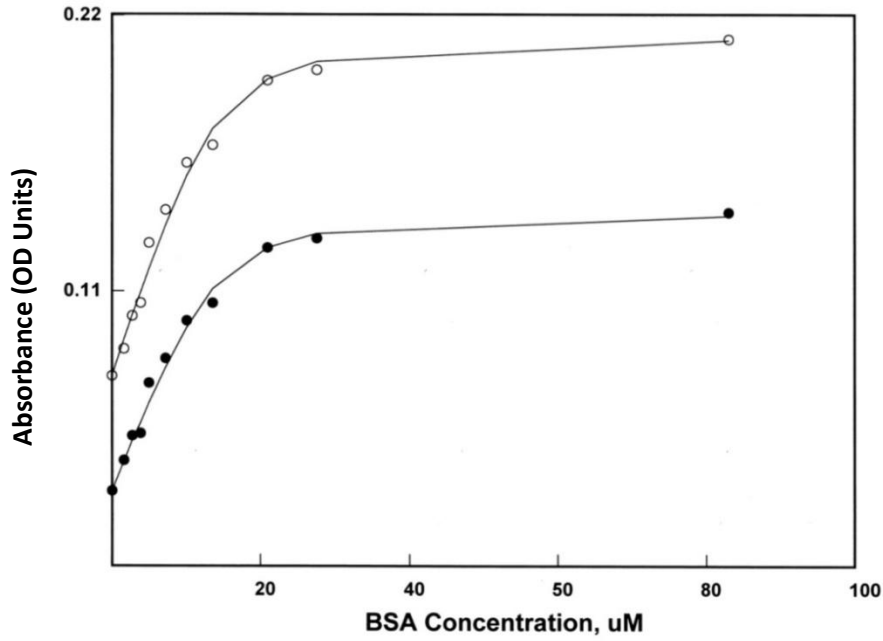


Figure 5.8a Fitted spectra for BSA binding of curcumin at 500nm, 525nm

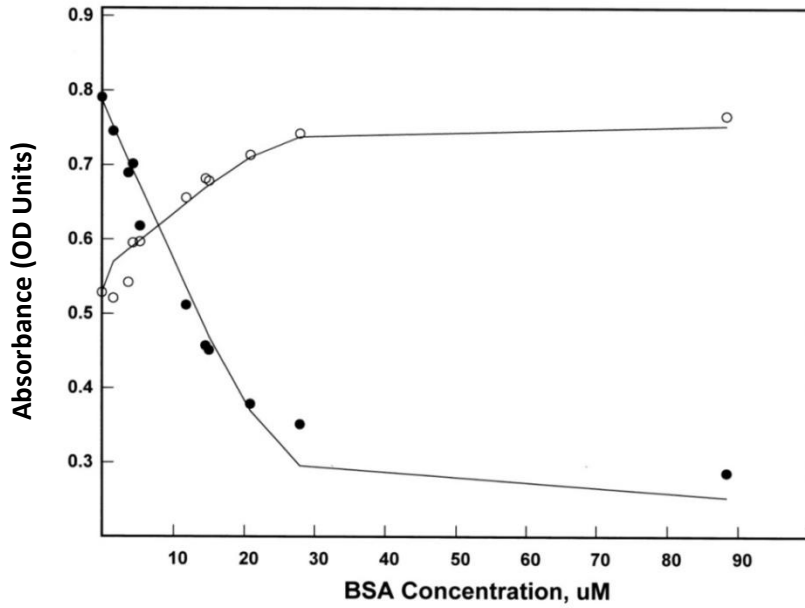


Figure 5.8b Fitted spectra for BSA binding of CMC2.24, 330nm, 421nm

## **E. *In vitro* antimicrobial activity of curcumin, CMC2.5 and CMC2.24**

### **1. Minimum Inhibitory Concentration (MIC)**

An antimicrobial (antibiotic) compound is defined as an agent that kills or slows down the growth of bacteria, and is used to treat infectious diseases. They are either bactericidal or bacteriostatic. Tetracyclines are a class of antibiotics, and are inhibitors of protein synthesis. Doxycycline is one of these. In 1983, Golub *et al.* found that tetracyclines could inhibit MMPs via a mechanism quite distinct from their antibiotic activity.<sup>8,9</sup> Even those tetracyclines having no antibiotic activity (lacking a dimethylamino group), still possess the ability to inhibit the MMPs. Because curcumin analogues contain the same binding site that is responsible for the MMP inhibitory activity as tetracyclines, namely the  $\beta$ -diketone assembly, it appeared important to determine if these novel chemically-modified curcumins possessed any antibiotic activity. Curcumin has been reported to lack anti-microbial activity in previous studies<sup>10-12</sup>, whereas the novel curcumin analogues CMC2.5 and CMC2.24 which show great inhibitory activity against human-derived MMPs *in vitro* and *in vivo* have never been tested. *E. coli* representing a Gram negative bacterium and *S. aureus* representing a Gram positive bacterium were selected as representative organisms to evaluate the minimum inhibition concentrations (MIC). The MIC is defined as the lowest serial dilution of the antimicrobial agents for which no growth of bacteria can be observed after overnight incubation. From the results obtained, doxycycline showed strong inhibition of bacterial growth with MIC=1.0  $\mu\text{g}/\text{mL}$  against *E.coli* and MIC=2.0  $\mu\text{g}/\text{mL}$  against *S. aureus*. However, curcumin and CMC2.5 did not show any observed inhibitory activity against these two bacterial species, whereas for CMC2.24, an MIC of 62.5  $\mu\text{g}/\text{mL}$  was revealed against *S. aureus* but there was no inhibition of *E.coli* at all the concentrations tested. Although CMC2.24 showed some activity against *S. aureus*, the effect is small.

Table 5.2 Minimum inhibitory concentrations (MIC) in  $\mu\text{g/mL}$  of curcumin and CMCs

Note: Doxycycline was used as a positive control.

Strains	Doxycycline (control)	Curcumin	CMC2.5	CMC2.24
<i>E.coli</i> (G-)	1.0	>500	>500	>500
<i>S. aureus</i> (G+)	2.0	>500	>500	62.5

## 2. $\beta$ -galactosidase inhibition

$\beta$ -Galactosidase is the enzyme that catalyzes the hydrolysis of  $\beta$ -D-galactose residues into monosaccharides. Kinetic studies carried out by Gasteiger *et al.* suggested that the onset inhibition of  $\beta$ -galactosidase synthesis inhibits protein synthesis at the initiation of translation.<sup>13</sup>  $\beta$ -Galactosidase was produced *in vitro* by an *E. coli* transcription / translation system.<sup>14-16</sup> The synthesis of  $\beta$ -galactosidase is used to determine the inhibition of ribosome protein synthesis.<sup>17</sup> The *E. coli* S30 extract system (Promega) utilizes a circular plasmid containing the  $\beta$ -galactosidase gene.  $\beta$ -Galactosidase activity assay (Promega) was conducted after the protein synthesis *in vitro* in the presence of various concentrations (1  $\mu\text{M}$ , 5  $\mu\text{M}$  and 10  $\mu\text{M}$ ) of potential protein inhibitors (doxycycline, curcumin and CMC2.24), whereas doxycycline, the known antibiotic, was used as a positive control.<sup>18,19</sup> The reaction mixture was maintained at 37°C for 1 hour, and the UV absorbance was measured in order to determine the residual activity of  $\beta$ -galactosidase. From the result of Table 5.2, doxycycline inhibits 6.4% production of  $\beta$ -galactosidase at 1  $\mu\text{M}$ , 12.2% at 5  $\mu\text{M}$  and 30.7% at 10  $\mu\text{M}$  in contrast to curcumin and CMC2.24, both of which show the inhibition of  $\beta$ -galactosidase production at less than 13.5% at 10  $\mu\text{M}$  (the highest concentration in the assay). The result strongly suggests that CMC2.24 is comparable to curcumin, regarding the inhibition of  $\beta$ -galactosidase production, and both of these compounds

exhibit much less inhibitory activities than doxycycline (the positive control), which is antibiotic at higher doses. Given the fact that curcumin is known to be safe for oral use as a natural product in the food ingredient curry powder, neither curcumin nor CMC2.24 shows any significant antibiotic activity. *P-value*, the probability in statistical significance for each two groups, was also calculated for the  $\beta$ -galactosidase inhibition. At 10  $\mu$ M, there is statistically significant difference between doxycycline and curcumin ( $p < 0.01$ ), and no statistical difference between curcumin and CMC2.24 ( $p > 0.05$ ). At 1  $\mu$ M and 5  $\mu$ M, no significant difference was observed between curcumin and CMC2.24. As for doxycycline, 1  $\mu$ M and 5  $\mu$ M are not statistically different ( $p < 0.05$ ), while both are significantly different at 10  $\mu$ M. The result strongly suggests that doxycycline exhibits inhibitory activities (30%) at 10  $\mu$ M as an antibiotic agent in comparison to its lower concentrations at 1  $\mu$ M or 5  $\mu$ M. For both curcumin and CMC2.24 at 1  $\mu$ M, 5  $\mu$ M or 10  $\mu$ M, no antimicrobial activity was observed.

Table 5.3  $\beta$ -galactosidase inhibition of curcumin and CMC2.24

	Doxycycline			Curcumin			CMC2.24		
	1 $\mu$ M	5 $\mu$ M	10 $\mu$ M	1 $\mu$ M	5 $\mu$ M	10 $\mu$ M	1 $\mu$ M	5 $\mu$ M	10 $\mu$ M
Inhibition %	0.3	6.7	26.8	3.6	6.1	10.1	2.1	4.3	9.1
Inhibition %	7.0	10.1	30.2	4.5	9.4	12.2	1.2	8.8	13.1
Inhibition %	6.4	12.2	34.1	0	0.9	14	0	8.2	17.1
AVE	4.6	9.7	30.7	2.7	5.5	12.1	1.1	7.1	13.1
S.D.	3.7	2.8	3.7	2.4	4.3	1.9	1.1	2.4	4.0
S.E.M.	2.14	1.60	2.11	1.37	2.47	1.13	0.61	1.41	2.31



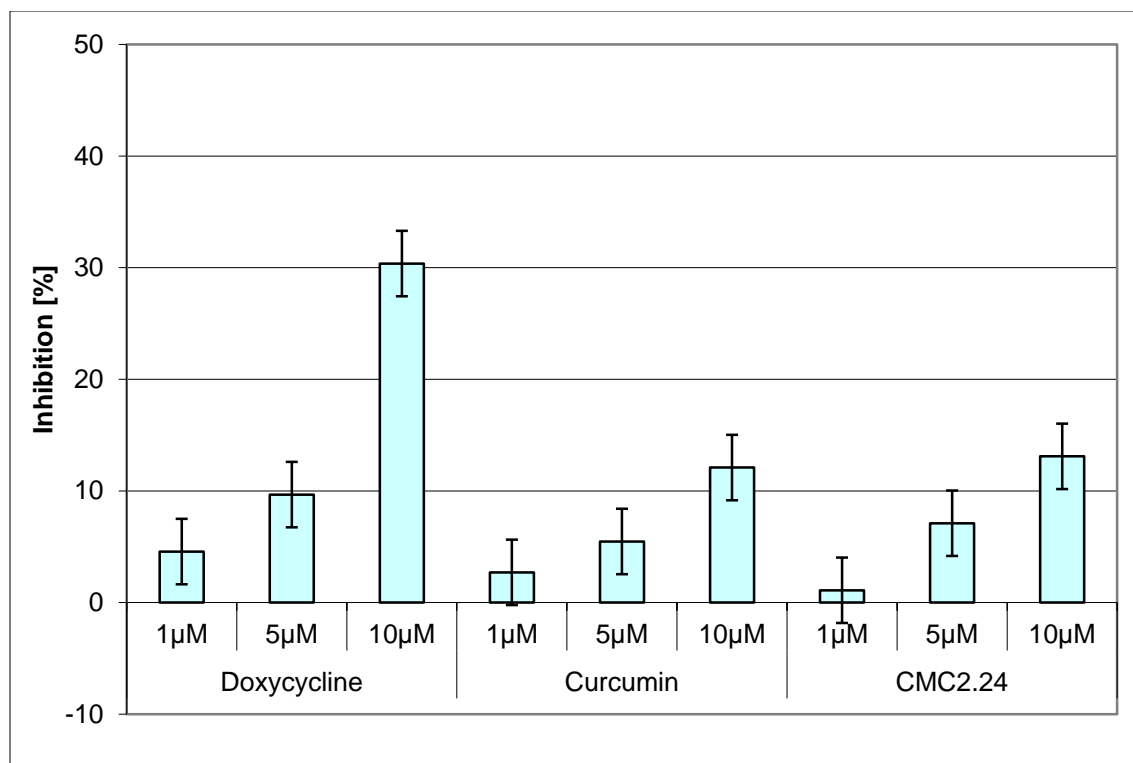


Figure 5.9  $\beta$ -galactosidase inhibition of curcumin and CMC2.24

## Materials and Methods

### 1. pH equilibria

Buffers containing 0.006 M  $\text{KH}_2\text{PO}_4$ , 0.001 M HCl, 0.093 M KCl or 0.003 M  $\text{KH}_2\text{PO}_4$ ,  $\text{K}_2\text{HPO}_4$ , 0.004 M  $\text{KHCO}_3$  and 0.090 M KCl, ionic strength 0.10 M (prepared by analytic techniques), were adjusted with 0.10 M KOH to span the range pH 3.0-12.0. Aliquots of 3.00 mL at each pH were delivered to the thermostatted dry cuvette, and the baseline re-zeroed. At zero time, 0.1000 mL fresh stock CMC 2.24, CMC 2.5, or curcumin, typically 450  $\mu\text{M}$  in acetonitrile, was added; efficient (99.9%) mixing was accomplished in 1 sec with a single mixer stroke. The UV-visible spectra sets were collected with an OceanOptics USB 2000 spectrophotometer, operated by SpectraSuite computer software. Acidity (pH) was measured with a Thermo/Orion Model 420+

meter using an MI-410 combination microelectrode from Microelectrodes, Inc. True pH values were calculated from the millivolt readings after linear correction for small drifts in the intervening standard pH buffer readings (commercial pH 4.00, 7.00 and 10.00 buffers from Fisher or J.T. Baker, standardized 0.00872 M KOH - 0.0900 M KCl for pH 11.82). Temperature was monitored to  $\pm 0.1^\circ\text{C}$  using a home-made thermistor bridge. Thirty-five to forty pH sets were obtained for each compound.

## 2. $\text{Zn}^{2+}$ and BSA binding

Crystalline bovine serum albumin from Pentex, shown to be fatty-acid-free was used without further treatment. Stock solutions of KCl-tris (hydroxymethyl)aminomethane (for  $\text{Zn}^{2+}$ , to avoid zinc phosphate precipitation) or KCl-phosphate (for BSA) with or without zinc acetate or BSA, all adjusted to pH 7.4, were prepared. Samples (5 mL) of varying zinc acetate or BSA concentration were prepared by analytical-balance weight-weight dilution. For two BSA series w/w dilution samples of CMC 2.24 in acetonitrile were prepared. Typically, 2.991  $\pm 0.005$  mL aliquots were added to the dry cuvette, and spectra were taken (primarily to establish the BSA concentration), after which the baseline was rezeroed to eliminate the BSA absorbance peak (the slight effect of further dilution with the 0.0981 mL acetonitrile aliquot is dealt with during post-processing). As before, data collection was initiated and the aliquot of compound in acetonitrile was added with one-second mixing, thus establishing "zero time" with an uncertainty smaller than the data interval. The final BSA concentration was determined from the corrected spectra using an absorptivity  $\epsilon_{279}$  at 279 nm of  $43,824 \text{ M}^{-1}\text{cm}^{-1}$ . The absorptivity of CMC 2.24 at 418.0 nm, in acetonitrile, was determined here as  $(4.19 \pm 0.15) \times 10^4 \text{ M}^{-1}\text{cm}^{-1}$ .

### 3. Data processing

The spectra for each pH, Zn<sup>2+</sup>, or BSA data set are fitted with a multiwavelength non-linear least-squares algorithm originally used to analyze the HgI<sub>n</sub><sup>2-n</sup> equilibria and later the thermorubin *pK<sub>a</sub>* equilibria.<sup>20,21</sup> The operative equations are Beer's Law and conservation of mass:

$$(1) A_{\lambda,j} = d \sum_i \epsilon_{\lambda,j} c_{i,j} \text{ for } M \text{ samples } j, N \text{ species } i. c_j^0 = \sum_i c_{i,j}$$

where the  $c_{i,j}$  are the concentrations of absorbing species  $i$  and the  $\epsilon_{\lambda,i}$  their intrinsic *absorptivities* at wavelength  $\lambda$ . The light path length  $d$  is 1.000 cm. The absorptivities  $\epsilon_{\lambda,i}$  and the equilibrium constants ( $pK_a$  or  $K_D$ ) that determine the  $c_{i,j}$  through the equilibrium expressions are adjusted to convergence by the algorithm, which minimizes the sum of squares of absorbance deviations ( $A_{\lambda,j}^{obs} - A_{\lambda,j}^{calc}$ ). Typically, 12 wavelengths, spaced to select those maximizing contrast among species, were used. With the  $pK_a$  values determined by the fitting then established, the entire spectral range for all samples was fitted with only the remaining absorptivities as fitting parameters. In many instances only two of the species (or internally-equilibrating populations, in kinetics cases), say A and B, that are interconverting, have non-negligible concentrations in the range of some data subset. Beer's Law reduces to

$$(2) A_{\lambda,j} = \epsilon_{\lambda,A} c_{A,j} + \epsilon_{\lambda,B} c_{B,j} = \epsilon_{\lambda,A} c_j^0 + (\epsilon_{\lambda,B} - \epsilon_{\lambda,A}) c_{B,j}$$

If the spectra for species or populations A and B cross at some wavelength  $\lambda_{iso}$ , there  $\epsilon_{\lambda,B} \equiv \epsilon_{\lambda,A}$ , and  $A_{\lambda,iso} = \epsilon_{\lambda,A} c_j^0$  is invariant. This is an *isosbestic point*, whose existence is *prima facie* evidence that in this data subset two and only two species or populations are interconverting.

### 4. MIC test

The MIC was determined by broth microdilution MIC test method, whereas the activity of an antimicrobial agent against different bacteria could be determined. Curcumin, CMC2.5 and

CMC2.24 dissolved in DMSO as stock solutions were used in the test, and doxycycline was used as a positive control. Serial dilutions were made to the final concentrations of 500, 250, 125, 62.5, 31.3, 15.7, 7.8, 3.9, 2.0, 1.0, 0.5, 0.25  $\mu\text{g}/\text{mL}$  by broth media (containing a final concentration of 10ppm  $\text{Mg}^{2+}$  and 20ppm  $\text{Ca}^{2+}$ ). Test bacterial *E. coli* (gram negative) and *S. aureus* (gram positive) were pre-incubated overnight on the sterilized plastic plate, and then inoculated to broth medium to grow at 37°C for 2 hours reaching the final concentrations of  $1 \times 10^8$  cells/mL with the O.D. reading at  $0.09 \pm 0.01$ . 100  $\mu\text{L}$  of bacterial at a final concentration of  $1 \times 10^6$  cells/mL was added to 100  $\mu\text{L}$  solutions of antimicrobial agents into optical quality round bottom 96-well susceptibility microtrays. The trays were incubated at 37 °C for 18 hours for these bacteria, and minimum inhibitory concentration (MIC) was evaluated as the lowest concentration of the antimicrobial agents above the dilution at which overnight growth is observed.

### **5. *In vitro* $\beta$ -galactosidase synthesis**

*In vitro*  $\beta$ -galactosidase synthesis was carried out by 1  $\mu\text{L}$  of  $\beta$ -galactosidase DNA plasmid (0.5  $\mu\text{g}/\mu\text{L}$ ), 5  $\mu\text{L}$  of complete amino acid mix (2.5  $\mu\text{L}$  of Amino Acid Mixture Minus Methionine, 1mM and 2.5  $\mu\text{L}$  of Amino Acid Mixture Minus Leucine, 1mM), 20  $\mu\text{L}$  of S30 Premix Without Amino Acid, 15  $\mu\text{L}$  of S30 Circular Extract and 9  $\mu\text{L}$  of inhibition solution to a final volume of 50  $\mu\text{L}$  in PCR tube and incubated at 37°C for 1 hour. The inhibition solutions including doxycycline, curcumin and CMC2.24 in concentrations of 1  $\mu\text{M}$ , 5  $\mu\text{M}$  and 10  $\mu\text{M}$  in DMSO (and DMSO only) were prepared separately. H<sub>2</sub>O was used as a negative control. The reaction mixtures were vortexed gently, then centrifuged for 5 seconds before use. Cell lysates from the previous step was obtained. 15  $\mu\text{L}$  of the cell lysates, 135  $\mu\text{L}$  of 1X Reporter Lysis Buffer and 150  $\mu\text{L}$  of 2X Assay Buffer were added together and vortexed gently. The reaction mixtures were

incubated in 37°C water bath for 1 hour and a faint yellow color has developed. All the reactions were stopped by an addition of 500 µL of 1M Na<sub>2</sub>CO<sub>3</sub>. Absorbance was read at 420nm after a brief vortexing. The inhibition was calculated upon the percentage of absorbance decrease in contrast to the blank, whereas H<sub>2</sub>O was used as a negative control.

## References

1. Bernabé-Pineda, M.; Ramirez-Silva, M.T.; Romero-Romob, M.; González-Vergara, E.; Rojas-Hernández, A. Determination of acidity constants of curcumin in aqueous solution and apparent rate constant of its decomposition. *Spectrochimica Acta Part A*, **2004**, *60*, 1091-1097
2. Bode, W.; Gomis-Rüth, F.X.; Stöckler, W. Astacins, serralysins, snake venom and matrix metalloproteinases exhibit identical zinc-binding environments (HEXXHXXGXXH and Met-turn) and topologies and should be grouped into a common family, the 'metzincins'. *FEBS Lett.*, **1993**, *27*, 134-140
3. Stöcker, W.; Grams, F.; Baumann, U.; Reinemer, P.; Gomis-Rüth, F.X.; McKay, D.B.; Bode, W. The metzincins--topological and sequential relations between the astacins, adamalysins, serralysins, and matrixins (collagenases) define a superfamily of zinc-peptidases. *Protein Sci.*, **1995**, *4*, 823-840
4. Ryan, M.E.; Usman, A.; Ramamurthy, N.S.; Golub, L.M. Greenwald, R.A. Excessive matrix metalloproteinase activity in diabetes: inhibition by tetracycline analogues with zinc reactivity. *Curr. Med. Chem.*, **2001**, *8*, 305-316
5. Carter, D. C.; Ho, J. X. Adv. Structure of serum albumin. *Protein Chem.*, **1994**, *45*, 153-203
6. Hsia, J.C.; Wong, L.T.; Tan, C.T.; Er, S.S.; Kharouba, S.; Balaskas, E.; Tinker, D.O.; Feldhoff, R.C. Bovine serum albumin: characterization of a fatty acid binding site on the N-terminal peptic fragment using a new spin-label. *Biochemistry*, **1984**, *23*, 5930-5932

7. Bourassa, P.; Kanakis, C.D.; Tarantilis, P.; Pollissiou, M.G.; Tajmir-Riahi, H.A. Resveratrol, Genistein, and Curcumin Bind Bovine Serum Albumin. *J. Phys. Chem. B*, **2010**, *114*, 3348-3354
8. Golub, L.M.; Lee, H.M.; Lehrer, G.; Nemiroff, A.; McNamara, T.F.; Kaplan, R.; Ramamurthy, N.S. Minocycline reduces gingival collagenolytic activity during diabetes: Preliminary observations and a proposed new mechanism of action. *J. Periodont. Res.*, **1983**, *18*, 516-526
9. Golub, L.M.; Greenwald, R.A.; Ramamurthy, N.S.; McNamara, T.F.; Rifkin, B.R. Tetracyclines inhibit connective tissue breakdown: New therapeutic implications for an old family of drugs. *Crit. Revs Oral Biol. Med.*, **1991**, *2*, 297-322
10. Wang, Y.; Lu, Z.; Wu, H.; Lv, F. Study on the antibiotic activity of microcapsule curcumin against foodborne pathogens. *International Journal of Food Microbiology*, **2009**, *136*, 71-74
11. Rai, D.; Singh, J.K.; Roy, N.; Panda, D. Curcumin inhibits FtsZ assembly: an attractive mechanism for its antibacterial activity. *Biochem J.*, **2008**, *410*, 147-155
12. Kim, M.K.; Park, J.C.; Chong, Y. Aromatic Hydroxyl Group Plays a Critical Role in Antibacterial Activity of the Curcumin Analogues. *Natural Product Communications*, **2012**, *7*, 57-58
13. Gasteiger, E.; Gattiker, A.; Hoogland, C.; Ivanyi, I.; Appel, R.D.; Bairoch, A. ExpASY: the proteomics server for in-depth protein knowledge and analysis. *Nucleic Acids Res.*, **2003**, *31*, 3784-3788

14. Kung, H.F.; Fox, J. E.; Spears, C.; Brot, N.; Weissbach, H. Studies on the role of ribosomal proteins L 7 and L 12 in the in vitro synthesis of  $\beta$ -galactosidase. *J. Biol. Chem.*, **1973**, *248*, 5012-5015
15. Kung, H.F.; Spears, C.; Schulz, T.; Weissbach, H. Studies on the in vitro synthesis of beta-galactosidase: necessary components in the ribosomal wash. *Arch. Biochem. Bwphys.*, **1974**, *162*, 578-584
16. Lindahl, L.; Sor, F.; Archer, R. H.; Nomura, M.; Zengel, J.M. Transcriptional organization of the S10, spc and alpha operons of *Escherichia coli*. *Biochim. Biophys. Acta.*, **1990**, *1050*, 337-342
17. Dennis, P. P.; Bremer, H. Differential rate of ribosomal protein synthesis in *Escherichia coli* B/r. *J. Mol. Biol.*, **1974**, *84*, 407-422
18. Zubay, G. In vitro synthesis of protein in microbial systems. *Annu. Rev. Genet.*, **1973**, *7*, 267-287
19. Zubay, G. The isolation and properties of CAP, the catabolite gene activator. *Meth. Enzymol.*, **1980**, *65*, 856-877
20. Stone, W.L.; Wishnia, A. Binding of iodo-mercurates to sulfhydryl-blocked beta-lactoglobulin-A, -B, and -C. *Bioinorg. Chem.*, **1978**, *8*, 517-529
21. Lin, F.W.; Wishnia, A. The Protein Synthesis Inhibitor Thermorubin. 1. Nature of the Thermorubin-Ribosome Complex. *Biochemistry*, **1982**, *21*, 477

## Chapter 6. An *in vitro* lipophilicity and an *in vivo* pharmacokinetic study of curcumin and CMC2.24

### A. Introduction

Lead candidates in drug discovery usually have suitable physicochemical properties beyond their potency, e.g., bioavailability, appropriate *in vivo* pharmacokinetics, safety. Lipinski's rule of five considers a partition coefficient value ( $\log P$ ), a known molar refractivity, molecular weight, the number of atoms (including H-bond donors and H-bond acceptors) and polar surface, all of which are needed to assess the pharmacological profile of the active drug substance.<sup>1</sup> The partition coefficient (P) value determined as the distribution between two separate solvent systems, usually 1-octanol /aqueous solution (which are immiscible with each other) is regarded as the distribution of the drug substance to be expected between the physiological phases of lipophilicity or hydrophilicity. The logarithm of the ratio in equilibrium concentrations of a single species,  $\log P$ , is used to assess the lipophilicity of a drug substance. Pharmacokinetics, including absorption, distribution, metabolism, and excretion (ADME), needs to be considered with regard to the drug disposition in the body. As mentioned in Chapter 2, curcumin is known to have poor bioavailability in the human system. Even with oral dosage up to 12g/day, only a small amount of curcumin (51.2ng/mL) can be detected in the serum.<sup>2-6</sup> Thus it is crucial to determine the biodistribution of the novel chemically-modified curcumins (CMCs) in comparison with curcumin, because they are more potent, more acidic, and more soluble at physiological pH. After considerable experimentation, ideal solution containing Solutol 15 and ethanol (v/v=1:1) was found to dissolve both curcumin and CMCs up to 40mg/mL, and this solution was used for the *in vivo* pharmacokinetics evaluation by intravenous (i.v.) route. No



precipitation occurred at the injection site. This is the first time that a CMC has been introduced intravenously.

### **B. *In vitro* lipophilicity**

Prior to any *in vivo* pharmacokinetic study, the *in vitro* lipophilicity study was conducted by Simon Tong *et al* using the same evaluation method (HPLC) as was used for doxycycline.<sup>7-9</sup> Curcumin and CMC2.24 at a concentration of 1mg/mL were dissolved separately in methanol and then diluted to 10 µg/mL by PBS buffer saturated with 1-octanol (used to mimic the lipid) (v/v=1:1), the separated layers were evaluated by HPLC to determine the concentrations by comparing to the standard curves obtained earlier, in order to calculate *log P*. However, both the concentrations of curcumin and CMC2.24 in the aqueous layers were below the detection limit of HPLC, whereas those in 1-octanol layers were close to the injection concentration, so the partition coefficient cannot be deduced from this assay (data not shown). Therefore we adopted a UV-Vis scanning spectrophotometer to study the distribution concentrations of curcumin and CMC2.24, where doxycycline (hydrophilic) and CMT-3 (lipophilic) were used as the control compounds. Scans were carried out at wavelengths ranging from 300nm to 500nm. As shown from Figure 6.1, a relatively large amount of doxycycline was found in the aqueous layer in contrast to CMT-3, which is known to be lipophilic. Curcumin and CMC2.24 are both very lipophilic according to the data, given that at the level of detection the concentration in the aqueous solution was close to zero. This strongly suggests that the lead compound, CMC2.24 is still very lipophilic, as is curcumin.

Figure 6.1 *In vitro* lipophilicity of doxycycline, CMT-3, curcumin and CMC2.24  
 Note: Spectrophotometric absorptions of compounds in methanol (blue line), PBS buffer (pink line) and 1-octanol (yellow line), wavelengths ranging from 300nm to 500nm.<sup>9</sup>

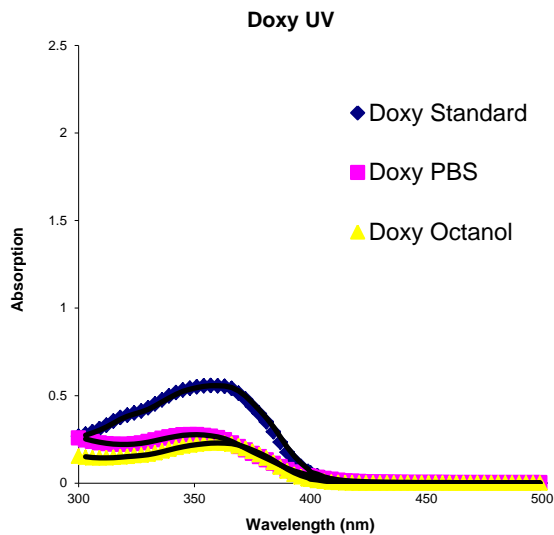


Figure 6.1a Lipophilicity study of doxycycline

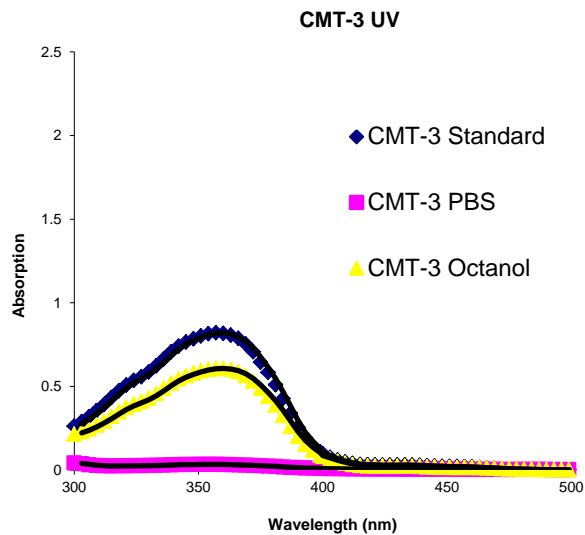


Figure 6.1b Lipophilicity study of CMT-3

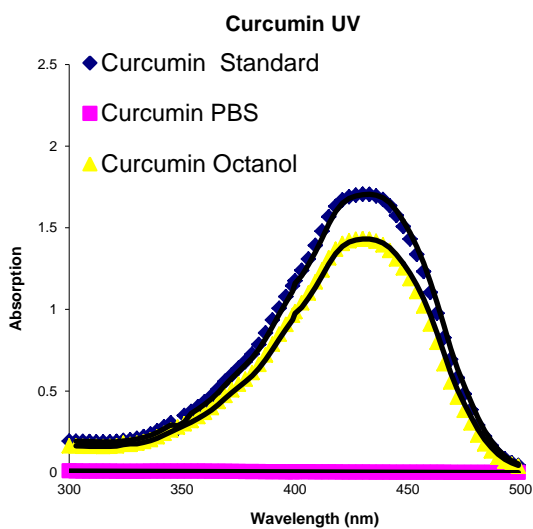


Figure 6.1c Lipophilicity study of curcumin

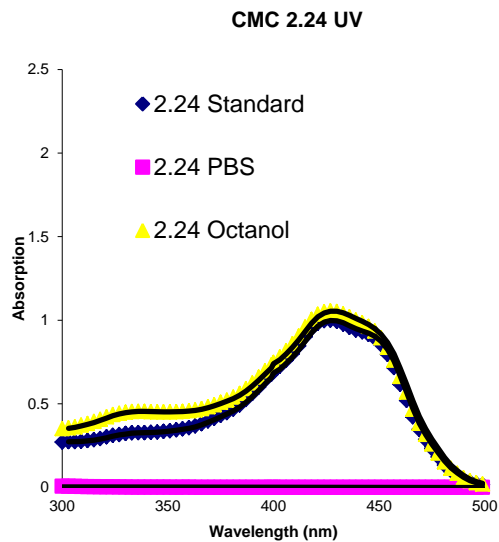


Figure 6.1d Lipophilicity study of CMC2.24

### C. *In vivo* pharmacokinetics by oral route

In order to evaluate the *in vivo* pharmacokinetics of curcumin and the lead compound, CMC2.24, a preliminary study was carried out by oral route. Both curcumin and CMC2.24 were administered at 500mg/kg to rats, and the rats were sacrificed 6 hours after the dosage. Blood was drawn at 2 hours and 6 hours before the rats were sacrificed, intestines were harvested and feces samples were collected. Results show that the concentrations of both curcumin and CMC2.24 from serum samples were below the detection limits in the serum samples at 2 hours and 6 hours. Most of the compounds were found in the stomach, intestine and feces (Figure 6.2). Control samples were spiked with either curcumin or CMC2.24 (data not shown), and were used as reference to determine the concentration of the compound in serum. This result suggests that both curcumin and CMC2.24 have very poor absorption by the oral administration, which leads to the poor bioavailability accordingly.

Figure 6.2 HPLC spectra of rat serum samples after oral dosages of curcumin and CMC2.24

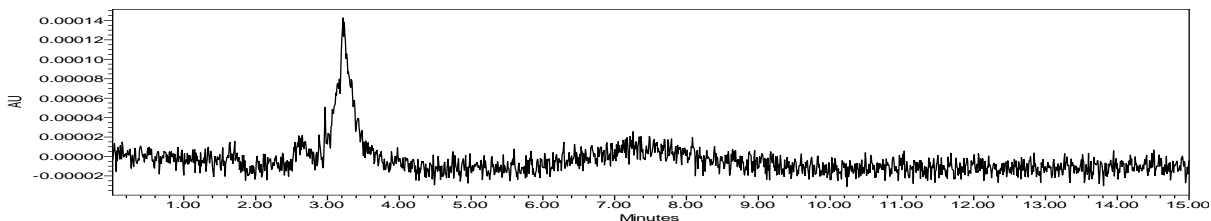


Figure 6.2a Blood sample from rats with no administration of curcumin or CMC2.24

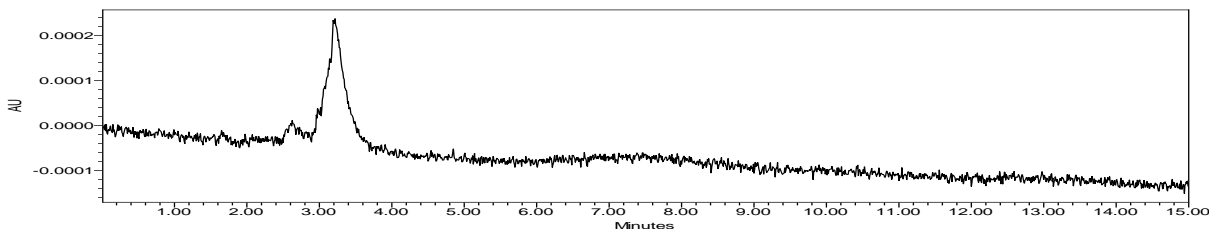


Figure 6.2b Blood sample from rats with oral administration of curcumin, 2h after dosage

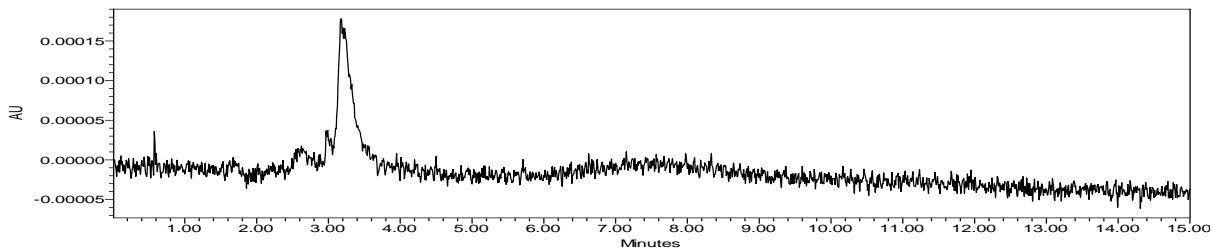


Figure 6.2c Blood sample from rats with oral administration of curcumin, 6h after dosage

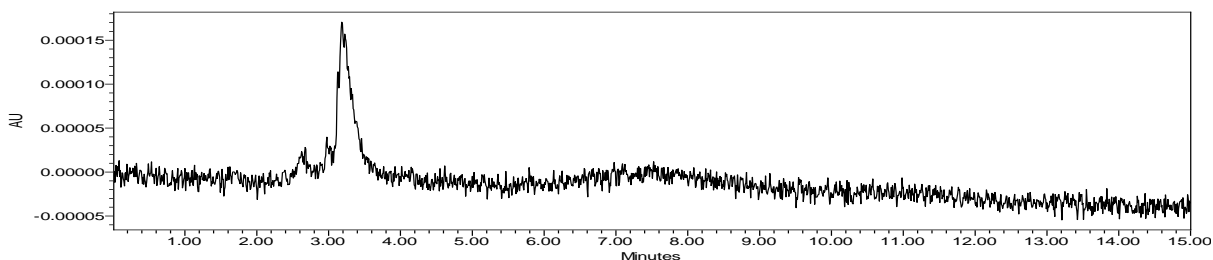


Figure 6.2d Blood sample from rats with oral administration of CMC2.24, 2h after dosage

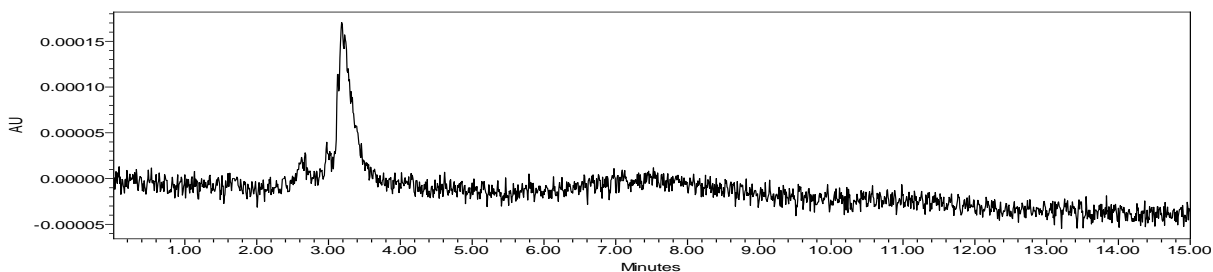


Figure 6.2e Blood sample from rats with oral administration of CMC2.24, 6h after dosage

#### D. *In vivo* pharmacokinetics by *i.v.* route

An *in vivo* pharmacokinetic study via the intravenous (*i.v.*) route was carried out for both curcumin and CMC2.24. Stock solutions were prepared in a combination of Solutol 15 and ethanol (v/v=1:1), the concentration of the drug substance being 40mg/mL.<sup>10,11</sup> Each rat was injected 20mg/kg (for a rat with the weight of 300g, 6mg of drug substance is injected). In the first pharmacokinetic study, rats were distributed to three groups, and each group contained three rats. Doxycycline was used as a control for the *in vivo* pharmacokinetics study, and blood was

drawn from retro-orbita (venous eye plexus) at 30min, 1h, 2h and 4h.<sup>12</sup> Serum samples was obtained for all the time points, and drug concentrations were calculated by comparison with standard curves. Curcumin, CMC2.24 and doxycycline showed relatively linear graphs for the standard concentrations ranging from 1  $\mu$ M to 50  $\mu$ M. When the rats were injected with curcumin, CMC2.24 and doxycycline, all of them remained alive and healthy, with no evidence of toxicity being observed. (Table 6.1a-6.1c, Figure 6.3a-6.3c)

Table 6.1 Standard curves for curcumin, CMC2.24 and doxycycline

Table 6.1a Standard curve for curcumin at concentrations at 1  $\mu\text{M}$ , 5  $\mu\text{M}$ , 10  $\mu\text{M}$  and 50  $\mu\text{M}$

Curcumin ( $\mu\text{M}$ )	0	1	5	10	50
Area Under Curve	0	47441	115230	200551	972782
$y=19523x, R^2=0.9982$ (y: area in Area Under Curve; x: concentration of curcumin in $\mu\text{M}$ )					

Table 6.1b Standard curve for CMC2.24 at concentrations at 1  $\mu\text{M}$ , 5  $\mu\text{M}$ , 10  $\mu\text{M}$  and 50  $\mu\text{M}$

CMC2.24 ( $\mu\text{M}$ )	0	1	5	10	50
Area Under Curve	0	41003	116088	182532	810628
$y=16366x, R^2=0.9950$ (y: Area Under Curve; x: concentration of CMC2.24 in $\mu\text{M}$ )					

Table 6.1c Standard curve for doxycycline at concentrations at 1  $\mu\text{M}$ , 5  $\mu\text{M}$ , 10  $\mu\text{M}$  and 50  $\mu\text{M}$

Doxycycline ( $\mu\text{M}$ )	0	1	5	10	50
Area Under Curve	0	3241	16223	33819	169689
$y=3391.9x, R^2=1.000$ (y: Area Under Curve; x: concentration of doxycycline in $\mu\text{M}$ )					

Figure 6.3 Standard curves for curcumin, CMC2.24 and doxycycline

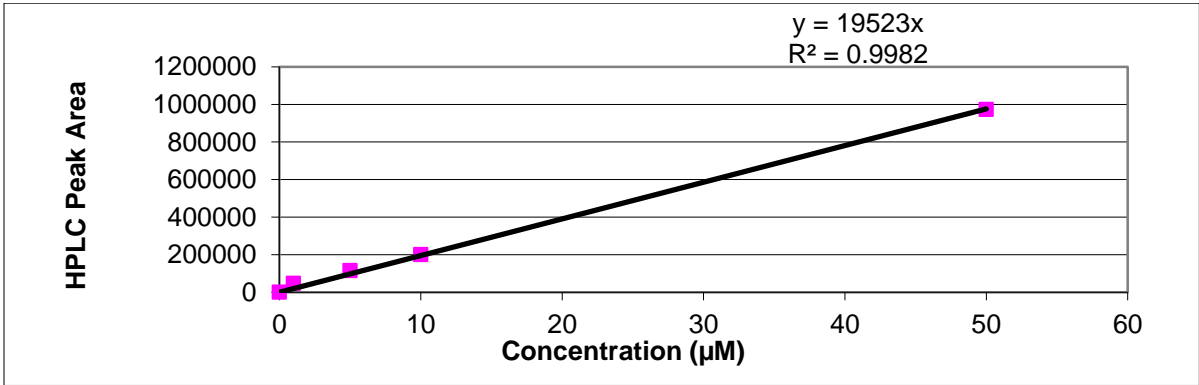


Figure 6.3a Curcumin standard curve

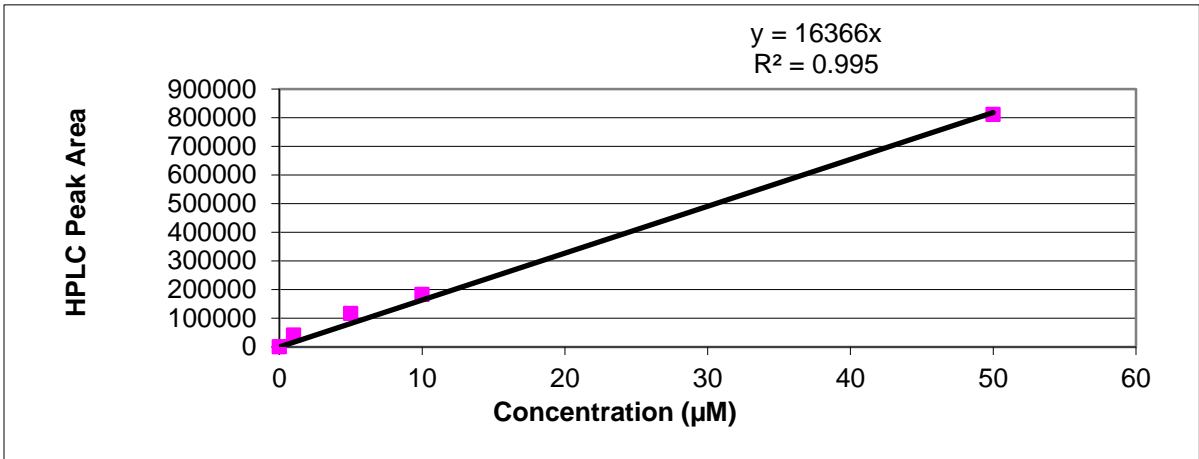


Figure 6.3b CMC2.24 standard curve

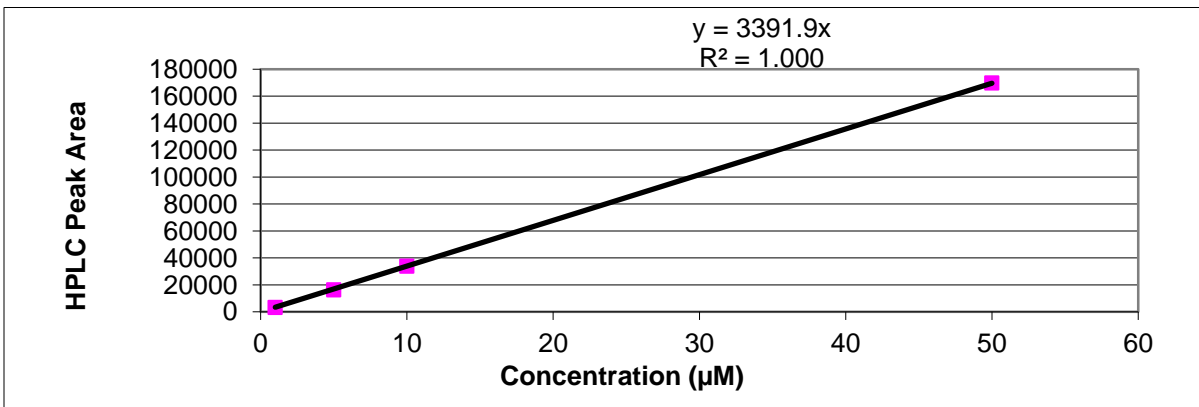


Figure 6.3c Doxycycline standard curve

According to the results (Table 6.4a-6.4c, Figure 6.2a-6.2c), doxycycline showed very high bioavailability in all the time points (30min, 1h, 2h, 4h), especially in the first 30min when the concentration rose to 4.84  $\mu\text{g}/\text{mL}$  in rat serum, and then decreased to 1.48  $\mu\text{g}/\text{mL}$  at the 4h time point. Curcumin at 0.5h showed 0.02  $\mu\text{g}/\text{mL}$  (0.07  $\mu\text{M}$ ) whereas CMC2.24 showed 0.71  $\mu\text{g}/\text{mL}$  (1.66  $\mu\text{M}$ ), about 23-fold over curcumin (in molar amount). The concentrations of both compounds decreased very quickly in the serum from 1h to 4h, and went under the detection limit at 4h. However, CMC2.24 showed higher concentrations in serum samples at 0.2824  $\mu\text{M}$  at 1h and 0.0561  $\mu\text{M}$  at 2h in contrast to curcumin, where the values were 0.0766  $\mu\text{M}$  at 1h and 0.0074  $\mu\text{M}$  at 2h. The observed concentration of CMC2.24 is about 3.7-fold at 1h and 7.6-fold at the 2h time point compared to curcumin. The result confirms that curcumin has a very short half-life (about 13min) in blood serum, whereas CMC2.24 showed considerably greater bioavailability in the serum in contrast to curcumin.



Table 6.2 *In vivo* pharmacokinetics of curcumin, CMC2.24 and doxycycline

Table 6.2a *In vivo* pharmacokinetics of curcumin in rat serum at 0.5h, 1h, 2h and 4h

	Rat	0.5h	1h	2h	4h
Concentration of curcumin in serum( $\mu\text{g}/\text{mL}$ )	1	0.040998	0.044824	0.008237	0
	2	0.014458	0.020659	0	0
	3	0.022846	0.019095	0	0
	AVE	0.026100	0.028193	0.002746	0
	S.D.	0.013566	0.014425	0.004756	----
	S.E.M.	0.007832	0.008328	0.002746	----

Table 6.2b *In vivo* pharmacokinetics of CMC2.24 in rat serum at 0.5h, 1h, 2h and 4h

	Rat	0.5h	1h	2h	4h
Concentration of CMC2.24 in serum( $\mu\text{g}/\text{mL}$ )	1	0.678227	0.019438	0.012915	0
	2	0.743715	0.147151	0.033735	0
	3	0.699961	0.195158	0.025491	0
	AVE	0.707301	0.120582	0.024047	0
	S.D.	0.033355	0.090823	0.010485	----
	S.E.M.	0.019258	0.052437	0.006054	----

Table 6.2c *In vivo* pharmacokinetics of doxycycline in rat serum at 0.5h, 1h, 2h and 4h

	Rat	0.5h	1h	2h	4h
Concentration of doxycycline in serum( $\mu\text{g}/\text{mL}$ )	1	4.742970	4.707733	2.801545	1.739768
	2	5.396904	3.797942	3.516189	2.218084
	3	4.361591	1.363625	0.866771	0.477608
	AVE	4.833822	3.289767	2.394835	1.478487
	S.D.	0.523602	1.729002	1.370735	0.734173
	S.E.M.	0.302302	0.998239	0.791394	0.423875

Figure 6.4 *In vivo* pharmacokinetics of curcumin, CMC2.24 and doxycycline

Figure 6.4a *In vivo* pharmacokinetics of curcumin in rat serum at 0.5h, 1h, 2h and 4h

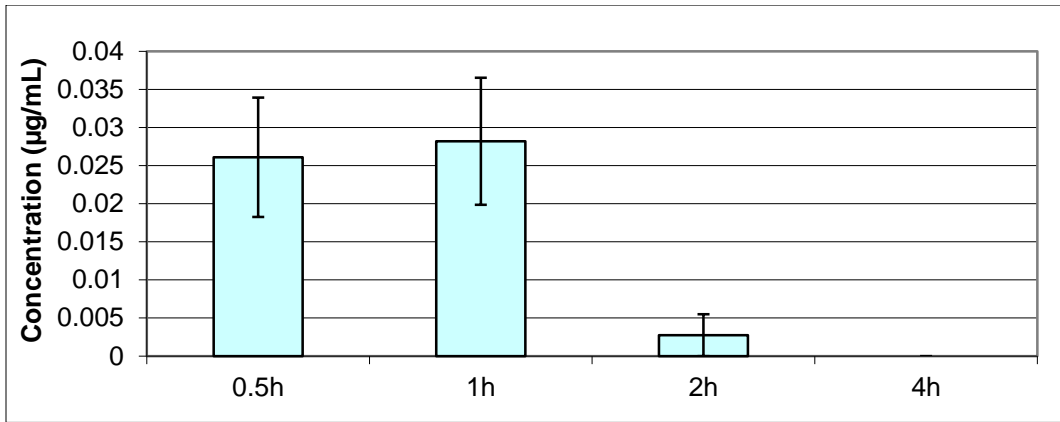


Figure 6.4b *In vivo* pharmacokinetics of CMC2.24 in rat serum at 0.5h, 1h, 2h and 4h

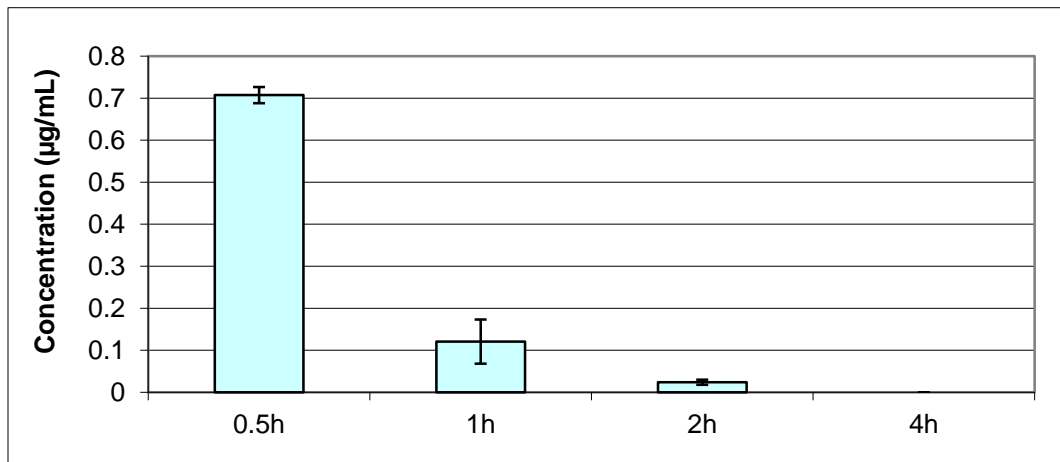
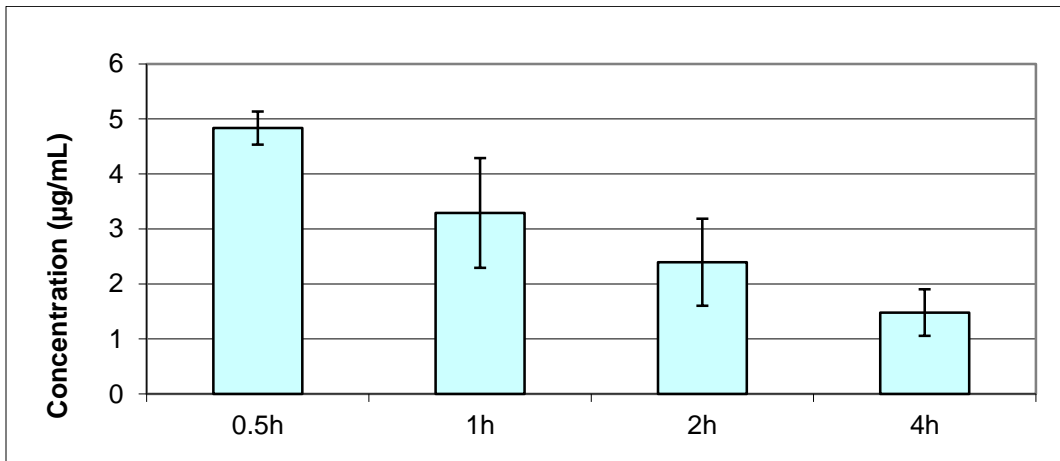


Figure 6.4c *In vivo* pharmacokinetics of doxycycline in rat serum at 0.5h, 1h, 2h and 4h



In order to study the dramatic changes of curcumin and CMC2.24 in serum during the first 0.5 hour, the second pharmacokinetics study with shorter intervals was carried out. Blood was taken at 5min, 10min and 20min. Blood pellets at each time point were collected and analyzed. All the rats were sacrificed at 1 hour time point, and organs including the liver, heart, spleen, kidney, lung and brain were collected and evaluated. From the data shown in Figure 6.5, Figure 6.6a-6.6b and Table 6.3a-6.3b, the 5min, 10min and 20min samples of both curcumin and CMC2.24 showed higher serum concentrations compared to the previous pharmacokinetics study. As for 5min sample, the concentration of CMC2.24 (11.00  $\mu\text{M}$ ) is about 2.2-fold in contrast to the one of curcumin (5.07  $\mu\text{M}$ ). Both 10min and 20min samples appeared to have decreased concentrations compared to 5min Samples.

Figure 6.5 HPLC analysis of rat serum samples by *i.v.* route of curcumin and CMC2.24

Figure 6.5a Blood sample from rats with no curcumin or CMC2.24

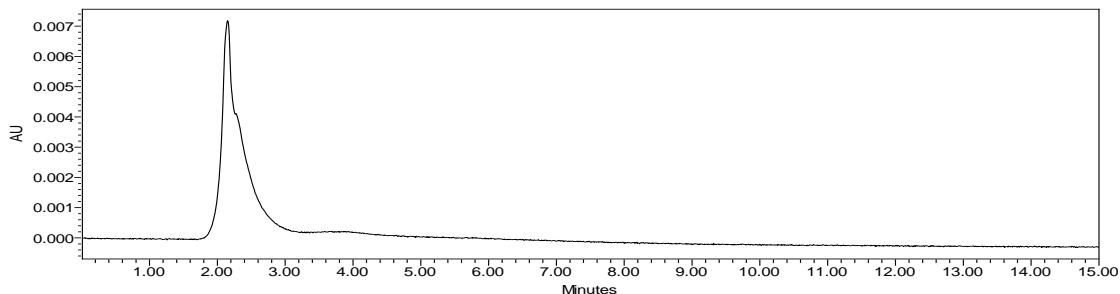


Figure 6.5b Blood sample from rats with *i.v.* administration of curcumin, 5min

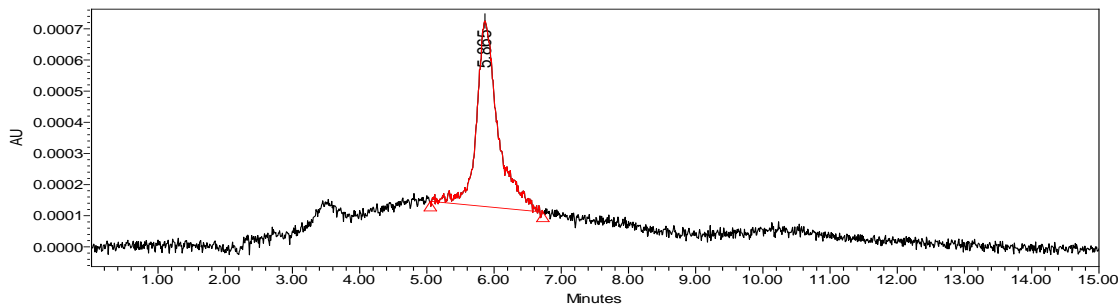


Figure 6.5c Blood sample from rats with *i.v.* administration of curcumin, 10min

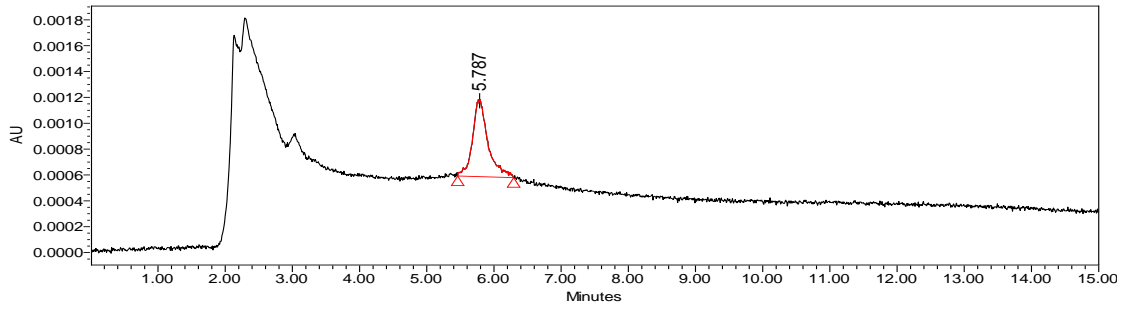


Figure 6.5d Blood sample from rats with *i.v.* administration of curcumin, 20min

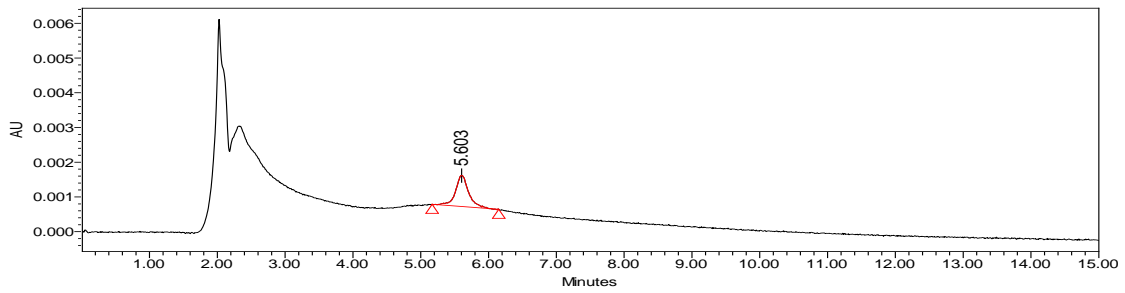


Figure 6.5e Blood sample from rats with *i.v.* administration of CMC2.24, 5min

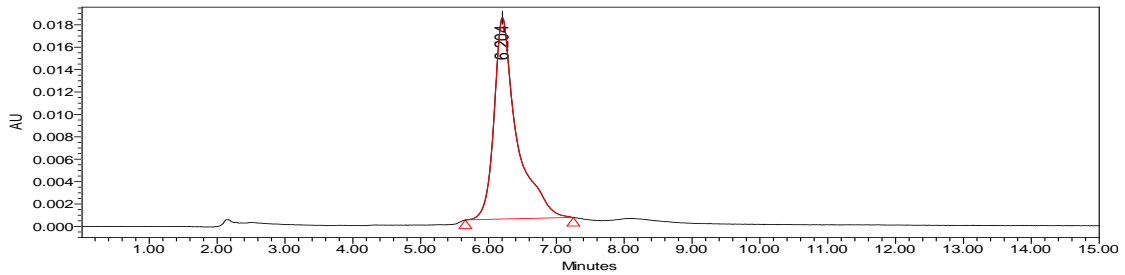


Figure 6.5f Blood sample from rats with *i.v.* administration of CMC2.24, 10min

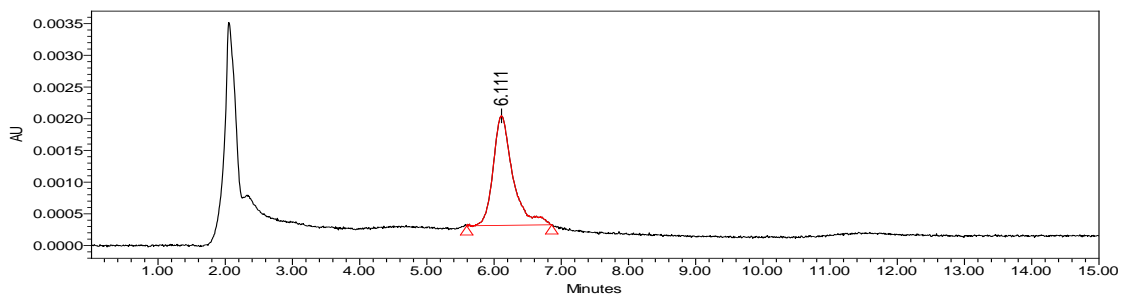


Figure 6.5g Blood sample from rats with i.v. administration of CMC2.24, 20min

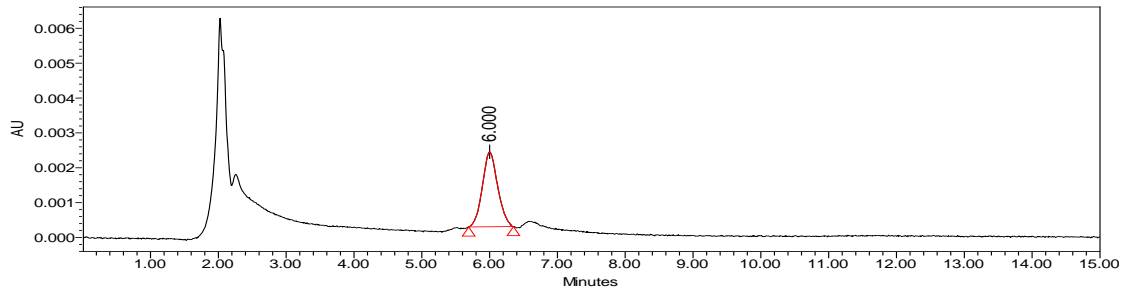


Table 6.3 *In vivo* pharmacokinetics of curcumin and CMC2.24 in 20min

Table 6.3a *In vivo* pharmacokinetics of curcumin in rat serum at 5min, 10min and 20min

\*For Rat #2, there was no detection of compound, so the data are from the Rat #1 and Rat #3

	Rat	5min	10min	20min
Concentration of curcumin in serum( $\mu\text{g/mL}$ )	1	0.264195	0.184707	0.051667
	2*	----	----	----
	3	1.865372	1.434979	0.172756
	AVE	1.064783	0.809843	0.112211
	S.D.	1.132202	0.884076	0.085623
	S.E.M.	0.653677	0.510422	0.049435

Table 6.3b *In vivo* pharmacokinetics of CMC2.24 in rat serum at 5min, 10min and 20min

	Rat	5min	10min	20min
Concentration of CMC2.24 in serum( $\mu\text{g/mL}$ )	1	2.124512	2.058946	0.876829
	2	1.561866	0.844868	0.340222
	3	10.40994	1.575225	1.438222
	AVE	4.698774	1.493013	0.885091
	S.D.	4.954013	0.6112	0.549047
	S.E.M.	2.860201	0.352876	0.316992

Figure 6.6 *In vivo* pharmacokinetics of curcumin and CMC2.24 within 20min

Figure 6.6a *In vivo* pharmacokinetics of curcumin in rat serum at 5min, 10min and 20min

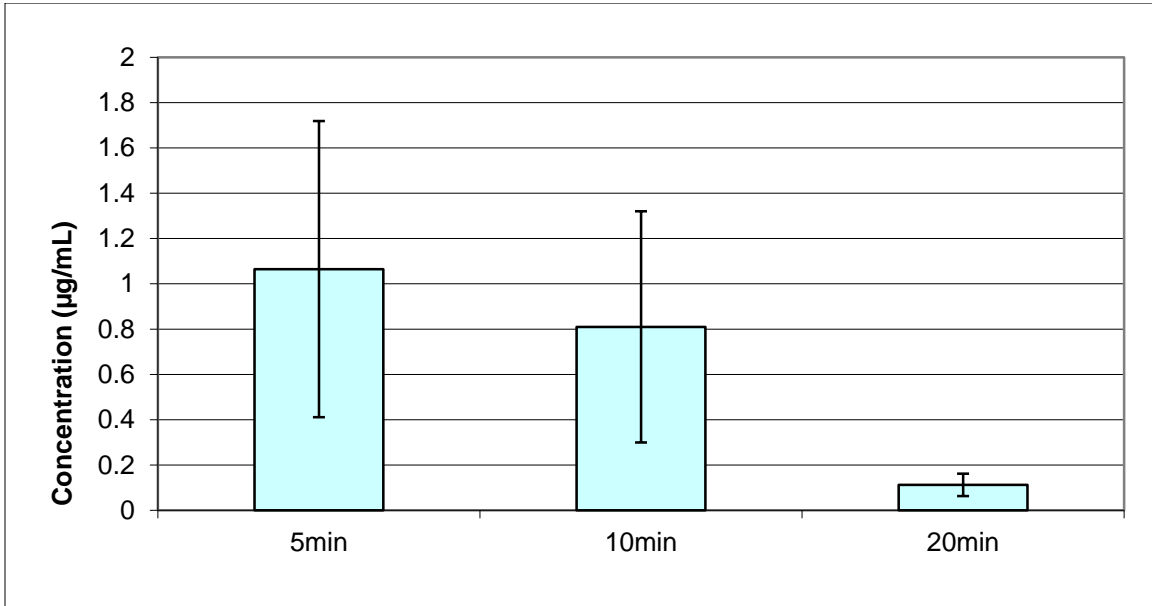
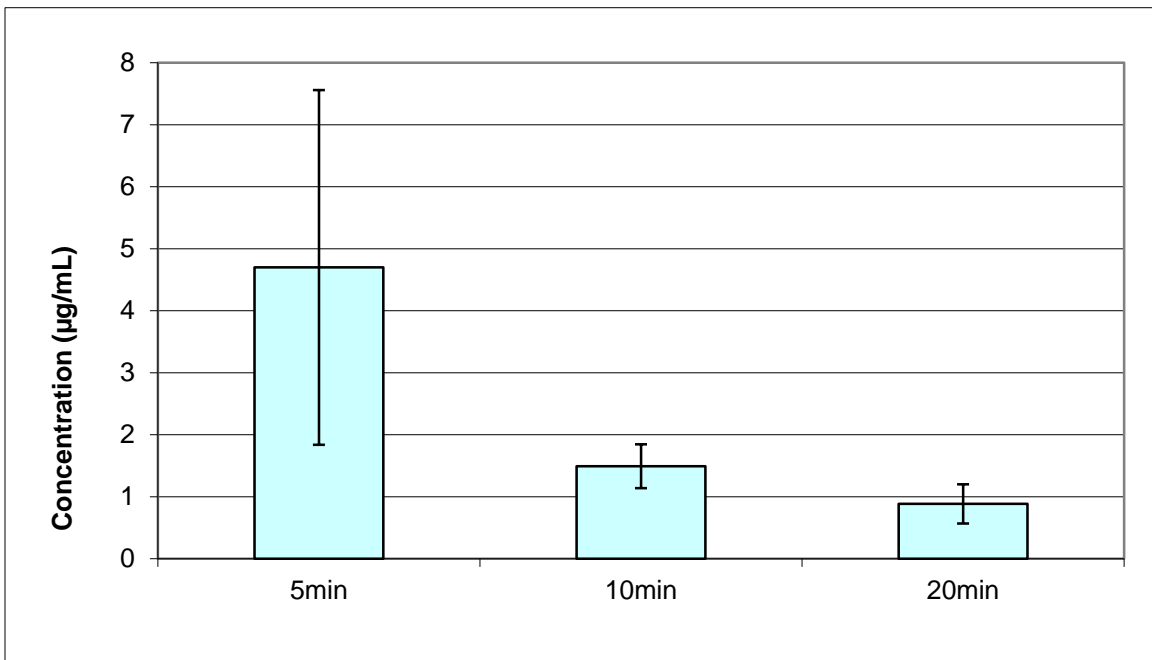


Figure 6.6b *In vivo* pharmacokinetics of CMC2.24 in rat serum at 5min, 10min and 20min



The concentrations of curcumin and CMC2.24 at 7 time points of 5min, 10min, 20min, 30min, 1h, 2h and 4h were shown in Figure 6.7, and then summarized in Table 6.4 and Figure 6.8. It appears that both these compounds have very short half-life within 30min. Pellets from rat blood (mainly blood cells), after removal of serum and washing three times by PBS buffer, were evaluated at these three time points, 5min, 10min and 20min. (Table 6.5, Figure 6.9) The data also indicate that only a relatively small amount of curcumin or CMC2.24 remains in the blood pellets. As for the 5min curcumin sample, about 1/5 of curcumin was found in the blood pellets (in  $\mu\text{g/mL}$ ) compared to serum (in  $\mu\text{g/mL}$ ) as well as CMC2.24. This finding contributes to a total blood distribution of curcumin and CMC2.24 in blood (not limited to serum).

Table 6.4 Summary of concentrations of curcumin and CMC2.24 in rat serum

	Curcumin( $\mu\text{g/mL}$ )	CMC2.24( $\mu\text{g/mL}$ )
5min	1.064783 $\pm$ 0.653677	4.698774 $\pm$ 2.860201
10min	0.809843 $\pm$ 0.510422	1.493013 $\pm$ 0.352876
20min	0.112211 $\pm$ 0.049435	0.885091 $\pm$ 0.316992
30min	0.026100 $\pm$ 0.007832	0.707301 $\pm$ 0.019258
1h	0.028193 $\pm$ 0.008328	0.120582 $\pm$ 0.052437
2h	0.002746 $\pm$ 0.002746	0.024047 $\pm$ 0.006054
4h	0	0



Figure 6.7 *In vivo* pharmacokinetics of curcumin and CMC2.24 in rat serum within 4h

Figure 6.7a *In vivo* pharmacokinetics of curcumin in rat serum within 4h

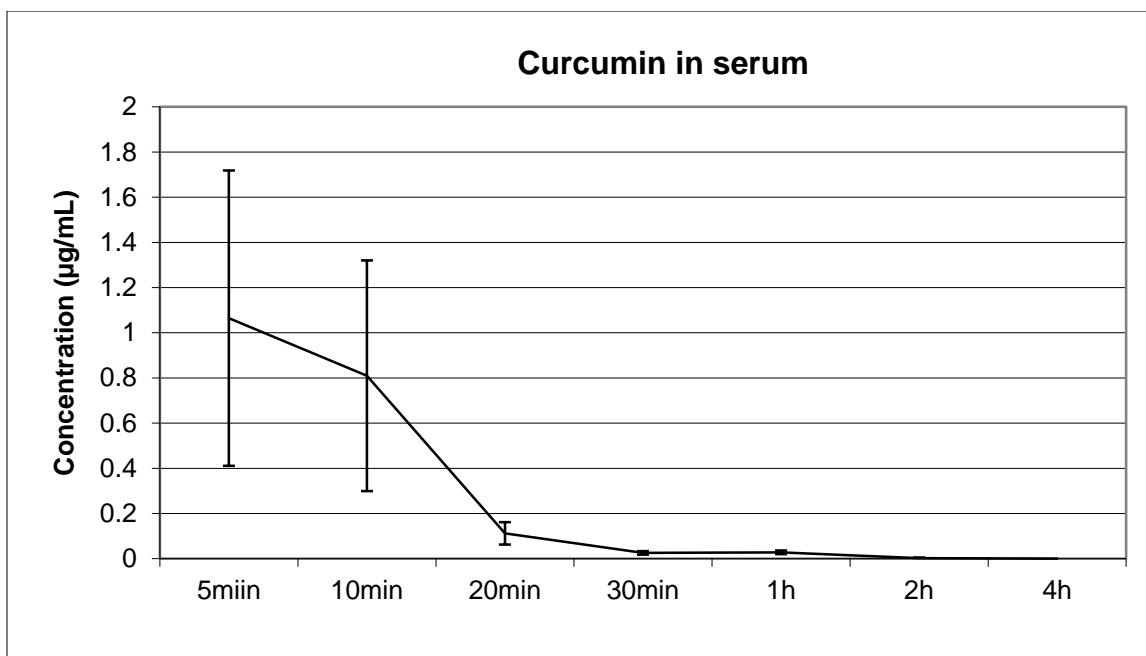


Figure 6.7b *In vivo* pharmacokinetics of CMC2.24 in rat serum within 4h

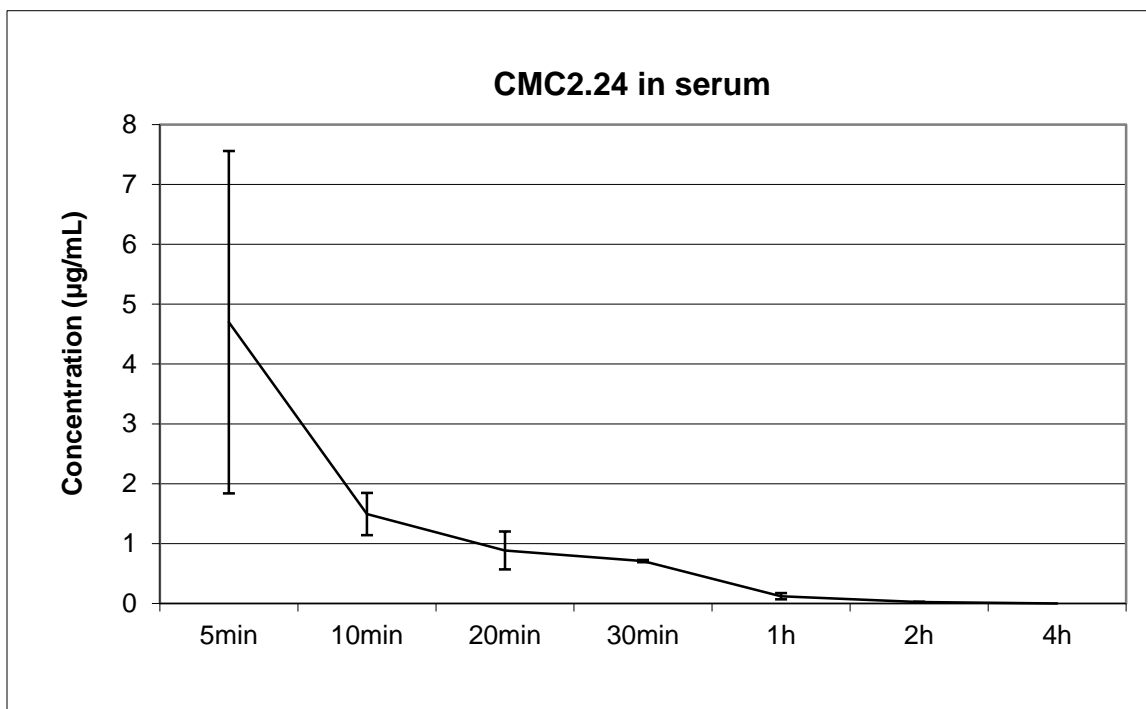


Figure 6.8 Comparison of curcumin and CMC2.24 in rat serum

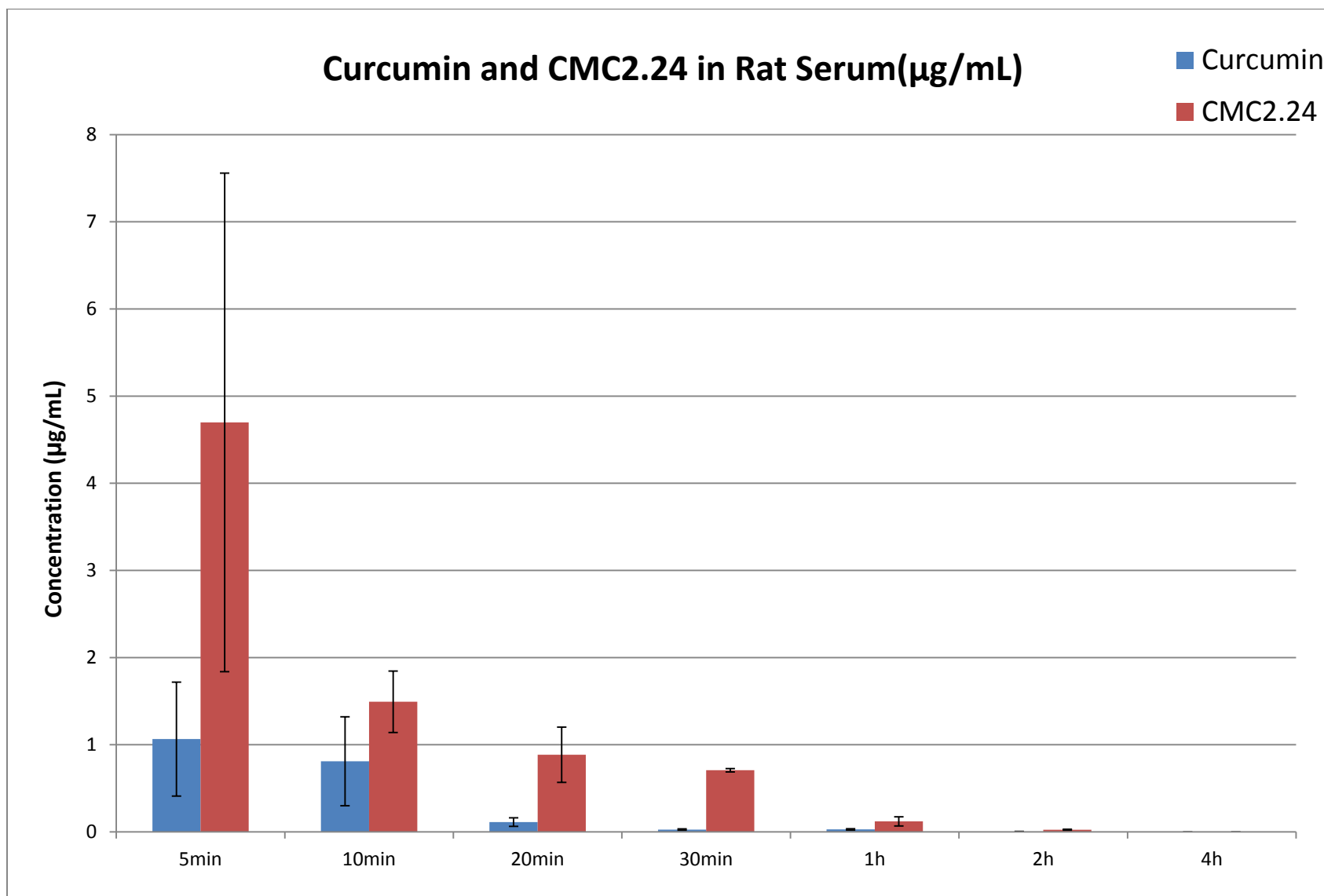


Table 6.5 *In vivo* pharmacokinetics of curcumin and CMC2.24 in rat blood pellets

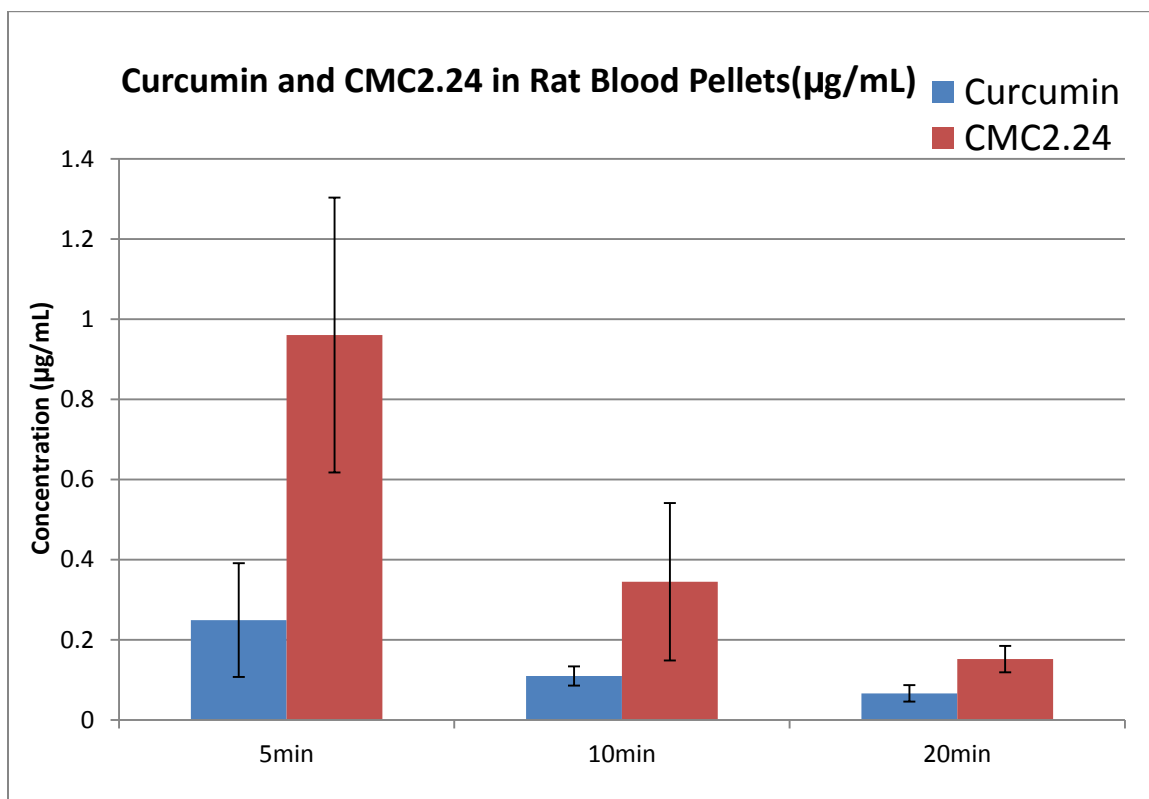
Table 6.5a *In vivo* pharmacokinetics of curcumin and CMC2.24 in rat blood pellets at 5min, 10min and 20min

		5min		10min		20min	
	Rat	Curcumin	CMC2.24	Curcumin	CMC2.24	Curcumin	CMC2.24
Concentration ( $\mu\text{g/mL}$ )	1	0.053853	1.077127	0.106198	0.074541	0.040018	0.146995
	2	0.168779	0.317158	0.070516	0.233616	0.052289	0.097605
	3	0.525262	1.487586	0.152776	0.727043	0.107348	0.211465
	AVE	0.249298	0.960624	0.10983	0.345067	0.066552	0.152022
	S.D.	0.245803	0.593848	0.04125	0.340229	0.03586	0.057096
	S.E.M.	0.141914	0.342858	0.023816	0.196431	0.020704	0.032964

Table 6.5b Comparison of curcumin and CMC2.24 in rat blood pellets at 5min, 10min and 20min

	Curcumin( $\mu\text{g/mL}$ )	CMC2.24( $\mu\text{g/mL}$ )
5min	0.249298 $\pm$ 0.141914	0.960624 $\pm$ 0.342858
10min	0.109830 $\pm$ 0.023816	0.345067 $\pm$ 0.196431
20min	0.066552 $\pm$ 0.020704	0.152022 $\pm$ 0.032964

Figure 6.9 Comparison of curcumin and CMC2.24 in rat blood pellets within 20min



Liver, heart, spleen, kidney, lung and brain were dissected from rats after 1 hour via i.v. injection of curcumin or CMC2.24. The samples were evaluated by HPLC, and the concentrations were calculated to  $\mu\text{g/g}$  for each organ. From the results obtained, it can be seen clearly that CMC2.24 has a significantly higher distribution in all the organs, compared to curcumin, generally about 1.5 folds. Also there are greater concentrations of both curcumin and CMC2.24 in spleen, compared to other organs including the heart and liver. It is also clear that the concentration of CMC2.24 in the lung is about 5 folds of that of curcumin, and also comparable to that of CMC2.24 in the spleen. Both curcumin and CMC2.24 showed low concentrations in brain tissue compared to other tissues at 1 hour time point. The results are shown in Table 6.6a-6.6b and Figure 6.10a-6.10b, and are summarized in Table 6.7 and Figure 6.11.

Table 6.6 *In vivo* pharmacokinetics of curcumin in rat organs

Table 6.6a *In vivo* pharmacokinetics of curcumin in rat organs including liver, heart, spleen, kidney, lung and brain at 1h after *i.v.* injection

Curcumin	Rat	Liver	Heart	Spleen	Kidney	Lung	Brain
Concentration ( $\mu\text{g/g}$ )	1	0.83041	2.841013	1.487927	0.403988	0.850426	0.095242
	2	0.012825	0.139508	2.468074	0.076898	0.307819	0.097746
	3	0.015486	0.152461	0.755557	0.014217	0.442845	0
	AVE	0.28624	1.044327	1.570519	0.165035	0.533696	0.064329
	S.D.	0.471267	1.555989	0.859241	0.2093	0.282482	0.055725
	S.E.M.	0.272086	0.898351	0.496083	0.120839	0.163091	0.032173

Table 6.6b *In vivo* pharmacokinetics of CMC2.24 in rat organs including liver, heart, spleen, kidney, lung and brain at 1h after *i.v.* injection

CMC2.24	Rat	Liver	Heart	Spleen	Kidney	Lung	Brain
Concentration ( $\mu\text{g/g}$ )	1	0.370603	1.253909	2.305669	0.50844	2.661765	0.099424
	2	0.729203	2.817656	2.588864	0.340268	1.503925	0.049081
	3	0.386824	1.620426	3.071122	1.347544	3.855265	0.106855
	AVE	0.495543	1.89733	2.655218	0.732084	2.673652	0.08512
	S.D.	0.202518	0.817822	0.387017	0.539596	1.175715	0.031431
	S.E.M.	0.116924	0.47217	0.223444	0.311536	0.678799	0.018147

Figure 6.10 *In vivo* pharmacokinetics of curcumin and CMC2.24 in rat organs

Figure 6.10a *In vivo* pharmacokinetics of curcumin in rat organs including liver, heart, spleen, kidney, lung and brain at 1h after *i.v.* injection

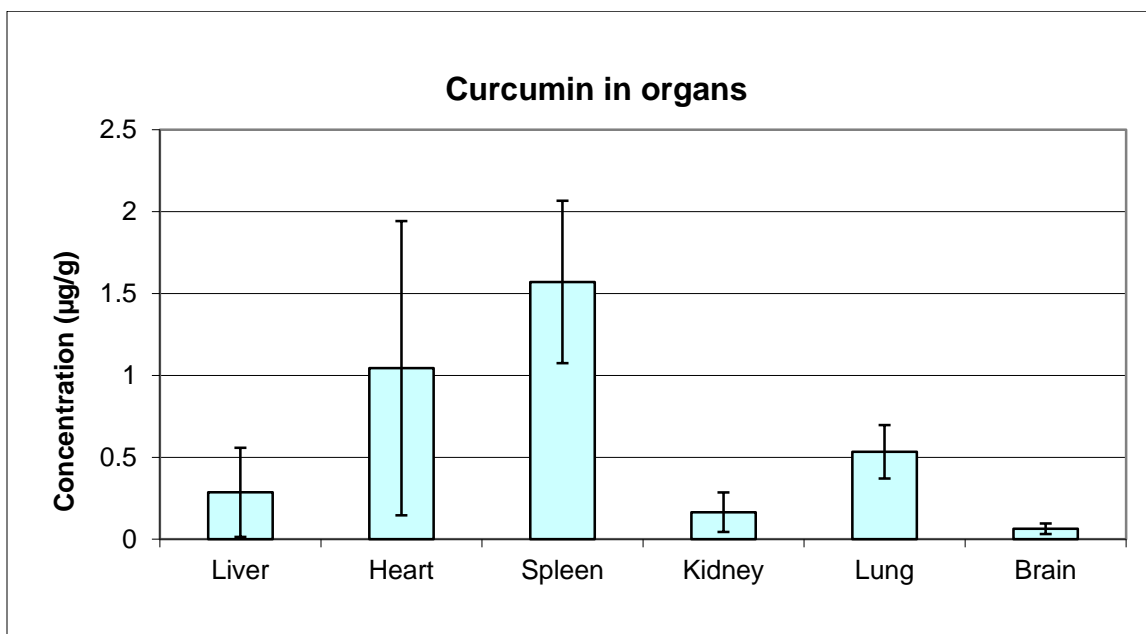


Figure 6.10b *In vivo* pharmacokinetics of curcumin in rat organs including liver, heart, spleen, kidney, lung and brain at 1h after *i.v.* injection

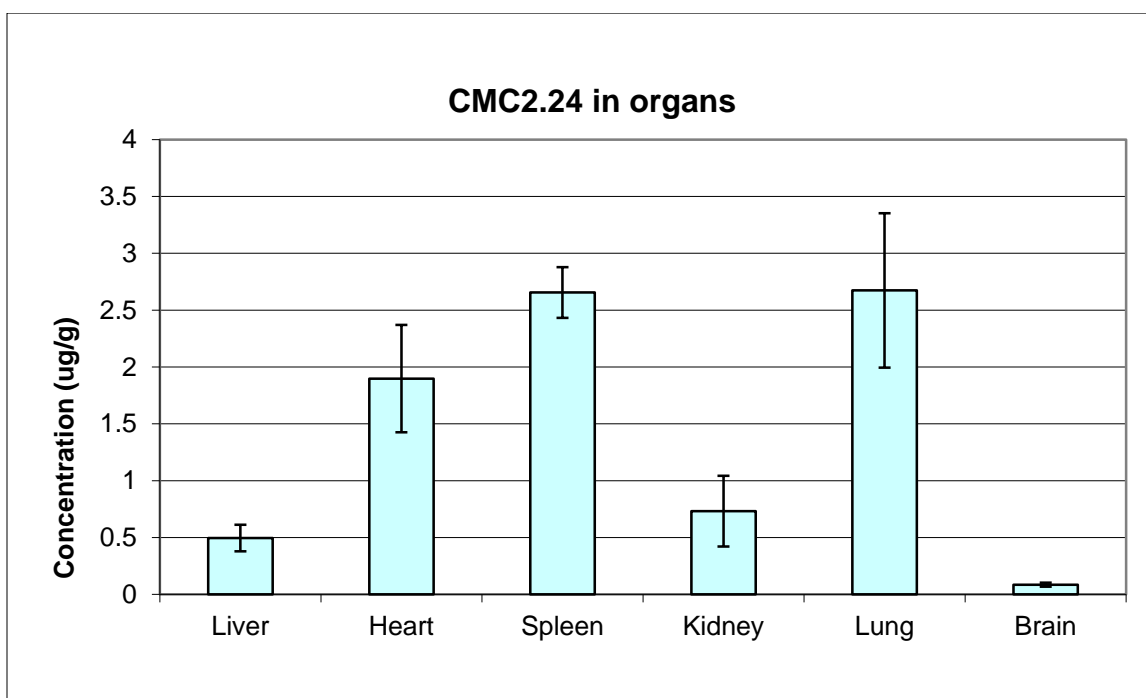
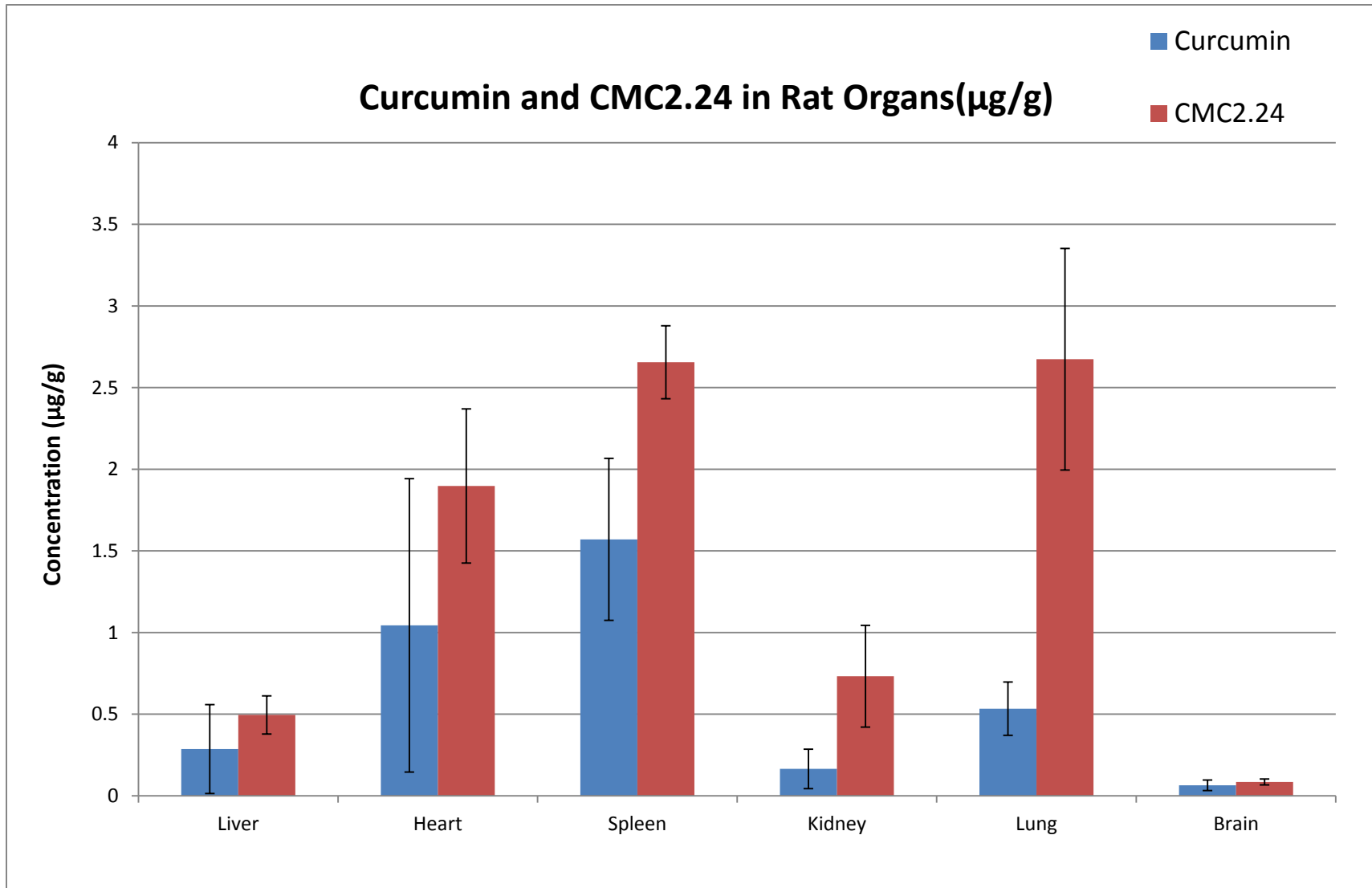


Table 6.7 Comparison of the distribution of curcumin and CMC2.24 in rat organs

	Curcumin( $\mu\text{g/g}$ )	CMC2.24( $\mu\text{g/g}$ )
Liver	0.286240 $\pm$ 0.272086	0.495543 $\pm$ 0.116924
Heart	1.044327 $\pm$ 0.898351	1.897330 $\pm$ 0.472170
Spleen	1.570519 $\pm$ 0.496083	2.655218 $\pm$ 0.223444
Kidney	0.165035 $\pm$ 0.120839	0.732084 $\pm$ 0.311536
Lung	0.533696 $\pm$ 0.163091	2.673652 $\pm$ 0.678799
Brain	0.064329 $\pm$ 0.032173	0.085120 $\pm$ 0.018147

Figure 6.11 Comparison of the distribution of curcumin and CMC2.24 in rat organs

Note: Liver, heart, spleen, kidney, lung and brain were dissected from rats after 1 hour via i.v. injection of curcumin or CMC2.24.





## **Materials and Methods**

### **1. Standard curve**

Curcumin and CMC2.24 were dissolved in Solultol HS 15 (BASF) and Ethyl alcohol (Fisher, 99.5%) (v/v =1:1) at a concentration of 100mM. Dilutions were made through Solultol 15 and ethanol mixture to 1  $\mu$ M, 5  $\mu$ M, 10  $\mu$ M, 50  $\mu$ M, where standard curves were extrapolated. 50  $\mu$ L of each dilution was added to the extraction buffer containing 5mM oxalic acid in water, acetonitrile, and methanol with volume ratio of 2.5:1.5:1. Then each sample was centrifuged down at 10,000rpm for 10min, and 120  $\mu$ L aliquot was taken for HPLC analysis. Both curcumin and CMC2.24 were eluted by HPLC for 20min with the mobile phase of 70% methanol and 30% distilled water eluting at 1.0mL per min, and the detection of peak was at 425nm. The retention time for curcumin and CMC2.24 are around 5.7min and 6.0min. Doxycycline was dissolved in 1X PBS buffer at concentration of 100mM, dilutions were made through PBS buffer to 50  $\mu$ M, 10  $\mu$ M, 5  $\mu$ M, 1  $\mu$ M, where the standard curve was extrapolated. Then each sample was centrifuged down at 10,000rpm for 10min, and 120  $\mu$ L aliquot was taken for HPLC analysis. Doxycycline was eluted by HPLC for 20min with the mobile phase of 20% Methanol, 30% Acetonitrile and 50% 5mM Oxalic acid eluting at 1.0mL per min, and the detection of peak was at 362nm.

### **2. Serum analysis**

Adult male Sprague-Dawley rats (297g average body weight, viral antibody free, Charles River Labs) were distributed into three groups: curcumin, CMC2.24 and doxycycline with three rats per group. Curcumin and CMC2.24 were dissolved in Solultol HS 15 and Ethyl alcohol (v/v=1:1) with the concentration of 40mg/mL, and doxycycline was dissolved in PBS buffer with the same concentration. 150  $\mu$ L of Injection was made through tail vein to each rat (20mg/kg).

Blood was taken at time 5min, 10min, 20min, 30min, 1h, 2h and 4h from orbital sinus. Serum samples were collected and analyzed by HPLC C-18 reverse phase column. For curcumin and CMC2.24, the elution system is 70% Methyl alcohol in double-distilled water with the peak of curcumin appearing at 5.7min and CMC2.24 appearing at 6.1min, while for doxycycline, the elution system is 20% Methanol, 30% Acetonitrile and 50% 5mM Oxalic acid with the peak of doxycycline appearing at 3.2min.

### **3. Pellets analysis**

200  $\mu$ L of blood from rats was drawn at 5min, 10min and 20min after i.v. injection of curcumin and CMC2.24. Serum was removed and the pellets were washed three times by 200  $\mu$ L of PBS buffer, then acetonitrile was added to each sample to reach a final volume of 200  $\mu$ L. 50  $\mu$ L of supernatant, after vortexing and centrifuge at 10,000rpm for 10min, was added to extraction buffer containing 5mM oxalic acid in water, acetonitrile, and methanol with volume ratio of 2.5:1.5:1. 120  $\mu$ L aliquot was taken for HPLC analysis. Both curcumin and CMC2.24 were eluted by HPLC for 20min with the mobile phase of 70% methanol and 30% distilled water eluting at 1.0mL per min, and the detection of peak was at 425nm.

### **4. Organ analysis**

Liver, heart, spleen, kidney, lung and brain from rats by i.v. injection of curcumin and CMC2.24 were dissected after 1h of dosage. These organs were washed with PBS buffer for three times, and dried by blotting with filter paper. Wet tissue was homogenized in 5.0mL of acetonitrile for 4min by polytron. 0.3mL of the homogenate was added to 0.6mL of extraction buffer containing 5mM oxalic acid in water, acetonitrile, and methanol with volume ratio of 2.5:1.5:1. Then each sample was centrifuged down at 10,000rpm for 10min, and 120  $\mu$ L aliquot was taken for HPLC analysis described above.

## References

1. Lipinski, C.A.; Lombardo, F.; Dominy, B.W.; Feeney, P.J. Experimental and computational approaches to estimate solubility and permeability in drug discovery and development settings. *Adv Drug Deliv Rev.*, **2001**, *46*, 3-26
2. Sharma, R.A.; Euden, S.A.; Platton, S.L.; Cooke, D.N.; Shafayat,A; Hewitt, H.R.; Marczylo, T.H.; Morgan, B.; Hemingway, D.; Plummer, S.M.; Pirmohamed, M; Gescher, A.J.; Steward, W.P. Phase I clinical trial of oral curcumin: biomarkers of systemic activity and compliance. *Clin. Cancer Res.*, **2004**, *10*, 6847-6854
3. Cheng, A.L.; Hsu, C.H.; Lin, J.K.; Hsu, M.M.; Ho, Y.F.; Shen, T.S.; Ko, J.Y.; Lin, J.T.; Lin, B.R.; Ming-Shiang, W; Yu, H.S.; Jee, S.H.; Chen, G.S.; Chen, T.M.; Chen, C.A.; Lai, M.K.; Pu, Y.S.; Pan, M.H.; Wang, Y.J.; Tsai, C.C.; Hsieh, C.Y. Phase I clinical trial of curcumin, a chemopreventive agent, in patients with high-risk or pre-malignant lesions. *Anticancer Res.*, **2001**, *21*, 2895-2900
4. Ravindranath, V.; Chandrasekhara, N. Absorption and tissue distribution of curcumin in rats. *Toxicology*, **1980**, *16*, 259-265
5. Maiti, K.; Mukherjee, K.; Gantait, A; Saha, B.P.; Mukherjee, P.K. Curcumin–phospholipid complex: Preparation, therapeutic evaluation and pharmacokinetic study in rats. *Int. J. Pharm.*, **2007**, *330*, 155-163
6. Sharma, R.A.; McLelland, H.R.; Hill, K.A.; Ireson, C. .; Euden, S.A.; Manson, M.M.; Pirmohamed, M; Marnett, L.J.; Gescher, A.J.; Steward, W.P. Pharmacodynamic and pharmacokinetic study of oral Curcuma extract in patients with colorectal cancer. *Clin. Cancer Res.*, **2001**, *7*, 1894-1900

7. Liu, Y.; Ramamurthy, N.; Marecek, J.; Lee, H.M.; Chen, J.L.; Ryan, M.E.; Rifkin, B.R.; Golub, L.M. The lipophilicity, pharmacokinetics, and cellular uptake of different chemically-modified tetracyclines (CMTs). *Curr. Med. Chem.*, **2001**, *8*, 243-252.
8. Yu, Z.; Leung, M.K.; Ramamurthy, N.S.; McNamara, T.F.; Golub, L.M. HPLC determination of a chemically modified nonantimicrobial tetracycline: biological implications. *Biochem. Med. Metab. Biol.*, **1992**, *47*, 10-20.
9. Tong, S.; Johnson, F. Investigation of Curcumin and CMCs. *Undergraduate Senior Thesis*, **2011**, Stony Brook University
10. Coon, J.S.; Knudson, W.; Clodfelter, K.; Lu, B.; Weinstein, R.S. Solutol HS 15, nontoxic polyoxyethylene esters of 12-hydroxystearic acid, reverses multidrug resistance. *Cancer Res.*, **1991**, *51*, 897-902
11. Fang, Y.; Xiang, B.; Pan, Z.H.; Cao, D.Y. Studies on preparation and dissolution test in vitro of sustained-release dropping pills of curcumin. *Zhong Yao Cai*, **2010**, *33*, 111-114
12. Van Herck, H.; Baumans, V.; Brandt, C.J.; Boere, H.A.; Hesp, A.P.; van Lith, H.A.; Schurink, M.; Beynen, A.C. Blood sampling from the retro-orbital plexus, the saphenous vein and the tail vein in rats: comparative effects on selected behavioral and blood variables. *Lab Anim.*, **2001**, *35*, 131-139

## **Chapter 7. X-Ray Crystallography of the MMP-8 catalytic subunit with and without curcumin and CMC2.24 as inhibitors**

### **A. Introduction**

#### **1. X-ray crystallography**

X-ray crystallography as well as NMR spectroscopy is the advanced technology used to study the structural interactions between biologically-interesting molecules including proteins at an atomic level. Such information can help to elucidate the mechanisms of protein-protein or protein-inhibitor interactions.<sup>1,2</sup> The crystals that are needed for X-ray analysis would be obtained after protein expression, purification and crystallization under certain conditions with or without other bound molecules, including proteins, peptides, regulators or small drug molecules. These crystals are exposed to certain X-ray wavelengths in a beamline to obtain three-dimensional diffraction patterns from which the crystal packing symmetry aspects and repeating units can be determined, all of which contribute to understanding the physical properties of the crystals.<sup>3,4</sup> These data are processed by specific software such as Phenix Refinement to determine the crystal structures based on the electron density map. Figure 7.1 shows the general procedure of X-ray crystallography. Protein would be obtained after cloning (the process to create copies of DNA fragments), transformation (the genetic alteration of a cell resulting from the incorporation of exogenous DNA from its surroundings), expression (the process in which proteins are synthesized, modified and regulated in living organisms) and purification (the process intended to isolate a single type of protein from a complex mixture), and then crystallized in certain conditions, ready for X-ray diffraction and data process.

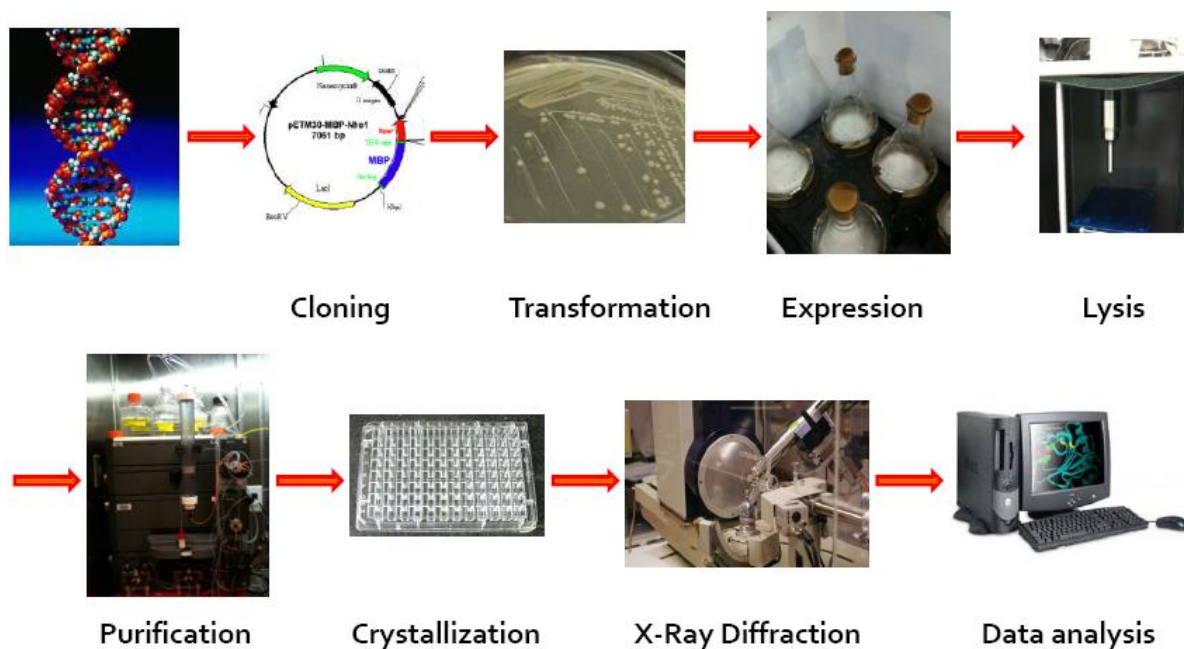


Figure 7.1 General procedures of X-ray crystallography

## 2. X-ray crystallography study of MMP-8

MMP-8, a neutrophil collagenase, possesses the ability to cleave the triple-helical domain of native fibrillar collagens I, II and III, generating the fragments of  $\frac{1}{4}$  and  $\frac{3}{4}$  length of a standard collagen monomer as mentioned in Chapter 2. Thus it is one of the collagenases of the matrix metalloproteinases family.<sup>5,6</sup> MMP-8, mainly produced by neutrophils, is crucial in a variety of pathological conditions related to inflammation and cancer because of its role in the regulation of immune response.<sup>7,8</sup> The glycosylated MMP-8 has a molecular weight of 75-80kD in the latent form. The catalytic subunit of MMP-8 lacking the hemopexin-like domain was first purified by Schnierer *et al.*<sup>9</sup>, and since then the crystal structures of MMP-8 with a variety of inhibitors have been studied by X-ray crystallography.<sup>10-24</sup> The MMP-8 catalytic domain has a sphere-like structure consisting of a five-stranded  $\beta$ -sheet and two  $\alpha$ -helices.<sup>10-12</sup> The two histidines and a catalytic glutamic acid residue of His197-Glu198-Xaa-Xaa-His201 (Xaa = acidic amino acid) comprise the zinc binding site, to the right of which sits the S1' pocket. Three amino acid

residues lie to the entrance to this pocket: Ile159, Leu160, and Ala161, and three other amino acid residues form the wall of the pocket: Tyr216, Pro217, and Asn218. Also in the interior of this pocket are the side chains of Tyr219-Tyr227, Leu214-Asp213, and Leu193.<sup>12</sup> The crystal structure of the MMP-8 catalytic domain (Met80 to Gly242) bearing one hydroxamate inhibitor, namely Pro-Leu-Gly-NHOH, was first studied by Bode *et al.*<sup>10</sup> From their crystal structure (2.0 Å resolution), penta-coordination with the catalytic zinc atom is formed by the two oxygens from the hydroxamic acid inhibitor as well as three histidines His197, His201 and His207 (Note: The example of penta-coordination with zinc is not known in inorganic chemistry, thus the assignment is questionable).<sup>10-13</sup>

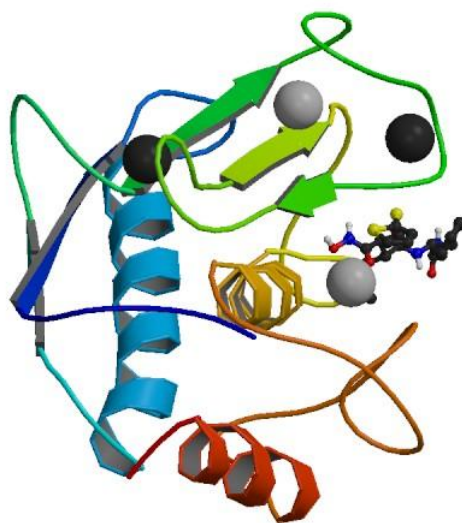


Figure 7.2 Crystal structure of MMP-8 catalytic domain with Batimastat

Note: This figure is adapted from Protein Data Bank (PDB) code: 1MMB. Five-stranded  $\beta$ -sheet and two  $\alpha$ -helices are shown in the figure with two calcium atoms are shown black and two zinc atoms are shown in white. The inhibitor, Batimastat is interacting with the catalytic zinc atom.<sup>13</sup>

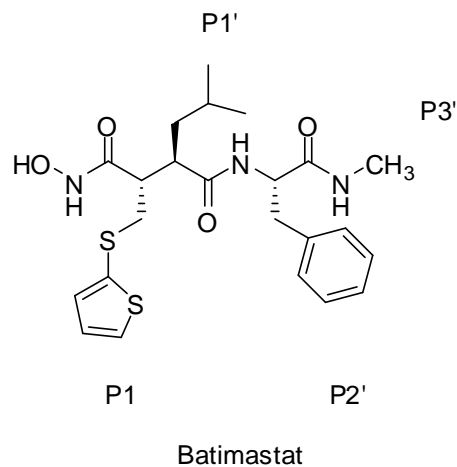


Figure 7.3 Structure of Batimastat (BB-94)

Batimastat (BB-94), {4-(N-hydroxyamino)-2(R)-isobutyl-3(S)-[ (2 thienylthiomethyl) succinyl]-L-phenylalanine-N-methylamide}, one of the most potent MMP inhibitors so far, was developed by British Biotech and evaluated in X-ray crystallography studies.<sup>13</sup> This hydroxamate inhibitor possesses the  $IC_{50}$  of 10nM against MMP-8.<sup>14</sup> Besides the penta-coordination between the catalytic zinc with its oxygens as well as the three histidine residues as mentioned above, the residues from Batimastat also displayed a strong interaction with MMP-8 in the pockets of catalytic domains. The P1' residue is the hydrophobic moiety of the compound (Figure 7.2), and it associates with the S1' pocket of MMP-8 catalytic domain. The P2' residue relates with the residues of Gly158, Ile159, Pro217 and Am218. The P3' residue was found to be responsible for solvent exposure (The solvent exposure of an amino acid in a protein defines as the extent to which the amino acid is accessible to the solvent, usually water, surrounding the protein).<sup>13</sup> Several other inhibitors have been crystallized together with MMP-8 catalytic domain, including phosphonate, carboxylate, peptide and non-zinc binding inhibitors.<sup>15-24</sup> Since curcumin and CMC2.24 are potent inhibitors of MMPs from the data discussed in Chapter 4, it is important to study the binding at the molecular level by X-ray crystallography. Although doxycycline as the MMP inhibitor was approved by the FDA at sub-antimicrobial doses for the treatment of



periodontal inflammation and chronic skin disease, the mechanism at the molecular level has still not been elucidated despite the proof by Golub *et al.*<sup>24</sup> that zinc binding is involved. It is important to attempt to define how the inhibitor binds in the catalytic pocket of the MMPs beyond the attachment to the zinc atom. Also the crystal structure of MMP-8 with curcumin and its analogues will definitely improve the further design and development of more specific inhibitors for different MMPs, based on the specific interactions between the inhibitors and their protein targets.

### **B. Recombinant protein expression with His-tag**

The MMP-8 catalytic domain purification method reported in the literature utilizes a hydroxamate affinity column. However, after reviewing this method, the alternate method using recombinant protein, with a His-tag was chosen because of the experience of this procedure in our laboratory. Recombinant protein expression with polyhistidine residues have been developed during the past decades, whereby immobilized metal-affinity chromatography using  $\text{Co}^{2+}$ ,  $\text{Ni}^{2+}$ ,  $\text{Cu}^{2+}$  or  $\text{Zn}^{2+}$  ions was introduced for protein purification.<sup>25,26</sup> Because histidine can bind to the immobilized metal ion resins through its electron-donating imidazole group, it has the ability to retain the protein on the pre-loaded metal-affinity column. The pure protein then can be eluted out by free imidazole solution at a different pH after the elution of other protein fractions. The primary structure is given below for the catalytic domain of MMP-8.<sup>9</sup> Metal ions binding involved are as follows: H197, H201, H207 for catalytic zinc (Zn999); H147, D149, H162, H175 for structural zinc (Zn998); D154, G155, N157, 1159, D177, E180 for calcium site Ka997; D137, G169, G171, D173 for calcium site Ka996.

80

MLTPGNPKWERTNLTYRIRNYTPQLSEAEVERAIKDAFELW

121

SVASPLIFTRISQGEADINIAFYQRDHGDNSPFDGPNGLAH

162

AFQPGQGIGGDAHFDAEETWTNTSANYNLFLVAAHEFGHSL

203

GLAHS SDPGALMYPNYAFRETSNYSLPQDDIDGIQAIYG

Figure 7.4 Primary structure of MMP-8 catalytic domain

PCR reaction was carried out by MMP8R255FWD (primer 1: 5'-GATGAAAAGCCTCGCTGTG-3') and MMP81037REV (primer 2: 5'-CAGAGCCCAGTATTGGTTGC-3'). After purification by QIAGEN MINElute purification kit, the PCR product was then cloned into a pET-7 vector (Novagen) using the 5' NdeI and 3' XhoI restriction enzymes, so that a His-tag was encoded at the N-terminus. Protein with a His-tag was obtained after the insertion into a plasmid, digestion, ligation, transformation and expression in *E. coli*. Cells were harvested by centrifugation, and the cell pellets were resuspended and sonicated to remove the cell debris, followed by centrifugation. The clear supernatant was then loaded onto a His-bind column (1.5cm x 15cm) containing 4mL His-bind resin (Novagen) that had been charged with 10mL of buffer ( $\text{Ni}^{2+}$ ). The eluted protein fractions were then collected and concentrated (Figure 7.5). TEV (tobacco etch virus) protease was added to the desired protein fraction and left overnight in order to remove the His-tag. Following this the protein fraction was loaded on to a Q-Sepharose ion-exchange column because it carries a negative charge at this pH (pH=6.0), and the purity of the eluted fractions was determined by sodium dodecyl sulfate polyacrylamide gel electrophoresis (SDS-PAGE) after Fast protein liquid chromatography (FPLC). However, the separation was not achieved, as can be seen from Figure 7.6, even after four additional purifications on a Q-Sepharose column. A second concern was the

low yield (about 30%) after the attempted purification. Thus, this method was not pursued further.

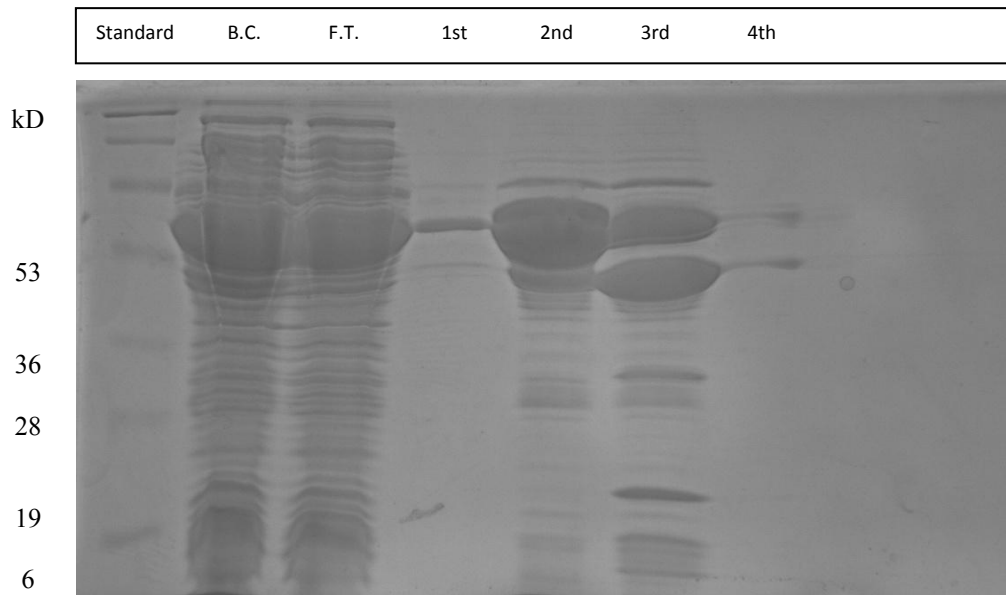


Figure 7.5 SDS gel of MMP-8 catalytic subunit after nickel column purification

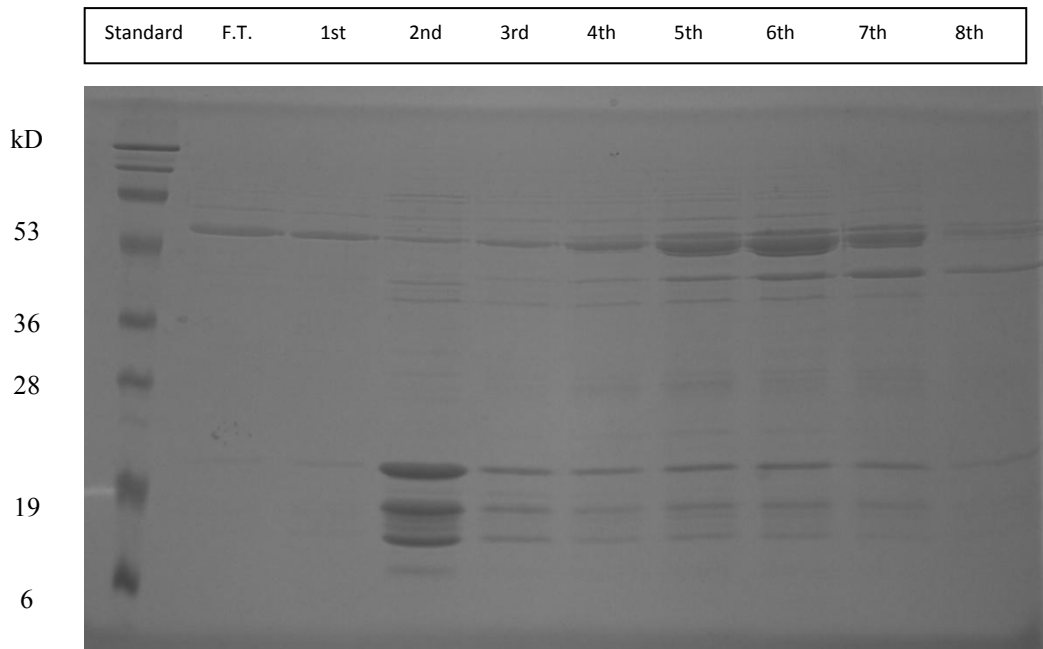


Figure 7.6 SDS gel of MMP-8 catalytic subunit after Q-Sepharose purification

### C. Recombinant protein expression without His-tag

Since the protein expression with His-tag didn't give either a desirable yield or purity, a recombinant protein expression without His-tag attempted. Protein can be denatured by high concentrations of urea (above 6M), and thereafter dialyzed to refold the three-dimensional natural structure. The digestion of the plasmid insert was first transformed to the vector, namely pET-22b(+), and then transferred into TOP-10F' competent cells by electroporation. Expression of the MMP-8 catalytic subunit was carried out in *E.coli* strain BL21(DE3), and inclusion bodies were isolated. Pellets were resuspended, sonicated, and then dissolved in 6M urea to denature the protein. The stock protein solution was diluted to 1mg/mL and then dialyzed to refold to the three-dimensional structure in the absence of urea. Refolding was confirmed by Circular Dichroism, which indicated the reformation of the secondary structures, the  $\alpha$ -helix and the  $\beta$ -sheet which corresponds to the native protein, as shown in Figure 7.7. The purity was determined by 15% SDS-PAGE (Figure 7.8) and MALDI (Figure 7.9). In Figure 7.8, the lower band is the *E. coli* heat shock protein with the MW of 16.0kD, and the upper band is the MMP-8 catalytic subunit with the MW of 18.5kD. The MMP-8 catalytic subunit was concentrated by centrifugation and loaded onto a superdex gel filtration column to remove the *E. coli* heat shock protein because of their differences in molecular weight. (Figure 7.10) The MMP-8 activity assay was also carried out for the MMP-8 catalytic subunit, which showed collagenase activity in its ability to degrade the fluorogenic substrate, Mca-Lys-Pro-Leu-Gly-Leu-Dpa-Ala-Arg-NH<sub>2</sub> which was used in the *in vitro* inhibition assay as mentioned in Chapter 4. The MMP-8 catalytic subunit, the major peak in Figure 7.8, was collected and concentrated for crystallization.

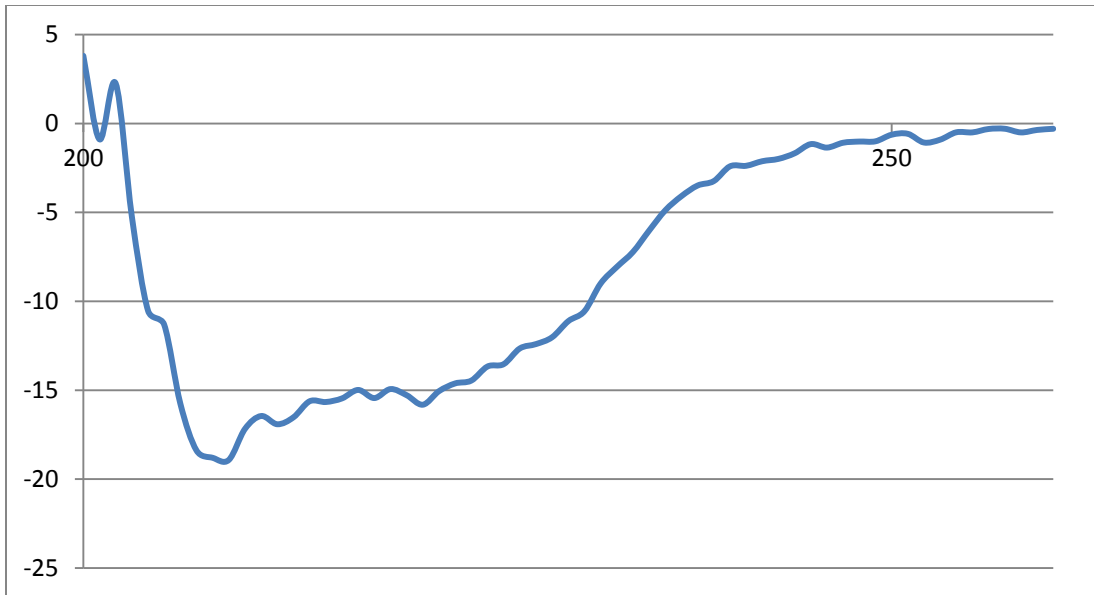


Figure 7.7 Circular Dichroism determination of MMP-8 refolding after dialysis

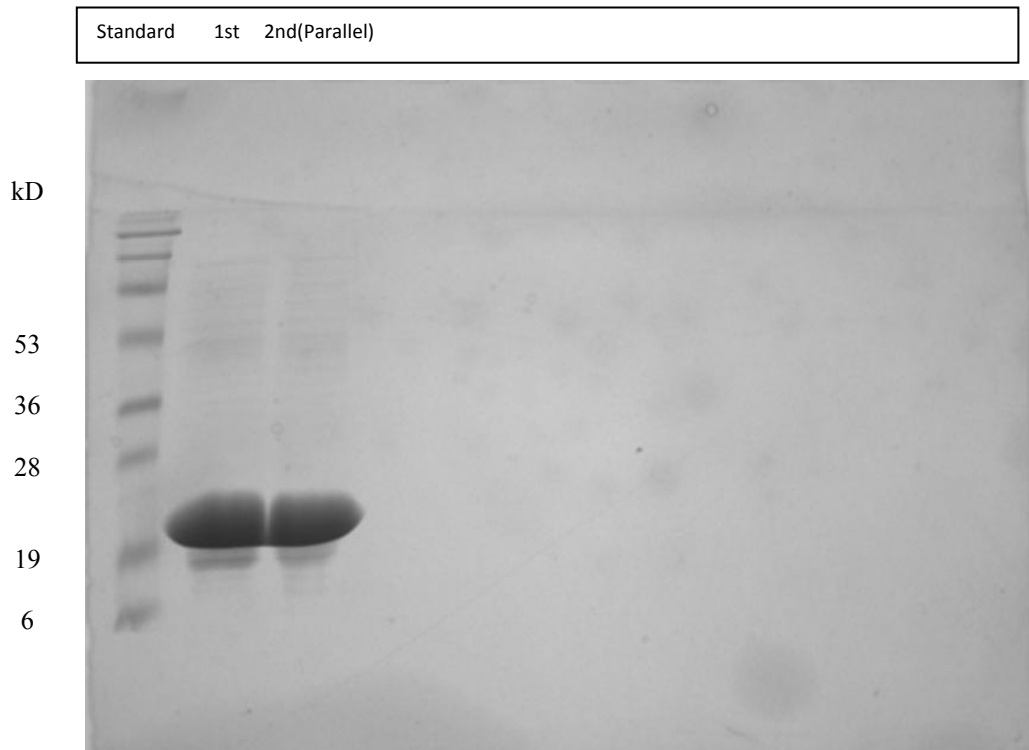


Figure 7.8 SDS gel of MMP-8 after dialysis

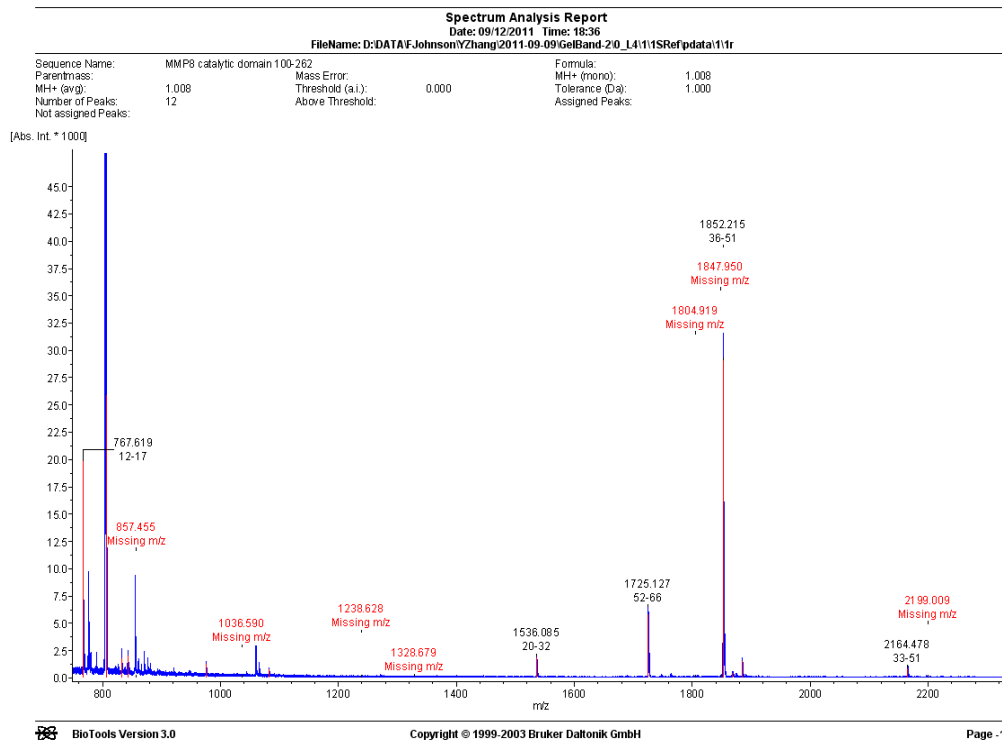


Figure 7.9 MALDI determination of MMP-8 after dialysis

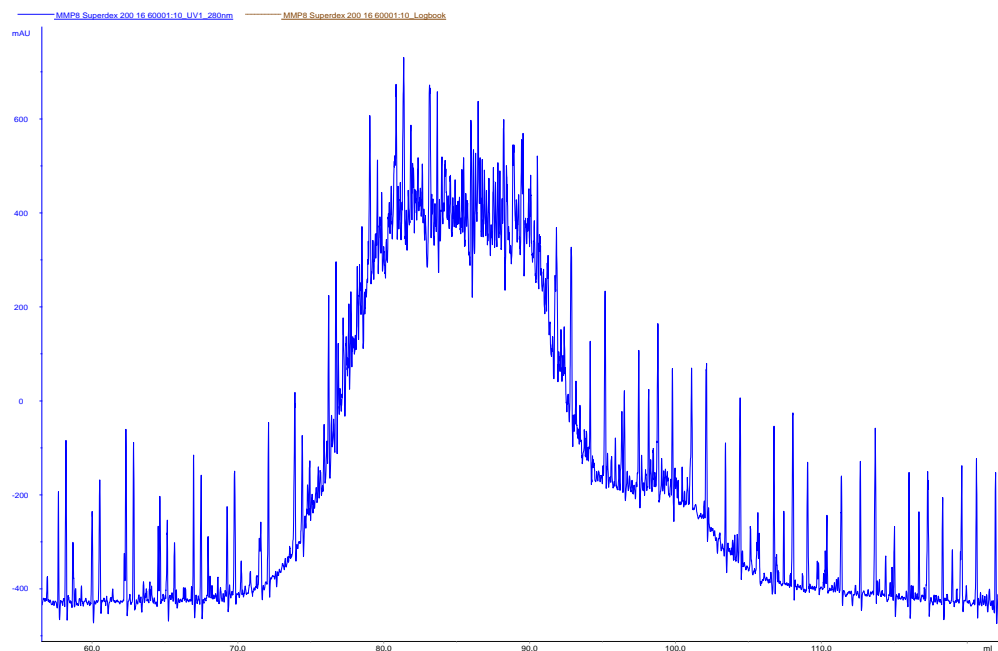


Figure 7.10 Gel filtration after dialysis

#### **D. Crystallization of MMP-8 with or without the inhibitor present**

The purified MMP-8 catalytic subunit was crystallized using the hanging drop method.<sup>16,17</sup> A 3-fold molar excess of curcumin or CMC2.24 (50mM) in DMSO was added to a solution of 12mg/mL MMP-8 catalytic subunit in the buffer containing 25mM MES, 100mM NaCl, 10mM CaCl<sub>2</sub>, 0.1mM ZnCl<sub>2</sub> (pH=6.0) to give a total volume of 4  $\mu$ L. The solution contained 10-25% (w/w) PEG6000, and was equilibrated against a 500  $\mu$ L reservoir solution of 1M Na<sub>2</sub>HPO<sub>4</sub>/NaH<sub>2</sub>PO<sub>4</sub> at pH 6.0. Parallel experiments were also carried out for the protein alone without any inhibitors to obtain the density map for structural analysis. Needle-shaped crystals appeared in 4 days. Crystal X-ray data were collected at 1.3-2.5 Å on Beamline 25 from the National Synchrotron Light Source (NSLS) at Brookhaven Lab. From the results shown in Figure 7.11 and 7.12, the crystal structure without inhibitors showed a similar density in the catalytic zinc-binding domain as those harboring an inhibitor (either curcumin or CMC2.24). This strongly indicates that the protein itself needs further purification to remove what appears to be the endogenous inhibitor (peptide or protein fragment) in the catalytic domain of MMP-8 to allow the synthetic inhibitor, curcumin and CMC2.24, to bind the catalytic domain. A recent study (unpublished data) by Dr. Sanford R. Simon shows that Triton buffer (used as one component in the buffer for the MMP-8 catalytic subunit expression) could bind to the elastase and prevent the inhibitor from binding. Thus this fragment in the crystal structure of MMP-8 catalytic subunit might be the molecule from the buffers used for protein expression or purification.

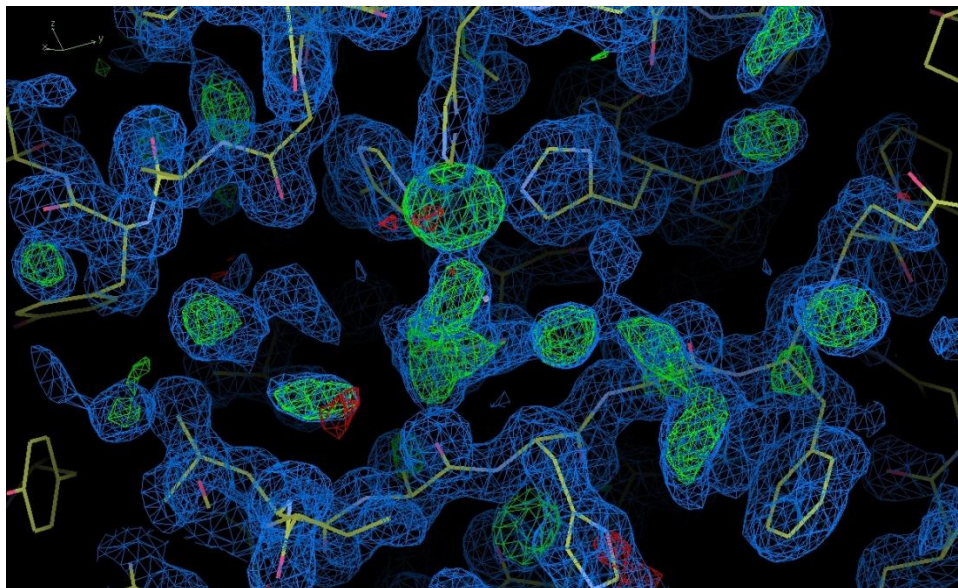


Figure 7.11 Density map from the X-ray data collection without any inhibitor

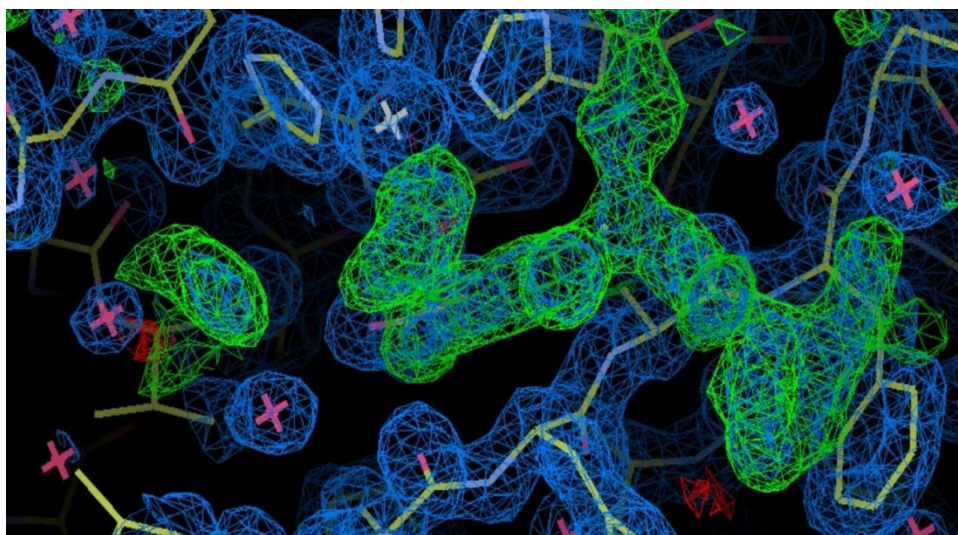


Figure 7.12 Density map from the X-ray data collection with an inhibitor CMC2.24

Note: The above figures seem the same, which strongly indicates that the protein itself needs further purification to remove what it appears to be as the endogenous inhibitor (or fragment) in the catalytic domain of MMP-8 to allow the synthetic inhibitor, curcumin and CMC2.24, to bind the catalytic domain.



## Materials and Methods

### 1. Cloning and protein expression of MMP-8 in an MBP fusion system

The cDNA of MMP-8 was purchased from Thermo Scientific. For the sub-cloning of the 209bp fragment which corresponds to the 18.5kDa MMP-8 catalytic subunit, forward oligomers (5'-GATGAAAAAGCCTCGCTGTG-3') and reverse oligomers (5'-CAGAGCCCAGTATTGGTTGC-3') were used as primers. The PCR reaction contained 1X PFU buffer [200mM Tris-HCl (pH=8.8 at 25 °C), 100mM (NH<sub>4</sub>)<sub>2</sub>SO<sub>4</sub>, 100mM KCl, 1% (v/v) Triton X-100, 1mg/ml BSA](5 µL), 2.5mM dNTPs (5 µL), pfu (1 µL), cDNA of MMP-8(1 µL) forward and reverse oligomers (5 µL) at 100 µM and H<sub>2</sub>O (28 µL) to a total of 50 µL. The 209bp fragment was amplified by polymerase chain reaction (PCR). After amplification the PCR product was purified by means of a QIAGEN MINElute purification kit and then digested with NdeI and XhoI restriction enzymes at the 5' and 3' end respectively, and thereafter purified by electrophoresis on agarose gel. The expression vector pET7-HMBP3 and the PCR product were digested in the following reaction: pET7-HMBP3 (7 µL), NdeI (1.5 µL), XhoI (1.5 µL), New England Biolabs (NEB) buffer 2 (5 µL) and H<sub>2</sub>O (35 µL) at 37°C, for 3 hours. The digestion was run on 1% agarose gel stained with ethidium bromide. The PCR and the pT7-HMBP3 were then cut out and purified by QIAGEN QIAQUICK Gel Extraction kit. The insert (PCR product) (5ng/µL) and the vector (10.5ng/µL) were used in ligation reactions of ratios 1:3, 1:7 and 1:10 in a T4 ligase Buffer (1 µL), containing T4 ligase (1 µL) and H<sub>2</sub>O (6 µL). The ligation reaction mixture was then transfected into TOP10F' *E.coli* competent cells by electroporation. With the 1:7 ratio ligation reactions, a subcloned pT7-HMBP3 vector containing the MMP-8 catalytic subunit was obtained. The positive colonies containing the MMP-8 catalytic subunit were grown in order to amplify the DNA necessary for protein expression. The 209bp fragment was then

subcloned into pT7TEV-HMBP3 vector (Novagen) adjacent to the maltose binding protein (MBP) under the control of a T7 promoter, where MBP is responsible for the increase of the solubility of recombinant proteins expressed in *E. coli*. MMP-8 was expressed in (DE3)-RIL arctic express *E. coli* cells as a fusion protein with MBP containing a tobacco etch virus (TEV, used for the removal of affinity tags from purified proteins) protease restriction site. The pT7TEV-HMBP3 vector containing the MMP-8 gene was then transformed in DE3 arctic express cells which were plated on kanamycin-containing lysogeny broth (LB) plates. After 24 hours, one of the colonies that grew was selected for growth in a 300mL LB culture containing 100 µg/ml of kanamycin. This pre-culture was grown overnight, and 20mL were then used to inoculate a 1.5L 2XYT medium. A total of 12 flasks (1.5L each) were grown at 37°C up to 0.8 O.D and then were induced for the protein expression with isopropyl β-D-1-thiogalactopyranoside (IPTG) and cells were grown at 14°C for 18 hours. The cells were then harvested by centrifugation and frozen at -80°C.

## **2. Nickel NTA chromatography for purification of the MBP-fusion protein**

The first purification strategy selected was to bind the MBP-MMP-8 fusion protein containing six histidine residues onto a Nickel-NTA column. This step removes most of the impurities from *E. coli* and allows the purification to continue using the isoelectric point of MMP-8. The cell pellets were resuspended in 30mL of lysis buffer (5% Glycerol, 20mM imidazole, 1M KCl, 20mM Tris-HCl, pH 7.0). In order to degrade further the cell walls, they were sonicated for 4min at 0°C. Cell debris was removed by centrifugation at 20,000rpm for 30min at 4 °C and the clear supernatant was loaded onto a Nickel-NTA (nitrilotriacetic acid) column 4mL (1.5cm x 15cm). Before loading the lysate, the Nickel column was equilibrated by 5% glycerol, 20mM imidazole and 0.5M KCl buffer. After adsorption on the column the protein was then eluted by using buffer

containing 5% glycerol, 0.5mM imidazole, 0.5M KCl, and 20 mM Tris-HCl, at pH 7.0. After the protein was eluted TEV (2.5mg) protease was added to the protein solution in order to separate MBP from the MMP-8 catalytic subunit.

### **3. Q-Sepharose for purification of the MMP-8 catalytic subunit**

After the MBP-MMP-8 fusion protein had been cleaved with TEV, the protein solution was loaded to a Q-Sepharose ion exchange column based on the isoelectric point (IP) of MMP-8 (-8.9) at pH 7.0, where the charged group of Q-Sepharose is a quarternary amine which carries a non-titratable positive charge, in order to separate the MMP-8 catalytic subunit which carries a negative charge at pH 7.0. The protein fraction was loaded onto a Q-Sepharose (1.5cm x 55cm) fast protein liquid chromatography (FPLC) column and the protein was eluted in a linear gradient by means of buffer A (5% Glycerol, 1mM DTT and 20mM Tris/HCl, pH 7.0) then buffer B (5% Glycerol, 1mM DTT and 1M KCl and 20mM Tris/HCl, pH 7.0). The purity of MMP-8 catalytic subunit was determined by 15% SDS-PAGE which gave a molecular weight as 18.5kDa. The yield of this protein expression method is only about 10%, and the purity is only 30% accordingly.

### **4. Cloning and protein expression of MMP-8 in pET-22b(+) vector**

Because the protein expression with His-tag didn't give the desired yield or purity, the recombinant protein expression without MBP was carried out. By using the same primers as before, the MMP-8 catalytic subunit was cloned into pET-22b(+) vector under the control of T7 promoter. The protein expression was accomplished in BL21(DE3) for 4 hours at 37°C after IPTG.

## **5. Protein purification of MMP-8 catalytic subunit by purification of inclusion bodies**

In order to purify the inclusion bodies pellets which contain the MMP-8 catalytic subunit and are found in the cell debris, the *E.coli* cells was resuspended in a 1.5L flask and sonicated for 4min in the following buffer: 50mM Tris/HCl (pH=8.0), 10mM DTT and 100mM NaCl. The lysate was then centrifuged and spun-down. The material that was collected, was washed by 30mL of 50mM Tris/HCl (pH=8.0), 1% Triton X-100, 100mM NaCl and 1mM DTT and then washed three times with 50mM of Tris/HCl (pH=8.0), 100mM NaCl and finally 1mM DTT. In order to denature the protein after the washing procedures, the pellets were dissolved in 50mL of 6M urea, 50mM Tris/HCl (pH=8.0), 200mM NaCl, 5mM CaCl<sub>2</sub>, 0.1mM ZnCl<sub>2</sub> and 1mM DTT and held at 37°C for 4 hours. To renature the protein, the solution was diluted to 1.5mg/mL, and then 10mL of the protein solution was dialysed for 2 days against 4L of 50mM Tris/HCl (pH=7.5), 200mM NaCl, 5mM CaCl<sub>2</sub>, 0.1mM ZnCl<sub>2</sub> and 0.005% Brij-35 buffer at 4°C. This buffer was changed twice. Refolding of the MMP-8 catalytic subunit was confirmed by Circular Dichroism (CD).

## **6. Gel Filtration Chromatography**

After the dialysis, the MMP-8 catalytic subunit was concentrated by centrifugation and loaded onto a Superdex 200 gel filtration column 16/60, pre-equilibrated with buffer of 25mM MES (pH=6.0), 100mM NaCl, 10mM CaCl<sub>2</sub>, and 0.2mM ZnCl<sub>2</sub>. The eluted fractions from the gel filtration were collected and the purity was determined by 15% SDS-PAGE and MALDI. The protein solution was concentrated to 12mg/mL for use. The yield is about 80% in total, and the purity is about 95%.

## 7. Crystallization

The purified MMP-8 catalytic subunit was crystallized by using the hanging drop method.<sup>16,17</sup> A 3-fold excess of curcumin or CMC2.24 (50mM) in DMSO was added to a solution of 12mg/mL of the protein (MMP-8 catalytic subunit) in buffer (25mM MES, 100 mM NaCl, 10mM CaCl<sub>2</sub>, 0.1mM ZnCl<sub>2</sub>, pH 6.0) to give a total volume of 4μL. The solution contained 10-25% (w/w) PEG6000 (Polyethylene Glycol with a molecular weight of 6000), and equilibrated against a 500μL reservoir solution of 1M Na<sub>2</sub>HPO<sub>4</sub>/NaH<sub>2</sub>PO<sub>4</sub> at pH 6.0 to initiate the crystallization in the protein solution. Parallel experiments were also carried out with the MMP-8 catalytic subunit without inhibitors. Needle-shaped crystals appeared in 4 days. The crystals diffracted to 1.3-2.5Å and data was collected at Beam line X25 and X29 in Brookhaven National Laboratory. Data processing was carried out using Phenix (this is a software suite for the automated determination of macromolecular structures using X-ray crystallography and other methods) and by model building by the Crystallographic Object-Oriented Toolkit (Coot) program.

## References

1. Wilson, L.J.; Bray, T.L.; Suddath, F.L. Crystallization of proteins by dynamic control of evaporation. *Journal of Crystal Growth*, 1991, *110*, 142-147
2. Smyth, M.S.; Martin, J.H. X ray crystallography. *Mol. Pathol.*, 2000, *5*, 8-14
3. Blundell, T.L.; Johnson, L.N. *Protein crystallography*. London, Academic Press, 1976
4. Luft, J. R.; Arakali, S.V.; Kirisits, M.J.; Kalenik, J.; Wawrzak, I.; Cody, V.; Pangborn, W. A.; DeTitta, G. T. A macromolecular crystallization procedure employing diffusion cells of varying depths as reservoirs to tailor the time course of equilibration in hanging- and sitting-drop vapor-diffusion and microdialysis experiments. *J. Appl. Cryst.*, 1994, *27*, 443-453

5. Weiss, S.J.; Peppin, G.; Ortiz, X.; Ragsdale, C.; Test, S.T. Oxidative autoactivation of latent collagenase by human neutrophils. *Science*, 1985, 227, 747-749
6. Prikk, K.; Maisi, P.; Pirila, E.; Sepper, R.; Salo, T.; Wahlgren, J.; Sorsa, T. In vivo collagenase-2 (MMP-8) expression by human bronchial epithelial cells and monocytes/macrophages in bronchiectasis. *J. Pathol.*, 2001, 194, 232-238
7. Balbin, M.; Fueyo, A.; Tester, A.M.; Pendas, A.M.; Pitiot, A.S.; Astudillo, A.; Overall, C.M.; Shapiro, S.D.; López-Otín, C. Loss of collagenase-2 confers increased skin tumor susceptibility to male mice. *Nat. Genet.*, 2003, 35, 252-257
8. Saari, H.; Suomalainen, K.; Lindy, O.; Kontinen, Y.T.; Sorsa, T. Activation of latent human neutrophil collagenase by reactive oxygen species and serine proteases. *Biochem. Biophys. Res. Commun.*, 1990, 171, 979-987
9. Schnierer, S.; Kleine, T.; Gote, T.; Hillemann, A.; Knauper, V.; Tschesche, H. The recombinant catalytic domain of human neutrophil collagenase lacks type I collagen substrate specificity. *Biochem. Biophys. Res. Commun.*, 1993, 191, 319-326
10. Bode, W.; Reinemer, P.; Huber, R.; Kleine, T.; Schnierer, S.; Tschesche, H. The X-ray crystal structure of the catalytic domain of human neutrophil collagenase inhibited by a substrate analogue reveals the essentials for catalysis and specificity. *EMBO J.*, 1994, 13, 1263-1269
11. Reinemer, P.; Grams, F.; Huber, R.; Kleine, T.; Schnierer, S.; Piper, M.; Tschesche, H.; Bode, W. Structural implications for the role of the N terminus in the 'superactivation' of collagenases. A crystallographic study. *FEBS Lett.*, 1994, 338, 227-233
12. Stams, T.; Spurlino, J.C.; Smith, D.L.; Wahl, R.C.; Ho, T.F.; Qoronfleh, M.W.; Banks, T.M.; Rubin, B. Structure of human neutrophil collagenase reveals large S1' specificity pocket. *Nat. Struct. Biol.*, 1994, 1, 119-123

13. Grams, F.; Crimmin, M.; Hinnes, L.; Huxley, P.; Pieper, M.; Tschesche, H.; Bode, W. Structure determination and analysis of human neutrophil collagenase complexed with a hydroxamate inhibitor. *Biochemistry*, 1995, *34*, 14012-14020
14. Grams, F.; Reinemer, P.; Powers, J.C.; Kleine, T.; Pieper, M.; Tschesche, H.; Huber, R.; Bode, W. X-ray structures of human neutrophil collagenase complexed with peptide hydroxamate and peptide thiol inhibitors. Implications for substrate binding and rational drug design. *Eur.J.Biochem.*, 1995, *228*, 830-841
15. Betz, M.; Huxley, P.; Davies, S.J.; Mushtaq, Y.; Pieper, M.; Tschesche, H.; Bode, W.; Gomis-Ruth, F.X. 1.8-A crystal structure of the catalytic domain of human neutrophil collagenase (matrix metalloproteinase-8) complexed with a peptidomimetic hydroxamate primed-side inhibitor with a distinct selectivity profile. *Eur.J.Biochem.*, 1997, *247*, 356-363
16. Brandstetter, H.; Engh, R.A.; Von Roedern, E.G.; Moroder, L.; Huber, R.; Bode, W.; Grams, F. Structure of malonic acid-based inhibitors bound to human neutrophil collagenase. A new binding mode explains apparently anomalous data. *Protein Sci.*, 1998, *7*, 1303-1309
17. Matter, H.; Schwab, W.; Barbier, D.; Billen, G.; Haase, B.; Neises, B.; Schudok, M.; Thorwart, W.; Schreuder, H.; Brachvogel, V.; Lonze, P.; Weithmann, K.U. Quantitative structure-activity relationship of human neutrophil collagenase (MMP-8) inhibitors using comparative molecular field analysis and X-ray structure analysis. *J.Med.Chem.*, 1999, *42*, 1908-1920
18. Gavuzzo, E.; Pochetti, G.; Mazza, F.; Gallina, C.; Gorini, B.; D'Alessio, S.; Pieper, M.; Tschesche, H.; Tucker, P.A. Two crystal structures of human neutrophil collagenase, one complexed with a primed- and the other with an unprimed-side inhibitor: implications for drug design. *J.Med.Chem.*, 2000, *43*, 3377-3385

19. Schroder, J.; Henke, A.; Wenzel, H.; Brandstetter, H.; Stammler, H.G.; Stammler, A.; Pfeiffer, W.D.; Tschesche, H. Structure-based design and synthesis of potent matrix metalloproteinase inhibitors derived from a 6H-1,3,4-thiadiazine scaffold. *J.Med.Chem.*, 2001, *44*, 3231-3243
20. Brandstetter, H.; Grams, F.; Glitz, D.; Lang, A.; Huber, R.; Bode, W.; Krell, H.W.; Engh, R.A. The 1.8-Å crystal structure of a matrix metalloproteinase 8-barbiturate inhibitor complex reveals a previously unobserved mechanism for collagenase substrate recognition. *J.Biol.Chem.*, 2001, *276*, 17405-17412
21. Bertini, I.; Calderone, V.; Fragai, M.; Luchinat, C.; Maletta, M.; Yeo, K.J. Snapshots of the reaction mechanism of matrix metalloproteinases. *Angew. Chem. Int. Ed.*, 2006, *45*, 7952-7955
22. Pochetti, G.; Gavuzzo, E.; Campestre, C.; Agamennone, M.; Tortorella, P.; Consalvi, V.; Gallina, C.; Hiller, O.; Tschesche, H.; Tucker, P.A.; Mazza, F. Structural insight into the stereoselective inhibition of MMP-8 by enantiomeric sulfonamide phosphonates. *J.Med.Chem.*, 2006, *49*, 923-931
23. Campestre, C.; Agamennone, M.; Tortorella, P.; Preziuso, S.; Biasone, A.; Gavuzzo, E.; Pochetti, G.; Mazza, F.; Hiller, O.; Tschesche, H.; Consalvi, V.; Gallina, C. N-Hydroxyurea as zinc binding group in matrix metalloproteinase inhibition: Mode of binding in a complex with MMP-8. *Bioorg.Med.Chem.Lett.*, 2006, *16*, 20-24
24. Golub, L.M.; Greenwald, R.A.; Ramamurthy, N.S.; McNamara, T.F.; Rifkin, B.R. Tetracyclines inhibit connective tissue breakdown: New therapeutic implications for an old family of drugs. *Crit. Revs Oral Biol. Med.*, **1991**, *2*, 297-322

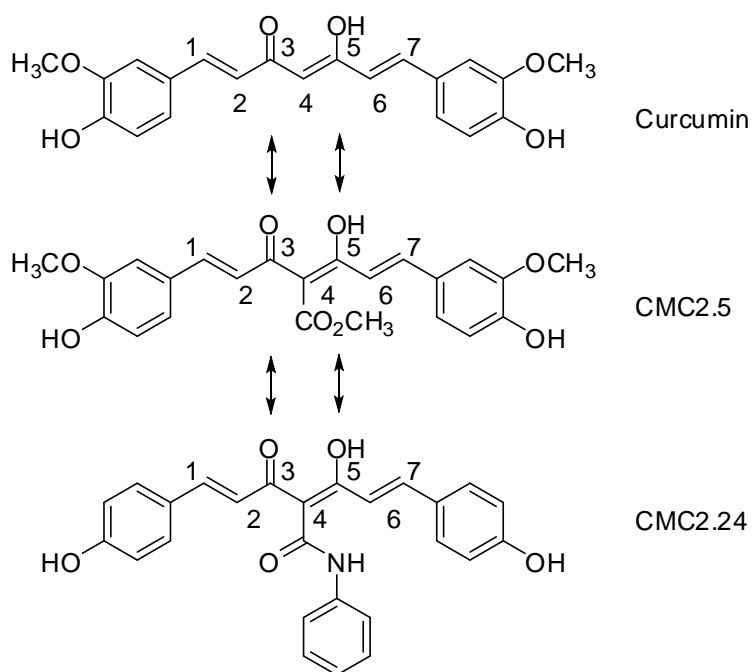


25. Makrides, S.C. Strategies for achieving high-level expression of genes in *Escherichia coli*. *Microbiol. Rev.*, 1996, 60, 512-538
26. Baneyx, F. Recombinant protein expression in *Escherichia coli*. *Current Opinion in Biotechnology*, 1999, 10, 411-421

## Chapter 8. Collateral studies and conclusion

### A. Introduction

Because several chemically-modified curcumins (CMCs) have shown excellent inhibitory activity against nine different matrix metalloproteinases, namely MMP-1, -2, -3, -7, -8, -9, -12, -13 and -14, as well as better zinc and serum albumin binding activity in contrast to curcumin in the previous chapters, both CMC2.5 and CMC2.24 were selected as lead compounds. In particular CMC2.24, the current lead compound, was evaluated for its efficacy in the reduction of chemokines and cytokines in cell culture (human peripheral blood monocytes) and tissue culture (bovine cartilage).<sup>1-7</sup> Also, curcumin and a group of CMCs were tested for their therapeutic potentials as inhibitors of inflammatory mediators (cytokines and prostaglandins) in a variety of *in vivo* disease models including osteoarthritis, periodontitis, acute respiratory disease syndrome (ARDS) and type-I diabetes. Of extreme importance, CMC2.24 is highly efficacious and non-toxic regardless as to whether it is administered systemically, by either the oral or the intraperitoneal (i.p.) route, or topically, in successful wound healing studies.<sup>7</sup>



Scheme 8.1 Structures of curcumin, CMC2.5 and CMC2.24

## B. Cell Culture Studies

CMC2.5 and CMC2.24 were found to inhibit the production of various mediators of inflammation and connective tissue destruction, induced in human monocytes either by endotoxin from *E. coli*, or by a complex of C-reactive protein (CRP) oxidized low-density lipoprotein (LDL) cholesterol from the studies carried out by Dr. Ying Gu (Department of Dentistry, Stony Brook University). These mediators include not only pro-inflammatory cytokines and mediators such as TNF- $\alpha$  (Figure 8.2a) and IL-1 $\beta$  (Figure 8.2b) but also PGE<sub>2</sub>, MCP-1 and several others (data not shown).<sup>1-4</sup> The expression of pathologically-excessive levels of MMP-2, -8 and -13 (data not shown) by monocytes in culture, was also reduced to normal levels by treatment with CMC2.24 at a low concentration. Regarding the effect on viable cells, as illustrated in Figure 8.1a and 8.1b, human peripheral blood monocytes were cultured in serum-free media with and without lipopolysaccharide (LPS). Curcumin at 2 or 5  $\mu$ M did not appear to

decrease the MMP-9 levels in the conditioned media Figure 8.1a. In contrast, when CMC2.24 was added to the culture at the same concentration either 2 or 5  $\mu\text{M}$ , the extracellular MMP-9 levels were reduced in a dose-dependent manner Figure 8.1b with a lesser effect at 2  $\mu\text{M}$ , but dramatically reduced at the 5  $\mu\text{M}$  concentration. CMC2.24 (2 and 5  $\mu\text{M}$ ) can inhibit the activities of inflammatory mediators, TNF- $\alpha$  (Figure 8.2a) and IL-1 $\beta$  (Figure 8.2b).

Figure 8.1 Illustration of the attenuating effect of curcumin and CMC2.24 on MMP-9 levels in conditioned media from human monocytes stimulated by LPS in cell culture

Note: Human peripheral mononuclear cells (PBMC) ( $5 \times 10^5$  cells/well) were cultured in serum-free media ( $37^\circ\text{C}$ , 5%  $\text{CO}_2$ ) overnight with LPS (*P. gingivalis*, 50 ng/mL) containing vehicle alone or curcumin or CMC2.24 at different concentrations (Figure 8.2a and 8.2b). Conditioned medium from both experiments were analyzed for MMP-9 levels by gelatin zymography.

Figure 8.1a The effect of curcumin on MMP-9 levels

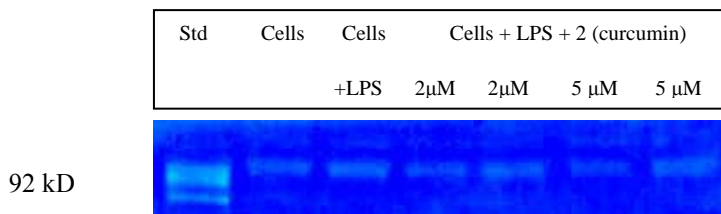


Figure 8.1b The effect of CMC2.24 on MMP-9 levels

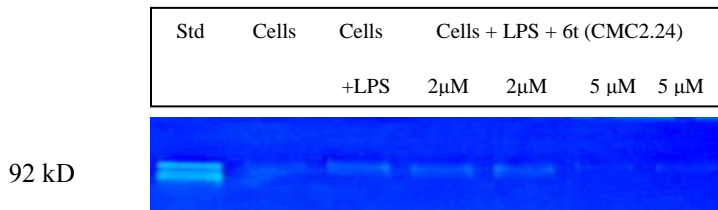


Figure 8.2 CMC2.24 (2 and 5  $\mu\text{M}$ ) inhibits the activities of inflammatory mediators (cytokine levels) TNF- $\alpha$  and IL-1 $\beta$  produced by human monocytes stimulated with *P. gingivalis* LPS (50ng/ml). Each bar represents the mean of 3 cultures  $\pm$  S.E.M.

Figure 8.2a CMC2.24 (2 and 5  $\mu\text{M}$ ) inhibits the activities of  $\text{TNF-}\alpha$

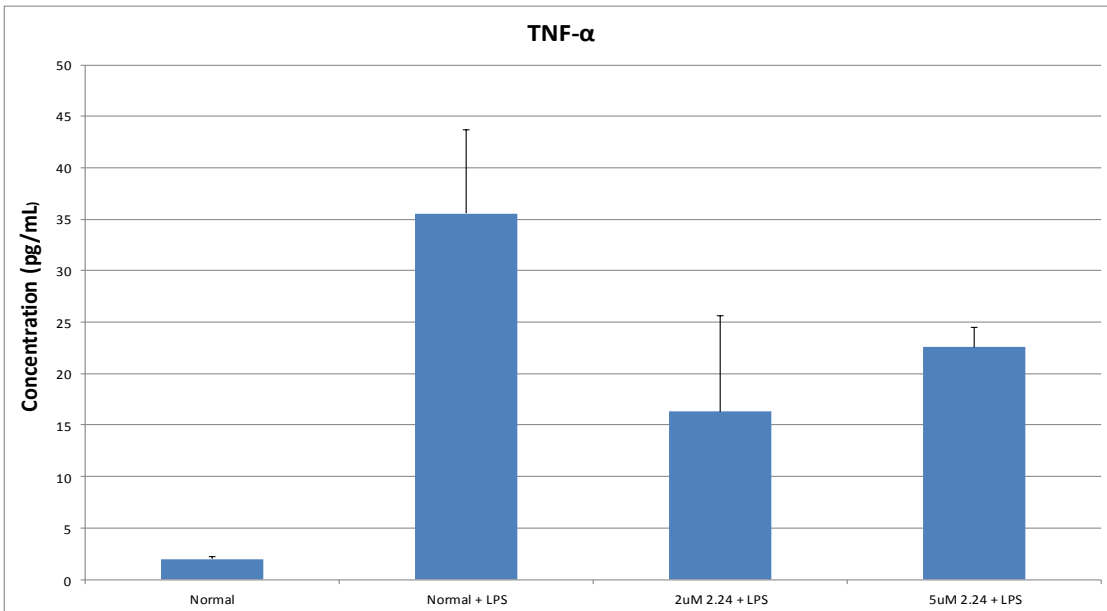
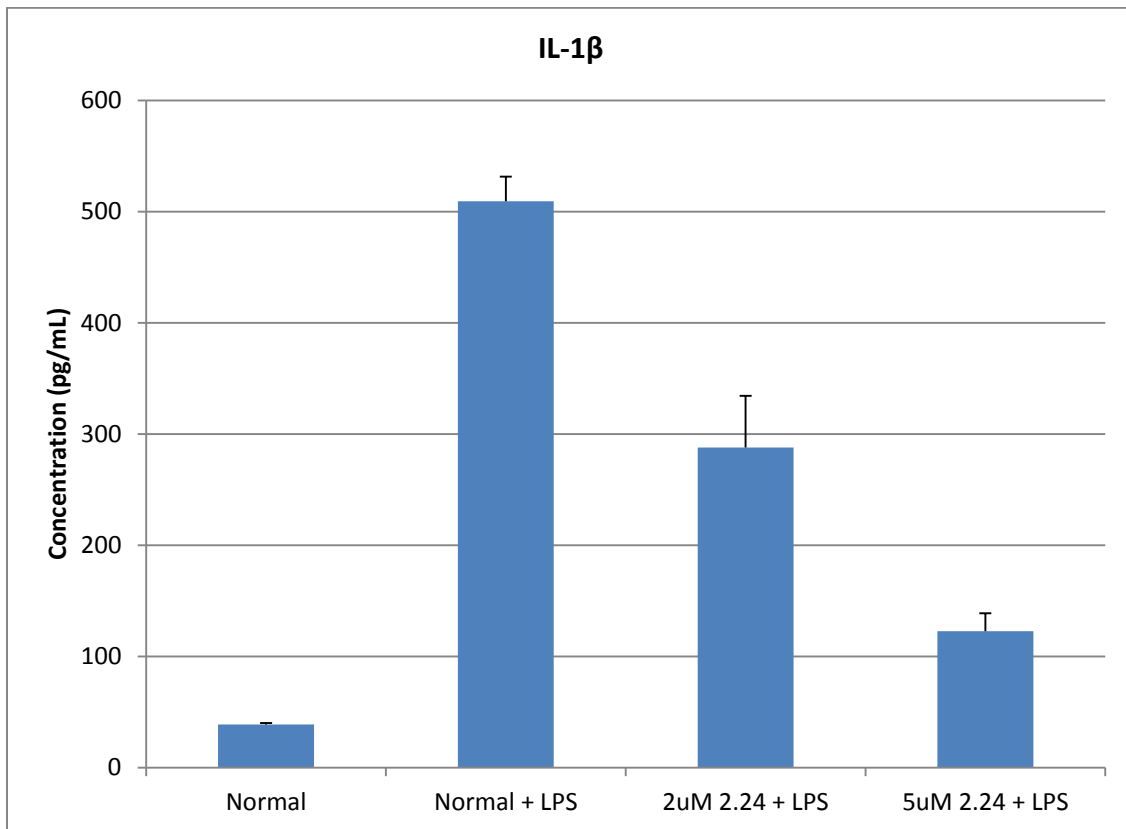


Figure 8.2b CMC2.24 (2 and 5  $\mu\text{M}$ ) inhibits the activities of  $\text{IL-1}\beta$



CMC2.23 and CMC2.24 were also studied by Dr. Balakrishna L. Lokeshwar (School of Medicine, University of Miami) in cancer cells in culture, and the result revealed that CMC2.24 was more effective in terms of inhibiting the cancer cell growth, than CMC2.23 in the study of prostate and pancreatic cancer cell lines (unpublished). (Figure 8.3)

Figure 8.3 Effect of CMC2.23 and CMC2.24 ( $\mu\text{M}$ ) against prostate (PC-3) and pancreatic (MiaPaCa) cancer cells in culture

Figure 8.3a Effect of CMC2.23 and CMC2.24 ( $\mu\text{M}$ ) against prostate (PC-3) cancer cells in culture

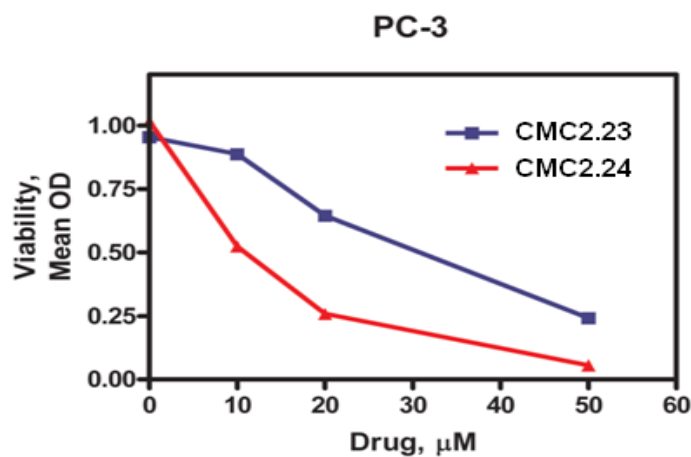
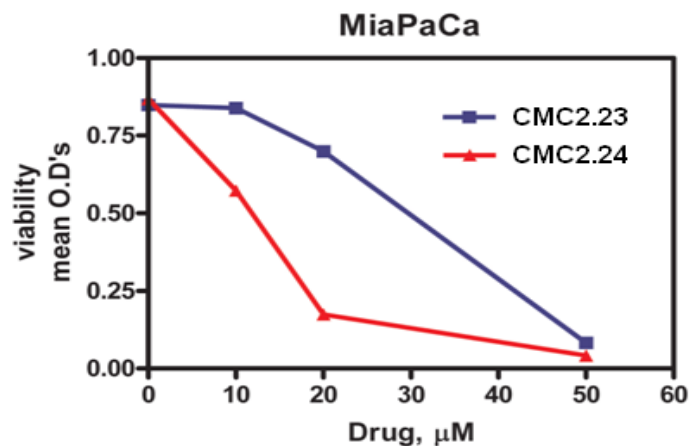


Figure 8.3b Effect of CMC2.23 and CMC2.24 ( $\mu\text{M}$ ) against pancreatic (MiaPaCa) cancer cells in culture



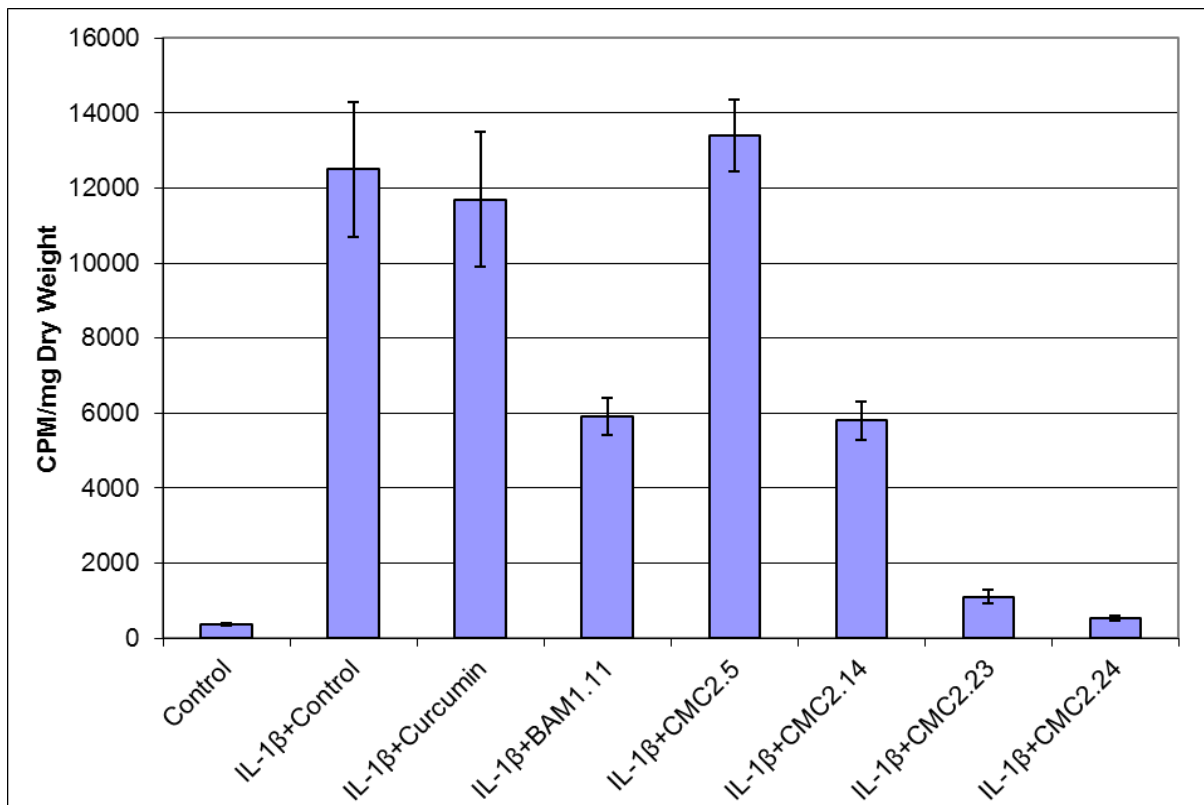
### C. Tissue Culture Studies

Osteoarthritis (OA) is considered to be the result of aging, and one of the leading causes of disability among the elder people.<sup>8,9</sup> OA is characterized by continuous degradation of articular cartilage. Once the chondrocytes (the only cells exist in healthy cartilage, that produce and maintain the cartilaginous matrix, comprising mainly of collagens and proteoglycans) are stimulated by pro-inflammatory cytokines including but not limited to interleukin-1 $\beta$  (IL-1 $\beta$ ), the release of cartilage-degrading enzymes such as MMPs will be triggered. Chondrocytes are responsible for the synthesis of proteoglycans, which are initially synthesized in endoplasmic reticulum, then go through the addition and sulfation of the glycosaminoglycan chains (within Golgi apparatus). As for the synthesis of proteoglycans, sulfation is the crucial and final step, so radioactive labeling with  $^{35}\text{SO}_4^{2-}$  has been utilized to monitor the synthesis of proteoglycan.<sup>10</sup> Dr. Daniel Grande (Department of Orthopaedic Surgery, Long Island Jewish Medical Center) reported recently that IL-1 $\beta$ -induced excessive proteoglycan ( $\text{S}^{35}$ -labeled) degradation of bovine cartilage in culture (a model for osteoarthritis) was reduced to basal/control levels by CMC2.23 and CMC2.24 but not by curcumin or CMC2.5.<sup>7</sup> In this experiment, three millimeter full-thickness bovine articular cartilage explants were trephined from femoral condyles of the knee and placed in tissue culture. Explants were labeled with  $^{35}\text{S}$  sulfate control cartilage explants (media only, negative control) demonstrated a baseline level of  $^{35}\text{S}$  sulfate release throughout the 72-hour period. IL-1 $\beta$  and Oncostatin M (OsM) -challenged explants (positive control) demonstrated high release of  $^{35}\text{S}$  compared to that of negative controls at all time-points. Curcumin derivatives, specifically CMC2.14, CMC2.23, and CMC2.24 exhibited significant chondroprotective effect, as evidenced by lower release of  $^{35}\text{S}$ . The results demonstrate improved chondroprotective effects of novel curcumin derivatives against IL-1 $\beta$  and OsM-induced

chondrolysis. This new evidence allows for speculation that these compounds may play a role in the future treatment of OA.

Figure 8.4 Analysis of  $^{35}\text{SO}_4^{2-}$  release following treatment with curcumin and CMCs (10  $\mu\text{M}$ ) after 72 Hours

Note: Three millimeter full-thickness bovine articular cartilage explants were trephined from femoral condyles of the knee and placed in tissue culture. Explants were labeled with  $^{35}\text{S}$  sulfate and separated into eight study groups: negative/positive controls, curcumin, novel derivatives labeled. Explants were challenged with IL-1 $\beta$  and OsM or with IL-1 $\beta$ , OsM and one of the derivatives.  $^{35}\text{S}$  sulfate release was evaluated at 24, 48, and 72 hours post-treatment by scintillation counting. Explants were then lyophilized to obtain dry weights (mg) and data expressed as counts per minute (CPM)/mg dry weight. Mean and standard deviation of CPM/mg for each group were used for statistical analysis using unpaired t-tests ( $\alpha = 0.05$ ).





## **D. *In Vivo* Studies.**

### **1. Type-I diabetes**

One of the leading causes of mortality for diabetic people is cardiovascular complication, characterized by the changes in vascular structure, including ECM deposition, intimal proliferation (the characteristic feature of the response of human saphenous vein to arterial implantation) and media-to-lumen ratio (the basis that the force-producing smooth muscle cells lie within the media) increase.<sup>11-13</sup> As discussed in the previous chapters, MMPs are essential in the regulation of ECM turnover. Nephropathy, the damage to kidney, is mainly due to the dysregulation of MMPs and TIMPs, characterized by collagen deposition in basement membrane.<sup>11</sup> When rats are rendered diabetic by LPS, we found that the diabetics exhibited a 4-fold increase in MMP-9 levels as estimated, from their peritoneal macrophages in cell culture, compared to the non-diabetic control rats (Figure 8.5a). However, when the diabetic rats were administered CMC2.24 (30mg/kg) orally, the pathologically-elevated levels of MMP-9 were reduced to normal levels (Figure 8.5b) despite the severely hyperglycemic state of these animals which remained unchanged (Figure 8.5c). We had previously demonstrated that either inducing diabetes with streptozotocin (STZ), or causing periodontitis locally by endotoxin injection into the gingiva, leads to an increase in the production of pro-inflammatory cytokines and MMPs. In these studies, both CMC2.5 and CMC2.24 were found to inhibit the production of pathologically-excessive levels of these inflammatory mediators and MMPs in tissue from rats that had been orally-administered these curcumin analogues (data not shown). Of particular significance, administration of CMC2.5 or CMC2.24 by the oral route in doses as high as 500mg/kg body-weight per diem, showed no evidence of toxicity in these already seriously-ill

animals. This suggests that the continuing tissue-degradation associated with diabetes, might be arrested by the use of CMC2.24 (unpublished).

Figure 8.5 Effect of CMC2.24 on levels of MMP-9 secreted by peritoneal macrophages from diabetic rats

Note: Thioglycollate-induced peritoneal macrophages derived from N, D and D rats treated with CMC2.24 daily for three weeks were isolated as described in the methods section. Cells at  $1 \times 10^6$  cells/mL were cultured in serum-free media ( $37^\circ\text{C}$ ,  $5\% \text{CO}_2/95\% \text{O}_2$ ) overnight, and conditioned media were analyzed for MMP-9 levels by gelatin zymography. **Std:** MMP standards; **N:** Non-diabetic control; **D:** Diabetic control; **D+2.24:** diabetics orally administered CMC2.24 (30mg/kg) daily for three weeks. Pro-MMP-9 has a MW of 92kD, while activated MMP-2 is 72kD (Representative zymogram is shown in Figure 8.5a). The band densities from the gelatin zymogram were measured by scanning on a laser densitometer, and image analysis was performed using Image J (Figure 8.5b). Each value represents the mean of 3 analyses  $\pm$  S.E.M. Blood glucose levels (mg/100mL) for the three groups of rats are shown in Figure 8.5c. Each value represents the mean  $\pm$  S.E.M. for 3 analyses per group.

Figure 8.5a Effect of CMC2.24 on levels of MMP-9 secreted by peritoneal macrophages from diabetic rats

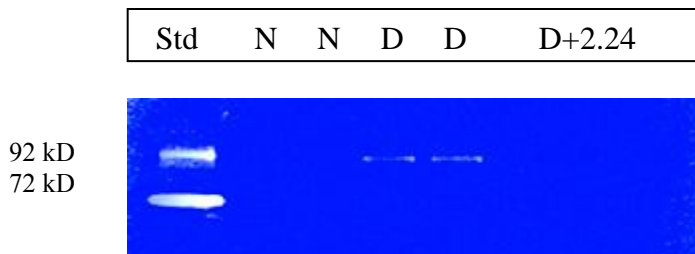


Figure 8.5b Densitometric scanning of CMC2.24 on levels of MMP-9 secreted by peritoneal macrophages from diabetic rats

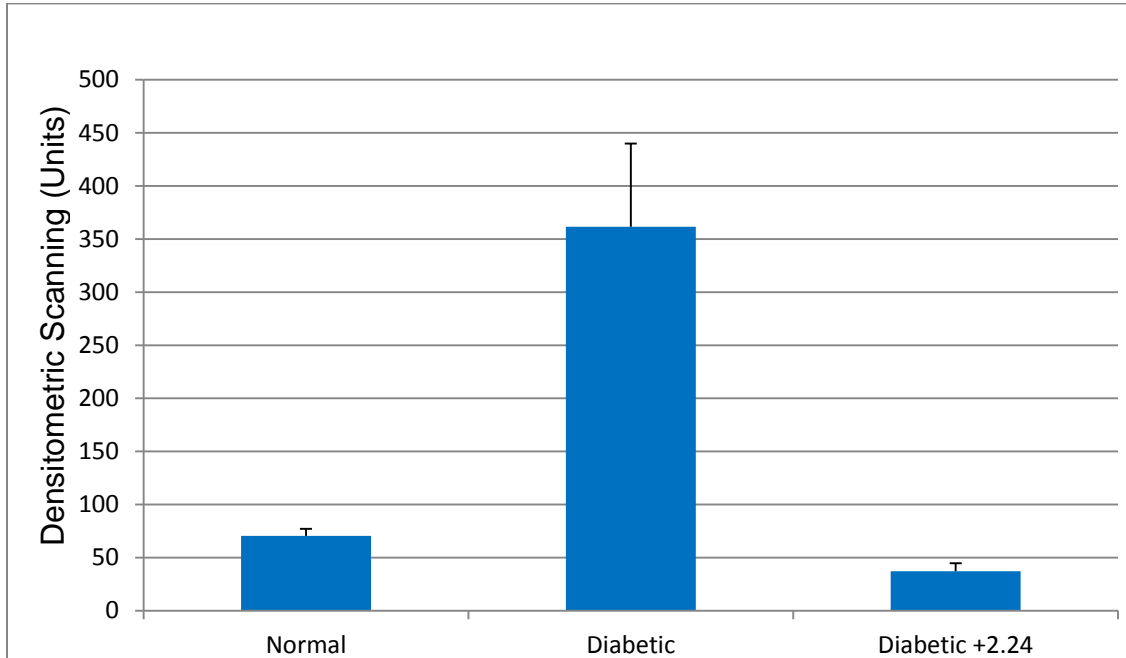
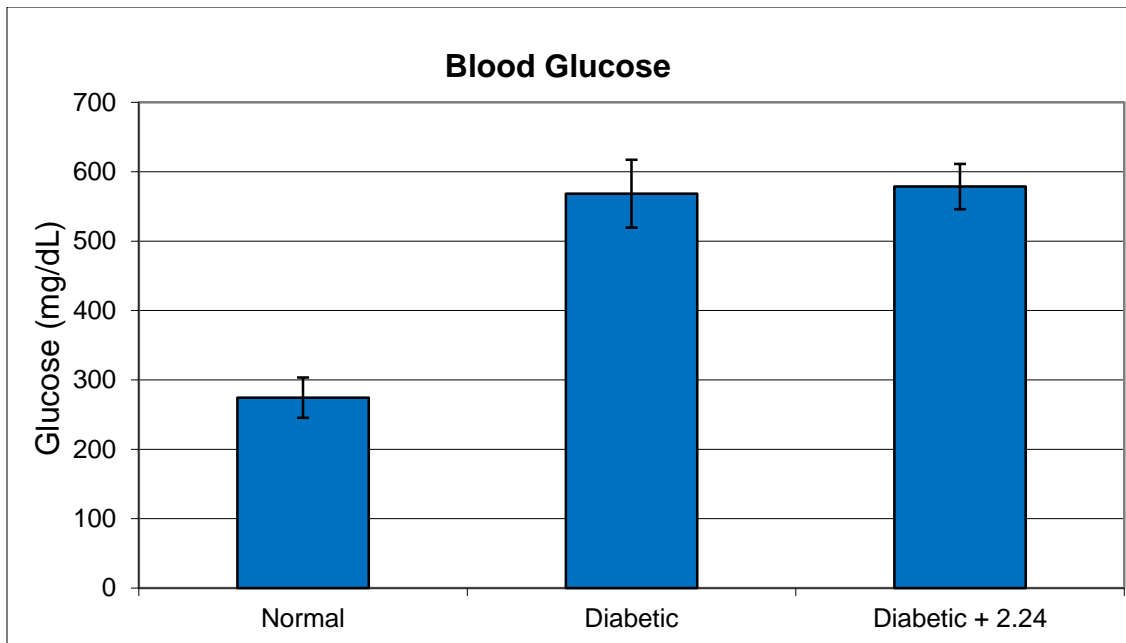


Figure 8.5c Blood glucose levels of normal and diabetic rats



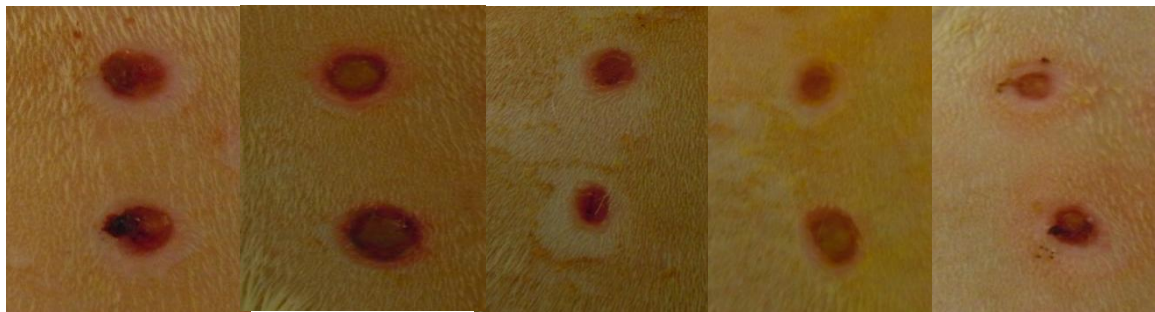


The healing cascade starts immediately with hemostasis and fibrin deposition, which release the clotting factors to prevent bleeding and generate cellular signals for the healing process. Then in the inflammatory phase, neutrophils, macrophages and lymphocytes sterilize and clear tissue debris, and then secrete additional chemokines and cytokines to promote healing. This is followed by the proliferation phase, whereas fibroblasts proliferate and synthesize collagen, producing a matrix for the injured tissue. The final stage is the remodeling phase, whereas collagen deposition and cross-linking occur to create new epithelium and seal the wound permanently. Because MMPs are responsible for the degradation of ECM, and they are secreted by various types of cells in wound healing process, they play an essential role in the regulation of wound repair.<sup>14-16</sup> In our current study, CMC2.24 was either topically (1% or 3% CMC2.24 in petrolatum jelly) or systematically (30mg/kg) administered to Type-I diabetic rats for 7 days to evaluate the efficacy on impaired wound-healing. Diabetic rats were divided to five groups: normal; diabetic; diabetic treated with 1% CMC2.24 in petrolatum jelly for topical administration; diabetic treated with 3% CMC2.24 in petrolatum jelly for topical administration; diabetic treated with 30mg/kg of CMC2.24 for oral route. The result revealed that 1% topical treatment of CMC2.24 produced the greatest improvements (about 34% reduction in healing) in healing of both the surface epithelium and the underlying connective tissue, according to the data on the biochemical and histological measurements (Figure 8.8).

Figure 8.8 Clinical appearances of wound healing studies

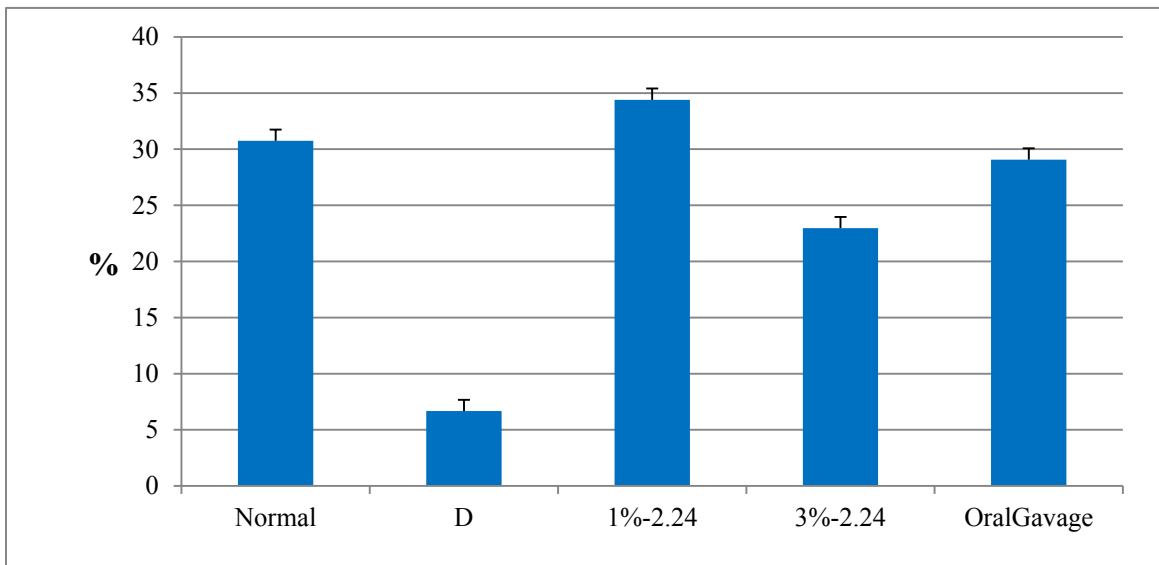
Note: Figure 8.6a Clinical appearance of standardized skin wounds in normal and diabetic rats after 7 days of healing: effect of topical and systemic administration of CMC2.24; Figure 8.6b Healing (% reduction) of skin wounds in Normal, Diabetic, and Diabetic Rats Treated with Vehicle Alone or with topical or Systemic Administration of CMC2.24.

Figure 8.8a Standardized skin wounds in normal and diabetic rats



Normal                      D                      D+1% CMC2.24                      D+3% CMC2.24                      D+CMC2.24 Oral 30mg/kg

Figure 8.8b Healing (% reduction) of skin wounds in normal, diabetic, and diabetic rats treated with vehicle alone or with topical or systemic administration of CMC2.24



### 3. Acute respiratory distress syndrome (ARDS)

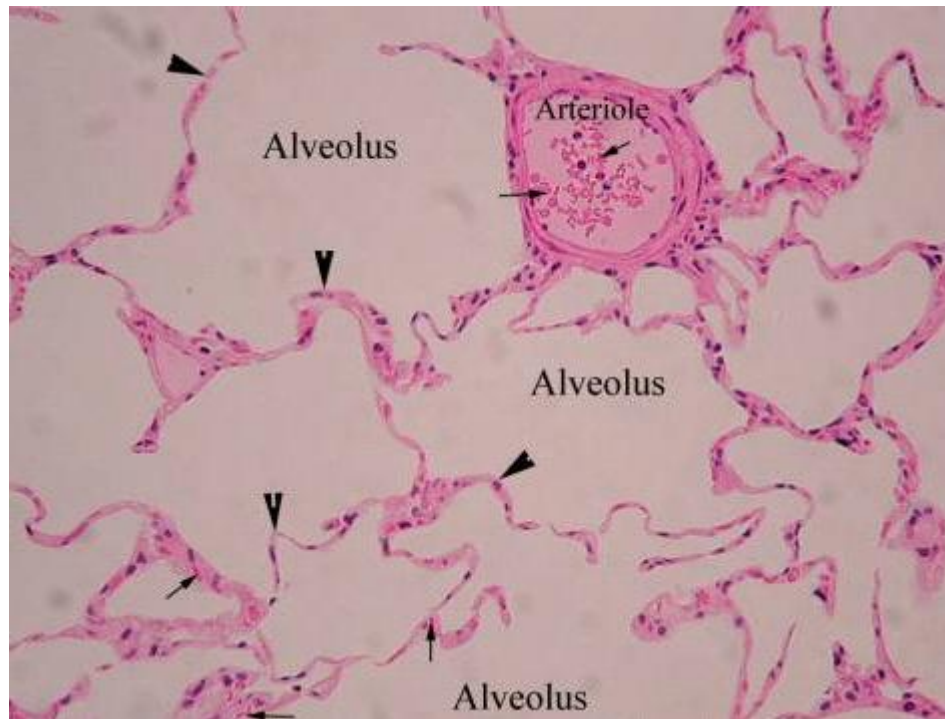


Figure 8.9 Normal lung histology

Note: There are large alveolar volumes, the septal spaces are very thin, and there is no cellular congestion.

Acute respiratory distress syndrome (ARDS) is a severe lung disease that prevents oxygen from passing into the blood thus rendering breathing difficulty. The mortality varies from 40-60%, and is caused by the accumulation of protein-loaded fluid in the alveolar spaces, which leads to a dramatic decrease in diffusing capacity and results in hypoxemia.<sup>19-20</sup> Studies have shown that sepsis, including but not limited to pneumonia, is one of the leading causes of ARDS, however other conditions such as multiple transfusions and trauma can also initiate the ARDS syndrome.<sup>21-22</sup> ARDS is generally characterized by alveolar inflammation, including thickened septal caused by protein release, congestion and decreased alveolar volume, while in the normal lung, septal spaces are very thin, and show no cellular congestion. A preliminary study

(unpublished) by Dr. Lucille London (Department of Oral Biology and Pathology, Stony Brook University) has been carried out by using a mouse model of ARDS. The condition is induced by reovirus, and the *in vivo* model was used to study the efficacy of curcumin, CMC2.5 and CMC2.24 in preventing the progression of the disease. The results revealed that 2% CMC2.24 in carboxymethyl cellulose administered 40mg/kg body-weight per diem over 19 days by the intraperitoneal route was able to completely suppress the lung inflammation and prevent the lung tissue destruction (Day 14). However, it did not suppress the initial inflammatory response in the lungs (Day 9) as can be seen from Figure 8.10, the alveolar space is large and clear. Fibrosis is not observed in Day 14 with the treatment of CMC2.24. When tested, CMC2.5 was proved to be less effective in this mouse model compared to CMC2.24. Curcumin was also able to suppress both the lung fibrosis and inflammatory response (Day 9 and Day 14).

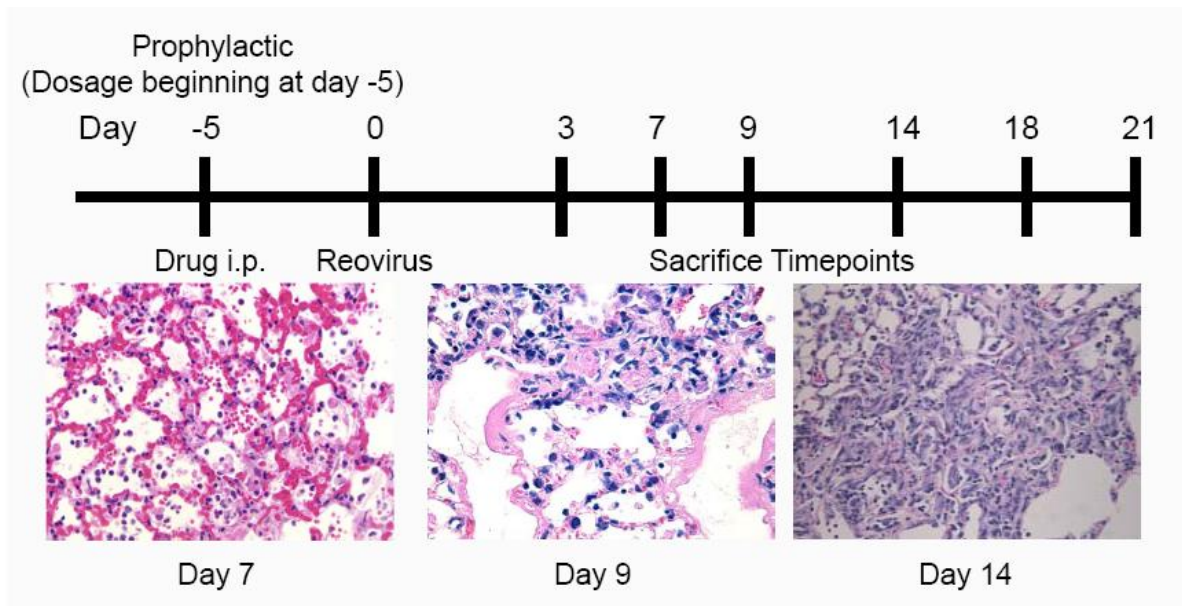


Figure 8.10 Histology of lung tissue in the mouse model of ARDS



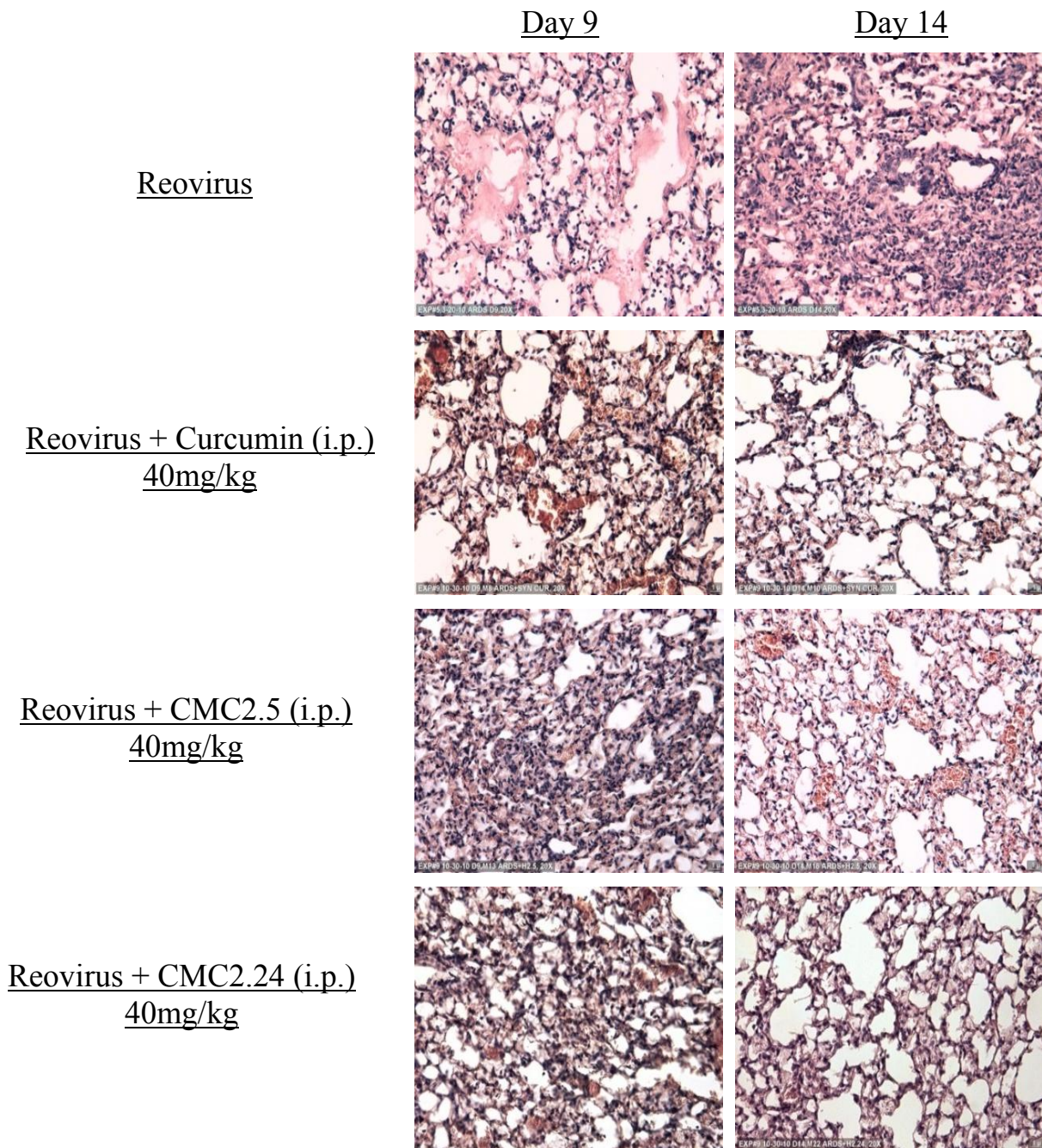


Figure 8.11 ARDS treatment with curcumin, CMC2.5 and CMC2.24

Note: All three compounds were administered to the mice 5 days ahead of the induction of reovirus. Lung tissues were obtained at Day 9 and Day 14. The group induced by reovirus without treatment of any compound was used as a control.

## E. Conclusion

In general, curcumin and chemically-modified curcumins required for the structure-activity relationship (SAR) studies were synthesized by a modified Pabon reaction. The synthetic route is shown in Chapter 3, and a series of the fully characterized compounds are documented. MMP inhibition assays were then carried out for pre-selected compounds with MMPs -1, -2, -3, -7, -8, -9, -12, -13 and -14. CMC2.24, the current lead compound, exhibited inhibitory  $IC_{50}$  values *in vitro*, ranging from 2-8 $\mu$ M against two collagenases (MMPs-8, -13), two gelatinases (MMPs-2, -9), and MMPs- 3, -7 and -12. In addition, the membrane-type MMP, MMP-14, was also effectively inhibited more by CMC2.24 ( $IC_{50}$ =15.3  $\mu$ M) than by the other known MMP inhibitors such as 1,10-phenanthroline ( $IC_{50}$ =43.8  $\mu$ M) and curcumin ( $IC_{50}$ =29.5  $\mu$ M). These MMPs are significantly up-regulated during a variety of tissue-destructive diseases such as (but certainly not limited to) arthritis, cardiovascular disease, periodontal disease, and cancer. In contrast, MMP-1 is often considered constitutive due, in part, to its involvement in the degradation of the triple-helical collagen molecule during physiological connective-tissue turnover. This collagenase requires much higher concentrations of CMC2.24 to inhibit its activity ( $IC_{50}$ =69.8  $\mu$ M). As illustrated in Figure 8.1, human peripheral blood monocytes were cultured in serum-free media and stimulated by lipopolysaccharide (LPS). Curcumin at 2 or 5  $\mu$ M did not appear to decrease the MMP-9 levels in the conditioned media (Figure 8.1a). In contrast, when CMC2.24 was added to the culture at a final concentration of 2 or 5  $\mu$ M, the extracellular MMP-9 levels were reduced in a dose-dependent manner (Figure 8.1b) and dramatically so at the 5  $\mu$ M concentration. When rats were rendered severely diabetic, we found that they exhibited a 4-fold increase in MMP-9 levels (Figure 8.2) produced by peritoneal macrophages in cell culture, compared to the non-diabetic control rats; These rats when administered CMC2.24 (30mg/kg

body weight) show normal levels of MMP-9 despite the severely hyperglycemic state of these animals. A significant number of CMCs are, in general, much more active than curcumin and do not share the latter's insolubility characteristics. Significantly, these CMCs appear to have the ability to reduce the pathological levels of only the inducible and not the constitutive MMPs to essentially normal homeostatic levels, which may be one of the reasons that these substances show little or no demonstrable toxicity at oral doses as high as 500mg/kg body-weight per diem. We have found that these compounds have no antibiotic or photosensitizing properties (similar to curcumin), and we are currently studying the potential of these compounds to control diseases of tissue loss/breakdown, especially those associated with aging, inflammation and cancer. Future studies will focus on the larger animals (e.g., pigs, dogs) to determine the toxicity and pharmacokinetic characteristics of chemically-modified curcumins in preparation for an Investigational New Drug (IND) application to the FDA.

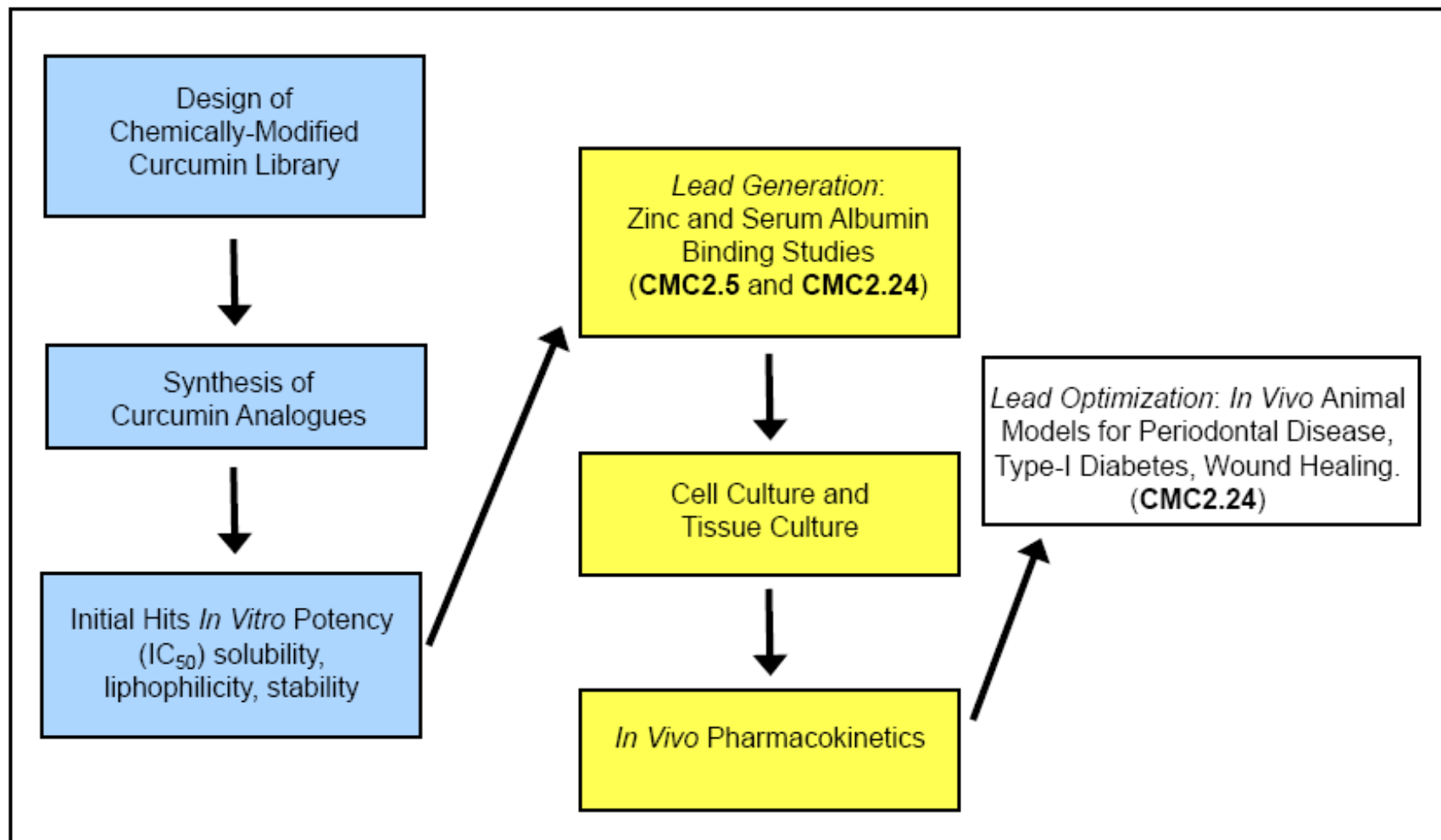


Figure 8.12 Pre-clinical developments of novel curcumin analogues as inhibitors of MMPs

## References

1. Clemens M.; Kang, D.; Napolitano, N.; Lee, H.M.; Golub, L.M.; Gu, Y. LPS or CRP/oxLDL Cholesterol-Complex: Temporal Study of Cytokine/MMP Production. *J. Dent. Res.* **2011**, *90*, Special Issue 2284
2. Napolitano, N.; Kang, D.; Clemens, M.; Lee, H.M.; Johnson, F.; Golub, L.M.; Gu, Y. Chemically Modified Curcumins Suppress Human Mononuclear Cell Cytokines. *J. Dent. Res.* **2011**, *90*, Special Issue 2292
3. Clemens, M.; Napolitano, N.; Lee, H.M.; Zhang, Y.; Johnson, F.; Golub, L.M.; Gu, Y. Chemically modified Curcumin Normalizes Chronic Inflammation in Diabetic Rats. *J. Dent. Res.* **2012**, *91*, Special Issue 1526
4. Napolitano, N.; Clemens, M.; Lee, H.M.; Zhang, Y.; Johnson, F.; Golub, L.M.; Gu, Y. Novel Curcumin Derivatives Suppress Inflammatory Mediators in Periodontally-relevant Cells. *J. Dent. Res.* **2012**, *91*, Special Issue 1527
5. Elburki, M.; Lee, H.M.; Gupta, N.; Balacky, P.; Zhang, Y.; Johnson, F.; Zhang, Y.; Golub, L.M. Chemically-Modified Curcumins Inhibit Alveolar Bone Loss in Diabetic Rats with Periodontitis. *J. Dent. Res.* **2012**, *91*, Special Issue 1528
6. Yu, H.W.; Zhang, Y.; Zhang, Y.; Lee, H.M.; McClain, S.A.; Johnson, F.; Golub, L.M.. A Novel Chemically-modified Curcumin (CMC2.24) Improves Diabetic Wound-Healing. *J. Dent. Res.* **2012**, *91*, Special Issue 1529
7. Katzap, E.; Goldstein, M.J.; Shah, N.V.; Schwartz, J.; Razzano, P.; Golub, L.M.; Johnson, F.; Greenwald, R.; Grande, D. The chondroprotective capability of curcumin (*curcuma longa*) and its derivatives against IL-1 $\beta$  and OsM-mediated chondrolysis. *Trans. Orthoped. Res. Soc.*,

2011, 36

8. Wang, M.; Shen, J.; Jin, H.; Im, H.J.; Sandy, J.; Chen, D. Recent progress in understanding molecular mechanisms of cartilage degeneration during osteoarthritis. *Ann. NY Acad. Sci.*, **2011**, *1240*, 61-69
9. Chun, J.S.; Oh, H.; Yang, S.; Park, M. Wnt signaling in cartilage development and degeneration. *BMB. Rep.*, **2008**, *41*, 485-494
10. Todhunter, R.J.; Fubini, S.L.; Wooton, J.A.; Lust, G. Effect of methylprednisolone acetate on proteoglycan and collagen metabolism of articular cartilage explants. *J. Rheumatol.*, **1996**, *23*, 1207-1213
11. Bangstad, H.J.; Osterby, R.; Rudberg, S.; Hartmann, A.; Brabrand, K.; Hanssen, K.F. Kidney function and glomerulopathy over 8 years in young patients with Type I (insulin-dependent) diabetes mellitus and microalbuminuria. *Diabetologia*, **2002**, *45*, 253-261
12. Osterby, R.; Hartmann, A.; Bangstad, H.J. Structural changes in renal arterioles in Type I diabetic patients. *Diabetologia*, **2002**, *45*, 542-549
13. Bangstad, H.J.; Osterby, R.; Dahl-Jorgensen, K.; Berg, K.J.; Hartmann, A.; Hanssen, K.F. Improvement of blood glucose control in IDDM patients retards the progression of morphological changes in early diabetic nephropathy. *Diabetologia*, **1994**, *37*, 483-490
14. Yin, J.; Yu, F.S. ERK1/2 mediate wounding- and G-proteincoupled receptor ligands-induced EGFR activation via regulating ADAM17 and HB-EGF shedding. *Invest. Ophthalmol. Vis. Sci.*, **2009**, *50*, 132-139
15. Chin, G.A.; Thigpin, T.G.; Perrin, K.J.; Moldawer, L.L.; Schultz, G.S. Treatment of chronic ulcers in diabetic patients with a topical metalloproteinase inhibitor, doxycycline. *Wounds*, **2003**, *15*, 315-323

16. Gill, S.E.; Parks, W.C. Metalloproteinases and their inhibitors: regulators of wound healing. *Int. J. Biochem. Cell Biol.*, **2008**, *40*, 1334-1347
17. Brew, K.; Kinakarandian, J.; Nagase, H. Tissue inhibitors of metalloproteinases: evolution, structure and function. *Biochim. Biophys. Acta.*, **2000**, *1477*, 267-283
18. McCulloch, J. Physical modalities in wound management: ultrasound, vasopneumatic devices and hydrotherapy. *Ostomy. Wound Manage*, **1995**, *41*, 32-37
19. Ware, L.B.; Matthay, M.A. The acute respiratory distress syndrome. *N. Engl. J. Med.*, **2000**, *342*, 1334-1349
20. Idell, S. Endothelium and disordered fibrin turnover in the injured lung: newly recognized pathways. *Crit. Care Med.*, **2002**, *30*, S274-S280
21. Johnson, M.D.; Widdicombe, J.H.; Allen, L.; Barbry, P.; Dobbs, L.G. Alveolar epithelial type I cells contain transport proteins and transport sodium, supporting an active role for type I cells in regulation of lung liquid homeostasis. *Proc. Natl. Acad. Sci. USA*, **2002**, *99*, 1966-1971
22. Dobbs, L.G.; Gonzalez, R.; Matthay, M.A.; Carter, E.P.; Allen, L.; Verkman, A.S. Highly water-permeable type I alveolar epithelial cells confer high water permeability between the airspace and vasculature in rat lung. *Proc. Natl. Acad. Sci. USA*, **1998**, *95*, 2991-2996

## Bibliography

- Aggarwal, B.B.; Kumar, A.; Bharti, A.C. Anticancer potential of curcumin: preclinical and clinical studies. *Anticancer Res.*, **2003**, *23*, 363-398
- Alberts, B.; Johnson, A.; Lewis, J.; Raff, M.; Roberts, K.; Walter, P. Molecular biology of the cell. **2002**, fourth edition, Garland Science, 1103-1105
- Allan, J.A.; Docherty, A.J.; Barker, P.J.; Huskisson, N.S.; Reynolds, J.J.; Murphy, G. Binding of gelatinases A and B to type-I collagen and other matrix components. *Biochem. J.*, **1995**, *309*, 299-306
- Amălinei, C.; Căruntu, I.D.; Giușcă, S.E.; Bălan, R.A. Matrix metalloproteinases involvement in pathologic conditions. Romanian Journal of Morphology and *Embryology*, **2010**, *51*, 215-228
- Anana-Apte, B.; Bao, L.; Smith, R.; Iwata, K.; Olsen, b.R.; Zetter, B. Apte, S.S. A review of tissue inhibitor of metalloproteinases-3 (TIMP-3) and experimental analysis of its effect on primary tumor growth. *Biochem. Cell Biol.*, **1996**, *74*, 853-862
- Anand, P.; Kunnumakkara, A.B.; Newman, R.A.; Aggarwal, B.B. Bioavailability of curcumin: problems and promises. *Mol. Pharm.*, **2007**, *4*, 807-818
- Bachmeier, B.E.; Mohrenz, I.V.; Mirisola, V.; Schleicher, E.; Romeo, F.; H öhneke, C.; Jochum, M.; Nerlich, A.G.; Pfeffer, U. Curcumin downregulates the inflammatory cytokines CXCL1 and -2 in breast cancer cells via NFκB. *Carcinogenesis*, **2008**, *29*, 779-789
- Balbin, M.; Fueyo, A.; Tester, A.M.; Pendas, A.M.; Pitiot, A.S.; Astudillo, A.; Overall, C.M.; Shapiro, S.D.; López-Ot ń, C. Loss of collagenase-2 confers increased skin



tumor susceptibility to male mice. *Nat. Genet.*, **2003**, *35*, 252-257

Baldwin, A.S. Control of oncogenesis and cancer therapy resistance by the transcription factor NFkappaB. *J. Clin. Invest.*, **2001**, *107*, 241-246

Banerji, A.; Chakrabarti, J.; Mitra, A.; Chatterjee, A. Effect of curcumin on gelatinase A (MMP-2) activity in B16F10 melanoma cells. *Cancer Lett.*, **2004**, *211*, 235-242

Baneyx, F. Recombinant protein expression in *Escherichia coli*. *Current Opinion in Biotechnology*, 1999, *10*, 411-421

Banfi, L.; Basso, A.; Bevilacqua, E.; Gandolfo, V.; Giannini, G.; Guanti, G.; Musso, L.; Paravidino, M.; Riva, R. Synthesis and DNA-cleaving activity of lactenediynes conjugated with DNA-complexing moieties. *Bioorg. Med. Chem.*, **2008**, *16*, 3501-3518

Bangstad, H.J.; Osterby, R.; Dahl-Jorgensen, K.; Berg, K.J.; Hartmann, A.; Hanssen, K.F. Improvement of blood glucose control in IDDM patients retards the progression of morphological changes in early diabetic nephropathy. *Diabetologia*, **1994**, *37*, 483-490

Bangstad, H.J.; Osterby, R.; Rudberg, S.; Hartmann, A.; Brabrand, K.; Hanssen, K.F. Kidney function and glomerulopathy over 8 years in young patients with Type I (insulin-dependent) diabetes mellitus and microalbuminuria. *Diabetologia*, **2002**, *45*, 253-261

Banji, D.; Pinnapureddy, J.; Banji, O.J.; Kumar, A.R.; Reddy, K.N. Evaluation of the concomitant use of methotrexate and curcumin on Freund's complete adjuvant-induced arthritis and hematological indices in rats. *Indian J. Pharmacol.*, **2011**, *43*, 546-550

Bartlett, J.D.; Ryu, O.H.; Xue, J.; Simmer, J.P.; Margolis, H.C. Enamelysin mRNA displays a developmentally defined pattern of expression and encodes a protein which

degrades amelogenin. *Connect. Tissue Res.*, **1998**, *39*, 101-109

Bauer, E.A.; Stricklin, G.P.; Jeffraey, J.J.; Eisen, A.Z. Collagenase production by human skin fibroblasts. *Biochem. Biophys. Res. Commun.*, **1975**, *64*, 232-240

Baum L.; Ng, A. Curcumin interaction with copper and iron suggests one possible mechanism of action in Alzheimer's disease animal models. *J. Alzheimers Dis.*, **2004**, *6*, 367-377

Begum, A.N. Jones, M.R.; Lim, G.P.; Morihara, T.; Kim, P.; Heath, D.D.; Rock, C.L.; Pruitt, M.A.; Yang F.; Hudspeth, B.; Hu, S.; Faull, K.F.; Teter, B.; Cole, G.M.; Frautschy, S.A. Curcumin structure-function, bioavailability, and efficacy in models of neuroinflammation and Alzheimer's disease. *J. Pharmacol. Exp. Ther.*, **2008**, *326*, 196-208

BernabéPineda, M.; Ramirez-Silva, M.T.; Romero-Romob, M.; González-Vergara, E.; Rojas-Hernández, A. Determination of acidity constants of curcumin in aqueous solution and apparent rate constant of its decomposition. *Spectrochimica Acta Part A*, **2004**, *60*, 1091-1097

Bertini, I.; Calderone, V.; Fragai, M.; Luchinat, C.; Maletta, M.; Yeo, K.J. Snapshots of the reaction mechanism of matrix metalloproteinases. *Angew. Chem. Int. Ed.*, 2006, *45*, 7952-7955

Betz, M.; Huxley, P.; Davies, S.J.; Mushtaq, Y.; Pieper, M.; Tschesche, H.; Bode, W.; Gomis-Ruth, F.X. 1.8-A crystal structure of the catalytic domain of human neutrophil collagenase (matrix metalloproteinase-8) complexed with a peptidomimetic hydroxamate primed-side inhibitor with a distinct selectivity profile. *Eur.J.Biochem.*,

1997, 247, 356-363

Bingham, S.J.; Tyman, J.H.P. Improved synthesis of alkyl diacetylacetates. *Organic Preparations and Procedures INT.*, **2001**, 33, 357-409

Birkedal-Hansen, H.; Moore, W.G.; Bodden, M.K.; Windsor, L.J.; Birkedal-Hansen, B.; DeCarlo, A.; Engler, J.A. Matrix metalloproteinases: a review. *Crit. Rev. Oral. Biol. Med.*, **1993**, 4, 197-250

Bjorklund, M.; Koivunen, E. Gelatinase-mediated migration and invasion of cancer cells. *Biochim. Biophys. Acta.*, **2005**, 25, 37-69

Blenis, J.; Hawkes, S.P. Transformation-sensitive protein associated with the cell substratum of chicken embryo fibroblasts. *Proc. Natl. Acad. Sci. USA*, **1983**, 80, 770-774

Blundell, T.L.; Johnson, L.N. *Protein crystallography*. London, Academic Press, 1976

Bode, W.; Gomis-Rüth, F.X.; Stöckler, W. Astacins, serralytins, snake venom and matrix metalloproteinases exhibit identical zinc-binding environments

(HEXXHXXGXXH and Met-turn) and topologies and should be grouped into a common family, the 'metzincins'. *FEBS Lett.*, **1993**, 27, 134-140

Bode, W.; Reinemer, P.; Huber, R.; Kleine, T.; Schnierer, S.; Tschesche, H. The X-ray crystal structure of the catalytic domain of human neutrophil collagenase inhibited by a substrate analogue reveals the essentials for catalysis and specificity. *EMBO J.*, 1994, 13, 1263-1269

Bourassa, P.; Kanakis, C.D.; Tarantilis, P.; Pollissiou, M.G.; Tajmir-Riahi, H.A.

Resveratrol, Genistein, and Curcumin Bind Bovine Serum Albumin. *J. Phys. Chem. B*,

**2010**, *114*, 3348-3354

Brandstetter, H.; Engh, R.A.; Von Roedern, E.G.; Moroder, L.; Huber, R.; Bode, W.; Grams, F. Structure of malonic acid-based inhibitors bound to human neutrophil collagenase. A new binding mode explains apparently anomalous data. *Protein Sci.*, 1998, *7*, 1303-1309

Brandstetter, H.; Grams, F.; Glitz, D.; Lang, A.; Huber, R.; Bode, W.; Krell, H.W.; Engh, R.A. The 1.8-Å crystal structure of a matrix metalloproteinase 8-barbiturate inhibitor complex reveals a previously unobserved mechanism for collagenase substrate recognition. *J.Biol.Chem.*, 2001, *276*, 17405-17412

Brew, K.; Kinakarpandian, J.; Nagase, H. Tissue inhibitors of metalloproteinases: evolution, structure and function. *Biochim. Biophys. Acta.*, **2000**, *1477*, 267-283

Brown, B.; Lindberg, K.; Reing, J.; Stolz, D.B.; Badylak, S.F. The Basement Membrane Component of Biologic Scaffolds Derived from Extracellular Matrix. *Tissue Engineering*, **2006**, *12*, 519-526

Brown, P.D. Matrix metalloproteinase inhibitors. *Angiogenesis*, **1998**, *1*, 142-154

Brown, P.D.; Davidson, A.H.; Drummond, A.H.; Gearing, A.; Whittaker, M. Hydroxamic acid matrix metalloproteinase inhibitors. Matrix metalloproteinases in cancer therapy. HUMANA PRESS. **2001**, 113-142

Brown, P.D.; Giavazzi, R. Matrix metalloproteinase inhibition: a review of anti-tumour activity. *Ann. Oncol.*, **1995**, *6*, 967-974

Buechi, G.; Wuest, H. Synthetic Studies on Damascenones. *Helvetica Chimica Acta*, **1971**, *54*, 1767-1775

Caesar, I.; Jonson, M.; Nilsson, K.P.; Thor, S.; Hammarström, P. Curcumin promotes A-beta fibrillation and reduces neurotoxicity in transgenic *Drosophila*. *PLoS One*, **2012**, *7*, e31424

Campestre, C.; Agamennone, M.; Tortorella, P.; Preziuso, S.; Biasone, A.; Gavuzzo, E.; Pochetti, G.; Mazza, F.; Hiller, O.; Tschesche, H.; Consalvi, V.; Gallina, C. N-Hydroxyurea as zinc binding group in matrix metalloproteinase inhibition: Mode of binding in a complex with MMP-8. *Bioorg.Med.Chem.Lett.*, 2006, *16*, 20-24

Caputi, M.; Groeger, A.M.; Esposito, V.; Dean, C.; De Luca, A.; Pacilio, C.; Muller, M.R.; Giordano, G.G.; Baldi, F.; Wolner, E.; Giordano, A. Prognostic role of cyclin D1 in lung cancer: relationship to proliferating cell nuclear antigen. *Am. J. Respir. Cell Mol. Biol.*, **1999**, *20*, 746-750

Caraveri, R.; Coronelli, C.; Pagani, H.; Sensi, P. Thermorubin, a new antibiotic from a thermoactinomycete. *Clin. Med.*, **1964**, *71*, 511-521

Carter, D. C.; Ho, J. X. Adv. Structure of serum albumin. *Protein Chem.*, **1994**, *45*, 153-203

Cavalleri, B.; Turconi, M.; Pallanza, R. Synthesis and antibacterial activity of some derivatives of the antibiotic thermorubin. *J. Antibiot. (Tokyo)*, **1985**, *38*, 1752-1760

Chen, S.Y.; Chen, Y.; Li, Y.P.; Chen, S.H.; Tan, J.H.; Ou, T.M.; Gu, L.Q.; Huang, Z.S. Design, synthesis, and biological evaluation of curcumin analogues as multifunctional agents for the treatment of Alzheimer's disease. *Bioorg. Med. Chem.*, **2011**, *19*, 5596-5604

Cheng, A.L.; Hsu, C.H.; Lin, J.K.; Hsu, M.M.; Ho, Y.F.; Shen, T.S.; Ko, J.Y.; Lin, J.T.;

Lin, B.R.; Ming-Shiang, W.; Yu, H.S.; Jee, S.H.; Chen, G.S.; Chen, T.M.; Chen, C.A.;  
Lai, M.K.; Pu, Y.S.; Pan, M.H.; Wang, Y.J.; Tsai, C.C.; Hsieh, C.Y. Phase I clinical  
trial of curcumin, a chemopreventive agent, in patients with high-risk or pre-malignant  
lesions. *Anticancer Res.*, **2001**, *21*, 2895-2900

Chin, G.A.; Thigpin, T.G.; Perrin, K.J.; Moldawer, L.L.; Schultz, G.S. Treatment of  
chronic ulcers in diabetic patients with a topical metalloproteinase inhibitor,  
doxycycline. *Wounds*, **2003**, *15*, 315-323

Chin, J.R.; Murphy, G.; Werb, Z. Stromelysin, a connective tissue-degrading  
metalloendopeptidases secreted by stimulated rabbit synovial fibroblasts in parallel  
with collagenase. Biosynthesis, isolation, characterization, and substrates. *J. Biol.*  
*Chem.*, **1985**, *260*, 12367-12376

Chun, J.S.; Oh, H.; Yang, S.; Park, M. Wnt signaling in cartilage development and  
degeneration. *BMB. Rep.*, **2008**, *41*, 485-494

Clemens, M.; Kang, D.; Napolitano, N.; Lee, H.M.; Golub, L.M.; Gu, Y. LPS or  
CRP/oxLDL Cholesterol-Complex: Temporal Study of Cytokine/MMP Production. *J.*  
*Dent. Res.*, **2011**, *90*, Special Issue 2284

Clemens, M.; Napolitano, N.; Lee, H.M.; Zhang, Y.; Johnson, F.; Golub, L.M.; Gu, Y.  
Chemically modified Curcumin Normalizes Chronic Inflammation in Diabetic Rats. *J.*  
*Dent. Res.*, **2012**, *91*, Special Issue 1526

Coon, J.S.; Knudson, W.; Clodfelter, K.; Lu, B.; Weinstein, R.S. Solutol HS 15,  
nontoxic polyoxyethylene esters of 12-hydroxystearic acid, reverses multidrug  
resistance. *Cancer Res.*, **1991**, *51*, 897-902

Coussens, L.M.; Fingleton, B.; Matrisian, L. M. Matrix metalloproteinase inhibitors and cancer: trials and tribulations. *Science*, **2002**, *295*, 2387-2392

Coussens, L.M.; Werb, Z. Matrix metalloproteinases and the development of cancer. *Chem. Biol.*, **1996**, *3*, 895-904

Curry, T.E.; Osteen, K.G. The matrix metalloproteinases system: changes, regulations, and impact throughout the ovarian and uterine reproductive cycle. *Endocr. Rev.*, **2003**, *24*, 429-465

Dennis, P. P.; Bremer, H. Differential rate of ribosomal protein synthesis in Escherichia coli B/r. *J. Mol. Biol.*, **1974**, *84*, 407-422

Dezube, B.J.; Krown, S.E.; Lee, J.Y.; Bauer, K.S.; Aboulafia, D.M. Randomized Phase II trial of matrix metalloproteinase inhibitor COL-3 in AIDS-related Kaposi's sarcoma: an AIDS malignancy consortium study. *Journal of Clinical Oncology*, **2006**, *24*, 1389-1394

Di Lullo, G.A.; Sweeney, S.M.; Korkko, J.; Ala-Kokko, L.; San Antonio, J. D. Mapping the Ligand-binding Sites and Disease-associated Mutations on the Most Abundant Protein in the Human, Type I Collagen. *J. Biol. Chem.*, **2002**, *277*, 4223-4231

Ding, Y.; Uitto, V.J.; Haapasalo, M.; Lounatmaa, K.; Kontinen, Y.T.; Salo, T.; Gienier, D.; Sorsa, T. Membrane components of Treponema denticola trigger proteinase release from human polymorphonuclear leukocytes. *J. Dent. Res.*, **1996**, *75*, 1986-1993

Dobbs, L.G.; Gonzalez, R.; Matthay, M.A.; Carter, E.P.; Allen, L.; Verkman, A.S.

Highly water-permeable type I alveolar epithelial cells confer high water permeability between the airspace and vasculature in rat lung. *Proc. Natl. Acad. Sci. USA*, **1998**, *95*, 2991-2996

Dove, A. MMP inhibitors: Glimmers of hope amidst clinical failures. *Nature Med.*, **2002**, *8*, 95

Drobnjak, M.; Osman, I.; Scher, H.I.; Fazzari, M.; Cordon-Cardo, C. Overexpression of cyclin D1 is associated with metastatic prostate cancer to bone. *Clin. Cancer Res.*, **2000**, *6*, 1891-1895

Duggar, B.M. Aureomycin: a product of the continuing search for new antibiotics. *Ann. NY Acad. Sci.*, **1948**, *51*, 177-181

Eckberg, R.P.; Nelson, J.H.; Kenney, J.W.; Howells, P.N.; Henry, R.A. Reactions of bis(2,4-pentanedionato)nickel(II) with isocyanates and other electrophiles. Electrophilic addition to 2,4-pentanedione catalyzed by bis(2,4-pentanedionato)nickel(II) *Inorganic Chemistry*, **1977**, *16*, 3128-3129

Egeblad, M.; Werb, Z. New functions for the matrix metalloproteinases in cancer progression. *Nat. Rev. Cancer*, **2002**, *2*, 161-174

Elburki, M.; Lee, H.M.; Gupta, N.; Balacky, P.; Zhang, Y.; Johnson, F.; Zhang, Y.; Golub, L.M. Chemically-Modified Curcumins Inhibit Alveolar Bone Loss in Diabetic Rats with Periodontitis. *J. Dent. Res.*, **2012**, *91*, Special Issue 1528

Fang, Y.; Xiang, B.; Pan, Z.H.; Cao, D.Y. Studies on preparation and dissolution test in vitro of sustained-release dropping pills of curcumin. *Zhong Yao Cai*, **2010**, *33*, 111-114



Fisher, J.F.; Mobashery, S. Recent advances in MMP inhibitor design. *Cancer Metastasis Rev.*, **2006**, *25*, 115-136

Freije, J.M.; Diez-Itza, I.; Balbín, M.; Sánchez, L.M.; Blasco, R.; Tolivia, J.; López-Otín, C. Molecular cloning and expression of collagenase-3, a novel human matrix metalloproteinase produced by breast carcinomas. *J. Biol. Chem.*, **1994**, *269*, 16766-16773.

Fridman, R.; Toth, M.; Pena, D.; Mobashery, S. Activation of progelatinase B (MMP-9) by gelatinase A (MMP-2). *Cancer Res.*, **1995**, *55*, 2548-2555

Gabler, W.L.; Creamer, H.R. Suppression of human neutrophil functions by tetracyclines. *J. Periodontal Res.*, **1991**, *26*, 52-58

Gasteiger, E.; Gattiker, A.; Hoogland, C.; Ivanyi, I.; Appel, R.D.; Bairoch, A. ExPASy: the proteomics server for in-depth protein knowledge and analysis. *Nucleic Acids Res.*, **2003**, *31*, 3784-3788

Gavuzzo, E.; Pochetti, G.; Mazza, F.; Gallina, C.; Gorini, B.; D'Alessio, S.; Pieper, M.; Tschesche, H.; Tucker, P.A. Two crystal structures of human neutrophil collagenase, one complexed with a primed- and the other with an unprimed-side inhibitor: implications for drug design. *J. Med. Chem.*, **2000**, *43*, 3377-3385

Giannelli, G.; Falk-marzillier, J.; Schiraldi, O.; Stetlerstevenson, W.G.; Quaranta, V. Induction of cell migration by matrix metalloproteinase-2 cleavage of laminin-5. *Science*, **1997**, *277*, 225-228

Gill, S.E.; Parks, W.C. Metalloproteinases and their inhibitors: regulators of wound healing. *Int. J. Biochem. Cell Biol.*, **2008**, *40*, 1334-1347

Golub, L.M.; Greenwald, R.A.; Ramamurthy, N.S.; McNamara, T.F.; Rifkin, B.R.  
Tetracyclines inhibit connective tissue breakdown: New therapeutic implications for an old family of drugs. *Crit. Revs Oral Biol. Med.*, **1991**, *2*, 297-322

Golub, L.M.; Lee, H.M.; Lehrer, G.; Nemiroff, A.; McNamara, T.F.; Kaplan, R.; Ramamurthy, N.S. Minocycline reduces gingival collagenolytic activity during diabetes: Preliminary observations and a proposed new mechanism of action. *J. Periodont. Res.*, **1983**, *18*, 516-526

Golub, L.M.; Lee, H.M.; Ryan, M.E.; Giannobile, W.V.; Payne, J.; Sorsa, T.  
Tetracyclines inhibit connective tissue breakdown by multiple non-antimicrobial mechanisms. *Adv. Dent. Res.*, **1998**, *12*, 12-26

Golub, L.M.; Ramamurthy, N.S.; McNamara, T.F.; Greenwald, R.A.; Rifkin, B.R.  
Tetracyclines inhibit connective tissue breakdown: new therapeutic implications for an old family of drugs. *Crit. Rev. Oral Biol. Med.*, **1991**, *2*, 297-321

Golub, L.M.; Wolff, M.; Roberts, S.; Lee, H.M.; Leung, M.; Payonk, G.S. Treating periodontal diseases by blocking tissue-destructive enzymes. *J. Am. Dent. Assoc.*, **1994**, *125*, 163-171

Gomez, D.E.; Alonso, D.F.; Yoshiji, H.; Thorgeirsson, U.P. Tissue inhibitors of metalloproteinases- structure, regulation and biological functions. *Eur. J. cell. Biol.*, **1997**, *74*, 111-122.

Grams, F.; Crimmin, M.; Hinnes, L.; Huxley, P.; Pieper, M.; Tschesche, H.; Bode, W.  
Structure determination and analysis of human neutrophil collagenase complexed with a hydroxamate inhibitor. *Biochemistry*, 1995, *34*, 14012-14020

Grams, F.; Reinemer, P.; Powers, J.C.; Kleine, T.; Pieper, M.; Tschesche, H.; Huber, R.; Bode, W. X-ray structures of human neutrophil collagenase complexed with peptide hydroxamate and peptide thiol inhibitors. Implications for substrate binding and rational drug design. *Eur.J.Biochem.*, 1995, 228, 830-841

Gross, J.; Lapiere, C.M. Collagenolytic activity in amphibian tissues - a tissue culture assay. *Proc. Natl. Acad. Sci. USA*, **1962**, 48, 1014-1022

Gumbiner, L.M.; Gumerlock, P.H.; Mack, P.C.; Chi, S.G.; deVere White, R.W.; Mohler, J.L.; Pretlow, T.G.; Tricoli, J.V. Overexpression of cyclin D1 is rare in human prostate carcinoma. *Prostate*, **1999**, 38, 40-45

Hagglund, A.C.; Ny, A.; Leonardsson, G.; Ny, T. Regulation and localization of matrix metalloproteinases and tissue inhibitors of metalloproteinases in the mouse ovary during gonadotropin-induced ovulation. *Endocrinology*, **1999**, 140, 4351-4358

Hayashi, K.; Dombou, M.; Sekiya, M.; Nakajima, H.; Fujita, T. Nakayama, M. Thermorubin and 2-hydroxyphenyl acetic acid, aldose reductase inhibitors. *J. Antibiot. (Tokyo)*, **1995**, 48, 1345-1346

Hiratsuka, S.; Nakamura, K.; Iwai, S.; Murakami, M.; Itoh, T.; Kijima, H.; Shipley, J.M.; Senior, R.M.; Shibuya, M. MMP-9 induction by vascular endothelial growth factor receptor-1 is involved in lung-specific metastasis. *Cancer Cell*, **2002**, 2, 289-300

Hojilla, C.V.; Mohammed, F.F.; Khokha, R. Matrix metalloproteinases and their tissue inhibitors direct cell fate during cancer development. *Br. J. Cancer*, **2003**, 89, 1817-1821

Holmgren, L. Antiangiogenesis restricted tumor dormancy. *Cancer Metast. Rev.*, **1996**,

15, 241-245

Hotary, K.B.; Allen, E.D.; Brooks, P.C.; Datta, N.S.; Long, M.W.; Weiss, S.J.

Membrane type I matrix metalloproteinase usurps tumor growth control imposed by the three-dimensional extracellular matrix. *Cell*, **2003**, *114*, 33-45

Hsia, J.C.; Wong, L.T.; Tan, C.T.; Er, S.S.; Kharouba, S.; Balaskas, E.; Tinker, D.O.;

Feldhoff, R.C. Bovine serum albumin: characterization of a fatty acid binding site on the N-terminal peptic fragment using a new spin-label. *Biochemistry*, **1984**, *23*, 5930-5932

[http://www.chemicalbook.com/ChemicalProductProperty\\_EN\\_CB4145842.htm](http://www.chemicalbook.com/ChemicalProductProperty_EN_CB4145842.htm) for physical properties of tributyl borate

[http://www.chemicalbook.com/ProductMSDSDetailCB1126251\\_EN.htm](http://www.chemicalbook.com/ProductMSDSDetailCB1126251_EN.htm) for physical properties of trimethyl borate

Huang, M.T.; Ma, W.; Yen, P.; Xie, J.G.; Han, J.; Frenkel, K.; Grunberger, D.;

Conney, A.H. Inhibitory effects of topical application of low doses of curcumin on 12-O-tetradecanoylphorbol-13-acetate-induced tumor promotion and oxidized DNA bases in mouse epidermis. *Carcinogenesis*, **1997**, *18*, 83-88

Huang, S.Y.; Van Arsdall, M.; Tedjarati, S.; McCarty, M.; Wu, W.J.; Langley, R.;

Fidler, I.J. Contributions of stromal metalloproteinases-9 to angiogenesis and growth of human ovarian carcinoma in mice. *J. Natl. Cancer. Inst.*, **2002**, *94*, 1134-1142

Huhtala, P. Chow, L.T.; Tryggvason, K. Structure of the human type IV collagenase gene. *J. Biol. Chem.*, **1990**, *265*, 11077-11082

Hulboy, D.L.; Rudolph, I.A.; Matrisian, L.M. Matrix metalloproteinases as mediators

of reproductive function. *Mol. Hum. Reprod.*, **1997**, *3*, 27-45

Hulmes, D. J. Building collagen molecules, fibrils, and suprafibrillar structures. *J. Struct. Biol.*, **2002**, *137*, 2-10

Hulmes, D.J. The collagen superfamily-diverse structures and assemblies. *Essays Biochem.*, **1992**, *27*, 49-67

Hynes, R.O. The extracellular matrix: not just pretty fibrils. *Science*, **2009**, *326*, 1216-1219

Idell, S. Endothelium and disordered fibrin turnover in the injured lung: newly recognized pathways. *Crit. Care Med.*, **2002**, *30*, S274-S280

Ingber, D. Extracellular matrix as a solid-state regulator in angiogenesis: identification of new targets for anti-cancer therapy. *Semin. Cancer Biol.*, **1992**, *3*, 57-63.

Ireson, C.; Orr, S.; Jones, D.J.; Verschoyle, R.; Lim, C.K.; Luo, J.L.; Howells, L.; Plummer, S.; Jukes, R.; Williams, M.; Steward, W.P.; Gescher, A. Characterization of metabolites of the chemopreventive agent curcumin in human and rat hepatocytes and in the rat in vivo, and evaluation of their ability to inhibit phorbol ester-induced prostaglandin E2 production. *Cancer Res.*, **2001**, *61*, 1058-1064

Ireson, C.R.; Jones, D.J.; Orr, S.; Coughtrie, M.W.; Boocock, D.J.; Williams, M.L.; Farmer, P.B.; Steward, W.P.; Gescher, A.J. Metabolism of the cancer chemopreventive agent curcumin in human and rat intestine. *Cancer Epidemiol Biomarkers Prev.*, **2002**, *11*, 105-111

Itoh, Y.; Kajita, M.; Kinoh, H.; Mori, H.; Okada, A.; Seiki, M. Membrane type 4 matrix metalloproteinase (MT4-MMP, MMP-17) is a glycosyl-phosphatidyl inositol-anchored

proteinase. *J. Biol. Chem.*, **1999**, *274*, 34260-34266

Johnson, F.; Chandra, B.; Iden, C.R.; Naiksatam, P.; Kahen, R.; Okaya, Y.; Lin, S. Y.

Thermorubin. 1. Structure studies. *J. Am. Chem. Soc.*, **1980**, *102*, 5580-5585

Johnson, M.D.; Widdicombe, J.H.; Allen, L.; Barbry, P.; Dobbs, L.G. Alveolar epithelial type I cells contain transport proteins and transport sodium, supporting an active role for type I cells in regulation of lung liquid homeostasis. *Proc. Natl. Acad. Sci. USA*, **2002**, *99*, 1966-1971

Jung, K.; Nowak, L.; Lein, M.; Priem, F.; Schnorr, D.; Loening, S.A. Matrix metalloproteinases 1 and 3, tissue inhibitor of metalloproteinase-1 and the complex of metalloproteinase-1 tissue inhibitor in plasma of patients with prostate cancer. *Int. J. Cancer*, **1997**, *74*, 220-223

Jung, S.; Rutka, J.T.; Hinek, A. Tropoelastin and elastin degradation products promote proliferation of human astrocytoma cell lines. *J. Neuropathol. Exp. Neurol.*, **1998**, *57*, 439-448

Kafienah, W.; Bromme, D.; Buttle, D.J.; Croucher, L.J.; Hollander, A.P. Human cathepsin K cleaves native type I and II collagens at the N-terminal end of the triple matrix. *Biochem.*, **1998**, *331*, 727-732

Katzap, E.; Goldstein, M.J.; Shah, N.V.; Schwartz, J.; Razzano, P.; Golub, L.M.;

Johnson, F.; Greenwald, R.; Grande, D. The chondroprotective capability of curcumin (curcuma longa) and its derivatives against IL-1 $\beta$  and OsM-mediated chondrolysis.

*Trans. Orthoped. Res. Soc.*, **2011**, 36

Kaur, G.; Tirkey, N.; Bharrhan, S.; Chanana, V.; Rishi, P.; Chopra, K. Inhibition of

oxidative stress and cytokine activity by curcumin in amelioration of endotoxin-induced experimental hepatotoxicity. *Clin. Exp. Immunol.*, **2006**, *145*, 313-321

Khurana, J.M.; Sehgal, A. An efficient and convenient procedure for ester hydrolysis. *OPPI BRIEFS*, **1994**, *26*, 580-583

Kim, M.K.; Park, J.C.; Chong, Y. Aromatic Hydroxyl Group Plays a Critical Role in Antibacterial Activity of the Curcumin Analogues. *Natural Product Communications*, **2012**, *7*, 57-58

Knauper, V.; Lopez-Otin, C.; Smith, B.; Knight, G.; Murphy, G. Biochemical characterization of human collagenase-3. *J. Biol. Chem.*, **1996**, *271*, 1544-1550

Knauper, V.; Will, H.; Lopez-Otin, C.; Smith, B.; Atkinson, S.J.; Stanton, H.; Hembry, R.M.; Murphy, G. Cellular mechanisms for human procollagenase-3 (MMP-13) activation. Evidence that MT1-MMP (MMP-14) and gelatinase a (MMP-2) are able to generate active enzyme. *J. Biol. Chem.*, **1996**, *271*, 17124-17131

Knight, C.G.; Willenbrock, F; Murphy, G. A novel coumarin-labelled peptide for sensitive continuous assays of the matrix metalloproteinases. *FEBS Lett.*, **1992**, *296*, 263-266

Kojima, S.; Itoh, Y.; Matsumoto, S.; Masuho, Y.; Seiki, M. Membrane-type 6 matrix metalloproteinase is the second glycosyl-phosphatidyl inositol-anchored MMP. *FEBS Lett.*, **2000**, *480*, 142-146

Kolb, C.; Mauch, S.; Krawinkel, U.; Sedlacek, R. Matrix metalloproteinase-19 in capillary endothelial cells: expression in acutely, but not in chronically, inflamed synovium. *Exp. Cell Res.*, **1999**, *250*, 122-130

Kontinen, Y.T.; Salo, T.; Hanemaaijer, R.; Valleala, H.; Sorsa, T.; Sutinen, M.; Ceponis, A.; Xu, J.W.; Santavirta, S.; Teronen, O.; López-Otín, C. Collagenase-3 (MMP-13) and its activators in rheumatoid arthritis: localization in the pannus-hard tissue junction and inhibition by alendronate. *Matrix Biol.*, **1999**, *18*, 401-412

Kung, H.F.; Fox, J. E.; Spears, C.; Brot, N.; Weissbach, H. Studies on the role of ribosomal proteins L 7 and L 12 in the in vitro synthesis of  $\beta$ -galactosidase. *J. Biol. Chem.*, **1973**, *248*, 5012-5015

Kung, H.F.; Spears, C.; Schulz, T.; Weissbach, H. Studies on the in vitro synthesis of beta-galactosidase: necessary components in the ribosomal wash. *Arch. Biochem. Biophys.*, **1974**, *162*, 578-584

Lal, B.; Kapoor, A.K.; Agrawal, P.K.; Asthana, O.P.; Srimal, R.C. Role of curcumin in idiopathic inflammatory orbital pseudotumours. *Phytother Res.*, **2000**, *14*, 443-447

Lampe, V. Synthese von Curcumin. *Ber. Dtsch. Chem. Ges.*, **1918**, *51*, 1347-1355;

Lampe, V.; Milobedzka, J.; Kostanecki, St. V. Zur Kenntnis des Curcumins. *Berichte.*, **1910**, *43*, 2163

Lao, C.D.; Ruffin, M.T.; Normolle, D.; Heath, D.D.; Murray, S.I.; Bailey, J.M.; Boggs, M.E.; Crowell, J; Rock, C.L.; Brenner, D.E. Dose escalation of a curcuminoid formulation. *BMC Complement Altern. Med.*, **2006**, *6*, 10

Lawbart, M.L.; Schneider, J.J. Preparation and properties of steroidal 17,20- and 20,21-acetonides epimeric at C-20. I. Derivatives of 5.beta.-pregnan-3.alpha.-ol. *J. Org. Chem.*, **1969**, *34*, 3505-3512

Lee, H.; Arsur, M.; Wu, M.; Duyao, M.; Buckler, A.J.; Sonenshein, G.E., Role of Rel-



related factors in control of c-myc gene transcription in receptor-mediated apoptosis of the murine B cell WEHI 231 line. *J. Exp. Med.*, **1995**, *181*, 1169-1177

Leff, R.L. Osteoarthritis. Matrix Metalloproteinase inhibition, cartilage loss. Surrogate markers, and clinical implications. *Ann. N.Y. Acad. Sci.*, **1999**, *878*, 201-207

Lin, F.W.; Wishnia, A. The Protein Synthesis Inhibitor Thermorubin. 1. Nature of the Thermorubin-Ribosome Complex. *Biochemistry*, **1982**, *21*, 477

Lindahl, L.; Sor, F.; Archer, R. H.; Nomura, M.; Zengel, J.M. Transcriptional organization of the S10, spc and alpha operons of *Escherichia coli*. *Biochim. Biophys. Acta.*, **1990**, *1050*, 337-342

Lindy, O.; Konttinen, Y.T.; Sorsa, T.; Ding, Y.; Santavirta, S.; Ceponis, A.; López-Otín, C. Matrix metalloproteinase 13 (collagenase-3) in human rheumatoid synovium. *Arthritis Rheum.*, **1997**, *40*, 1391-1399

Liotta, L.A.; Abe, S.; Robey, P.G.; Martin, G.R. Preferential digestion of basement membrane collagen by an enzyme derived from a metastatic murine tumor. *Proc. Natl. Acad. Sci. USA*, **1979**, *76*, 2268-2272

Lipinski, C.A.; Lombardo, F.; Dominy, B.W.; Feeney, P.J. Experimental and computational approaches to estimate solubility and permeability in drug discovery and development settings. *Adv Drug Deliv Rev.*, **2001**, *46*, 3-26

Liu, Y.; Ramamurthy, N.; Marecek, J.; Lee, H.M.; Chen, J.L.; Ryan, M.E.; Rifkin, B.R.; Golub, L.M. The lipophilicity, pharmacokinetics, and cellular uptake of different chemically-modified tetracyclines (CMTs). *Curr. Med. Chem.*, **2001**, *8*, 243-252.

Lohi, J.; Wilson, C.L.; Roby, J.D.; Parks, W.C. Epilysin, a novel human matrix

metalloproteinase (MMP-28) expressed in testis and keratinocytes and in response to injury. *J. Biol. Chem.*, **2001**, 276, 10134-10144

Luft, J.R.; Arakali, S.V.; Kirisits, M.J.; Kalenik, J.; Wawrzak, I.; Cody, V.; Pangborn, W. A.; DeTitta, G. T. A macromolecular crystallization procedure employing diffusion cells of varying depths as reservoirs to tailor the time course of equilibration in hanging- and sitting-drop vapor-diffusion and microdialysis experiments. *J. Appl. Cryst.*, 1994, 27, 443-453

Maiti, K.; Mukherjee, K.; Gantait, A; Saha, B.P.; Mukherjee, P.K. Curcumin–phospholipid complex: Preparation, therapeutic evaluation and pharmacokinetic study in rats. *Int. J. Pharm.*, **2007**, 330, 155-163

Makrides, S.C. Strategies for achieving high-level expression of genes in *Escherichia coli*. *Microbiol. Rev.*, 1996, 60, 512-538

Manicourt, D.H.; Fujimoto, N.; Obata, K.; Thonar, E.J. Levels of circulating collagenase, stromelysin-1, and tissue inhibitor of matrix metalloproteinases 1 in patients with rheumatoid arthritis. Relationship to serum levels of antigenic keratan sulfate and systemic parameters of inflammation. *Arthritis Rheum.*, **1995**, 38, 1031-1039

Mathy-Hartert, M.; Jacquemond-Collet, I.; Priem, F.; Sanchez, C.; Lambert, C.; Henrotin, Y. Curcumin inhibits pro-inflammatory mediators and metalloproteinase-3 production by chondrocytes. *Inflamm. Res.*, **2009**, 58, 899-908

Matter, H.; Schwab, W.; Barbier, D.; Billen, G.; Haase, B.; Neises, B.; Schudok, M.; Thorwart, W.; Schreuder, H.; Brachvogel, V.; Lonze, P.; Weithmann, K.U.

Quantitative structure-activity relationship of human neutrophil collagenase (MMP-8) inhibitors using comparative molecular field analysis and X-ray structure analysis.

*J.Med.Chem.*, 1999, *42*, 1908-1920

McCawley, L.J.; Matrisian, L.M. Matrix metalloproteinases: they're not just for matrix anymore! *Curr. Opin. Cell Biol.*, **2001**, *13*, 534-540

McCulloch, J. Physical modalities in wound management: ultrasound, vasopneumatic devices and hydrotherapy. *Ostomy. Wound Manage*, **1995**, *41*, 32-37

Meikle, M.C.; Bord, S.; Hembry, R.M.; Comston, J.; Croucher, P.I.; Reynolds, J.J.

Human osteoblasts in culture synthesize collagenase and other matrix metalloproteinases in response to osteotropic hormones and cytokines. *J.Cell Sci.*, **1992**, *103*, 1093-1099

Minieri, P.P.; Firman, M.C.; Mistretta, A. G.; Abbey, A.; Bricker, C.E.; Rigler, N.E.;

Sokol, H. A new broad spectrum antibiotic product of the tetracycline group.

*Antibiotics Ann. 1953-54.*,**1954**, 81-87

Mitsiades, N.; Yu, W.H.; Poulaki, V.; Tsokos, M.; Stamenkovic, I. Matrix metalloproteinase-7-mediated cleavage of Fas ligand protects tumor cells from chemotherapeutic drug cytotoxicity. *Cancer Res.*, **2001**, *61*, 577-581

Mizoguchi H, Yamada K, Nabeshima T. Matrix metalloproteinases contribute to neuronal dysfunction in animal models of drug dependence, Alzheimer's disease, and epilepsy. *Biochem. Res. Int.*, **2011**, 681385

Morimoto, T.; Yamasaki, M.; Nakata, K.; Tsuji, M.; Nakamura, H. The expression of macrophage and neutrophil elastases in rat periradicular lesions. *J. Endod.*, **2008**, *34*,

1072-1076

Mukhopadhyay, A.; Banerjee, S.; Stafford, L.J.; Xia, C.X.; Liu, M.; Aggarwal, B.B.,  
Curcumin-induced suppression of cell proliferation correlates with downregulation of  
cyclin D1 expression and CDK4-mediated retinoblastoma protein phosphorylation.

*Oncogene*, **2002**, *21*, 8852-8862

Murphy, G.; Allan, J.A.; Willenbrock, F.; Cockett, M.I.; O'Connell, J.P.; Docherty,  
A.J. The role of the C-terminal domain in collagenase and stromelysin specificity. *J.*

*Biol. Chem.*, **1992**, *267*, 9612-9618

Murphy, G.; Crabbe, T. Gelatinases A and B. *Methods Enzymol.*, **1995**, *248*, 470-484

Murphy, G.; Knauper, V. Relating matrix metalloproteinase structure to function: why  
the 'hemopexin' domain? *Matrix Biol.*, 1997, *15*, 511-518

Nagase, H. Human stromelysins 1 and 2. *Methods Enzymol.*, **1995**, *248*, 449-470

Nagase, H.; Engild, J.J.; Suzuki, K.; Salvesen, G. Stepwise activation mechanisms of  
the precursor of matrix metalloproteinase 3 (stromelysin) by proteinases and (4-  
aminophenyl) mercuric acetate. *Biochemistry*, **1990**, *29*, 5783-5789

Nagase, H.; Fields, C.G.; Fields, G.B. Design and Characterization of a Fluorogenic  
Substrate Selectively Hydrolyzed by Stromelysin 1 (Matrix Metalloproteinase-3). *J.*

*Biol. Chem.*, **1994**, *269*, 20952-20957

Nagase, H.; Visse, R.; Murphy, G. Structure and function of matrix metalloproteinases  
and TIMPs. *Cardiovasc. Res.*, **2006**, *69*, 562-573

Nagase, H.; Woessner, J.F. Jr. Matrix metalloproteinases. *J. Biol. Chem.*, **1999**, *274*,  
21491-21494

Napolitano, N.; Clemems, M.; Lee, H.M.; Zhang, Y.; Johnson, F.; Golub, L.M.; Gu, Y. Novel Curcumin Derivatives Suppress Inflammatory Mediators in Periodontally-relevant Cells. *J. Dent. Res.*, **2012**, *91*, Special Issue 1527

Napolitano, N.; Kang, D.; Clemems, M.; Lee, H.M.; Johnson, F.; Golub, L.M.; Gu, Y. Chemically Modified Curcumins Suppress Human Mononuclear Cell Cytokines. *J. Dent. Res.*, **2011**, *90*, Special Issue 2292

O'Brien, P.M.; Sliskovic, D.R.; Blankley, C. J.; Roth, B.D.; Wilson, M.W.; Hamelehle, K.L.; Krause, B.R.; Stanfield, R.L. Inhibitors of Acyl-CoA:Cholesterol O-Acyl Transferase (ACAT) as Hypocholesterolemic Agents. 8. Incorporation of Amide or Amine Functionalities into a Series of Disubstituted Ureas and Carbamates. Effects on ACAT Inhibition in vitro and Efficacy in vivo. *J. Med. Chem.*, **1994**, *37*, 1810-1822

Okada, N.; Ishida, H.; Murata, N.; Hashimoto, D.; Seyama, Y.; Kubota, S. Matrix metalloproteinase-2 and -9 in bile as a marker of liver metastasis in colorectal cancer. *Biochem. Biophys Res. Commun.*, **2001**, *288*, 212-216

Osterby, R.; Hartmann, A.; Bangstad, H.J. Structural changes in renal arterioles in Type I diabetic patients. *Diabetologia*, **2002**, *45*, 542-549

Overall, C. M.; Lopez-Otin, C. Strategies for MMP inhibition in cancer: innovations for the post-trial era. *Nature Rev. Cancer*, **2002**, *2*, 657-672

Overall, C.M.; Kleifeld, O. Towards third generation matrix metalloproteinase inhibitors for cancer therapy. *British Journal of Cancer*, **2006**, *94*, 941-946

Overall, C.M.; Lopez-Otin, C. Strategies for MMP inhibition in cancer: innovations for the post-trial era. *Nat. Rev. Cancer*, **2002**, *2*, 657-672

Pabon, H.J.J. A synthesis of curcumin and related compounds. *Recueil.*, **1964**, *83*, 379-386

Pankov, R.; Yamada, K.M. Fibronectin at a glance. *Journal of Cell Science*, **2002**, *115*, 3861-3863

Pavolini, T. Nuova sintesi della Curcumina. *Riv. Ital. Essenze, Profumi, Piante Officinali*, **1937**, *19*, 167-168

Pedersen, U.; Rasmussen, P.B.; Lawesson, S.O. Synthesis of naturally occurring curcuminoids and related compounds. *Liebigs Ann. Chem.*, **1985**, 1557-1569

Pei, D.; Majmudar, G.; Weiss, S.J. Hydrolytic inactivation of a breast cancer carcinoma cell-derived serpin by human stromelysin-3. *J. Biol. Chem.*, **1994**, *269*, 25849-25855

Pei, D.; Weiss, S.J. Transmembrane-deletion mutants of the membrane-type matrix metalloproteinase-1 process progelatinase A and express intrinsic matrix-degrading activity. *J. Biol. Chem.*, **1996**, *271*, 9135-9140

Pendás, A.M.; Knäuper, V.; Puente, X.S.; Llano, E.; Mattei, M.G.; Apte, S.; Murphy, G.; López-Otín, C. Identification and characterization of a novel human matrix metalloproteinase with unique structural characteristics, chromosomal location, and tissue distribution. *J. Biol. Chem.*, **1997**, *272*, 4281-4286

Peterson, J.T. The importance of estimating the therapeutic index in the development of matrix metalloproteinase inhibitors. *Cardio. Res.*, **2006**, *69*, 677-687

Pochetti, G.; Gavuzzo, E.; Campestre, C.; Agamennone, M.; Tortorella, P.; Consalvi, V.; Gallina, C.; Hiller, O.; Tschesche, H.; Tucker, P.A.; Mazza, F. Structural insight into the stereoselective inhibition of MMP-8 by enantiomeric sulfonamide

phosphonates. *J.Med.Chem.*, 2006, 49, 923-931

Polette, M.; Birembaut, P. Membrane-type metalloproteinases in tumor invasion. *Int. J. Biochem. Cell Biol.*, **1998**, 30, 1195-1202

Polette, M.; Nawrocki-Raby, B.; Gilles, C.; Clavel, C.; Birembaut, P. Tumour invasion and matrix metalloproteinases. *Crit. Rev. Oncol. Hematol.*, **2004**, 49, 179-186

Potempa, J.; Banbula, A.; Travis, J. Role of bacterial proteinases in matrix destruction and modulation of host responses. *Periodontol 2000*, **2000**, 24, 153-192

Powell, W.C.; Fingleton, B.; Wilson, C.L.; Boothby, M.; Matrisian, L.M. The metalloproteinase matrilysin proteolytically generates active soluble Fas ligand and potentiates epithelial cell apoptosis. *Curr. Biol.*, **1999**, 9, 1441-1447

Powell, W.C.; Knox, J.D.; Navre, M.; Grogan, T.M.; Kittelson, J.; Nagle, R.B.; Bowden, G.T. Expression of the metalloproteinase matrilysin in DU-145 cells increases their invasive potential in severe combined immunodeficient mice. *Cancer Res.*, **1993**, 53, 417-422

Prikk, K.; Maisi, P.; Pirila, E.; Sepper, R.; Salo, T.; Wahlgren, J.; Sorsa, T. In vivo collagenase-2 (MMP-8) expression by human bronchial epithelial cells and monocytes/macrophages in bronchiectasis. *J. Pathol.*, 2001, 194, 232-238

Rai, D.; Singh, J.K.; Roy, N.; Panda, D. Curcumin inhibits FtsZ assembly: an attractive mechanism for its antibacterial activity. *Biochem J.*, **2008**, 410, 147-155

Ravindran, J.; Subbaraju, G.V.; Ramani, M.V.; Sung, B.; Aggarwal, B.B. Bisdemethylcurcumin and structurally related hispolon analogues of curcumin exhibit enhanced prooxidant, anti-proliferative and anti-inflammatory activities in vitro.

*Biochem Pharmacol.*, **2010**, *79*, 1658-1666

Ravindranath, V.; Chandrasekhara, N. Absorption and tissue distribution of curcumin in rats. *Toxicology*, **1980**, *16*, 259-265

Reinemer, P.; Grams, F.; Huber, R.; Kleine, T.; Schnierer, S.; Piper, M.; Tschesche, H.; Bode, W. Structural implications for the role of the N terminus in the 'superactivation' of collagenases. A crystallographic study. *FEBS Lett.*, 1994, *338*, 227-233

Riaz, M.; Pilpel, N. Effects of ultraviolet light on lecithin monolayers in the presence of fluorescein dyes and tetracycline drugs. *J. Pharm. Pharmacol.*, **1983**, *35*, 215-218

Richards, C.; Pantanowitz, L.; Dezube, B.J. Antimicrobial and non-antimicrobial tetracyclines in human cancer trials. *Pharmacological Research*, **2011**, *63*, 151-156

Ruby, A.J.; Kuttan, G; Babu, K.D.; Rajasekharan, K.N.; Kuttan, R. Anti-tumour and antioxidant activity of natural curcuminoids. *Cancer Lett.*, **1995**, *94*, 79-83

Ruhul Amin, A.R.; Senga, T.; Oo, M.L.; Thant, A.A.; Hamaguchi, M. Secretion of matrix metalloproteinase-9 by the proinflammatory cytokine, IL-1 beta: a role for the dual signalling pathways, Akt and Erk. *Genes Cells*, **2003**, *8*, 515-523

Ryan, M.E.; Ramamurthy, N.S.; Golub, L.M. Matrix metalloproteinases and their inhibitors in periodontal treatment. *Curr. Opin. Periodontol.*, **1996**, *3*, 85-96

Ryan, M.E.; Usman, A.; Ramamurthy, N.S.; Golub, L.M. Greenwald, R.A. Excessive matrix metalloproteinase activity in diabetes: inhibition by tetracycline analogues with zinc reactivity. *Curr. Med. Chem.*, **2001**, *8*, 305-316

Saari, H.; Suomalainen, K.; Lindy, O.; Kontinen, Y.T.; Sorsa, T. Activation of latent human neutrophil collagenase by reactive oxygen species and serine proteases.



*Biochem. Biophys. Res. Commun.*, **1990**, *171*, 979-987

Sandberg, S.; Glette, J.; Hopen, G.; Solberg, C.O. Doxycycline induced photodamage to human neutrophils and tryptophan. *Photochem. Photobiol.*, **1984**, *39*, 43-48

Sandur, S.K.; Pandey, M.K.; Sung, B.; Ahn, K.S.; Murakami, A.; Sethi, G.; Limtrakul, P.; Badmaev, V.; Aggarwal, B.B. Curcumin, demethoxycurcumin, bisdemethoxycurcumin, tetrahydrocurcumin, and turmerones differentially regulate antiinflammatory and antiproliferative responses through a ROS independent mechanism. *Carcinogenesis*, **2007**, *28*, 1765-1773

Sang, Q.X.; Birkedal-Hansen, H.; Van Wart, H.E. Proteolytic and non-proteolytic activation of human neutrophil progelatinase B. *Biochim. Biophys. Acta.*, **1995**, *1251*, 99-108.

Sato, H.; Kinoshita, T.; Takino, T.; Nakayama, K.; Seiki, M. Activation of a recombinant membrane type 1-matrix metalloproteinase (MT1-MMP) by furin and its interaction with tissue inhibitor of metalloproteinases (TIMP)-2. *FEBS Lett.*, **1996**, *393*, 101-104

Sato, H.; Takino, T.; Okada, Y.; Cao, J.; Shinagawa, A.; Yamamoto, E.; Seiki, M. A matrix metalloproteinase expressed on the surface of invasive cells. *Nature*, **1994**, *370*, 61-65

Schnierer, S.; Kleine, T.; Gote, T.; Hillemann, A.; Knauper, V.; Tschesche, H. The recombinant catalytic domain of human neutrophil collagenase lacks type I collagen substrate specificity. *Biochem. Biophys. Res. Commun.*, **1993**, *191*, 319-326

Schroder, J.; Henke, A.; Wenzel, H.; Brandstetter, H.; Stammli, H.G.; Stammli, A.;

Pfeiffer, W.D.; Tschesche, H. Structure-based design and synthesis of potent matrix metalloproteinase inhibitors derived from a 6H-1,3,4-thiadiazine scaffold.

*J.Med.Chem.*, 2001, *44*, 3231-3243

Seiki M. Membrane-type matrix metalloproteinases. *APMIS.*, **1999**, *107*, 137-143

Sellers, A.; Reynolds, J.J.; Meikle, M.C. Neutral metallo-proteinases of rabbit bone. Separation in latent forms of distinct enzymes that when activated degrade collagen, gelatin and proteoglycans. *Biochem. J.*, **1978**, *171*, 493-496

Sellers, A.; Woessner, J.F. The extraction of a neutral metalloproteinase from the involuting rat uterus, and its action on cartilage proteoglycan. *Biochem. J.*, **1980**, *189*, 521-531

Shapiro, S.D.; Griffin, G.L.; Gilbert, D.J.; Jenkins, N.A.; Copeland, N.G.; Welgus, H.G.; Senior, R.M.; Ley, T.J. Molecular cloning, chromosomal localization, and bacterial expression of a murine macrophage metalloelastase. *J. Biol. Chem.*, **1992**, *267*, 4664-4671

Sharma, O.P. Antioxidant activity of curcumin and related compounds. *Biochem Pharmacol.*, **1976**, *25*, 1811-1812

Sharma, R.A.; Euden, S.A.; Platton, S.L.; Cooke, D.N.; Shafayat, A.; Hewitt, H.R.; Marcylo, T.H.; Morgan, B.; Hemingway, D.; Plummer, S.M.; Pirmohamed, M.; Gescher, A.J.; Steward, W.P. Phase I clinical trial of oral curcumin: biomarkers of systemic activity and compliance. *Clin. Cancer Res.*, **2004**, *10*, 6847-6854

Sharma, R.A.; McLelland, H.R.; Hill, K.A.; Ireson, C. ; Euden, S.A.; Manson, M.M.; Pirmohamed, M.; Marnett, L.J.; Gescher, A.J.; Steward, W.P. Pharmacodynamic and

pharmacokinetic study of oral Curcuma extract in patients with colorectal cancer. *Clin.*

*Cancer Res.*, **2001**, *7*, 1894-1900

Shoba, G.; Joy, D.; Joseph, T.; Majeed, M.; Rajendran, R.; Srinivas, P. S. Influence of piperine on the pharmacokinetics of curcumin in animals and human volunteers.

*Planta. Med.*, **1998**, *64*, 353-356

Sledge, G.W.; Qulali, M.; Goulet, R.; Bone, E.A.; Fife, R. Effect of matrix metalloproteinase inhibitor batimastat on breast cancer regrowth and metastasis in athymic mice. *J. Natl. Cancer Inst.*, **1995**, *87*, 1546-1550

Smyth, M.S.; Martin, J.H. X ray crystallography. *Mol. Pathol.*, 2000, *5*, 8-14

Song, F.; Wisithphrom, K.; Zhou, J.; Windsor, L.J. *Frontiers in Bioscience*, **2006**, *11*, 3100 -3120

Sorsa T, Mäntylä P, Rönkä H, Kallio P, Kallis GB, Lundqvist C, Kinane DF, Salo T, Golub LM, Teronen O, Tikanoja S. Scientific basis of a matrix metalloproteinase-8 specific chair-side test for monitoring periodontal and peri-implant health and disease.

*Ann. N. Y. Acad. Sci.*, **1999**, *878*, 130-140

Sorsa T.; Tjäderhane L.; Konttinen Y.T.; Lauhrio A.; Salo, T.; Lee, H.M.; Golub, L.M.; Brown, D.L.; Mäntylä P. Matrix metalloproteinases: contribution to pathogenesis, diagnosis and treatment for periodontal inflammation. *Ann. Med.*, **2006**, *38*, 306-321

Sorsa, T.; Ding, Y.L.; Ingman, T.; Salo, T.; Westerlund, U.; Haapasalo, M.; Tschesche, H.; Konttinen, Y.T. Cellular source, activation and inhibition of dental plaque collagenase. *J. Clin. Periodontol.*, **1995**, *22*, 709-717

Sorsa, T.; Ingman, T.; Suomalainen, K.; Haapasalo, M.; Konttinen, Y.T.; Lindy, O.;

Saari, H.; Uitto, V.J. Identification of proteases from periodontopathogenic bacteria as activators of latent human neutrophil and fibroblast-type interstitial collagenases.

*Infect. Immun.*, **1992**, *60*, 4491-4495

Sorsa, T.; Tjaderhane, L.; Salo, T. Matrix metalloproteinases (MMPs) in oral diseases.

*Oral. Dis.*, **2004**, *10*, 311-318

Sovak, M.A.; Bellas, R.E.; Kim, D.W.; Zanieski, G.J.; Rogers, A.E.; Traish, A.M.;

Sonenshein, G.E. Aberrant nuclear factor-kappaB/Rel expression and the pathogenesis of breast cancer. *J. Clin. Invest.*, **1997**, *100*, 2952-2960

Springman, E.B.; Angleton, E.L.; Birkedalhansen, H.; Vanwart, H.E. Multiple-modes of activation of latent human fibroblast collagenase-evidence for the role of a Cys-73 active-site zinc complex in latency and a cysteine switch mechanism for activation.

*Proc. Natl. Acad. Sci. USA*, **1990**, *87*, 364-368

Stams, T.; Spurlino, J.C.; Smith, D.L.; Wahl, R.C.; Ho, T.F.; Qoronfleh, M.W.; Banks, T.M.; Rubin, B. Structure of human neutrophil collagenase reveals large S1' specificity pocket. *Nat. Struct. Biol.*, 1994, *1*, 119-123

Stöcker, W.; Grams, F.; Baumann, U.; Reinemer, P.; Gomis-Rüth, F.X.; McKay, D.B.;

Bode, W. The metzincins-topological and sequential relations between the astacins, adamalysins, serralysins, and matrixins (collagenases) define a superfamily of zinc-peptidases. *Protein Sci.*, **1995**, *4*, 823-840

Stolow, M.A.; Bauzon, D.D.; Li, J.; Sedgwick, T.; Liang, V.C.; Sang, Q.A.; Shi, Y.B.

Identification and characterization of a novel collagenase in *Xenopus laevis*: possible roles during frog development. *Mol. Biol. Cell*, **1996**, *7*, 1471-1483

Stone, W.L.; Wishnia, A. Binding of iodo-mercurates to sulfhydryl-blocked beta-lactoglobulin-A, -B, and -C. *Bioinorg. Chem.*, **1978**, *8*, 517-529

Strongin, A.Y.; Collier, I.; Bannikov, G.; Marmer, B.L.; Grant, G.A. Goldberg, G.I. Mechanism of cell-surface activation of 72-kDa type-IV collagenase-isolation of the activated form of the membrane metalloproteinase. *J. Biol. Chem.*, **1995**, *270*, 5331-5338

Suzuki, M. Raab, G.; Moses, M.A.; Fernandez, C.A.; Klagsbrun, M. Matrix metalloproteinase-3 releases active heparin-binding EGF-like growth factor by cleavage at a specific juxtamembrane site. *J. Biol. Chem.*, **1997**, *272*, 31730-31737

Takagi, H.; Manabe, H.; Kawai, N.; Goto, S.N.; Umemoto, T. Circulating matrix metalloproteinase-9 concentrations and abdominal aortic aneurysm presence: a meta-analysis. *Interact. Cardiovasc. Thorac. Surg.*, **2009**, *9*, 437-440

Thapliyal, R.; Maru, G.B. Inhibition of cytochrome p450 isoenzymes by curcumins in vitro and in vivo. *Food Chem. Toxicol.*, **2001**, *39*, 541-547

Todhunter, R.J.; Fubini, S.L.; Wooton, J.A.; Lust, G. Effect of methylprednisolone acetate on proteoglycan and collagen metabolism of articular cartilage explants. *J. Rheumatol.*, **1996**, *23*, 1207-1213

Tong, S.; Johnson, F. Investigation of Curcumin and CMCs. *Undergraduate Senior Thesis*, **2011**, Stony Brook University

Tummalapali, C.M.; Heath, B.J.; Tyagi, S.C. Tissue inhibitor of metalloproteinase-4 instigates apoptosis in transformed cardiac fibroblasts. *J. Cell Biochem.*, **2001**, *80*, 512-521

Van Herck, H.; Baumans, V.; Brandt, C.J.; Boere, H.A.; Hesp, A.P.; van Lith, H.A.; Schurink, M.; Beynen, A.C. Blood sampling from the retro-orbital plexus, the saphenous vein and the tail vein in rats: comparative effects on selected behavioral and blood variables. *Lab Anim.*, **2001**, *35*, 131-139

Vanwart, H.E.; Birkedalhansen, H. The cysteine switch-a principle of regulation of metalloproteinase activity with potential applicability to the entire matrix metalloproteinase gene family. *Proc. Natl. Acad. Sci. USA*, **1990**, *87*, 5578-5582

Vartio, T.; Hovi, T.; Vaheri, A. Human macrophages synthesize and secrete a major 95,000-dalton gelatin-binding protein distinct from fibronectin. *J. Biol. Chem.*, **1982**, *257*, 8862-8868

Venkatesan, N. Curcumin attenuation of acute adriamycin myocardial toxicity in rats. *Br. J. Pharmacol.*, **1998**, *124*, 425-427

Visse R.; Nagase H. Matrix metalloproteinases and tissue inhibitors of metalloproteinases: structure, function, and biochemistry. *Circ Res.*, **2003**, *92*, 827-839

Vu, T.H.; Werb. Z. Matrix metalloproteinases: effectors of development and normal physiology. *Genes. Dev.*, **2000**, *14*, 2123-2133

Wang, L.; Li, C.; Guo, H.; Kern, T.S.; Huang, K.; Zheng, L. Curcumin inhibits neuronal and vascular degeneration in retina after ischemia and reperfusion injury. *PLoS One*, **2011**, *6*, e23194

Wang, M.; Shen, J.; Jin, H.; Im, H.J.; Sandy, J.; Chen, D. Recent progress in understanding molecular mechanisms of cartilage degeneration during osteoarthritis. *Ann. NY Acad. Sci.*, **2011**, *1240*, 61-69

Wang, Y.; Lu, Z.; Wu, H.; Lv, F. Study on the antibiotic activity of microcapsule curcumin against foodborne pathogens. *International Journal of Food Microbiology*, **2009**, *136*, 71-74

Ware, L.B.; Matthay, M.A. The acute respiratory distress syndrome. *N. Engl. J. Med.*, **2000**, *342*, 1334-1349

Warner, R.L.; Lewis, C.S.; Beltran, L.; Youkin, E.M.; Varani, J.; Johnson, K.J. The role of metalloelastase in immune complex-induced acute lung injury. *Am. J. Pathol.*, **2001**, *158*, 2139-2144

Weiss, S.J.; Peppin, G.; Ortiz, X.; Ragsdale, C.; Test, S.T. Oxidative autoactivation of latent collagenase by human neutrophils. *Science*, **1985**, *227*, 747-749

Werb, Z.; Gordon, S. Elastase secretion by stimulated macrophages. Characterization and regulation. *J. Exp. Med.*, **1975**, *142*, 361-377

Whittaker, M.; Floyd, C.D.; Brown, P.; Gearing, A.J.H. Design and therapeutic application of matrix metalloproteinase inhibitors. *Chem. Rev.*, **1999**, *99*, 2735-2776.

Wilhelm, S.M.; Collier, I.E.; Marmer, B.L.; Eisen, A.Z.; Grant, G.A.; Goldberg, G.I. SV 40-transformed human lung fibroblasts secrete a 92 kDa type IV collagenase which is identical to that secreted by normal human macrophages. *J. Biol. Chem.*, **1989**, *264*, 17213-17221

Wilson, L.J.; Bray, T.L.; Suddath, F.L. Crystallization of proteins by dynamic control of evaporation. *Journal of Crystal Growth*, 1991, *110*, 142-147

Woessner, J.F.; Taplin, C.J. Purification and properties of a small latent matrix metalloproteinases of the rat uterus. *J. Biol. Chem.*, **1988**, *263*, 16918-16925

Wojtowicz-Praga, S.; torri, J. Johnson, M.; Steen, V.; Marshal, J.; Ness, E.; Dickson, R.; Sale, M.; Rasmussen, H.S.; Chiodo, T.A.; Hawkins, M.J. Phase I trial of Marimastat, a novel matrix metalloproteinase inhibitor, administered orally to patients with advanced lung cancer. *J. Clin. Oncol.*, **1998**, *16*, 2150-2156.

Wolf, K.; Mazo, I.; Leung, H.; Engelke, K.; Von Andrian, U.H.; Deryugina, E.I.; Strongin, A.Y.; Bocker, E.B.; Friedl, P. Compensation mechanism in tumor cell migration : mesenchymal-amoeboid transition after blocking of pericellular proteolysis. *J. Cell Biol.*, **2003**, *160*, 267-277

Woo, M.S.; Jung, S.H.; Kim, S.Y.; Hyun, J.W.; Ko, K.H.; Kim, W.K.; Kim, H.S. Curcumin suppresses phorbol ester-induced matrix metalloproteinase-9 expression by inhibiting the PKC to MAPK signaling pathways in human astroglioma cells. *Biochem. Biophys. Res. Commun.*, **2005**, *335*, 1017-1025

Wooley, D.E.; Roberts, D.R.; evanson, J.M. Inhibition of human collagenase activity by a small molecular weight serum protein. *Biochem. Biophys. Res. Commun.*, **1975**, *66*, 747-754

Wu, I.M.; Moses, M.A. Molecular cloning and expression analysis of the cDNA encoding rat tissue inhibitor of metalloproteinase-4. *Matrix Biol.*, **1998**, *16*, 339-342

Yin, J.; Yu, F.S. ERK1/2 mediate wounding- and G-proteincoupled receptor ligands-induced EGFR activation via regulating ADAM17 and HB-EGF shedding. *Invest. Ophthalmol. Vis. Sci.*, **2009**, *50*, 132-139

Ylipalosaari, M.; Thomas, G.J.; Nystrom, M.; Salhimi, S.; Marshall, J.F.; Huotari, V.; Tervahartiala, T.; Sorsa, T.; Salo, T. Alpha v beta 6 integrin down-regulates the MMP-



13 expression in oral squamous cell carcinoma cells. *Exp. Cell Res.*, **2005**, *309*, 273-283

Yu, H.W.; Zhang, Y.; Zhang, Y.; Lee, H.M.; McClain, S.A.; Johnson, F.; Golub, L.M.. A Novel Chemically-modified Curcumin (CMC2.24) Improves Diabetic Wound-Healing. *J. Dent. Res.*, **2012**, *91*, Special Issue 1529

Yu, Q.; Stamenkovic, I. Cell surface-localized matrix metalloproteinase-9 proteolytically activates TGF-beta and promotes tumor invasion and angiogenesis. *Genes. Dev.*, **2000**, *14*, 163-176

Yu, Z.; Leung, M.K.; Ramamurthy, N.S.; McNamara, T.F.; Golub, L.M. HPLC determination of a chemically modified nonantimicrobial tetracycline: biological implications. *Biochem. Med. Metab. Biol.*, **1992**, *47*, 10-20.

Zhou, D.; Lagoja, I.M.; Rozenski, J.; Busson, R.; Van Aerschot, A.; Herdewijn, P. Synthesis and properties of aminopropyl nucleic acids. *Chembiochem*, **2005**, *6*, 2298-2304

Zitka, O.; Kukacka, J.; Krizkova, S.; Huska, D.; Adam, V.; Masarik, M.; Prusa, R.; Kizek, R. Matrix metalloproteinases. *Current Medicinal Chemistry*, **2010**, *17*, 3751-3768

Zubay, G. In vitro synthesis of protein in microbial systems. *Annu. Rev. Genet.*, **1973**, *7*, 267-287

Zubay, G. The isolation and properties of CAP, the catabolite gene activator. *Meth. Enzymol.*, **1980**, *65*, 856-877

Zucker, S.; Cao, J.; Chen, W.T. Critical appraisal of the use of matrix metalloproteinase

inhibitors in cancer treatment. *Oncogene*, **2000**, *19*, 6642-6650

# Appendix

## A. Report on the boron analysis of CMC2.24

Report Number: 38546



Report Date: 2012-01-05

### Laboratory Report

**Report prepared for:**

Ramesh Gupta  
Stony Brook University  
622 Chemistry Bldg  
Stony Brook, NY 11794-3400  
Phone: 631-632-8862  
Email: [yuzhang.chn@gmail.com](mailto:yuzhang.chn@gmail.com)

**Report prepared by:**

Pat B Delozier

**Purchase Order:**

VISA,Gupta,741

**For further assistance, contact:**

Pat B Delozier  
Report Production Coordinator  
PO Box 51610  
Knoxville, TN 37950-1610  
(865) 546-1335  
[patdelozier@galbraith.com](mailto:patdelozier@galbraith.com)

<b>Sample:</b> C2.24		<b>Received:</b> 2011-12-13			
<b>Lab ID:</b> 2011-P-9675					
Analysis	Method	Result	Basis	Amount	Date (Time)
B : Boron	GLI Procedure ME-70	< 28 ppm	Dried	90.59 mg	2012-01-03
ZZX: Dry before analysis					
	GLI Procedure 3.2.3.6	Completed	As Received	Direct	2011-12-19

**Signatures:**

Published By: pat.b.delozier

2012-01-05T16:46:40.923-05:00

- Physical signatures are on file.
- "Published By" signature indicates authorized release of data.